
Economic Commission for Europe

English

Inland Transport Committee**29 May 2015****Working Party on the Transport of Dangerous Goods****Joint Meeting of Experts on the Regulations annexed to the European Agreement concerning the International Carriage of Dangerous Goods by Inland Waterways (ADN)****Twenty-seventh session**

Geneva, 24-28 August 2015

Agenda item 3 (b)

Implementation of the ADN:**Special authorizations, derogations and equivalents**

“Bunker vessel Argos-GL”

Transmitted by the Government of the Netherlands

I. Introduction

1. During its meeting in January 2015, the ADN Committee discussed the Report of the meeting of the technical expert group on the Argos-GL bunker vessel (2015/INF.27). Several delegations had additional questions about the project. The delegation of the Netherlands was requested to put in writing the oral replies and explanations on these questions as provided during the January session in a document. This document can serve as a basis for a decision during the August session (ECE/TRANS/WP.15/AC.2/54).

2. Additional questions about the project involved the following topics:

- the stability of the vessel,
- the consequences of possible interference of LNG and gas oil in case of loss of containment,
- the use of large tanks and the calculations done on them by the class society,
- the integrity of the tank,
- sloshing effects.

II. Further report

3. In Annex II the “Further Report on the Bunker vessel Argos-GL” is added. This Further Report also contains several appendices. In this Report the topics mentioned under (2) are explained in depth. The Appendices provide the results of technical research, calculations and tests on the topics such as stability, interaction of the bunker fuels, crashworthy structure and sloshing.

III. Further process

4. The revised derogation is attached (Annex I). The ADN Administrative Committee is requested to decide based upon this derogation based on the information provided in 2014/INF.11, 2015/INF.27 and the present document.

Annex I

Decision of the ADN Administrative Committee relating to the tank vessel “Argos-GL”

Derogation No. xx/2015 of 28 August 2015

The competent authority of the Netherlands is authorized to issue a trial certificate of approval to the motor tank vessel Argos-GL, yard number to be determined, type G tanker, as referred to in the ADN, for the use of membrane tanks for the carriage of liquefied natural gas (LNG).

Pursuant to paragraph 1.5.3.2 of the Regulations annexed to ADN, the above-mentioned vessel may deviate until 31 December 2018 from the requirements:

1. *Table C, UN 1972 (LNG), Column 7, cargo tank design: 1* (pressure tank).

Although the membrane tank is a pressurized tank (70 kPa), it does not comply with the definition of a pressure tank according to ADN (400 kPa).

2. *Table C, UN 1972 (LNG), Column 8, cargo tank type: 1* (independent tank). Although the tank is independent from the ship's structure for temperature, it is not independent from a structural point of view.

3. *9.3.1.0.1 Tank materials*. The membrane tanks are made of plywood, polyurethane foam, aluminium foil and stainless steel.

4. *9.3.1.0.2 Use of wood, aluminium and plastics in the cargo zone*. The membrane tanks are made of plywood, polyurethane foam, aluminium foil and stainless steel.

5. *9.3.1.23.1 Cargo tanks need to comply with the requirements of a classification society for pressure vessels*. As the tanks are not considered as a pressure vessel, these requirements are not applicable. But the membrane tanks are type approved by the classification society which classes the ship (Lloyd's Register) and other recognized classification societies.

The Administrative Committee has decided that the use of membrane tanks is sufficiently safe if the following conditions are met at all times:

1. All data related to the use of the membrane tanks shall be collected by the carrier. The data shall be sent to the competent authority on request;
2. An evaluation report shall be sent each year to the UNECE secretariat for information of the Administrative Committee.

The evaluation report shall contain at least information on the following:

- (a) operational data (e.g. temperature and pressure inside the tank);
- (b) abnormalities, repairs and modifications to the tank;
- (c) inspection report by the classification society which classed the vessel.

Annex II

Further Report to the "Bunker vessel Argos-GL"



May 2015

1. Introduction

During its meeting in January 2015 the ADN Committee discussed the Report of the meeting of the technical expert group on the Argos-GL bunker vessel (2015/IINF.27). The French company GTT also gave a presentation on the technical aspects of the membrane tank concept, the experiences with these types of tanks and its track record.

Several delegations had additional questions on the technical and safety aspects of the proposed vessel and the Membrane tanks. The delegation of the Netherlands was requested to put in writing the oral replies and explanations provided during the January session in a document.

The topics addressed during the January session involved:

- a. the stability of the vessel
- b. the consequences of possible interference of LNG and gas oil in case of loss of containment,
- c. the use of large tanks and the calculations done on them by the class society,
- d. the integrity of the tank;
- e. sloshing effects partly filling of the cargo tanks; .

In paragraph 2 a general introduction to the project. Paragraph 3 contains additional information on the topics above.

2. General Introduction

Description

Argos Bunkering B.V. in Rotterdam is considering the building of the Bunker vessel 'Argos-GL'.

The ship is designed for bunkering both seagoing vessels and inland waterway vessels, of either regular fuel oil or LNG. The working area of this ship is mainly in ARA (Amsterdam, Rotterdam, Antwerp) ports.

The 'Argos-GL' is a type G tanker which will be built for the carriage of LNG and diesel.

The vessel is designed as an inland waterway Type G tanker, according the ADN 2015, the Rhine Vessels Inspection Regulations (RVIR), and the Lloyd's Register Rules and Regulations for Inland Waterway Ships.

The ship will be equipped with four tanks of 380m³ for the carriage of diesel and two cargo tanks of 935m³ for the carriage of LNG. As the LNG tanks exceed 380m³ the ship will be build according to the requirements of ADN 9.3.4.

Attached is the general arrangement plan of the vessel (Appendix 1). These classification society involved in this project is Lloyds Register.

Dimensions

The main dimensions of the ship are:

- Length 110 meters
- With 13,5 meters

The following volumes are on this ship available for bunker operations:

Gasoil 4 tanks of 380 m³ total 1520 m³ (volume 100%)

LNG cargo 2 tanks of 935 m³ total 1870 m³ (volume 100%)

Construction

The ship is divided into the following compartments:

Forepeak - generator room - **cofferdam** – gas storage tank room – **cofferdam** – gasoil cargo tank 1 (PS & SB) – **cofferdam** - LNG cargo tank 1 – **cofferdam** – LNG cofferdam 2 – **cofferdam** – gasoil cargo tank 2 (PS & SB) – **cofferdam** – tanks – aft engine room and PS and SB thruster rooms– aft peak.

As tanks are used larger than 380m³ the ship is designed with an additional double side construction ("Schelde huid") to protect the ship for external impact.

With the use of this many cofferdams not only the cargo zone is separated from the fore- and aft ship, but also the LNG cargo tanks are separated from the gasoil tanks. All cofferdams can be flooded with water.

Propulsion

Three LNG-electric generators are installed for the ships' propulsion and power generation. For LNG propulsion a LNG tank of 40 m³ (volume 100%) is installed. In a separate engine room in the aft ship a diesel generator is installed for back-up power.

The maximum movability of this ship will be handled by, 2 L drives (650 kW each) in the after ship and 1 channel bow thruster (500 kW). Detail description and drawings of the LNG propulsion system are included in the HAZID report of Lloyd's Register, report number 50102448-R01, date 29-4-2014.

For the LNG propulsion the ship complies with the Lloyd's Register Rules and Regulations for Natural Gas Fuelled Ships (2014), and the draft Chapter 8b of the RVIR. A recommendation for the use of LNG as fuel has been granted by the Central Commission for Navigation on the Rhine in September 2014 (Recommendation 19/2014 dated 9-9-2014).

3. Membrane Tanks

In the ADN2015 it is allowed to carry LNG by inland vessel using a regular pressure tank.

However, the proposal includes the use of membrane type Mark III for the carriage of LNG.

This type of tank is pressure less, and consist of a layer of plywood, 300 mm of glass reinforced poly-urethane foam, a layer of reinforced aluminum foil, a second layer of 100 mm glass reinforced poly-urethane foam, and a layer of 1.2 mm stainless steel. Appendix 2 contains general information on the way the tanks are constructed.

Main difference to the carriage in a regular pressure tank is the reliquidfaction of the LNG on board the vessel. The boil off of the LNG is extracted from the cargo tank, made liquid again and pumped back into the tank. Due to this, the tank is almost pressure less.

In case of ARGOS GL, the reliquefaction plant is as follows:

- 4 units are fitted, operating in parallel;
- each unit is capable of treating 50% of the design BOG, so a total of 2 x 100% of design BOG;
- therefore, the performance of the system will be sufficient even after a double equipment failure; it should be noted that usually a single failure-proof system is considered as sufficient for safety;
- the ship is equipped with an emergency diesel generator independent from LNG fuel part of the installation ensuring energy for reliquefaction plant;
- the system has been approved by LR for this project.

These tanks and it's additional equipment will be delivered by the French company GTT. This type of tank was developed in the 1960s and has been installed on hundreds of seagoing LNG tankers since (Attachment 2, Membrane type Mark III overview). These tanks comply with the relevant class rules of Lloyds Register.

No cold transfer

The insulation by the two layers of foam is such that this has no effect on the type of steel used for the ships' structure. The heat transfer from the cargo to the ships' structure has been calculated by GTT and approved by Lloyd's Register.

As the use of these tanks is new for an inland waterway vessel and the type approval is based on seagoing ships, the requirements of the IMO IGC Code has been used as far as useful on an inland waterway vessel. Some parts of the IGC Code however aren't applicable on inland waterway vessels, such as the requirement for partly loaded tanks. On seagoing vessels these requirements make sense due to the occurrence of sloshing in these large tanks. Sloshing however doesn't occur on inland waterway vessels.

During the ships' operations the tanks aren't usually not completely emptied to keep them cold. Only for maintenance or surveys the tanks will be emptied according a procedure as described by GTT. The cooling down of the tanks at the first cargo intake or after a survey will also be done according a procedure from the tank manufacturer.

The tanks can't be considered as being independent from a strength point of view as they needed to be supported by the ships' steel structure. They are considered to be independent for temperature aspects. The tanks can't be considered as being pressure tanks according the ADN as the pressure will not exceed 70 kPa.

As the tanks are placed inside the double hull of the vessel the risk of being damaged by a collision is limited. However, due to the size of the tanks the whole vessel needs to comply with the requirements of ADN 9.3.4. The vessel isn't only equipped with a patented 'Schelde-huid', but also the double hull is 1065 mm, which is more than is needed according legislation.

The calculations according the requirements of ADN 9.3.4 have been made and have showed that the inner hull of the vessel will not be damaged until leakage. The membrane tanks have sufficient flexibility to withstand the deformation of the inner hull of the vessel due to the calculated collisions. So it can be concluded that the risk of leakage due to a collision isn't worse as on a vessel with conventional gas tanks.

Advantages to pressure tanks

From a safety point of view, as opposed to pressurized tank, this means:

- No risk of BLEVE (Boiling Liquid Expanding Vapour Explosion);
- No jet fire;
- Limited amount of spill and reduced dispersion range in case of a hypothetical catastrophic containment failure, as the leaking flowrate would be purely generated by gravity instead of pressure.

4. Remaining topics

During its meeting in January 2015 the ADN Committee discussed the Report of the meeting of the technical expert group on the Argos-GL bunker vessel (2015/INF.27). The French company GTT also gave a presentation on the technical aspects of the membrane tank concept, the experiences with these types of tanks and its track record.

Several delegations had additional questions on the technical and safety aspects of the proposed vessel and the Membrane tanks. The delegation of the Netherlands was requested to put in writing the oral replies and explanations provided during the January session in a document.

The topics addressed during the January session involved:

- a. the stability of the vessel

- b. the consequences of possible interference of LNG and gas oil in case of loss of containment,
- c. the use of large tanks and the calculations done on them by the class society,
- d. the integrity of the tank;
- e. sloshing effects partly filling of the cargo tanks;.

These topics are addressed below.

a. the stability of the vessel

When entering service the vessel has of course to comply fully with the current ADN regulations on intact and leak stability according to ADN 9.3.2.13, 9.3.2.14 and 9.3.2.15. A loading computer will be on board. Appendix 3 provides a detailed stability booklet on the vessel. This includes the stability in both loaded and unloaded conditions, for all tanks (both gas oil and LNG) and all stages in between.

The booklet is – as usual practice – a preliminary version. The final version will be drafted when the vessel is build, and practical test on the actual vessel can be executed.

b. the consequences of possible interference of LNG and gas oil in case of loss of containment & effects of release of large amounts of LNG on the water surface

Appendix 4 provides a study done by the RIVM (Dutch National Institute of Public Health and the Environment). The RIVM identifies no specific in case the LNG would come into contact with gas oil. No chemical reaction will occur.

The release of (large) amounts of LNG on the surface of the water will lead to more “Rapid phase transitions” i.c. bobbles of LNG evaporating into the air. These effects are expected – also in case of a largo spill – to be highly localized to the cargo tank breach. The further away from the breach, the thinner the layer of LNG on the water surface and the faster the process of evaporation.

c. the use of large tanks/ crashworthy side structure

Type G vessels has to comply with the building requirements in ADN 9.3.1. When the vessel is in compliance with these requirements the size of the cargo tank is maximized to 380m³.

Larger tank to a maximum of 1.000 m³ are allowed, but it that case the vessel has to be build with a “crashworthy side structure”. This is a hull structure which is capable to withstand an impact which is far greater than for regular type G vessel. ADN 9.3.4 provides extensive provisions how this has to be proven.

ADN 9.3.4.3.1 describes in detail the procedure to be followed for this calculation. This procedure contains of 13 steps.

Appendix 5 provides the calculation, based on the 13 steps, done by Damen Shipyards.

d. the integrity of the tank

Two issues are addressed specifically: fatigue and the resistance of the tank to deformation caused by external impact. Both these issues are addressed in Appendix 6.

Fatigue

The membrane system itself plus load standing associated elements are designed and validated for fatigue:

- in extreme conditions: 40 years of operation worldwide including in North Atlantic Winter Conditions
- in addition, consideration of 2,000 full thermal cycles (from ambient to -163°C temperature). These fatigue calculations are done considering a combination of the following loads
 - Hull bending moment
 - Cargo pressure
 - Thermal gradient.

Deformation

The GTT membrane containment systems have a great flexibility to withstand the large deformations of the tank structure. For Mark III system, the primary barrier is folded corrugated stainless steel, 1.2mm thick.

Tests have been performed at ambient temperature and cryogenic temperature: it is possible to totally unfold primary membrane without any crack apparition. Tightness of primary membrane is ensured under important deformation: the maximum transverse out of plane of tank structure is 150 mm/m.

The calculations according to the requirements of ADN 9.3.4 have been made and have showed that the damage of the inner hull of the vessel will be limited, so that the transverse deformation is less that the above limit, and no leakage will occur. The membrane tanks have sufficient flexibility to withstand the deformation of the inner hull of the vessel due to the calculated collisions

The membrane tanks have been tested on the possibility of being ruptured during collision. The way the membrane is fixed to the vessels structure allows for flexible tanks, which are to a large extent resisted to deformation. In addition, in case the tank indeed would get ruptured it could be considered safer than a pressure tank. In comparison to a regular type G tank the pressure inside the membrane tank is much lower. After a rupture there is no high pressure gas vapor release by the tank.

e. resistance of the membrane to sloshing

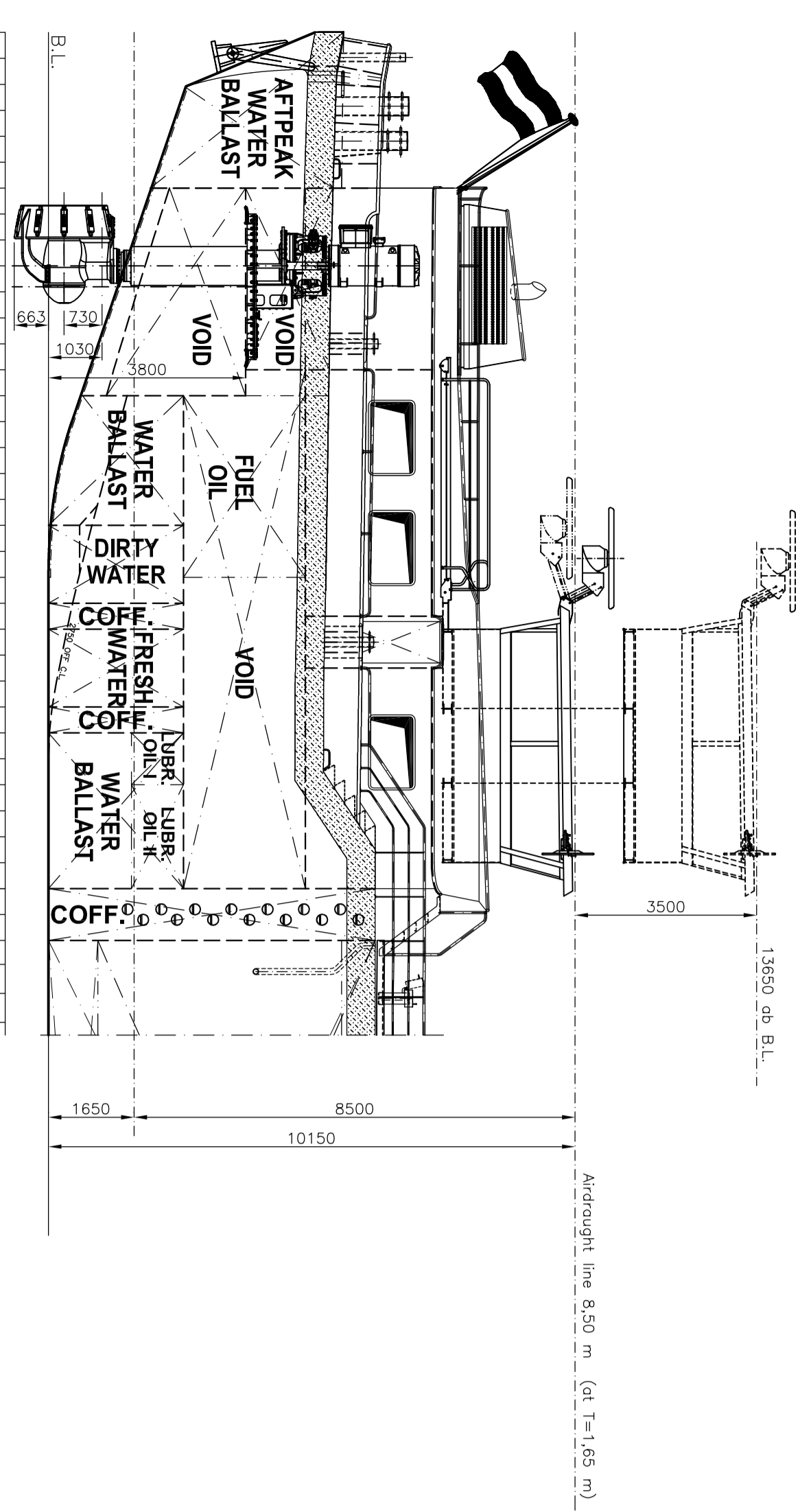
The membrane to be used on the Argos vessel is tested and approved for use on seagoing vessels and the impact of sloshing at sea. Appendix 7 provides coverage of large scale scientific test on the resistance of the membrane Mark III to sloshing.

During the test the Membrane Mark III was tested under very severe circumstances, circumstances only applicable on seagoing vessels. As an alternative for LNG regular water was used. The Mark III Membrane proved to be resisted to sloshing far greater then experienced in inland waterways.

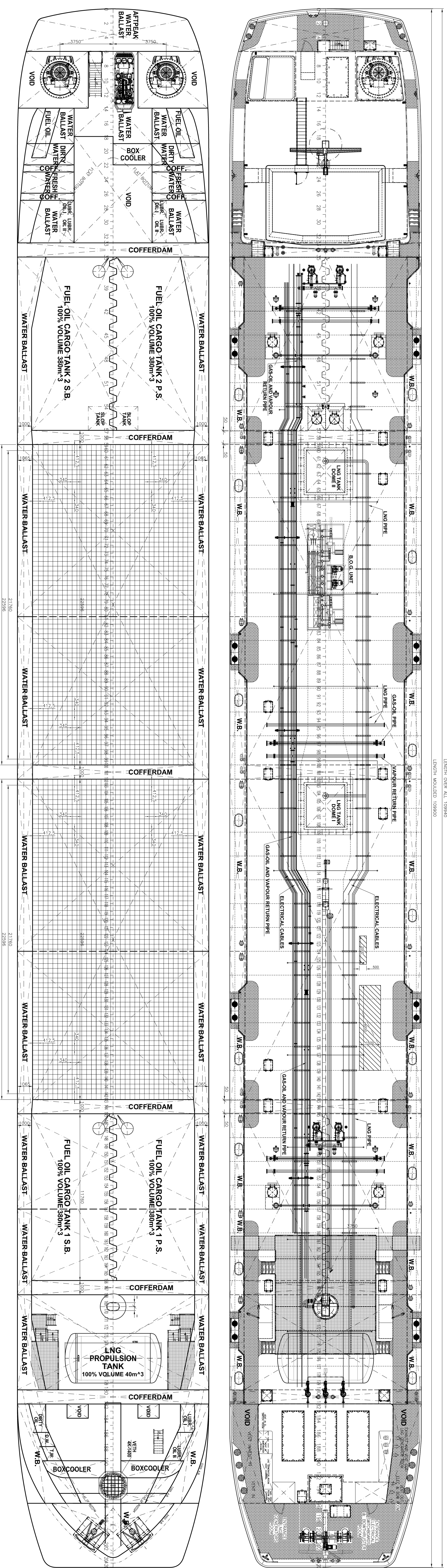
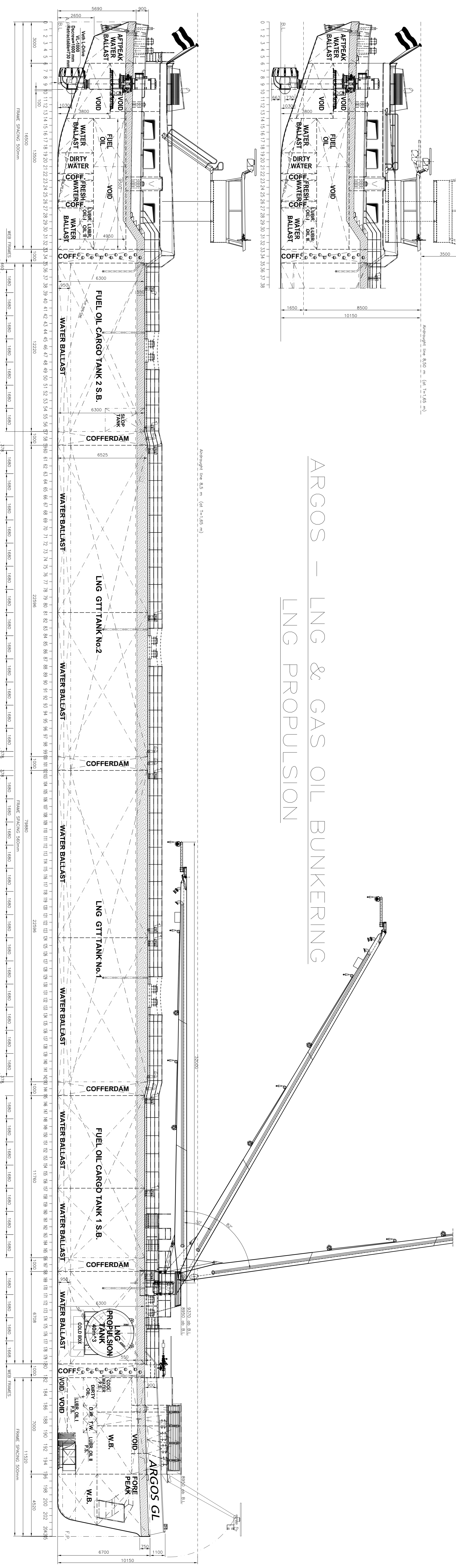
Therefore the possibility of the membrane or the integrity of the tanks being damaged when used on inland vessels on inland waterways is very slim, and less than on type C tankers due to the low density of LNG.

Other sources of interest

<https://www.youtube.com/watch?v= ghACzdfnak>



ARGOS - LNG & GAS OIL BUNKERING LNG PROPULSION



MAIN PARTICULARS

LENGTH O.A. (+2x20mm SHEERSTRAKE)	109.94	m
LENGTH M.I.D.	109.90	m
BREADTH M.I.D.	13.50	m
BREADTH O.A. (+2x20mm SHEERSTRAKE)	13.54	m
DEPTH M.I.D.	6.30/6.325	m
SCANTLING DEPTH	4.50	m
AIR DRAUGHT MAX. (at T=1.65m)	8.50	m

CLASSIFICATION Lloyd's Register

CLASS NOTATION:
 *A1 L1W1 Tanker Type G, p.v. +70 kPa, SG 0.5, in association with a List of Defined Carriage
 Zone 2, IS "D", with the descriptive note: "Gas tanks designed for the carriage of LNG at -165°C"
 Part of the cargo zone built as Tanker Type G, p.v. +50 kPa, SG 1.0, in association with a List of Defined Carriages.

CARGO ARRANGEMENT

LNG GTT BUNKER TANKS	
NUMBER OF LNG BUNKER TANKS	2
VOLUME 100%	935 m ³ x 2 = 1870 m ³
VOLUME 97%	850 m ³ x 2 = 1700 m ³
FUEL OIL BUNKER TANKS	
NUMBER OF FUEL OIL BUNKER TANKS	4
VOLUME 100%	380 m ³ x 4 = 1520 m ³
VOLUME 97%	388 m ³ x 4 = 1547 m ³

REV.	DATE	DRAWN	DESCRIPTION

Copyright © Rommerts Ship Design B.V. All rights reserved. No part thereof may be reproduced, stored, distributed or in any other way made available to the public without the prior written permission of Rommerts Ship Design B.V.
 ROMMERTS SHIP DESIGN
 Aegos Group B.V.

LNG & FUEL OIL BUNKER TANKER - m/s "ARGOS CL"
 GENERAL ARRANGEMENT (GTT TANKS)
 SCALE 1:100
 SHEET 10
 SHEETS 1

DATE: 14.10.2014
 SHEET NO.: 10



Technical Division

**GTT REPORT TO ADN - MEMBRANE CONTAINMENT
SYSTEM FOR LNG**

Report

DT-RPT-001158

Revision : 02




12/06/2015

Page : 1 / 17


Technical Division

**GTT REPORT TO ADN - MEMBRANE CONTAINMENT
SYSTEM FOR LNG**

Report

02	Update following Remarks by the German Delegation – Federal Ministry of Transport and Digital Infrastructure 13/05/2015	12/06/2015	 MAL	 CAB	 ARB
01	First issue	20/02/2015			
REVISION	DESCRIPTION	DATE DD/MM/YYYY	BY	CHECKED	APPROVED

document_simple-rev09

	Technical Division	DT-RPT-001158 Revision : 02 12/06/2015 Page : 2 / 17
	GTT REPORT TO ADN - MEMBRANE CONTAINMENT SYSTEM FOR LNG	
	Report	

CONTENTS

1. ABBREVIATIONS	5
2. INTRODUCTION	5
3. MEMBRANE DESIGN	6
3.1. INTEGRATED TANKS.....	6
3.2. ATMOSPHERIC TANKS	7
3.3. INSULATION MATERIALS.....	8
3.4. STRUCTURAL VALIDATION	8
3.4.1. FATIGUE.....	8
3.4.2. STRENGTH ASSESSMENT	8
3.4.3. SLOSHING.....	9
3.4.4. CONCLUSION TO STRUCTURAL VALIDATION	13
4. ARGOS GL GENERAL ARRANGEMENT AND SPECIFICITIES	13
4.1. LNG PROPULSION.....	13
4.2. SHIP COMPARTMENTS.....	13
4.3. STABILITY	14
4.4. PROTECTION TO SIDE COLLISION RISK.....	15
4.5. LNG PUMPS.....	16
4.6. RELIQUEFACTION	16
APPENDIX 1. GENERAL ARRANGEMENT	17



	Technical Division	DT-RPT-001158 Revision : 02 12/06/2015 Page : 3 / 17
	GTT REPORT TO ADN - MEMBRANE CONTAINMENT SYSTEM FOR LNG	
	Report	

TABLE OF ILLUSTRATIONS

Figure 1: IMO classification of LNG Containment System.....	6
Figure 2: Tank volume optimisation according to LNG containment system.....	7
Figure 3: 3D view of two LNG tanks at small scale.....	11
Figure 4: Picture of the 6 degree of freedom test rig	11
Figure 5: Experimental and numerical assessment of the CS.....	11
Figure 6: Probability of failure definition	12
Figure 7: ARGOS GL General Arrangement	13
Figure 8: DAMEN "Schelde-huid" structure, intact and deformed	15
Figure 9: Corrugated stainless steel primary membrane	15

REFERENCE DOCUMENTS

- [1] SIGTTO - Gas concentrations in the insulation spaces of membrane LNG carriers date March 2007
- [2] ISOPE - Reliability-based Methodology for Sloshing Assessment of Membrane LNG Vessels, E. Gervaise and al. ISOPE 2009
- [3] DAMEN - Royal Schelde Shipyard - Construction aspects for the Schelde Y-shape crashworthy hull structure, Bob van de Graaf
- [4] TU Delft - Ship collision, Joep Broekhuijzen , Flushing, Feb. 2003
- [5] ARGOS .b.v. - Gasoil/LNG bunker ship project - update
- [6] United Nations Economic and Social Council, Working Party on the Transport of Dangerous Goods - Joint Meeting of the RID Committee of Experts and the Working Party on the Transport of Dangerous Goods; Bern 17-21 March 2014 / Tanks.
ref.: ECE/TRANS/WP.15/AC.1/2014/24
- [7] Economic Commission for Europe , Inland Transport Committee, Working Party on the Transport of Dangerous Goods - Joint Meeting of Experts on the Regulation annexed to the European Agreement concerning the International Carriage of Dangerous Goods by Inland Waterways (ADN); Geneva, 26-30 January 2015 /
Report of the meeting of the informal Expert Group "Bunker vessel Argos-GL
ref.: INF 27 -

	Technical Division	DT-RPT-001158 Revision : 02 12/06/2015 Page : 4 / 17
	GTT REPORT TO ADN - MEMBRANE CONTAINMENT SYSTEM FOR LNG	
	Report	

EXECUTIVE SUMMARY

At present, LNG fuel transportation with inland vessels has only been allowed in pressurized, cylindrical tanks. The GTT membrane tank system offers several advantages but does not comply with some of the requirements of the ADN rules.

The membrane technology is the most used LNG cargo containment system for seagoing vessels, integrated into the ship structure. It is operated in near atmospheric conditions with advantages in case of a hypothetical failure and it features a proven, redundant tightness and insulation system.

Its robustness has been thoroughly tested with detailed investigations including very extensive model testing of the sloshing phenomenon, allowing to determine precisely the loads applied on the insulation in all conditions. However, the relevance of sloshing for inland vessels is substantially lower than for seagoing vessels.

The ARGOS GL bunker vessel is the very first application of the membrane system to inland vessels, adequately integrated in the vessel design, structure and systems in order to provide a safe and efficient storage solution, approved by the Classification Society.



Technical Division

**GTT REPORT TO ADN - MEMBRANE CONTAINMENT
SYSTEM FOR LNG**

Report

DT-RPT-001158

Revision : 02

12/06/2015

Page : 5 / 17

1. ABBREVIATIONS

ADN: European Agreement concerning the International Carriage of Dangerous Goods by Inland Waterways

Bara: bar absolute

Barg: bar gauge (above atmospheric pressure)

BLEVE: Boiling Liquid Expanding Vapour Explosion

BOG: Boil-Off Gas

CFD: Computerized Fluid Dynamics

CS: Containment System

EPF: Exceedance Probability Function

FEM: Finite Element Model

GTT: Gaztransport & Technigaz

IGC Code: International Code for the Construction and Equipment of Ships Carrying Liquefied Gases in Bulk

IMO: International Maritime Organisation

ISOPE: The International Society of Offshore and Polar Engineers

LNG: Liquefied Natural Gas

LR: Lloyd's Register of Shipping

NG: Natural Gas (at vapour stage)

PDF: Probability Density Function

PUF: PolyUrethane Foam

PS: Portside

R-PUF: Reinforced PolyUrethane Foam

RVIR: Rhine Vessels Inspection Regulations

SB: Starboard

SIGGTO: Society of International Gas Tanker and Terminal Operators Ltd

2. INTRODUCTION

With the implementation of new pollution regulation and the probable long term increase of fuel cost, the gas propulsion becomes a competitive alternative to the standard HFO fuelled Ship. The following years will see the development of LNG fuelled Ship designs. These Ships will need to bunker. Shipping and LNG distribution industries are currently developing LNG bunker Ships.

In this context, ARGOS as main bunker fuel operator wants to develop its activities in LNG bunkering. Thus, the ARGOS GL project is currently under development. This ship is designed for bunkering both seagoing vessels and inland waterway vessels, but can also be used for delivering LNG to bunkering stations.

The vessel is designed as an inland waterway Type G tanker, according to ADN 2015, to the Rhine Vessels Inspection Regulations (RVIR) and to the Lloyd's Register Rules and Regulations for Inland Waterway Ships. The working area of this ship is mainly Amsterdam, Rotterdam and Antwerp ports. This ship will be able to bunker as well Gasoil (four tanks of 380 m³ each) and LNG (two tanks of 935 m³ each). It will be the first combined LNG / Gasoil bunker vessel. This LNG bunker ship is not a standalone item, but an opportunity for the total chain.

This development is included in LNG Masterplan for Rhine-Main-Danube and will be co-financed by the European Union. This project is under development since beginning of 2013. The main next target dates are the followings:

- 2
- July 2015: signing contracts, beginning of hull construction in Romania
 - February 2016: arriving of hull in the Netherlands for outfitting
 - June 2016: tests and power up LNG gas generator systems
 - July 2016: LNG cargo system tests finalisation
 - August 2016: LR approvals and ship delivery

The technology chosen for LNG containment system is Mark III Flex membrane system developed by GTT.

GTT is a world leader in the LNGC market, thanks to its membrane containment system. The company is continuously adapting its technologies to meet new challenges. GTT's membrane technology is recognised by all industry players thanks to its compactness, reduced construction time, cost effectiveness, etc. These advantages, together with the large network of Shipyards proposing GTT systems have allowed GTT's market share to continuously increase.

This document aims at giving technical justification of the safety of the membrane system for inland waterway navigation.

3. MEMBRANE DESIGN

IMO classification of LNG containment system considers separately independent tanks from integrated tanks as explained in the following figure:

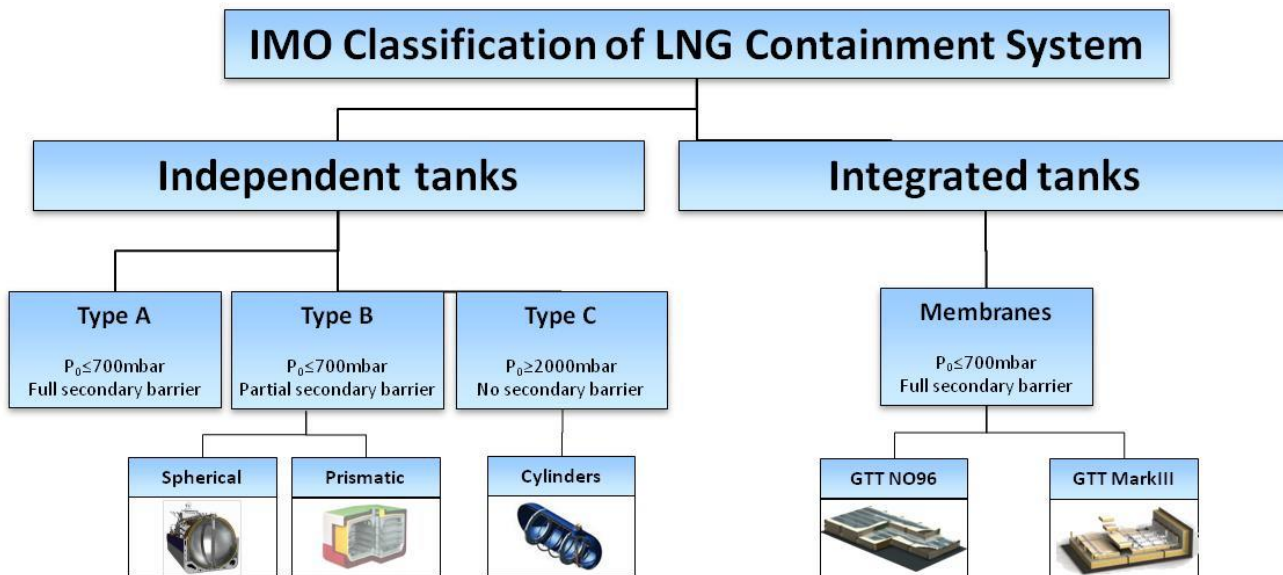


Figure 1: IMO classification of LNG Containment System

Membrane systems have two main characteristics:

- Integrated system: the tank is integrated into the ship structure;
- "Atmospheric" system: the pressure is maintained under 700 mbarg.

All GTT LNG containment systems are fully validated by the major Classification Societies including Lloyds Register which is in charge of the classification of ARGOS GL ship.

3.1. INTEGRATED TANKS

The tank is integrated to the ship: the insulation is supported by the adjacent hull structure. The functions of thermal insulation and tightness are realised by two separated components. For Mark III GTT containment system, the components are the following:

- Insulation is achieved by: R-PUF: Polyurethane Foam (PUF) reinforced (R) by glass fibre;
- Tightness is ensured by two barriers: Triplex – composite: two glass clothes and aluminium foil in between (so-called secondary barrier) - and Stainless steel 304L thickness 1.2mm (so-called primary barrier).

This separation of function allows optimizing the weight of the solution. GTT membrane systems are light (around 70 kg/m²). Thus, for the same cargo capacity, the ship lightweight is reduced with membrane system.

This LNG containment system does not create any particular points or stress concentrations on the ship structure because it is integrated: the loads are transferred in a uniform way to the hull structure. No thermal loads are transferred to the ship structure.

Because the system is integrated, no loss of space is induced by inspection room between hull structure and insulation. For ARGOS GL project, LNG cargo capacity is increased by 55,8% with membrane containment system compared to type C system as illustrated in the following figures:

Conceptual design: Type C LNG cargo tanks

$$4 \times 300 \text{ m}^3 = 1\,200 \text{ m}^3$$

Final design: Membrane LNG cargo tanks

$$2 \times 935 \text{ m}^3 = 1\,870 \text{ m}^3$$

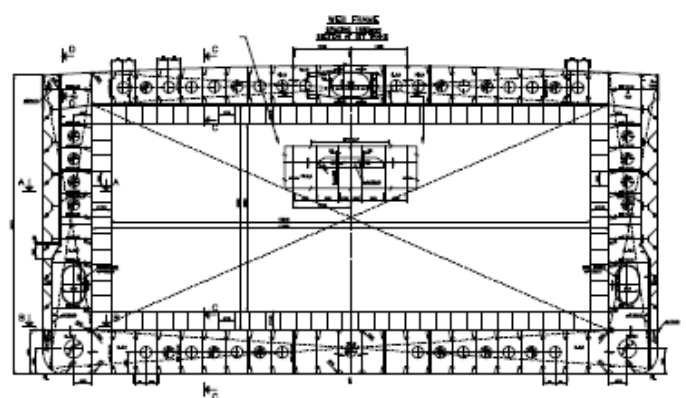
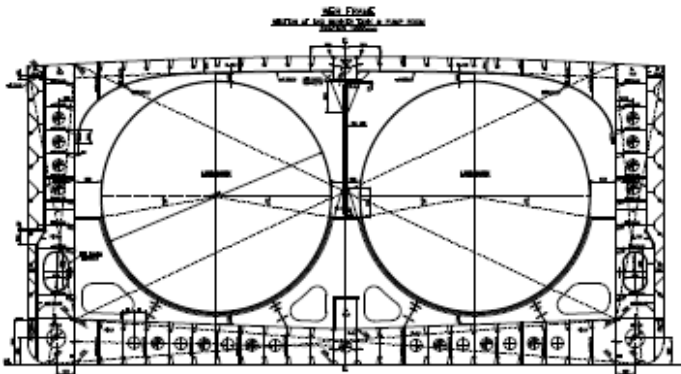


Figure 2: Tank volume optimisation according to LNG containment system

In addition type C tank cannot be filled up to the same level than the membrane tanks because of the higher pressure setting of their safety valves.

2 3.2. ATMOSPHERIC TANKS

According to IMO classification, membrane tanks are atmospheric tanks. The pressure is controlled under 700 mbarg. Pressure is permanently monitored inside the tank and controlled between 50 and 150 mbarg as the LNG is kept as cold as possible.

From a safety point of view and opposed to pressurized tank, this means:

- Limited amount of spill and reduced dispersion range in case of a hypothetic catastrophic containment failure, as the leaking flowrate would be purely generated by gravity instead of pressure. No jets of cryogenic liquid or jets of burning gas at high pressure (jet fire) are possible.

The total inventory (450 t of liquid) would not leak at once or in a short period of time. If the leak is not important, the LNG will instantaneously vaporize forming a small vapour cloud which will disperse quickly because NG is lighter than air. If the leak is more important, LNG will create a pool with NG evaporation.


Outside, in a non-enclosed area, if proportion of NG is 5 to 15% in the air and an ignition source causes inflammation of gas. No explosion phenomena will occur.

- No risk of BLEVE (Boiling Liquid Expanding Vapour Explosion);

In membrane tanks, as well as in pressurized tanks (IMO type C), LNG is boiling: liquid and gas are at the equilibrium.

When LNG is cold (meaning at the equilibrium at atmospheric pressure (1 atm)), more energy is needed to vaporize LNG than when LNG is pressurized. Thus, for a membrane tank, more time is needed to vaporize LNG and reached the tank pressure setting point than for type C tank.

BLEVE phenomena occurs when LNG suddenly vaporizes due to a very quick depressurization from tank pressure setting (or more) to atmospheric pressure. The vaporization creates an over-pressure which leads to an explosion. In the case of a fire around an LNG tank, pressure increases inside the tank up to the tank pressure setting.

	Technical Division	DT-RPT-001158 Revision : 02 12/06/2015 Page : 8 / 17
	GTT REPORT TO ADN - MEMBRANE CONTAINMENT SYSTEM FOR LNG	
	Report	

BLEVE phenomena more probably occurs when a fire is near a LNG tank increasing heat ingress and vaporization inside the tank and creating defect on the tank leading to rupture.

For a pressurized tank, pressure can go up to 10 barg. In case of tank failure, the LNG suddenly flashes from 11 bara to 1 bara. The expanding vapor generated is the cause of a brutal explosion, which is a BLEVE.

For an atmospheric tank, the LNG would flash from 1.7 bara to 1 bara. Less vapor is generated and no explosion could happen. NG produced will be released by PSV.

3.3. INSULATION MATERIALS

Mark III (and Mark III Flex) containment system is made of plywood, mastic, reinforced polyurethane foam, triplex and stainless steel. The selection of material is done according to classification society and GTT cooperation.

Testing methods are defined, after in-house GTT laboratory tests.

For each material used, a dedicated material specification is issued including explanation on performance characteristics. Suppliers are approved by GTT and classification society.

The main requirements are the following:

- To withstand LNG temperature (-163°C) and warming up temperature (up to 60°C);
- To be chemically compatible with LNG, water, sea water and nitrogen;
- To withstand dynamic pressure loads due to LNG motions inside the tank;
- To withstand pressure variations from - 800 mbarg to 3 barg.

All the insulation materials including R-PUF are enclosed between hull structure and primary barrier made of 1,2 mm thick Stainless steel sheet. This primary barrier is in direct contact with LNG. The fire risk within these spaces is null since there is no ignition source and no oxygen in the insulation spaces and inside the tank itself. So this situation is totally different from externally insulated tank of road trucks which may be exposed to ignition source in the presence of ambient air / oxygen - see ref. [6]

In case of fire, the heat ingress will increase and the BOG flow as well. The pressure safety valves are designed according to this fire case. In case of fire, the integrity of the tank is ensured.

Moreover, the insulation spaces are permanently inerted by nitrogen. The pressure is permanently controlled ensuring that no air ingress is possible. The insulation spaces are continuously monitored for detection of hydrocarbon traces.

For more explanations and risk assessment about the nitrogen system and insulation spaces of GTT membrane system, please refer to the document from SIGGTO *Gas concentrations in the insulation spaces of membrane LNG carriers* dated March 2007 - ref. [1]

3.4. STRUCTURAL VALIDATION

3.4.1. FATIGUE


The membrane system itself plus load standing associated elements are designed and validated for fatigue:

- in extreme conditions: 40 years of operation worldwide including in North Atlantic Winter Conditions
- in addition, consideration of 2,000 full thermal cycles (from ambient to -163°C temperature).

This fatigue calculations are done considering a combination of the following loads:

- Hull bending moment
- Cargo pressure
- Thermal gradient.

3.4.2. STRENGTH ASSESSMENT

	Technical Division	DT-RPT-001158 Revision : 02 12/06/2015 Page : 9 / 17
	GTT REPORT TO ADN - MEMBRANE CONTAINMENT SYSTEM FOR LNG	
	Report	

The membrane strength assessment combines the loads due to:

- internal cargo pressure;
- external ballast pressure;
- thermal loads;
- ship global and local deflection;
- dynamic loads due to ship motions;
- sloshing loads.

3.4.3. SLOSHING

3.4.3.1. Preamble

This section deals with the sloshing phenomenon in relation with the membrane system, because:

- this issue has been raised repeatedly during previous ADN discussions about the membrane;
- in the past, it has caused some concern in the LNG maritime industry, as opposed to pressurized tank.

However, sloshing does not occur on inland waterway vessels as discussed in section 3.4.3.6 below. Tanks are too small and ship motions are reduced. This load case is not to be considered for ARGOS GL project.

3.4.3.2. Nature of sloshing and GTT experience

Sloshing is the result of global cargo motions within a partially filled tank resulting from ship motions. When ship motions become significant, waves are generated inside the tank and lead to liquid impacts when they hit the tank walls. This local and dynamic phenomenon has no impact on the general stability of the ship but only with ship structure and containment system. Anyhow, the stability of any ship - inland or seagoing - is ensured by the compliance of the compulsory Stability Booklet with IMO and ADN regulations as well as Classification Societies rules for ships carrying a liquid cargo, including the free surface effect.

Sloshing is a resonance phenomenon, it means that the frequency of the impacts and their magnitude will tend to increase when the liquid natural periods coincides with the natural period of the excitation source (the ship motions in relation with the sea state and heading).

Sloshing is by nature a non-deterministic phenomenon. While the global ship motions are predictable, the magnitude, the location and the instant of a sloshing impact are rather unpredictable. Sloshing is hence studied through statistical approaches based on the description of the statistical pressure distributions and the frequency of the impacts.

GTT has developed a unique expertise in:

- assessing the impact of sloshing on the membrane system and its components;
- determining the areas of the tank where membrane reinforcement is required;
- designing suitably reinforced membrane components.

The methodology used for validation can be divided into three parts:


- 1) The sloshing load evaluation;
- 2) The Containment System strength evaluation;
- 3) The final strength assessment which compares both the loads and the containment strength.

The resistance of insulation material in cryogenic conditions (vs. ambient temperature) is tested separately in depth by GTT:

- in its own material laboratory, equipped with state-of-the art equipment, with a long experience considered as a worldwide reference;
- through measurements on board seagoing vessels in operation.

3.4.3.3. Loads evaluation

The sloshing loads are derived from laboratory tests at small scale (1/40).

	Technical Division	DT-RPT-001158 Revision : 02 12/06/2015 Page : 10 / 17
	GTT REPORT TO ADN - MEMBRANE CONTAINMENT SYSTEM FOR LNG	
	Report	

The tests consist in shaking with pre-determined motions a model tank filled with water and a specific gas mixture at ambient conditions in order to measure representative pressures of the real scale, at various locations of the model tank and for a set of conditions (filling level, heading, sea state).

Tank motion excitations at small scale are derived from the motions at full scale calculated through numerical simulations by means of the Froude similitude.

The model tanks made of PMMA (Plexiglas) represent the tanks shape at model scale:

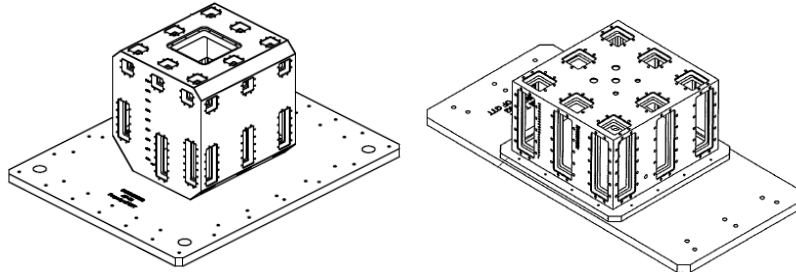


Figure 3: 3D view of two LNG tanks at small scale

Six (6) degrees of freedom motion generator called HEXAPOD is being used as a routine for the model tests (see Figure 4). It is based on the "Stewart Platform" principle, with six mechanical jacks and their associated electric-driven motors.



Figure 4: Picture of the 6 degree of freedom test rig

A long-term approach is considered for the sloshing study to determine the maximum expected sloshing loads on the containment system. This approach integrates the sloshing response of all the sea states the vessel will potentially face during her life. It is applied by determining short-term probability density functions (PDF) obtained at the critical filling level for a large set of sea states and headings. These PDFs are then combined, taking occurrence frequency of each sea state and heading into account, to generate the long-term exceedance probability function (EPF).

3.4.3.4. Containment System strength evaluation

The Containment System (CS) is submitted to both thermal (cryogenic conditions) and mechanical (dynamic loads) effects. The modeling of these effects in order to apprehend them from an experimental approach is very challenging.

In-service CS strengths are consequently determined through two complementary approaches:

- Experimental: GTT's finite elements models are calibrated with several kinds of experimental results, like static compression of the CS at ambient temperature or subsystems experiments under dynamic and temperature conditions;
- Numerical: The numerical models which have been validated during the previous step are used to determine the in-service capacities of the CS.

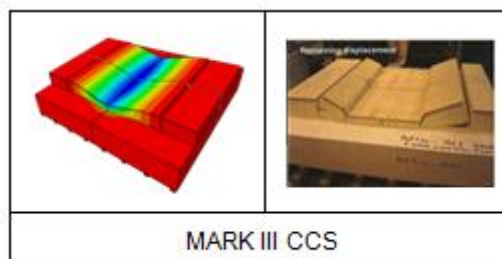


Figure 5: Experimental and numerical assessment of the CS

3.4.3.5. Reliability approach

A reliability method is proposed. Probabilities of failure are calculated for each failure mode of the CS and compared with GTT design acceptance criteria. GTT design acceptance criteria have been determined taking into account the type of CS and the consequences of a failure of one (or several) of its components.

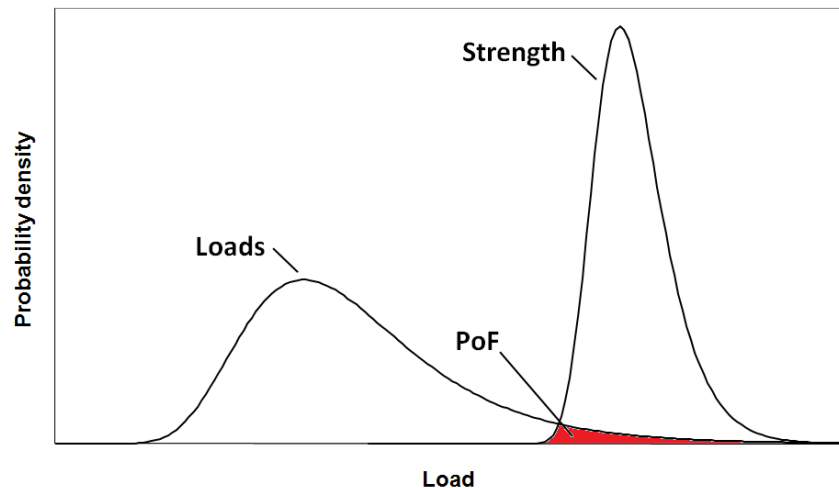


Figure 6: Probability of failure definition

The limit conditions considered for Mark III is the permanent crushing of the foam.

It can be noticed that the sloshing load evaluation is only based on model tests. Indeed, even if CFD simulations can give a good idea of the global liquid flow, today's computers and today's CFD programs are not powerful enough to model all the phenomena occurring during an impact and predict the sloshing pressure accurately enough.

From a liquid motion point-of-view, the overall design can be optimized by:

- modifying the tank shape;
- improving containment strength;
- shifting from one-row of tanks to two-row tanks design.

GTT has developed technical solutions to be able to adapt the containment system to the loads it copes with, even in very severe conditions.

For more details on this subject please refer to: *Reliability-based Methodology for Sloshing Assessment of Membrane LNG Vessels*, - ref. [2]

3.4.3.6. Inland waterway specificities

Seagoing vessels are concerned by sloshing loads because of the tank size allowing wave formation and sea states with large waves creating important ship motions.

Inland waterway vessels are not concerned by sloshing: tank sizes are relatively small (limited mass of liquid moving) and ship structure is anyway not designed to sustain wave patterns generating important ship motion.

Possible LNG accelerations and impacts on board inland vessels are of another nature and amplitude:

- in case of collision with another vessel or a fixed obstruction in the river (e.g. a bridge column), the liquid acceleration will not generate any fatigue stress due to repeated loads. According to GTT calculations, the risk of damaging the containment system by on shock is negligible (multiplied by 10^{-6}) compared to the risk of sloshing in North Atlantic condition navigation. In case of collision, the tank might be probably damaged by the impact itself and not by the wave caused by this impact. This point is specifically addressed by naval architect when calculating the scantling of ship structure according to applicable class rules (about the tank structure reinforcement, please refer to section 4.4);

- the liquid accelerations inside the tanks due to the turning of the vessel e.g. in a Rhine turn are much lower than the accelerations to be considered according to the maritime Classification Rules; typically 0.7g transverse - 0.4g vertical.

3.4.4. CONCLUSION TO STRUCTURAL VALIDATION

All the causes of the following loads on membrane have to be taken into account for the design of the ship whatever the LNG containment system chosen. It has to be done according to class rules and ADN regulation.

- Local and global deformations of the tank structure and internal and external pressure impact the scantling of the ship.
- Thermal loads imply a specific choice of steel grade for the tank structure.
- Free surface has an impact on the calculation of ship stability.

It is worth mentioning that after 50 years of operations not a single failure of the primary membrane has occurred, even after a few significant accidents and frequent rough sea conditions.

4. ARGOS GL GENERAL ARRANGEMENT AND SPECIFICITIES

As explained in introduction, this ship will be able to load Gasoil (four tanks of 380 m³ each) as well as LNG (two tanks of 935 m³ each).

4.1. LNG PROPULSION

Three LNG-electric generators are installed for the ship's propulsion and power generation. In a separate engine room in the aft ship a diesel generator is installed for emergency power. For LNG propulsion a separate LNG fuel tank of 40 m³ (volume 100%) is installed. Type C LNG containment system was chosen here.

LNG propulsion system and LNG cargo system are totally independent by design according to ADN §7.2.4.9. This implies that tank monitoring system, safety equipments, pressure management, piping for LNG fuel and LNG cargo parts are totally independent.

2

4.2. SHIP COMPARTMENTS

The ship is divided into the following compartments:

Forepeak – generator room – cofferdam – LNG fuel storage tank room – cofferdam – Gasoil cargo tank 1 (PS and SB) – cofferdam – LNG cargo tank 1 – cofferdam – LNG cargo tank 2 – cofferdam – Gasoil cargo tank 2 (PS and SB) – cofferdam – tanks – aft engine room and PS and SB thrusters rooms – aft peak.

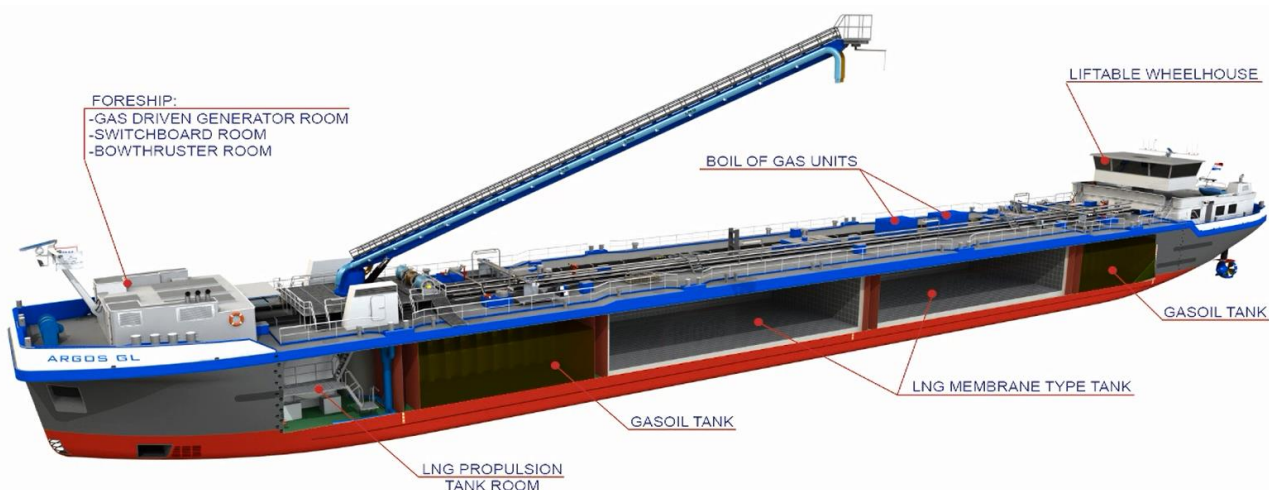



Figure 7: ARGOS GL General Arrangement

	Technical Division	DT-RPT-001158 Revision : 02 12/06/2015 Page : 14 / 17
	GTT REPORT TO ADN - MEMBRANE CONTAINMENT SYSTEM FOR LNG	
	Report	

The General Arrangement of the vessel is shown in APPENDIX 1.

With the use of so many cofferdams, not only the cargo zone is separated from the fore and aft ship but also the LNG cargo tanks are separated from the gasoil tanks. All cofferdams can be inerted in normal operation with nitrogen as a preventive mean to eliminate presence of oxygen. Alternatively, all cofferdams can be flooded with water. Thus, in case of an improbable leakage of a LNG cargo tank or of a gasoil tank, surrounding cofferdams would be flooded in order to avoid any ignition possibility.

Cofferdams are protected against any leak of LNG. By design, the membrane system has two independent liquid tight barriers. The two insulation spaces are permanently monitored by temperature sensors and gas detection.

During the 15 000 tank.years of membrane navigation recorded, no LNG leak in double hull or cofferdam has been experienced.

Interaction of LNG and gasoil can therefore be considered as not possible.

Moreover, **NG** is extracted from the same underground oil well as **the crude oil** from which gasoil is extracted as well. Consequently NG and gasoil are chemically compatible without any risk. Cold NG or LNG in contact with gasoil would just have the physical effect of freezing gasoil creating wax.

In the improbable case of fire in cargo gasoil tank (cargo gasoil tanks are inerted in normal operation by inert gas), no consequences on the LNG membrane tanks will happen (refer to §3.3):

- As already stated above, the cofferdam between both tanks can be inerted as preventive measure or flooded in case of leak detected. The increase of heat ingress in the LNG tank due to a fire would then be very limited.
- BOG flow will increase as well. The pressure safety valves are designed according to this fire case.
- Insulation foam is enclosed between hull structure and primary barrier. No risk of insulation material fire. The insulation keeps its insulation capacity.

4.3. STABILITY

2 The ship fully complies with the stability requirements of the ADN (refer §9.3.1.13.1 to 9.3.15.4).

The LNG will be carried in tanks with a large breadth, but the free surface moment is included in the ship's stability calculations and this does not lead to a large reduction in stability due to the light density of the LNG (around 0.45 t/m³). The gasoil tanks are divided into a PS and SB tank with a bulkhead in between, so their contribution to the free surface moment is limited but has, of course, been taken into account.

4.4. PROTECTION TO SIDE COLLISION RISK

The ship will be built with a double bottom, a double hull and a double deck. Inside this double hull, the membrane tanks will be placed. As the tanks are integrated inside the double hull of the vessel the risk of being damaged by a collision is limited.

1) However, due to the size of the tanks, the whole vessel needs to comply with the requirements of ADN §9.3.4. Thus, the vessel is equipped with a DAMEN patented 'Schelde-huid'. This Y-shaped crashworthy hull structure allows to sustain high impact loads by increasing the energy absorbing capability of the side shell.

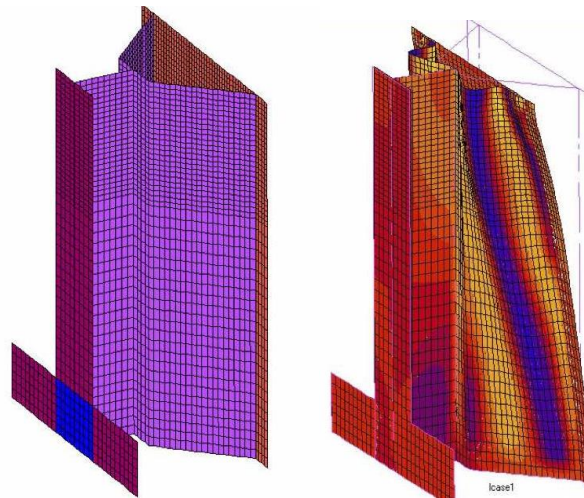


Figure 8: DAMEN "Schelde-huid" structure, intact and deformed

For more details on this crashworthiness structure, please refer to *Construction aspects for the Schelde Y-shape crashworthy hull structure*, ref. [3] and *Ship collision*, ref. [4].

2) The double hull width is 1,065 mm, which is more than required by legislation.

3) Lastly, the GTT membrane containment systems have a great flexibility to withstand the large deformations of the tank structure. For Mark III system, the primary barrier is folded corrugated stainless steel, 1.2mm thick.

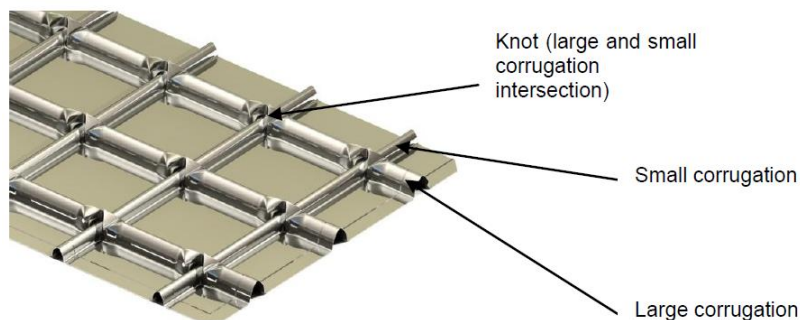



Figure 9: Corrugated stainless steel primary membrane

Tests have been performed at ambient temperature and cryogenic temperature: it is possible to totally unfold primary membrane without any crack apparition. Tightness of primary membrane is ensured under important deformation: the maximum transverse out of plane of tank structure is 150 mm/m

The calculations according to the requirements of ADN §9.3.4 have been made and have showed that the damage of the inner hull of the vessel will be limited, so that the transverse deformation is less that the above limit, and no leakage will occur. The membrane tanks have sufficient flexibility to withstand the deformation of the inner hull of the vessel due to the calculated collisions

	Technical Division	DT-RPT-001158 Revision : 02 12/06/2015 Page : 16 / 17
	GTT REPORT TO ADN - MEMBRANE CONTAINMENT SYSTEM FOR LNG	
	Report	

4.5. LNG PUMPS

Submerged pumps (with electrical motor inside LNG tank) are commonly used in any LNG installation onshore or offshore. Pressure inside tank is above atmospheric pressure ensuring that no oxygen is inside tank. There are no risks of explosion or fire.

ARGOS GL project will use deep well pumps which motor is installed on deck according to ADN requirement §9.3.1.52.1. No electric wire will be inside LNG tank.

4.6. RELIQUEFACTION

Membrane tanks pressure limitation to 0.7 barg requires the installation of a BOG treatment system to be started after a certain time of standstill without gas consumption.

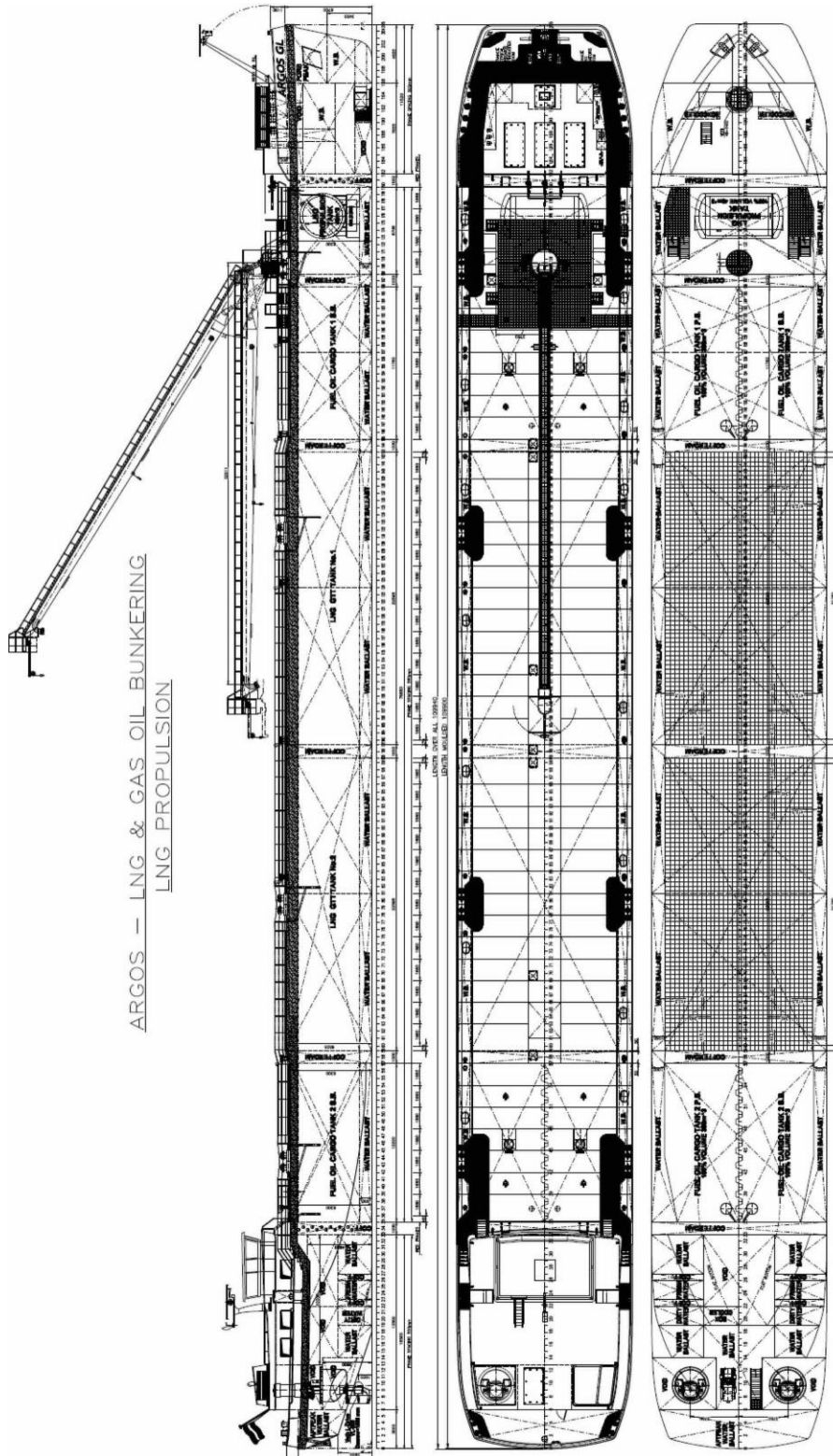
In case of ARGOS GL, BOG is treated by a reliquefaction plant as follows:

- 4 units are fitted, operating in parallel;
- each unit is capable of treating 50% of the design BOG, so a total of 2 x 100% of design BOG;
- therefore, the performance of the system will be sufficient even after a double equipment failure; it should be noted that usually a single failure-proof system is considered as sufficient for safety;
- the ship is equipped with an emergency diesel generator independent from LNG fuel part of the installation ensuring energy for reliquefaction plant;
- the system has been approved by LR for this project.

By design, even in case of failure, the risk to completely lose the reliquefaction function is so low that it can be considered as not possible.



APPENDIX 1. GENERAL ARRANGEMENT



LNG and Fuel Oil Bunker Tanker m.t.s. "Argos GL"
Inland Waterway Tanker type C and G

"Preliminary Stability information Booklets"

Booklet 1 of 1:

- View of Compartments
- Intact Stability calculations
- Loading conditinos

Yard:

Yard no.:

Class: Lloyd's Register

Class reg. no.:

National Authority: ILT

ID no.:

Flag State: NL

Date: 27 January 2015

Document no.:

Produced by:



ROMMERTS
S H I P D E S I G N

Building "Westgate 1"
Scheepmakerij 150
3331 MA Zwijndrecht
The Netherlands
Tel. 0(031) 78 - 744 01 35

PRELIMINARY

Index

Abbreviations & Units.....	3
General	4
Vessel’s Characteristics.....	4
Stability Criteria according “ADN art.9.3.2.13 – 9.3.2.15”	4
Intact Stability criteria tank width > 0.70 B	4
Damage Stability criteria “intermediate stage of flooding”	4
Damage Stability criteria “final stage of flooding”	4
Permeability of damaged compartments.....	4
Hullform.....	5
Bodyplan.....	5
Special Points.....	6
Compartments.....	7
Maximum tank capacities.....	7
Views of compartments.....	10
Hydrostatic particulars	36
Stability Calculation for Loading condition.....	39
Damage Stability.....	39
Intact Stability.....	40
LSW, 98% consumables with WB1 filled.....	40
LSW, 98% consumables, fully ballasted.....	44
LSW, 98% consumables, fully loaded FO and LNG with WB1 filled.....	48
LSW, 98% consumables, 97% FO, 50% LNG with WB1 filled.....	52
LSW, 98% consumables, 50% FO, 50% LNG with WB1 filled.....	56
LSW, 98% consumables, 10% FO, 10% LNG.....	60
LSW, 98% consumables, 50% FO and 50% LNG with additional external moment	64

Abbreviations & Units

Hydrostatic particulars

Trim	Total trim on the perpendiculars; by the stern is negative	[m]
Draught from US keel		[m]
Displacement		[ton]
Immersion		[ton/cm]
Moment change trim	Moment to change the trim 1 cm	[tonm/cm]
LCB from APP	Longitudinal centre of buoyancy measured from APP	[m]
LCF from APP	Longitudinal centre of floatation of the waterline measured from APP	[m]
KM transverse	Vertical distance between the transverse metacentre and the baseline	[m]

Damage cases

Displacement		[ton]
Intact draft	Draft from US keel	[m]
Maximum VCG	Maximum VCG to fulfill damage stability criteria	[m]
VCG	Vertical centre of gravity from baseline including calculated FSA	[m]
Wintact	Weight of compartment intact	[ton]
SWintact	Specific weight of compartment intact	[ton/m ³]
FSMintact	Free surface moment of compartment intact	[tonm]

Tank capacities

Volume		[m ³]
Weight		[ton]
VCG	Vertical centre of gravity from baseline	[m]
LCG	Longitudinal centre of gravity from App	[m]
TCG	Transverse centre of gravity from centreline	[m]
S.W.	Specific weight	[ton/m ³]

The aft perpendicular (APP) is frame 0.

The forward perpendicular (FPP) is 109.500m. forward of APP.

The draft aft is at the APP.

The draft forward is at the FPP.

The trim is the difference between draft aft and draft forward.

A negative trim is a trim to the stern; Positive trim is to the stem

The mean draft is measured at 54.750m forward of APP.

All vertical distances are related to the base line.

All longitudinal distances are related to App (aft end vessel)

General

Vessel's Characteristics

Type of vessel	Chemical tanker type C
Length over all	110.00 [m]
Breadth, over all	13.50 [m]
Depth from baseline	6.525 [m]

Stability Criteria according "ADN art.9.3.2.13 – 9.3.2.15"

Intact Stability criteria tank width > 0.70 B

Minimum GZ in range	0.10 meter
Minimum area under GZ curve	0.024 mrad
Minimum metacentric height (GM)	0.10 meter

Damage Stability criteria "intermediate stage of flooding"

Minimum GZ in range	0.03 meter
Minimum range	5.00 degrees

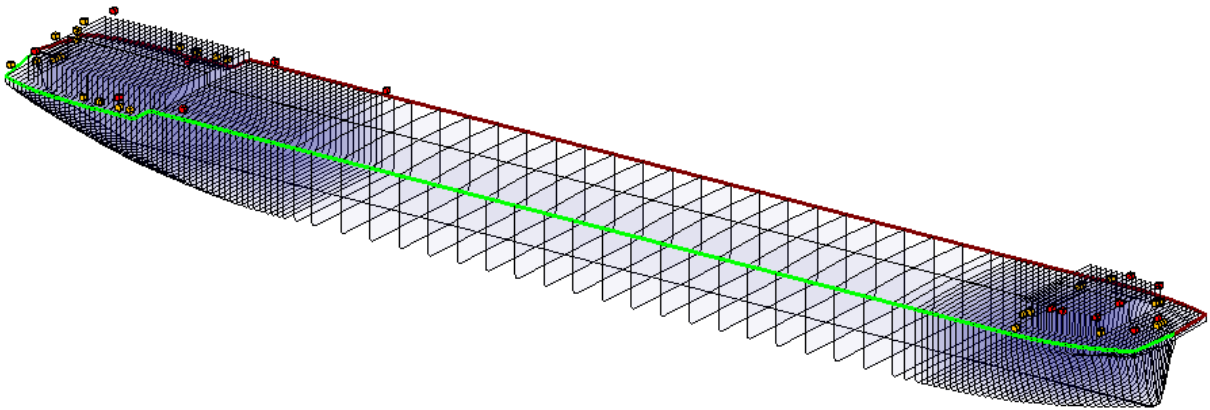
Damage Stability criteria "final stage of flooding"

Maximum static angle of inclination	12.00 degrees
Minimum GZ in range	0.05 meter
Minimum area under GZ curve	0.0065 mrad
Distance to openings (open and weathertight)	0.10 meter

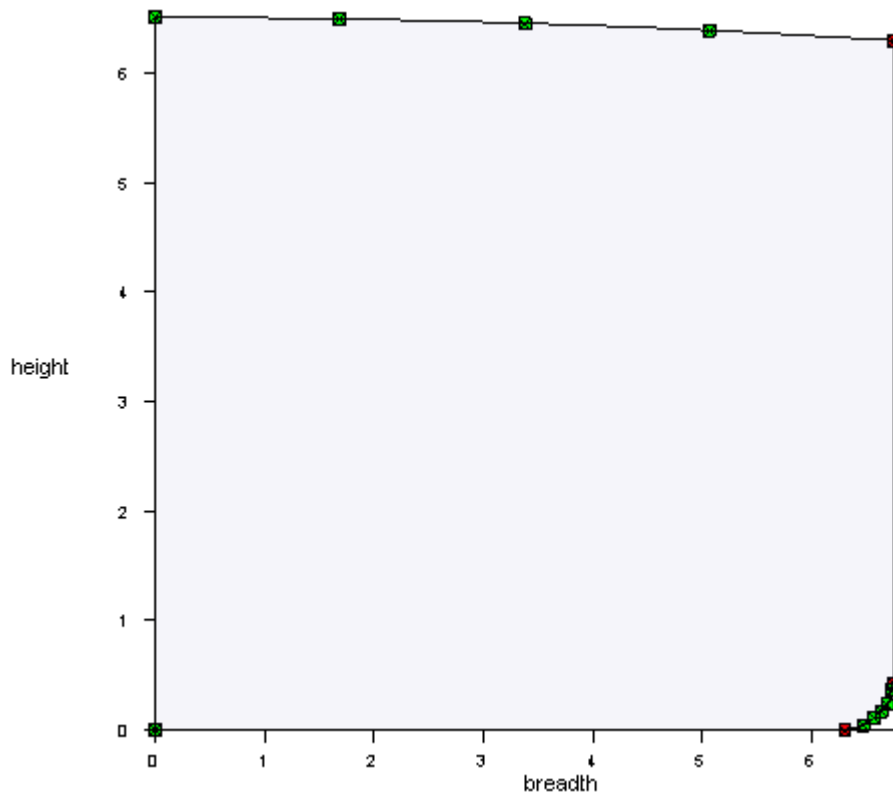
Permeability of damaged compartments

Engine room	95 %
All other compartments	95 %

Hullform



Bodyplan



Special Points

LIST OF SPECIAL POINTS mts "Argos GL"

22 Jan 2015 13:06:51

Description	Length	Breadth	Height	Type of point	Connected with compartment
Airvent WB AP PS	0.750	-4.500	6.090	Weathertight opening	Aftpeak WB
Airvent WB AP SB	0.750	4.500	6.090	Weathertight opening	Aftpeak WB
Entrance Aftpeak PS	2.000	-2.800	6.130	Weathertight opening	Aftpeak WB
Entrance Aftpeak SB	2.000	2.800	6.130	Weathertight opening	Aftpeak WB
Airvent WB aft CL at	3.250	-1.950	8.250	Weathertight opening	WB aft CL
Airvent WB aft CL at	3.250	1.950	8.250	Weathertight opening	WB aft CL
Airvent WB aft PS	9.250	-6.587	5.939	Weathertight opening	WB aft PS
Airvent WB aft SB	9.250	6.587	5.939	Weathertight opening	WB aft PS
Airvent DW aft PS	10.900	-6.600	5.915	Weathertight opening	DW aft PS
Airvent DW aft SB	10.900	6.600	5.915	Weathertight opening	DW aft PS
Airvent FW aft PS	12.750	-6.600	5.879	Weathertight opening	FW aft PS
Airvent FW aft SB	12.750	6.600	5.879	Weathertight opening	FW aft PS
Airvent WB aft 1 PS	13.750	-6.600	5.876	Weathertight opening	WB aft1 PS
Airvent WB aft 1 SB	13.750	6.600	5.876	Weathertight opening	WB aft1 PS
Airvent FO aft PS	10.700	-6.600	5.919	Weathertight opening	FO aft PS
Airvent FO aft SB	10.700	6.600	5.919	Weathertight opening	FO aft PS
Entrance Acco aft PS	11.350	-4.750	5.800	Weathertight opening	Accommodation
Entrance Acco aft SB	11.350	4.750	5.800	Weathertight opening	Accommodation
Em.exit Acco aft ???	0.000	0.000	0.000	Watertight	Accommodation
Entrance ER aftwall1	3.000	1.750	6.150	Weathertight opening	Engine Room
Entrance ER aftwall2	3.000	0.850	6.150	Weathertight opening	Engine Room
Em.exit ER aft ???	0.000	0.000	0.000	Watertight	Engine Room
Air IN ER aft PS	3.750	-5.343	8.160	Open opening	Engine Room
Air OUT ER aft SB	3.750	5.343	8.160	Open opening	Engine Room
Entrance CD fore PS	98.288	-3.294	6.960	Weathertight opening	CD fore
Entrance CD fore SB	98.288	3.294	6.960	Weathertight opening	CD fore
Airvent CD fore PS	98.069	-4.000	6.935	Weathertight opening	CD fore
Airvent CD fore SB	98.069	4.000	6.935	Weathertight opening	CD fore
Airvent WB 5 PS1	18.619	-6.234	6.959	Open opening	WB 8 U-Tank
Airvent WB 5 PS2	29.399	-6.234	6.959	Open opening	WB 8 U-Tank
Airvent WB 5 SB1	18.619	6.234	6.959	Open opening	WB 8 U-Tank
Em.exit Bowthr.rm SB	105.380	1.250	8.635	Open opening	DB bowthr.rm
Airvent WB fore PS	99.130	-6.500	6.800	Weathertight opening	WB fore PS
Airvent WB fore SB	99.130	6.500	6.800	Weathertight opening	WB fore PS
Air IN Bowthr.rm SB	102.330	4.635	8.380	Open opening	Bowthr.rm
Air OUT Bowthr.rm PS	105.330	-4.205	8.380	Open opening	Bowthr.rm
Entrance Bowthr.rm P	105.380	-3.675	7.055	Weathertight opening	Bowthr.rm
Air IN Elec. Switch	101.330	4.745	8.380	Open opening	Elec. Switch Room
Air OUT Elec. Switch	105.330	-4.205	8.380	Open opening	Elec. Switch Room
Entrance Elec. Switc	105.380	-3.675	7.055	Weathertight opening	Elec. Switch Room
Air IN LNG Generator	105.330	4.205	8.380	Open opening	LNG Generator Room
Air OUT LNG Generato	102.330	-4.635	8.380	Open opening	LNG Generator Room
Entrance LNG Generat	105.380	3.675	7.055	Weathertight opening	LNG Generator Room
Airvent WB Forepeak	105.530	-4.000	7.050	Weathertight opening	Forepeak WB
Airvent WB Forepeak	105.530	4.000	7.050	Weathertight opening	Forepeak WB
Chain Pipe PS	107.130	-1.580	6.855	Open opening	Forepeak
Chain Pipe SB	107.130	1.580	6.855	Open opening	Forepeak
Entrance Forepeak PS	108.480	-0.385	7.190	Weathertight opening	Forepeak
Entrance Forepeak SB	108.480	0.385	7.190	Weathertight opening	Forepeak

If in a damage case an opening is submerged which is connected to a damaged compartment, this points has no effect on this particular damage calculation.

Compartments

Maximum tank capacities

SUMMARY OF MAXIMUM TANK VOLUMES mts "Argos GL"

21 Jan 2015 11:42:27

Compartment	Volume	Weight	VCG	LCG	TCG	Mom. In. T	S.W.
FO aft PS	8.624	7.330	3.814	8.619	-4.713	0.77	0.850
FO aft SB	8.624	7.330	3.814	8.619	4.713	0.77	0.850
Subtotal	17.248	14.661	3.814	8.619	0.000		
Compartment	Volume	Weight	VCG	LCG	TCG	Mom. In. T	S.W.
LNG propulsion tank CL	53.805	34.973	3.780	95.153	0.000	52.75	0.650
Subtotal	53.805	34.973	3.780	95.153	0.000		
Compartment	Volume	Weight	VCG	LCG	TCG	Mom. In. T	S.W.
FW aft PS	8.812	8.812	1.724	12.276	-4.290	7.22	1.000
FW aft SB	8.812	8.812	1.724	12.276	4.290	7.22	1.000
Subtotal	17.624	17.624	1.724	12.276	0.000		
Compartment	Volume	Weight	VCG	LCG	TCG	Mom. In. T	S.W.
DW aft PS	6.140	6.140	1.911	10.294	-4.113	6.02	1.000
DW aft SB	6.140	6.140	1.911	10.294	4.113	6.02	1.000
Subtotal	12.280	12.280	1.911	10.294	0.000		
Compartment	Volume	Weight	VCG	LCG	TCG	Mom. In. T	S.W.
Aftpeak WB	66.413	66.413	4.277	1.806	0.000	317.45	1.000
WB aft CL	33.441	33.441	1.703	6.790	0.000	34.61	1.000
WB aft PS	5.792	5.792	2.093	8.432	-3.840	5.78	1.000
WB aft SB	5.792	5.792	2.093	8.432	3.840	5.78	1.000
WB aft1 PS	23.259	23.259	1.531	15.053	-4.444	15.64	1.000
WB aft1 SB	23.259	23.259	1.531	15.053	4.444	15.64	1.000
WB 8 U-Tank	279.499	279.499	2.071	23.906	0.000	2419.57	1.000
WB 7 U-Tank	287.652	287.652	1.976	36.789	0.000	2438.98	1.000
WB 6 U-Tank	260.952	260.952	2.037	48.375	0.000	2182.29	1.000
WB 5 U-Tank	287.652	287.652	1.976	60.385	0.000	2438.97	1.000
WB 4 U-Tank	260.547	260.547	2.035	71.962	0.000	2180.21	1.000
WB 3 U-Tank	147.050	147.050	1.980	81.272	0.000	1350.30	1.000
WB 2 U-Tank	122.701	122.701	2.102	87.458	0.000	1090.02	1.000
WB 1 U-Tank	157.629	157.629	1.973	94.053	0.000	1260.47	1.000
WB fore PS	42.200	42.200	3.339	101.705	-4.696	13.55	1.000
WB fore SB	42.200	42.200	3.339	101.705	4.696	13.55	1.000
Forepeak WB	35.377	35.377	1.924	106.571	0.000	25.90	1.000
Subtotal	2081.413	2081.413	2.126	56.218	0.000		
Compartment	Volume	Weight	VCG	LCG	TCG	Mom. In. T	S.W.
Cargo 02 PS	389.740	389.740	3.670	23.645	-2.827	192.90	1.000

SUMMARY OF MAXIMUM TANK VOLUMES
mts "Argos GL"

21 Jan 2015 11:42:27

Compartment	Volume	Weight	VCG	LCG	TCG	Mom. In. T	S.W.
Cargo 02 SB	389.740	389.740	3.670	23.645	2.827	192.90	1.000
Cargo 01 PS	377.761	377.761	3.654	83.792	-2.845	185.60	1.000
Cargo 01 SB	377.761	377.761	3.654	83.792	2.845	185.60	1.000
Subtotal	1535.002	1535.002	3.662	53.249	0.000		

Compartment	Volume	Weight	VCG	LCG	TCG	Mom. In. T	S.W.
LNG TANK GTT 02	932.007	932.007	3.412	42.023	0.000	2114.80	1.000
LNG TANK GTT 01	932.007	932.007	3.412	65.619	0.000	2114.84	1.000
Subtotal	1864.013	1864.013	3.412	53.821	0.000		

Compartment	Volume	Weight	VCG	LCG	TCG	Mom. In. T	S.W.
CD aft PS	2.512	2.512	1.816	11.254	-4.213	2.27	1.000
CD aft SB	2.512	2.512	1.816	11.254	4.213	2.27	1.000
CD aft1 PS	3.328	3.328	1.642	13.252	-4.349	2.52	1.000
CD aft1 SB	3.328	3.328	1.642	13.252	4.349	2.52	1.000
Void at side PS	4.610	4.610	4.693	4.806	-5.949	0.35	1.000
Void at side SB	4.610	4.610	4.693	4.806	5.949	0.35	1.000
Void at side2 PS	26.367	26.367	3.847	11.183	-6.038	2.78	1.000
Void at side2 SB	26.367	26.367	3.847	11.183	6.038	2.78	1.000
Void at side3 PS	5.109	5.109	5.314	12.703	-6.240	0.82	1.000
Void at side3 SB	5.109	5.109	5.314	12.703	6.240	0.82	1.000
POD compartment PS	20.300	20.300	3.025	5.324	-3.331	25.09	1.000
POD compartment SB	20.300	20.300	3.025	5.324	3.331	25.08	1.000
Void DB	18.924	18.924	0.308	13.513	0.084	81.56	1.000
Accommodation	436.364	436.364	5.422	12.250	0.000	1242.06	1.000
Engine Room	321.930	321.930	4.054	7.861	0.012	610.50	1.000
Boxcooler aft PS	4.401	4.401	0.735	10.277	-1.272	2.55	1.000
CD aft	82.281	82.281	3.322	17.001	0.000	201.85	1.000
CD fore	81.776	81.776	3.311	97.878	0.000	202.89	1.000
CD FO2LNG2	72.387	72.387	3.230	30.219	0.000	122.13	1.000
LNG TANK 02 W.O. GTT BLOCKS	325.491	325.491	3.433	42.004	0.000	2712.52	1.000
Void above GTT	144.801	144.801	6.174	42.018	0.000	2712.44	1.000
CD LNG1-2	71.982	71.982	3.230	53.816	0.000	120.04	1.000
LNG TANK 01 W.O. GTT BLOCKS	325.491	325.491	3.433	65.600	0.000	2712.48	1.000
Void Above GTT	144.801	144.801	6.174	65.614	0.000	2712.44	1.000
CD LNG1FO1	72.387	72.387	3.230	77.413	0.000	122.13	1.000
CD FO1-Propulsion	72.815	72.815	3.230	90.172	0.000	126.18	1.000
Cargo hold LNG prop Tank CL	331.858	331.858	3.725	93.721	0.000	833.21	1.000
DB bowthr.rm	40.150	40.150	0.363	101.418	0.000	464.78	1.000
Void fore PS	13.995	13.995	5.915	101.849	-5.558	4.92	1.000
Void fore SB	13.995	13.995	5.915	101.849	5.558	4.92	1.000

SUMMARY OF MAXIMUM TANKVOLUMES
mts "Argos GL"

21 Jan 2015 11:42:27

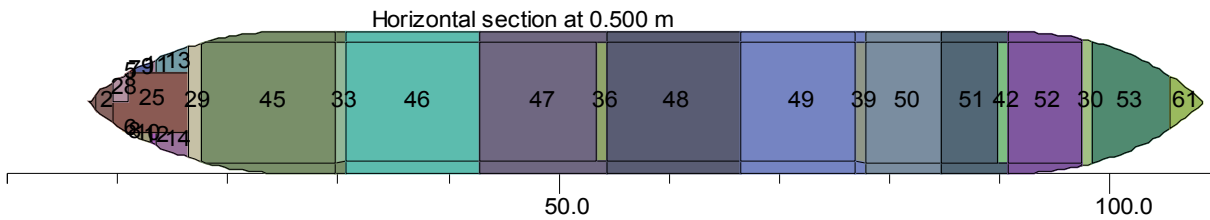
Compartment	Volume	Weight	VCG	LCG	TCG	Mom.In.T	S.W.
Bowthr.rm	215.861	215.861	3.273	102.203	-0.607	278.82	1.000
Elec. Switch Room	62.963	62.963	4.105	100.360	1.465	86.98	1.000
LNG Generator Room	163.715	163.715	6.877	101.341	0.237	404.30	1.000
Forepeak	77.768	77.768	5.470	107.092	0.000	480.93	1.000
Subtotal	3220.587	3220.587	4.210	55.539	0.000		
Total	8801.972	8780.554	3.441	54.937	0.000		

Views of compartments

COMPARTMENT LAYOUT
mts "Argos GL"

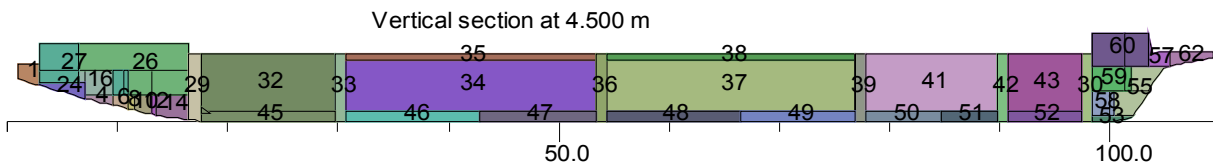
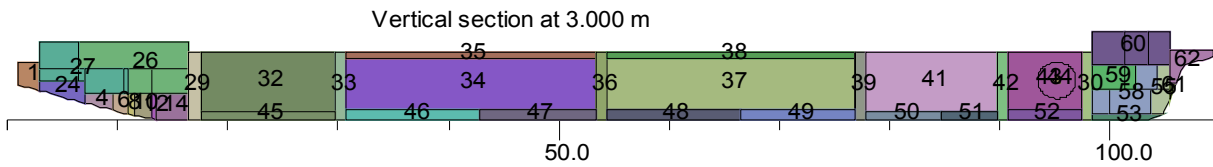
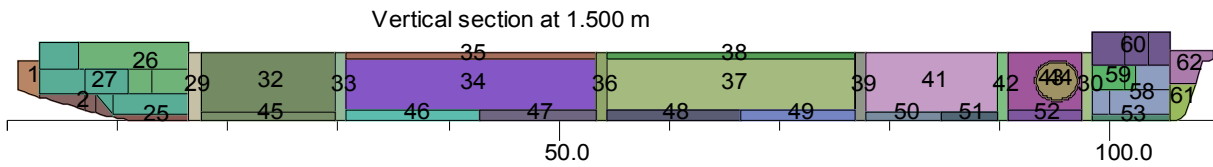
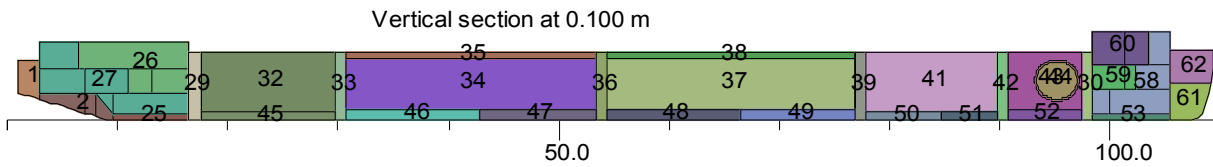
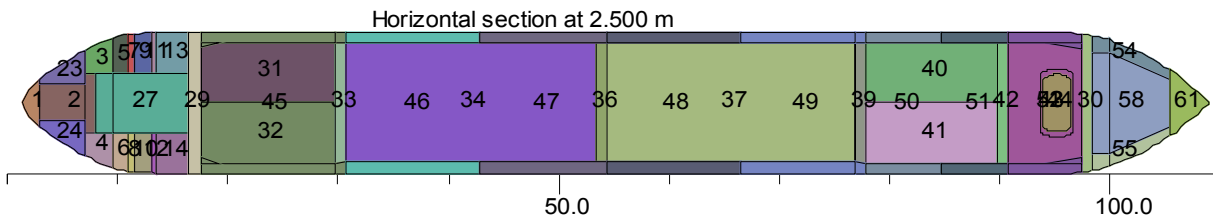
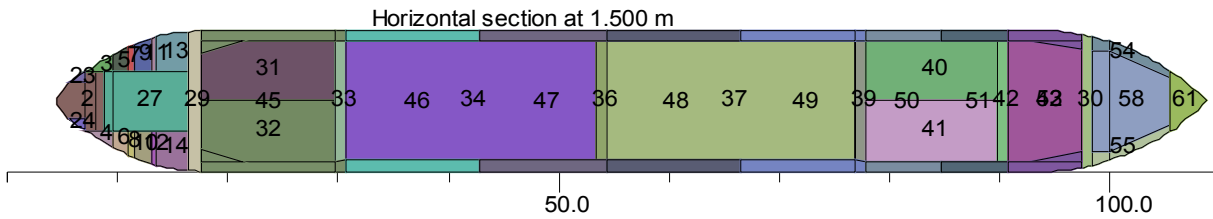
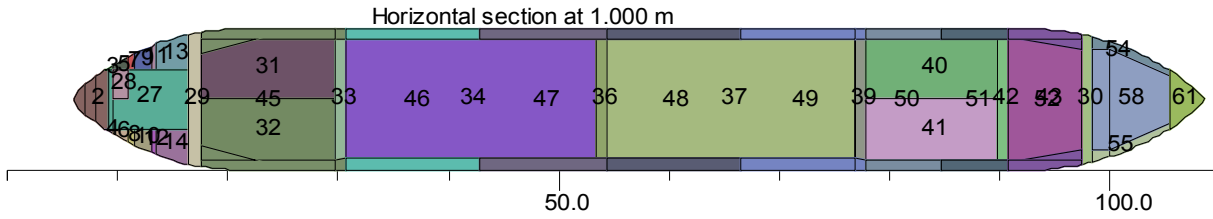
21 Jan 2015 11:19:33

- | | |
|--------------------------------|--------------------------------|
| 1 Aftpeak WB | 2 WB aft CL |
| 3 WB aft PS | 4 WB aft SB |
| 5 DW aft PS | 6 DW aft SB |
| 7 CD aft PS | 8 CD aft SB |
| 9 FW aft PS | 10 FW aft SB |
| 11 CD aft1 PS | 12 CD aft1 SB |
| 13 WB aft1 PS | 14 WB aft1 SB |
| 15 FO aft PS | 16 FO aft SB |
| 17 Void at side PS | 18 Void at side SB |
| 19 Void at side2 PS | 20 Void at side2 SB |
| 21 Void at side3 PS | 22 Void at side3 SB |
| 23 POD compartment PS | 24 POD compartment SB |
| 25 Void DB | 26 Accommodation |
| 27 Engine Room | 28 Boxcooler aft PS |
| 29 CD aft | 30 CD fore |
| 31 Cargo 02 PS | 32 Cargo 02 SB |
| 33 CD FO2LNG2 | 34 LNG TANK 02 W.O. GTT BLOCKS |
| 35 Void above GTT | 36 CD LNG1-2 |
| 37 LNG TANK 01 W.O. GTT BLOCKS | 38 Void Above GTT |
| 39 CD LNG1FO1 | 40 Cargo 01 PS |
| 41 Cargo 01 SB | 42 CD FO1-Propulsion |
| 43 Cargo hold LNG prop Tank CL | 44 LNG propulsion tank CL |
| 45 WB 8 U-Tank | 46 WB 7 U-Tank |
| 47 WB 6 U-Tank | 48 WB 5 U-Tank |
| 49 WB 4 U-Tank | 50 WB 3 U-Tank |
| 51 WB 2 U-Tank | 52 WB 1 U-Tank |
| 53 DB bowthr.rm | 54 WB fore PS |
| 55 WB fore SB | 56 Void fore PS |
| 57 Void fore SB | 58 Bowthr.rm |
| 59 Elec. Switch Room | 60 LNG Generator Room |
| 61 Forepeak WB | 62 Forepeak |



COMPARTMENT LAYOUT
mts "Argos GL"

21 Jan 2015 11:19:34



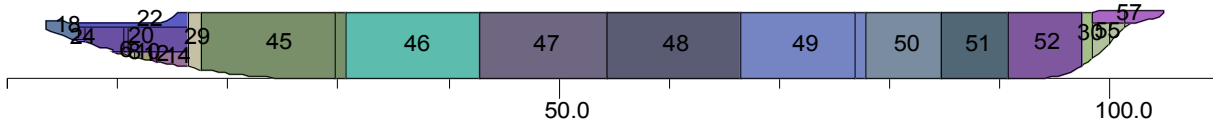
Preliminary Stability information Booklet mts "Argos GL"

Date: 27 January 2015

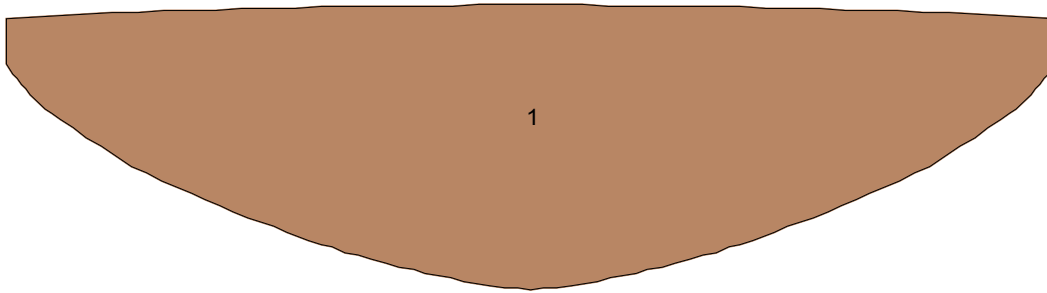
COMPARTMENT LAYOUT
mts "Argos GL"

21 Jan 2015 11:19:34

Vertical section at 6.250 m



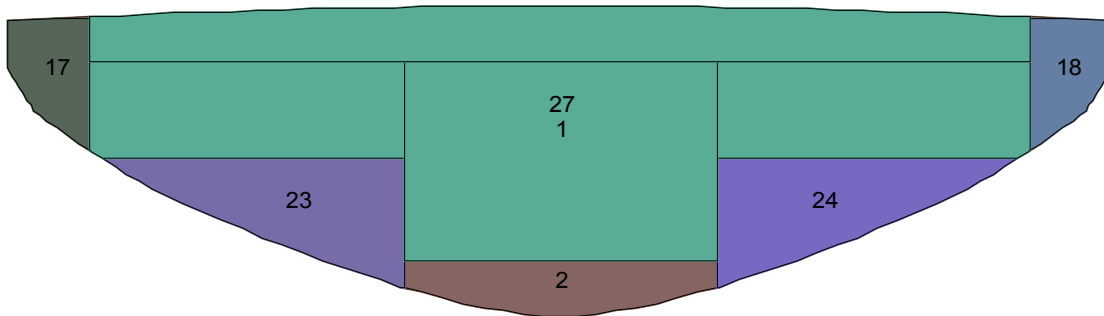
Cross section at 2.000 m



COMPARTMENT LAYOUT
mts "Argos GL"

21 Jan 2015 11:19:34

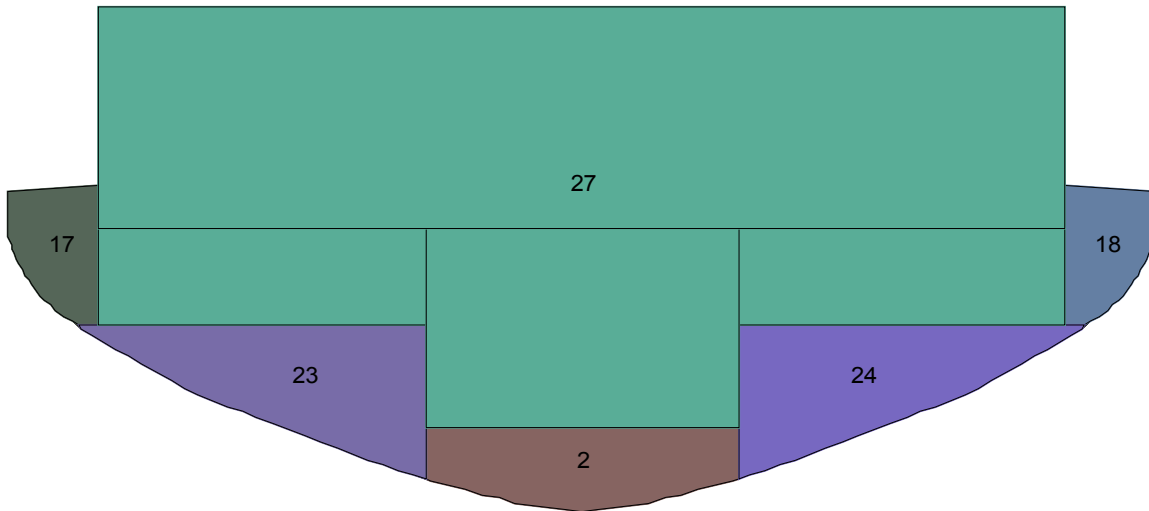
Cross section at 3.000 m



COMPARTMENT LAYOUT
mts "Argos GL"

21 Jan 2015 11:19:34

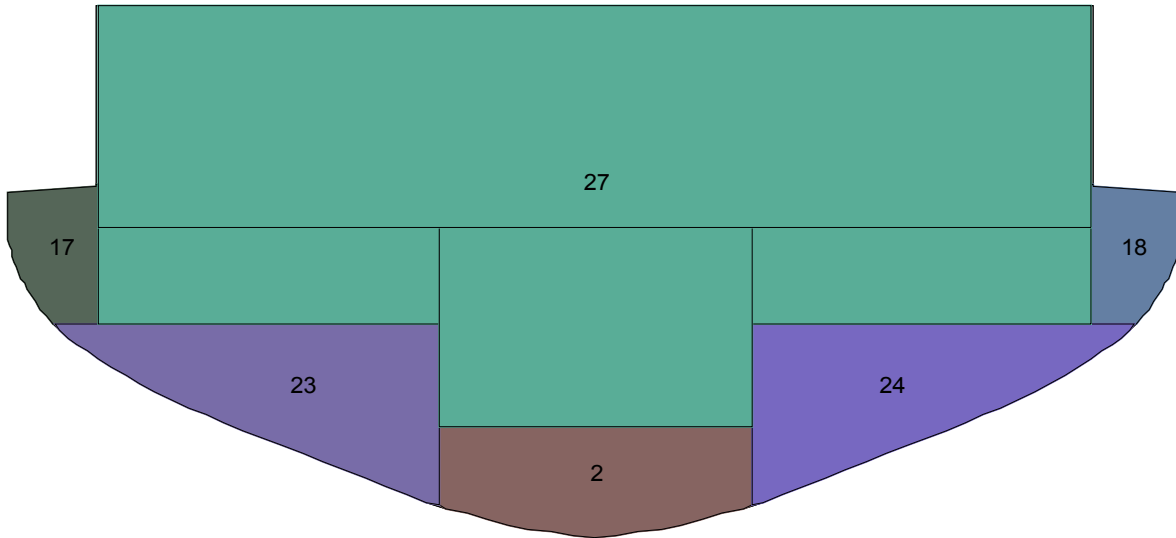
Cross section at 4.000 m



COMPARTMENT LAYOUT
mts "Argos GL"

21 Jan 2015 11:19:34

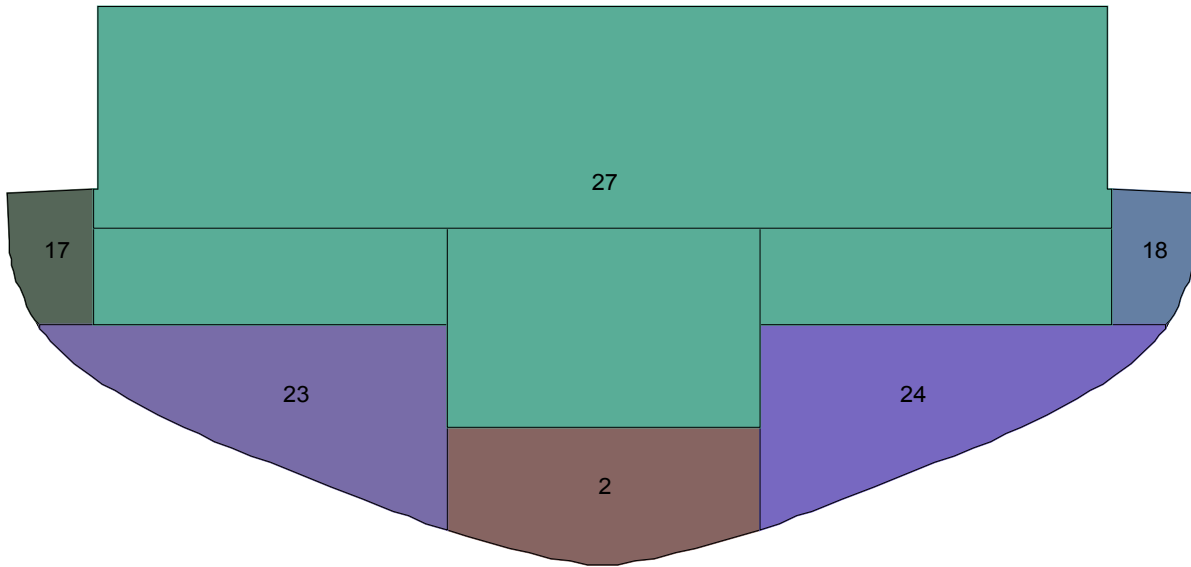
Cross section at 5.000 m



COMPARTMENT LAYOUT
mts "Argos GL"

21 Jan 2015 11:19:34

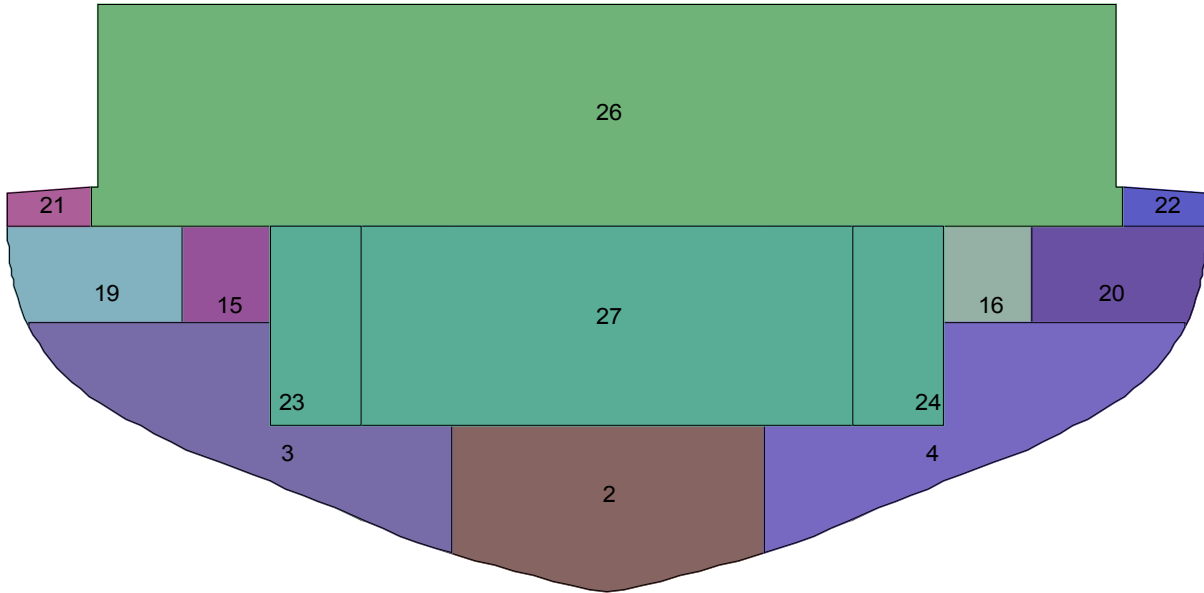
Cross section at 6.000 m



COMPARTMENT LAYOUT
mts "Argos GL"

21 Jan 2015 11:19:34

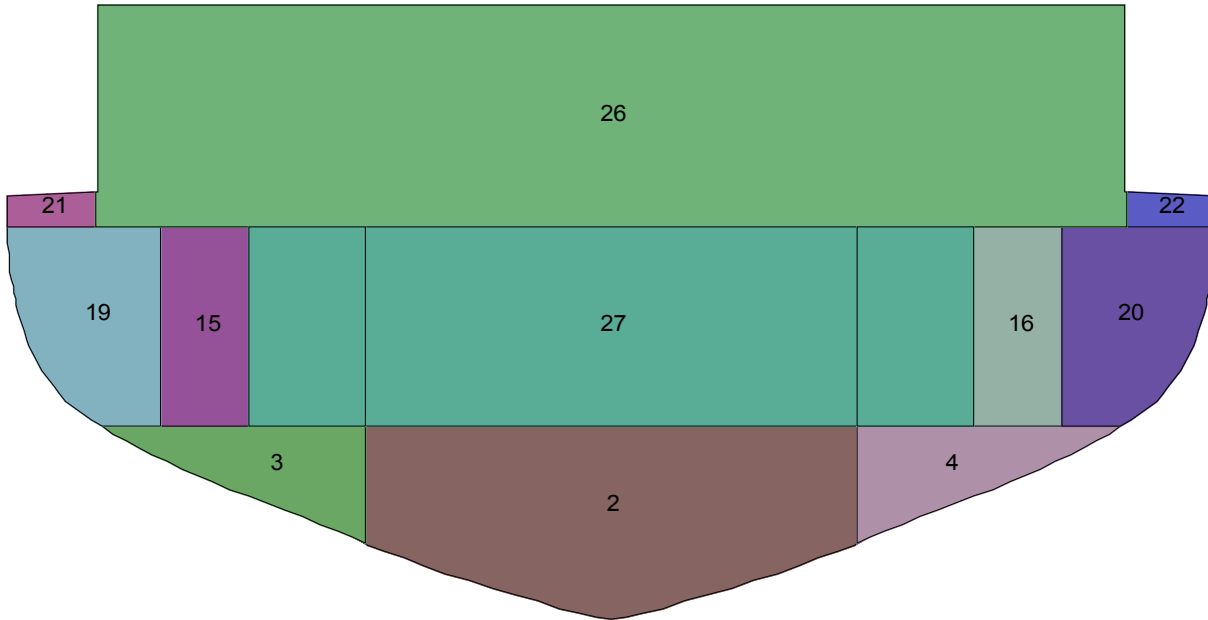
Cross section at 7.000 m



COMPARTMENT LAYOUT
mts "Argos GL"

21 Jan 2015 11:19:34

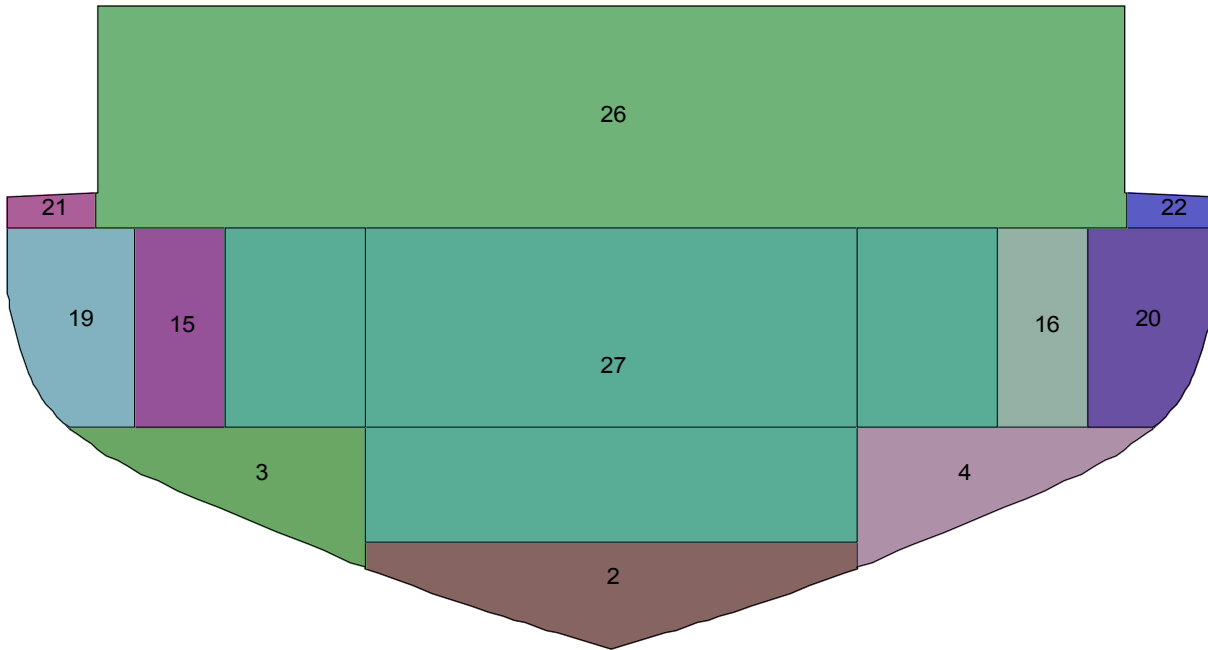
Cross section at 8.000 m



COMPARTMENT LAYOUT
mts "Argos GL"

21 Jan 2015 11:19:34

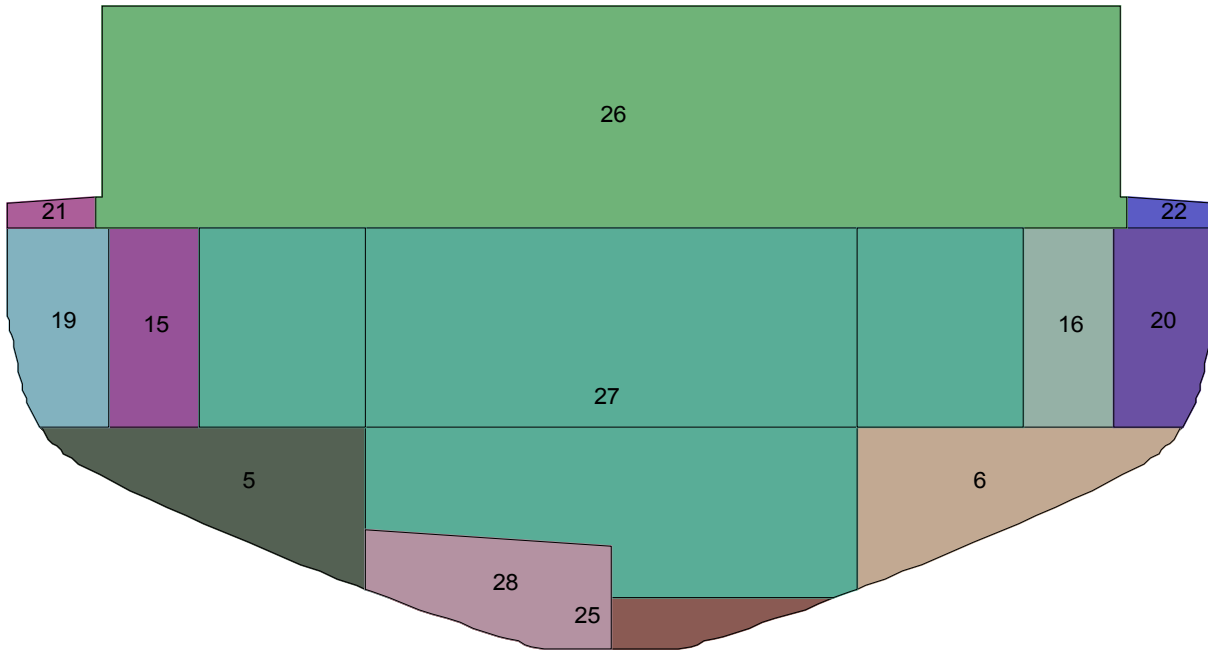
Cross section at 9.000 m



COMPARTMENT LAYOUT
mts "Argos GL"

21 Jan 2015 11:19:34

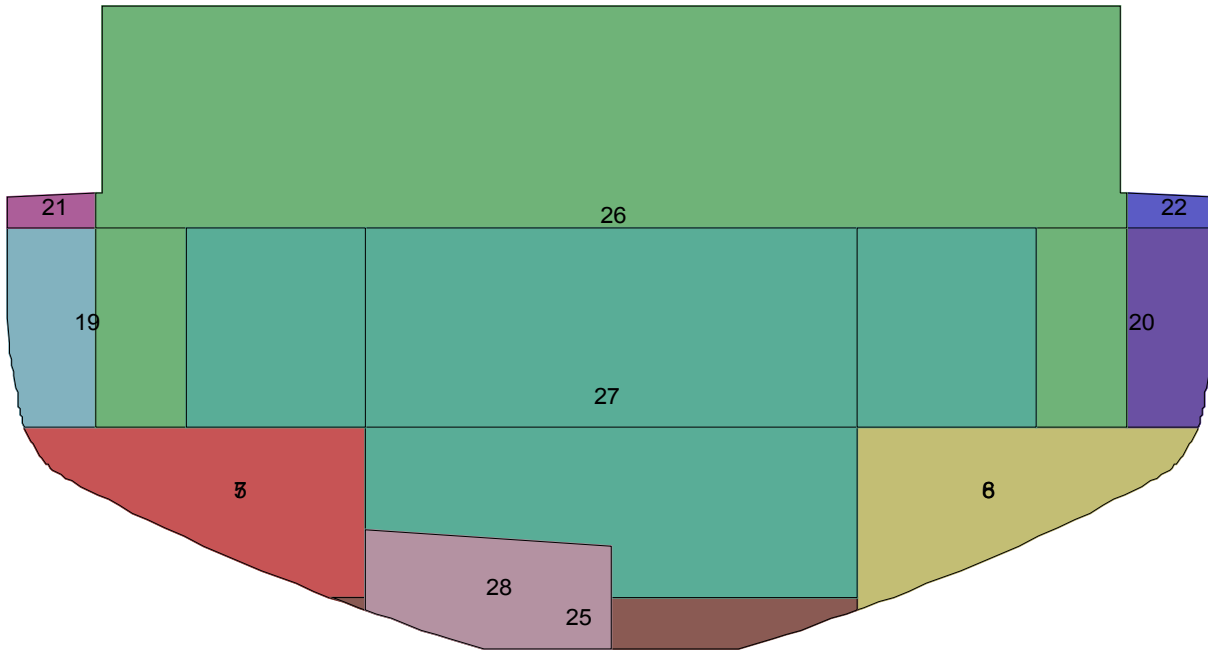
Cross section at 10.000 m



COMPARTMENT LAYOUT
mts "Argos GL"

21 Jan 2015 11:19:34

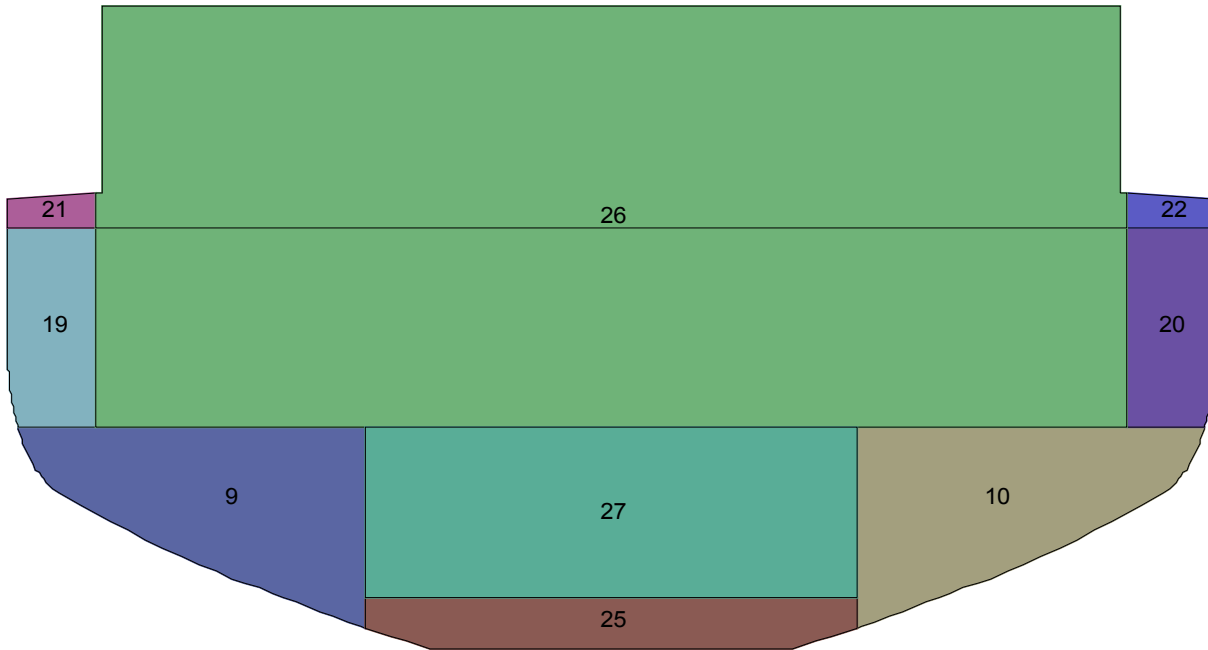
Cross section at 11.000 m



COMPARTMENT LAYOUT
mts "Argos GL"

21 Jan 2015 11:19:34

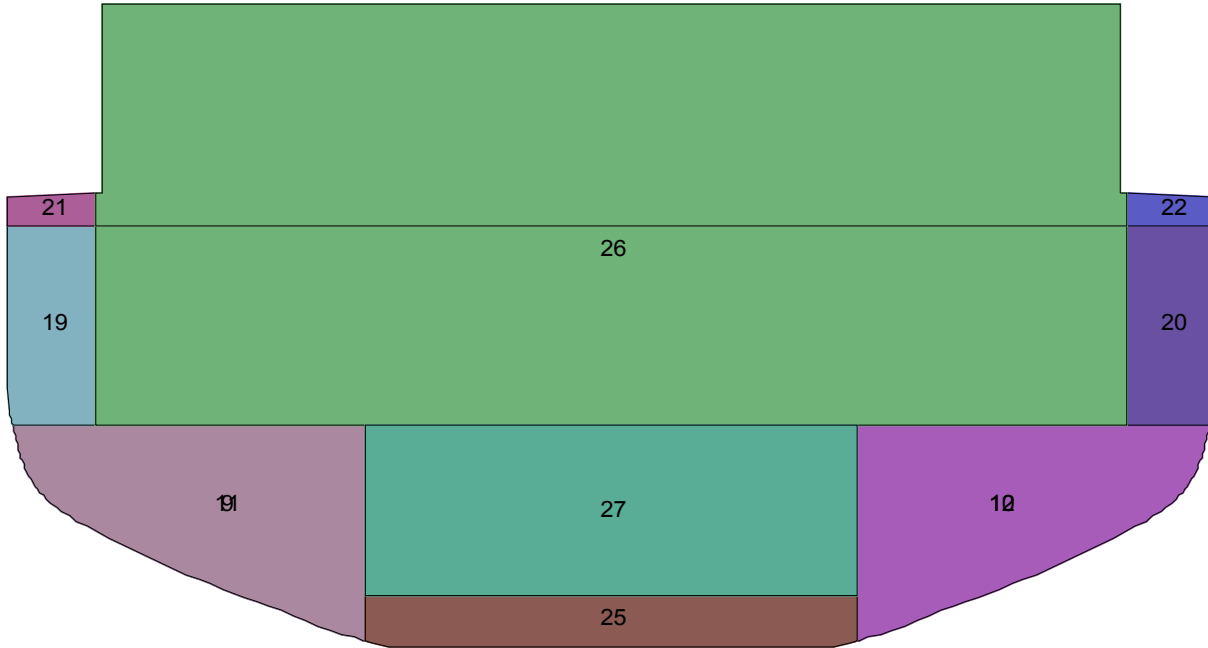
Cross section at 12.000 m



COMPARTMENT LAYOUT
mts "Argos GL"

21 Jan 2015 11:19:34

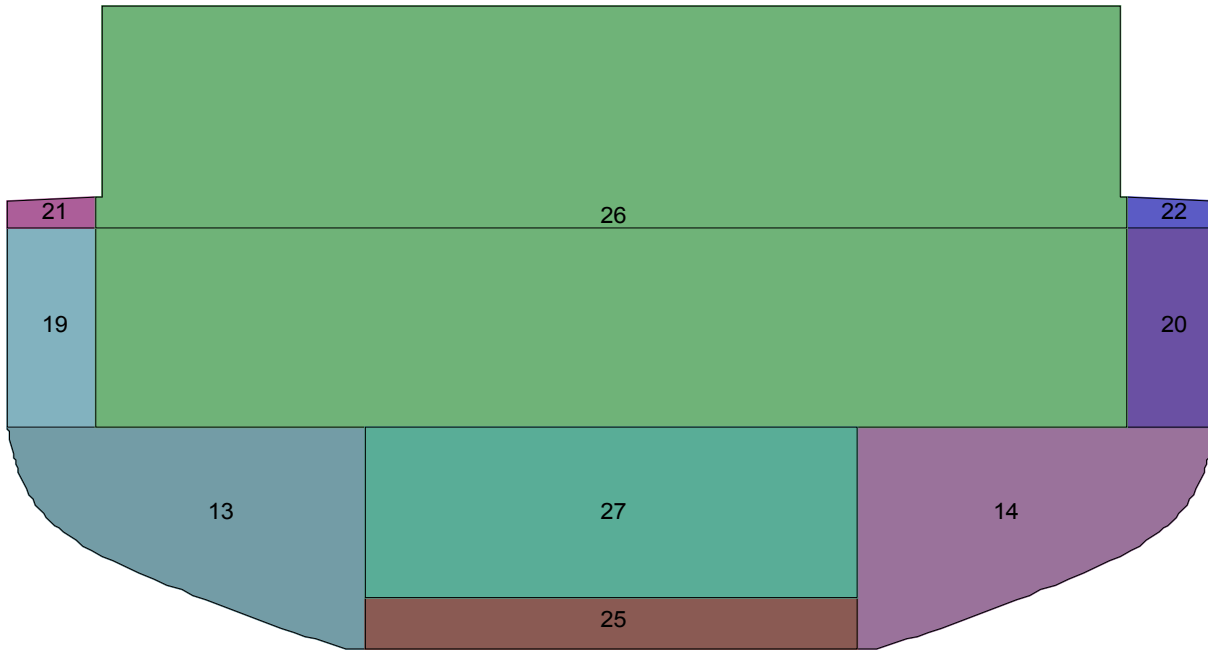
Cross section at 13.000 m



COMPARTMENT LAYOUT
mts "Argos GL"

21 Jan 2015 11:19:34

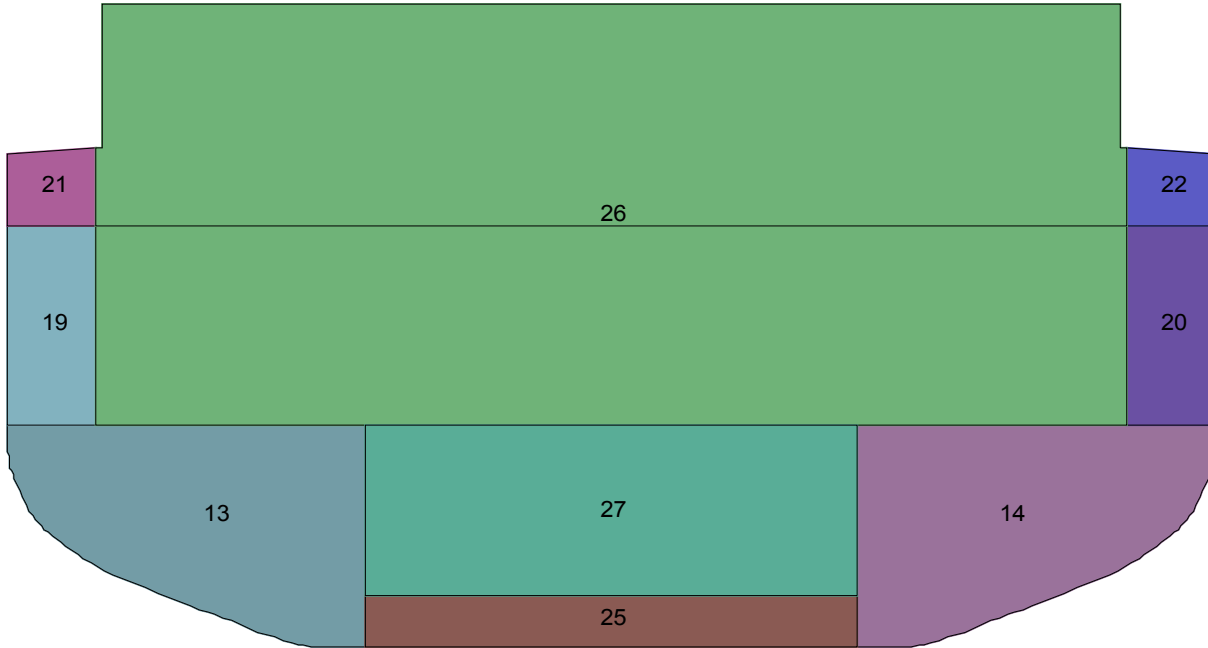
Cross section at 14.000 m



COMPARTMENT LAYOUT
mts "Argos GL"

21 Jan 2015 11:19:34

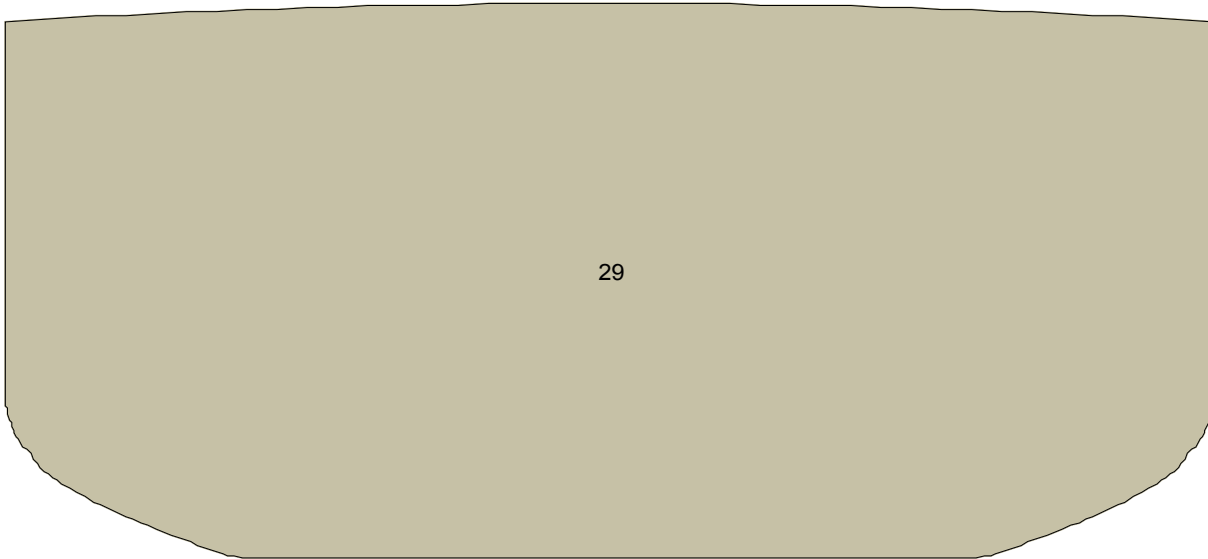
Cross section at 15.000 m



COMPARTMENT LAYOUT
mts "Argos GL"

21 Jan 2015 11:19:34

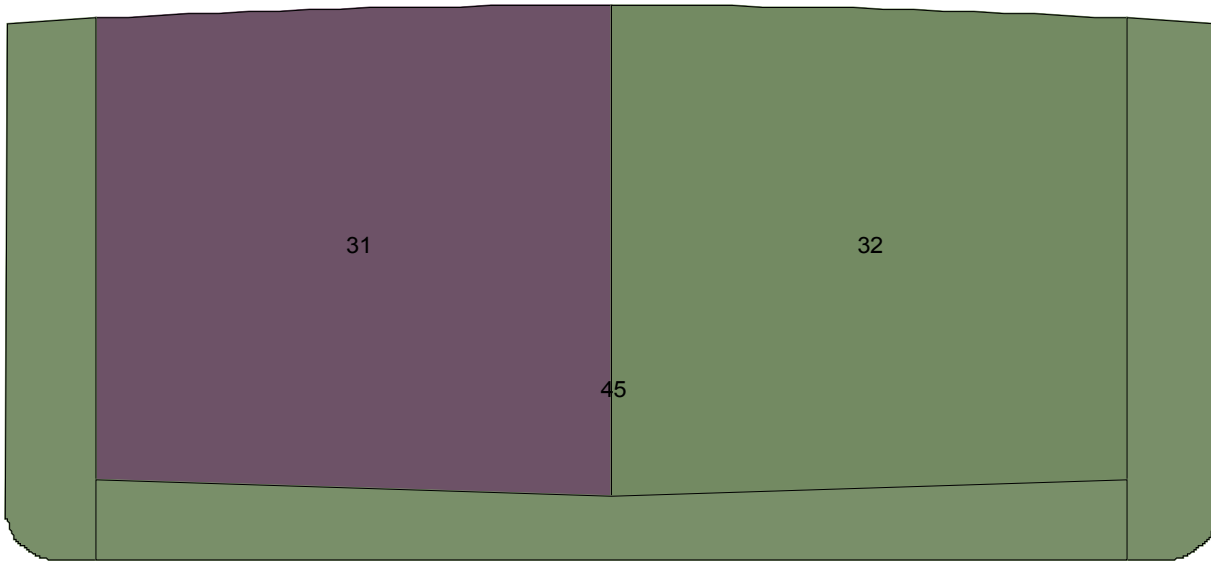
Cross section at 16.950 m



COMPARTMENT LAYOUT
mts "Argos GL"

21 Jan 2015 11:19:34

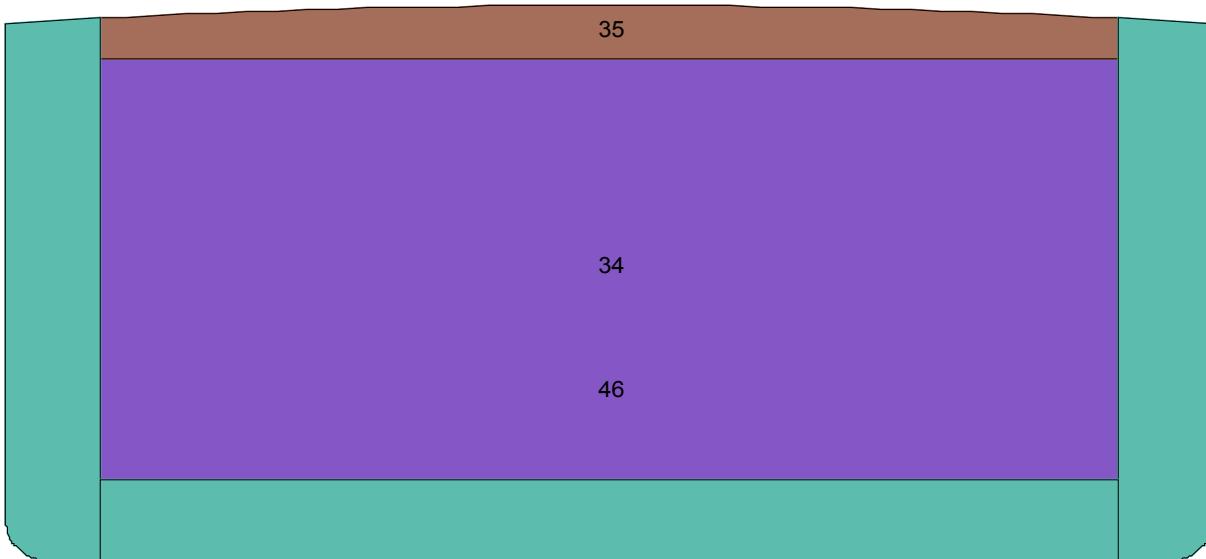
Cross section at 25.800 m



COMPARTMENT LAYOUT
mts "Argos GL"

21 Jan 2015 11:19:34

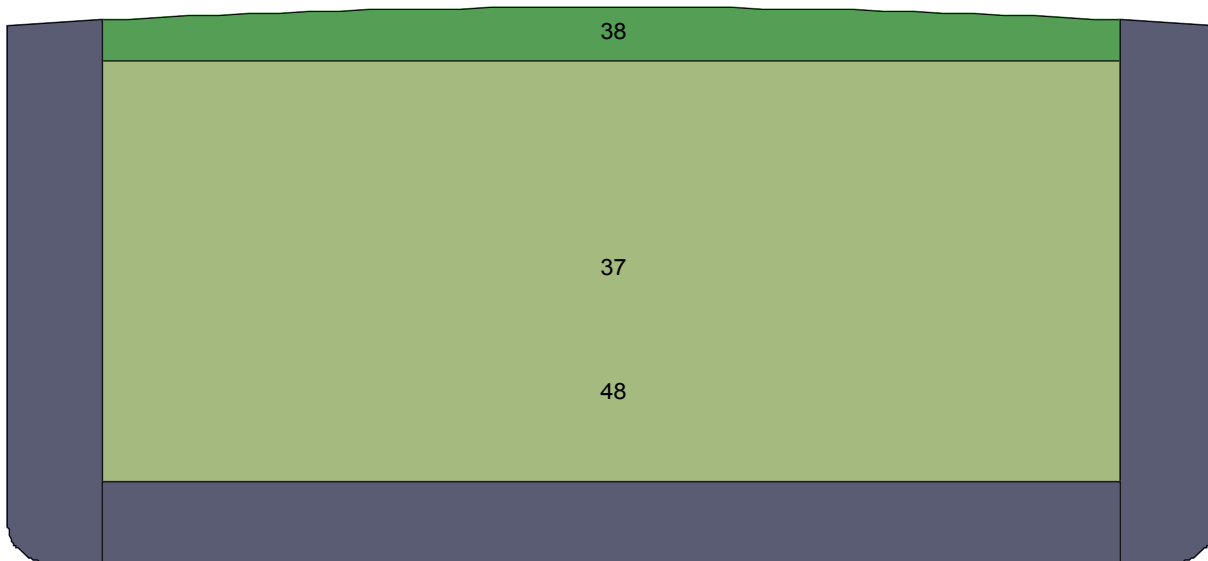
Cross section at 42.600 m



COMPARTMENT LAYOUT
mts "Argos GL"

21 Jan 2015 11:19:34

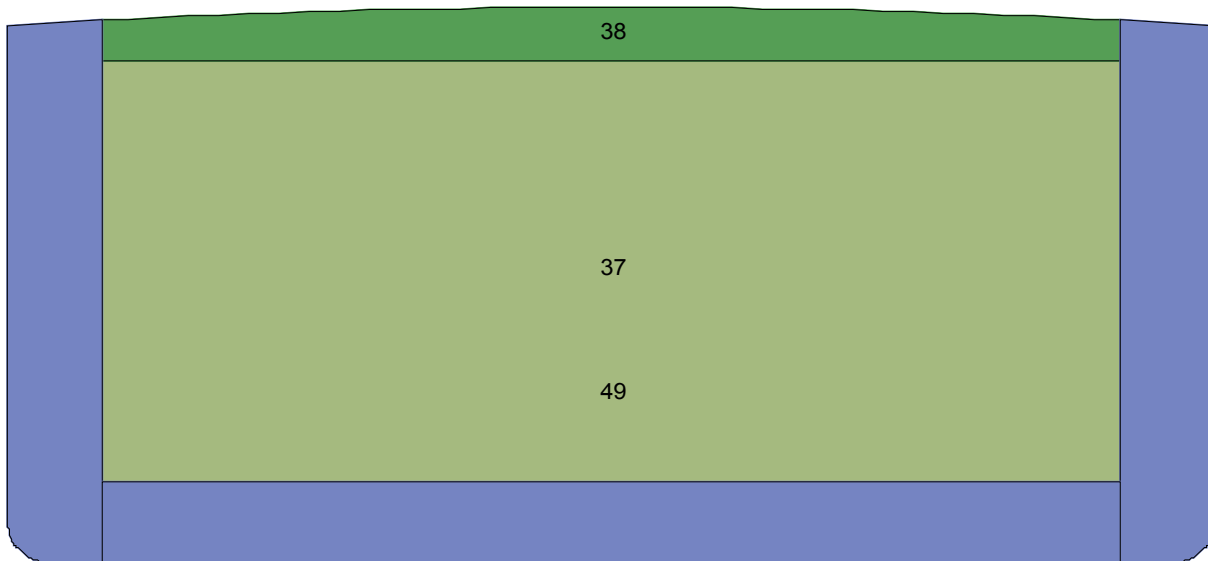
Cross section at 54.920 m



COMPARTMENT LAYOUT
mts "Argos GL"

21 Jan 2015 11:19:34

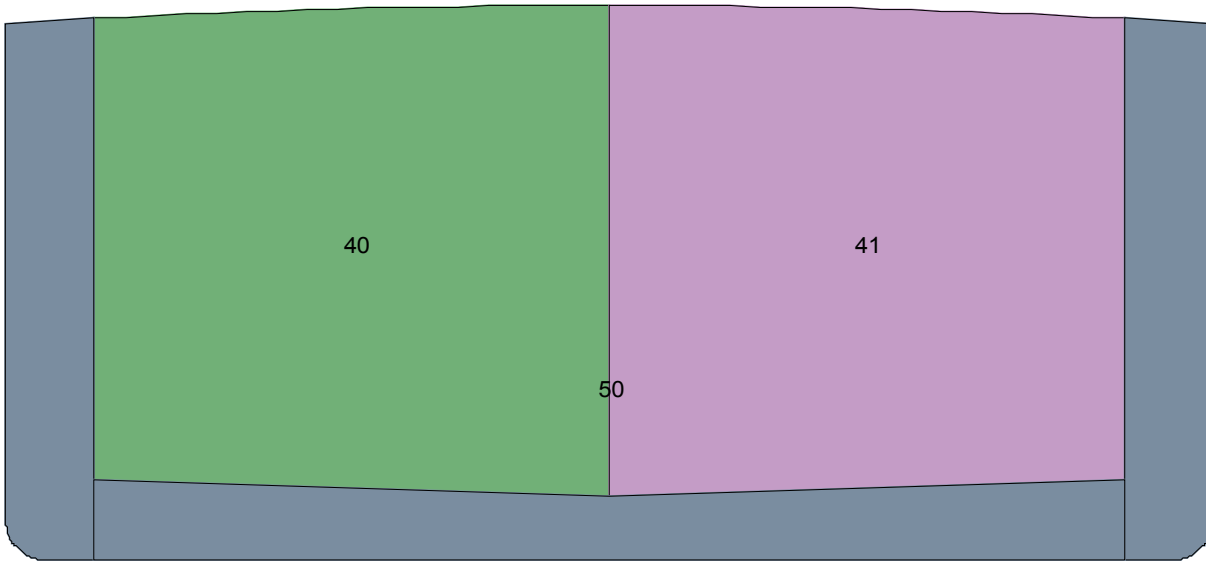
Cross section at 70.600 m



COMPARTMENT LAYOUT
mts "Argos GL"

21 Jan 2015 11:19:34

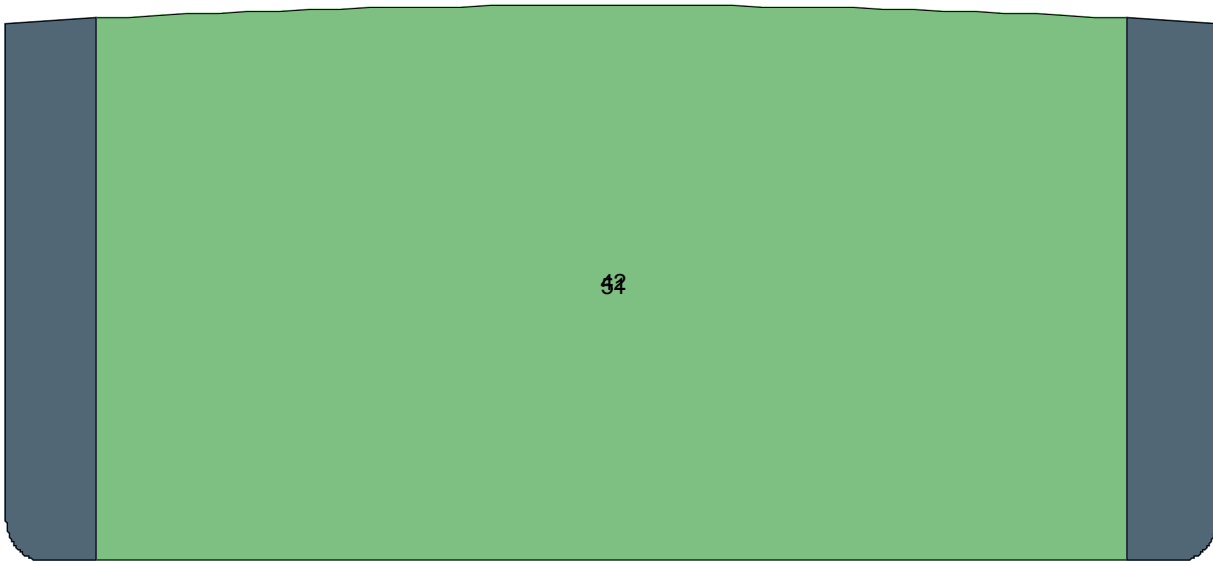
Cross section at 82.640 m



COMPARTMENT LAYOUT
mts "Argos GL"

21 Jan 2015 11:19:34

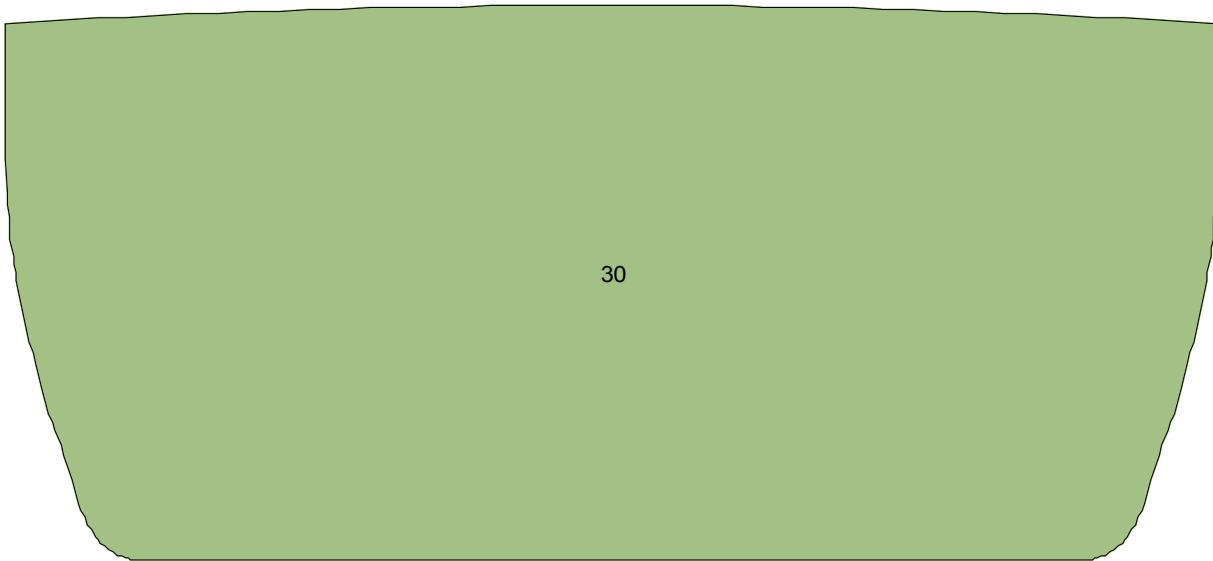
Cross section at 90.200 m



COMPARTMENT LAYOUT
mts "Argos GL"

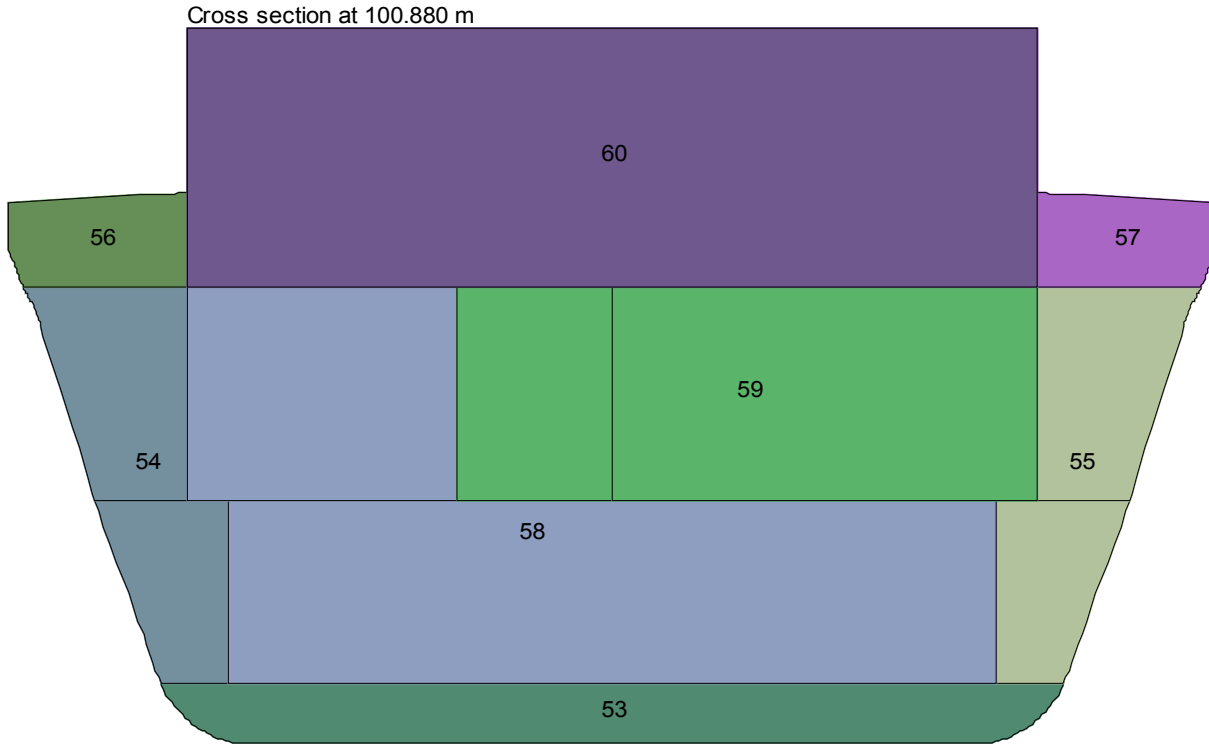
21 Jan 2015 11:19:34

Cross section at 97.930 m



COMPARTMENT LAYOUT
mts "Argos GL"

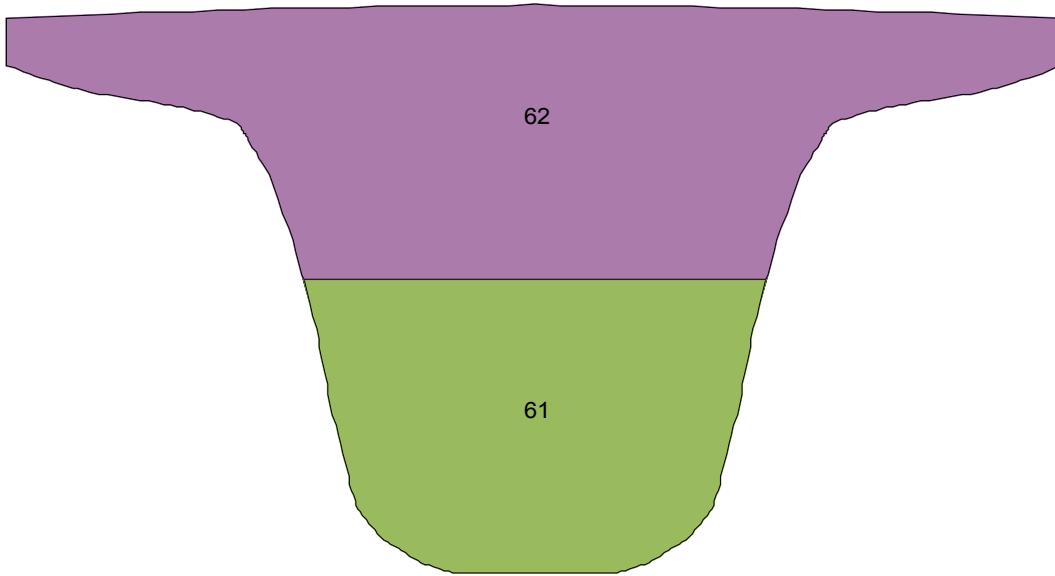
21 Jan 2015 11:19:34



COMPARTMENT LAYOUT
mts "Argos GL"

21 Jan 2015 11:19:34

Cross section at 106.380 m



Hydrostatic particulars

HYDROSTATIC PARTICULARS

mts "Argos GL"

Trim = 0.000 m						22 Jan 2015	13:08:27
Draft from base m	Displ. [S.W. 1.0000] ton	Immer- sion ton/cm	Moment change trim tonm/cm	LCB from APP m	TCB from CL m	LCF from APP m	KM transv. m
0.300	349.86	12.03	73.15	58.540	0.000	58.352	47.319
0.350	410.16	12.10	74.11	58.508	0.000	58.271	40.829
0.400	470.81	12.17	75.03	58.473	0.000	58.186	36.024
0.450	531.82	12.24	75.90	58.436	0.000	58.101	32.267
0.500	593.10	12.28	76.71	58.398	0.000	58.012	29.136
0.550	654.61	12.33	77.49	58.358	0.000	57.920	26.577
0.600	716.34	12.37	78.23	58.318	0.000	57.831	24.446
0.650	778.27	12.41	78.96	58.276	0.000	57.740	22.648
0.700	840.40	12.45	79.66	58.233	0.000	57.641	21.112
0.750	902.73	12.49	80.36	58.190	0.000	57.549	19.785
0.800	965.24	12.52	81.04	58.146	0.000	57.456	18.629
0.850	1027.94	12.56	81.71	58.101	0.000	57.361	17.611
0.900	1090.82	12.60	82.37	58.056	0.000	57.267	16.708
0.950	1153.87	12.63	83.02	58.011	0.000	57.170	15.903
1.000	1217.10	12.67	83.67	57.966	0.000	57.078	15.180
1.050	1280.49	12.70	84.31	57.920	0.000	56.989	14.528
1.100	1344.05	12.73	84.94	57.875	0.000	56.903	13.937
1.150	1407.76	12.76	85.56	57.829	0.000	56.825	13.400
1.200	1471.63	12.79	86.18	57.784	0.000	56.741	12.909
1.250	1535.66	12.82	86.78	57.739	0.000	56.661	12.460
1.300	1599.84	12.85	87.38	57.695	0.000	56.581	12.046
1.350	1664.18	12.89	87.98	57.650	0.000	56.491	11.666
1.400	1728.68	12.92	88.59	57.606	0.000	56.407	11.314
1.450	1793.32	12.95	89.20	57.561	0.000	56.333	10.989
1.500	1858.12	12.98	89.80	57.517	0.000	56.243	10.687
1.550	1923.07	13.01	90.40	57.473	0.000	56.169	10.405
1.600	1988.16	13.04	90.99	57.430	0.000	56.093	10.143
1.650	2053.39	13.07	91.58	57.386	0.000	56.015	9.898
1.700	2118.78	13.10	92.18	57.343	0.000	55.932	9.670
1.750	2184.32	13.12	92.77	57.300	0.000	55.855	9.456
1.800	2249.99	13.15	93.36	57.257	0.000	55.779	9.255
1.850	2315.81	13.18	93.96	57.214	0.000	55.691	9.066
1.900	2381.78	13.21	94.55	57.171	0.000	55.626	8.888
1.950	2447.88	13.24	95.14	57.128	0.000	55.551	8.720
2.000	2514.13	13.27	95.74	57.086	0.000	55.458	8.563
2.050	2580.53	13.30	96.33	57.043	0.000	55.383	8.413

Preliminary Stability information Booklet mts "Argos GL"

Date: 27 January 2015

HYDROSTATIC PARTICULARS
mts "Argos GL"

Trim = 0.000 m								22 Jan 2015 13:08:27
Draft from base m	Displ. [S.W. 1.0000] ton	Immer- sion ton/cm	Moment change trim tonm/cm	LCB from APP m	TCB from CL m	LCF from transv. APP m	KM m	
2.100	2647.06	13.32	96.93	57.001	0.000	55.323	8.272	
2.150	2713.72	13.35	97.53	56.959	0.000	55.235	8.139	
2.200	2780.53	13.38	98.12	56.917	0.000	55.172	8.013	
2.250	2847.47	13.40	98.70	56.875	0.000	55.095	7.893	
2.300	2914.55	13.43	99.28	56.833	0.000	55.015	7.779	
2.350	2981.76	13.46	99.87	56.791	0.000	54.947	7.672	
2.400	3049.11	13.48	100.44	56.750	0.000	54.872	7.569	
2.450	3116.58	13.51	101.02	56.709	0.000	54.795	7.472	
2.500	3184.19	13.54	101.60	56.668	0.000	54.727	7.380	
2.550	3251.93	13.56	102.17	56.627	0.000	54.656	7.292	
2.600	3319.79	13.59	102.74	56.586	0.000	54.587	7.208	
2.650	3387.79	13.62	103.33	56.545	0.000	54.498	7.128	
2.700	3455.93	13.64	103.93	56.504	0.000	54.439	7.053	
2.750	3524.19	13.67	104.52	56.463	0.000	54.363	6.981	
2.800	3592.58	13.69	105.13	56.423	0.000	54.302	6.912	
2.850	3661.09	13.71	105.69	56.383	0.000	54.239	6.846	
2.900	3729.72	13.74	106.24	56.343	0.000	54.174	6.785	
2.950	3798.45	13.76	106.77	56.303	0.000	54.115	6.726	
3.000	3867.30	13.78	107.28	56.264	0.000	54.062	6.670	
3.050	3936.25	13.80	107.77	56.225	0.000	54.011	6.616	
3.100	4005.30	13.82	108.25	56.186	0.000	53.963	6.565	
3.150	4074.44	13.84	108.71	56.148	0.000	53.908	6.517	
3.200	4143.70	13.86	109.15	56.111	0.000	53.876	6.470	
3.250	4213.02	13.88	109.58	56.074	0.000	53.841	6.426	
3.300	4282.45	13.89	109.99	56.037	0.000	53.794	6.384	
3.350	4351.95	13.91	110.39	56.001	0.000	53.748	6.344	
3.400	4421.54	13.93	110.77	55.966	0.000	53.720	6.306	
3.450	4491.20	13.94	111.15	55.931	0.000	53.693	6.270	
3.500	4560.95	13.96	111.51	55.896	0.000	53.655	6.235	
3.550	4630.77	13.97	111.86	55.862	0.000	53.629	6.202	
3.600	4700.66	13.98	112.18	55.829	0.000	53.618	6.171	
3.650	4770.62	14.00	112.53	55.796	0.000	53.567	6.141	
3.700	4840.65	14.02	112.86	55.764	0.000	53.542	6.113	
3.750	4910.75	14.03	113.13	55.732	0.000	53.525	6.086	
3.800	4980.90	14.04	113.44	55.701	0.000	53.505	6.060	
3.850	5051.13	14.06	113.78	55.670	0.000	53.458	6.035	

HYDROSTATIC PARTICULARS
mts "Argos GL"

Trim = 0.000 m							22 Jan 2015	13:08:27
Draft from base m	Displ. [S.W. 1.0000] ton	Immer- sion ton/cm	Moment change trim tonm/cm	LCB from APP m	TCB from CL m	LCF from transv. APP m	KM m	
3.900	5121.41	14.06	114.03	55.640	0.000	53.460	6.012	
3.950	5191.75	14.08	114.31	55.610	0.000	53.447	5.990	
4.000	5262.15	14.09	114.58	55.581	0.000	53.431	5.969	
4.050	5332.61	14.10	114.84	55.553	0.000	53.399	5.949	
4.100	5403.12	14.11	115.11	55.525	0.000	53.405	5.929	
4.150	5473.68	14.12	115.36	55.497	0.000	53.396	5.911	
4.200	5544.29	14.13	115.60	55.470	0.000	53.383	5.894	
4.250	5614.95	14.14	115.84	55.444	0.000	53.381	5.878	
4.300	5685.65	14.15	116.06	55.418	0.000	53.353	5.863	
4.350	5756.41	14.16	116.30	55.393	0.000	53.359	5.848	
4.400	5827.21	14.17	116.51	55.368	0.000	53.342	5.835	
4.450	5898.05	14.18	116.73	55.344	0.000	53.339	5.822	
4.500	5968.94	14.18	116.94	55.320	0.000	53.341	5.810	

Stability Calculation for Loading condition

Damage Stability

The damage stability calculations has been carried out in an earlier investigation of mts ARGOS GL. The conclusion of that investigation can be summarized as follows:

The stability criteria derived from ADN regulation 9.3.2.13, 9.3.2.14 and 9.3.2.15 valid for Type C Tankers are applied on the design and the watertight deviation of the compartments of the hull has been updated according the results of the damage calculations.. The so called Maximum allowable VCG table for damaged conditions is not critical for the expected loading conditions mts ARGOS GL will sail at. Till a (theoretical) draught of 4,50m a realistic loading condition can be achieved which complies to the regulations.

Intact Stability

LSW, 98% consumables with WB1 filled

TRIM AND STABILITY CALCULATION mts "Argos GL"

27 Jan 2015 13:11:27

Condition : LSW, 98% cons. with WB1 filled

Description	Filling %	S.W. ton/m ³	Weight ton	VCG m	LCG m	TCG m	FSM tonm
Empty ship	-	-	1733.480	3.975	53.588	0.000	0.000
Subtotals for group : Fuel Oil Tanks							
FO aft PS	98.0	0.850	7.184	3.791	8.622	-4.713	0.652
FO aft SB	98.0	0.850	7.184	3.791	8.622	4.713	0.652
SUBTOTAL	-	-	14.368	3.791	8.622	-0.000	1.303
Subtotals for group : LNG Propulsion Tanks							
LNG propulsion tank CL	98.0	0.650	34.274	3.746	95.153	0.000	10.554
SUBTOTAL	-	-	34.274	3.746	95.153	0.000	10.554
Subtotals for group : Fresh Water Tanks							
FW aft PS	98.0	1.000	8.636	1.706	12.277	-4.282	7.211
FW aft SB	98.0	1.000	8.636	1.706	12.277	4.282	7.211
SUBTOTAL	-	-	17.272	1.706	12.277	-0.000	14.421
Subtotals for group : Miscellaneous Tanks							
DW aft PS	98.0	1.000	6.017	1.898	10.295	-4.103	6.010
DW aft SB	98.0	1.000	6.017	1.898	10.295	4.103	6.010
SUBTOTAL	-	-	12.035	1.898	10.295	0.000	12.021
Subtotals for group : Water Ballast Tanks							
Aftpeak WB	0.0	1.000	0.000	1.954	2.833	0.000	0.000
WB aft CL	0.0	1.000	0.000	0.000	9.333	0.000	0.000
WB aft PS	0.0	1.000	0.000	0.838	9.333	-2.754	0.000
WB aft SB	0.0	1.000	0.000	0.838	9.333	2.754	0.000
WB aft1 PS	0.0	1.000	0.000	0.000	15.470	-3.155	0.000
WB aft1 SB	0.0	1.000	0.000	0.000	15.470	3.155	0.000
WB 8 U-Tank	0.0	1.000	0.000	0.000	24.044	0.000	0.000
WB 7 U-Tank	0.0	1.000	0.000	0.000	36.789	0.000	0.000
WB 6 U-Tank	0.0	1.000	0.000	0.000	48.142	0.000	0.000
WB 5 U-Tank	0.0	1.000	0.000	0.000	60.385	0.000	0.000
WB 4 U-Tank	0.0	1.000	0.000	0.000	71.735	0.000	0.000
WB 3 U-Tank	0.0	1.000	0.000	0.000	81.272	0.000	0.000
WB 2 U-Tank	0.0	1.000	0.000	-0.004	87.241	0.000	0.000
WB 1 U-Tank	98.0	1.000	154.476	1.886	94.054	0.000	527.623
WB fore PS	0.0	1.000	0.000	0.700	101.602	-4.249	0.000
WB fore SB	0.0	1.000	0.000	0.700	101.602	4.249	0.000
Forepeak WB	0.0	1.000	0.000	-0.010	107.244	0.000	0.000
SUBTOTAL	-	-	154.476	1.886	94.054	0.000	527.623
Subtotals for group : Cargo Tanks							
Cargo 02 PS	0.0	0.850	0.000	0.750	23.610	-0.095	0.000
Cargo 02 SB	0.0	0.850	0.000	0.750	23.610	0.095	0.000
Cargo 01 PS	0.0	0.850	0.000	0.750	83.792	-0.095	0.000
Cargo 01 SB	0.0	0.850	0.000	0.750	83.792	0.095	0.000
SUBTOTAL	-	-	0.000	0.000	0.000	0.000	0.000
Subtotals for group : LNG Cargo Tanks							
LNG TANK GTT 02	0.0	0.500	0.000	1.372	42.023	0.000	0.000
LNG TANK GTT 01	0.0	0.500	0.000	1.372	65.619	0.000	0.000
SUBTOTAL	-	-	0.000	0.000	0.000	0.000	0.000

Preliminary Stability information Booklet mts "Argos GL"

Date: 27 January 2015

TRIM AND STABILITY CALCULATION
mts "Argos GL"

27 Jan 2015 13:11:27

Condition : LSW, 98% cons. with WB1 filled

Description	Filling %	S.W. ton/m ³	Weight ton	VCG m	LCG m	TCG m	FSM tonm
Subtotals for group : Other Spaces and Compartments							
CD aft PS	0.0	1.000	0.000	0.361	11.333	-2.769	0.000
CD aft SB	0.0	1.000	0.000	0.361	11.333	2.769	0.000
CD aft1 PS	0.0	1.000	0.000	0.000	13.333	-2.764	0.000
CD aft1 SB	0.0	1.000	0.000	0.000	13.333	2.764	0.000
Void at side PS	0.0	1.000	0.000	3.800	5.294	-5.834	0.000
Void at side SB	0.0	1.000	0.000	3.800	5.294	5.834	0.000
Void at side2 PS	0.0	1.000	0.000	2.600	12.102	-5.997	0.000
Void at side2 SB	0.0	1.000	0.000	2.600	12.102	5.997	0.000
Void at side3 PS	0.0	1.000	0.000	4.950	11.536	-6.249	0.000
Void at side3 SB	0.0	1.000	0.000	4.950	11.536	6.249	0.000
POD compartment PS	0.0	1.000	0.000	1.117	6.833	-1.765	0.000
POD compartment SB	0.0	1.000	0.000	1.117	6.833	1.765	0.000
Void DB	0.0	1.000	0.000	0.000	13.794	0.026	0.000
Accommodation	0.0	1.000	0.000	2.600	13.750	0.000	0.000
Engine Room	0.0	1.000	0.000	0.600	13.236	0.143	0.000
Boxcooler aft PS	0.0	1.000	0.000	0.000	10.388	-0.522	0.000
CD aft	0.0	1.000	0.000	0.000	17.006	0.000	0.000
CD fore	0.0	1.000	0.000	-0.004	97.785	0.000	0.000
CD FO2LNG2	0.0	1.000	0.000	0.000	30.219	0.000	0.000
LNG TANK 02 W.O. GTT BLOCKS	0.0	1.000	0.000	0.950	42.018	0.000	0.000
Void above GTT	0.0	1.000	0.000	5.885	42.018	0.000	0.000
CD LNG1-2	0.0	1.000	0.000	0.000	53.816	0.000	0.000
LNG TANK 01 W.O. GTT BLOCKS	0.0	1.000	0.000	0.950	65.614	0.000	0.000
Void Above GTT	0.0	1.000	0.000	5.885	65.614	0.000	0.000
CD LNG1FO1	0.0	1.000	0.000	0.000	77.413	0.000	0.000
CD FO1-Propulsion	0.0	1.000	0.000	-0.004	90.160	0.000	0.000
Cargo hold LNG prop Tank CL	0.0	1.000	0.000	0.950	93.910	0.000	0.000
DB bowthr.rm	0.0	1.000	0.000	-0.001	101.311	0.000	0.000
Void fore PS	0.0	1.000	0.000	5.355	101.322	-5.500	0.000
Void fore SB	0.0	1.000	0.000	5.355	101.322	5.500	0.000
Bowthr.rm	0.0	1.000	0.000	0.700	101.446	0.000	0.000
Elec. Switch Room	0.0	1.000	0.000	2.855	100.360	1.465	0.000
LNG Generator Room	0.0	1.000	0.000	5.355	101.341	0.237	0.000
Forepeak	0.0	1.000	0.000	3.450	106.689	0.000	0.000
SUBTOTAL	-	-	0.000	0.000	0.000	0.000	0.000
TOTAL	-	-	1965.904	3.773	56.535	-0.000	565.922

TRIM AND STABILITY CALCULATION
mts "Argos GL"

27 Jan 2015 13:11:27

Condition : LSW, 98% cons. with WB1 filled

Hydrostatics

Volume 1951.270 m³
LCF 55.939 m
Mom. change trim 91.550 tonm/cm
Ton/cm immersion 13.063 ton/cm
Specific weight 1.000 ton/m³

Drafts and trim

Drafts above base :
Draft mean (Lpp/2) 1.585 m
Draft aft (App) 1.682 m
Draft fore (Fpp) 1.489 m
Trim -0.193 m

Transverse stability

KM transverse 10.259 m
VCG 3.773 m
GM solid 6.486 m
GG' correction 0.288 m
G'M liquid 6.198 m

VCG' 4.061 m

The stability values are calculated for the actual trim.

Statical and dynamical stability, calculated with constant LCB :

Angle(SB) degrees	Draft mld. m	Trim m	KNsinφ m	VCG'sinφ m	TCGcosφ m	G'Nsinφ m	Area mrad
0.00	1.585	-0.193	0.000	0.000	0.000	-0.000	0.000
2.00	1.585	-0.191	0.358	0.142	0.000	0.216	0.004
5.00	1.582	-0.180	0.897	0.354	0.000	0.543	0.024
7.00	1.579	-0.168	1.257	0.495	0.000	0.762	0.046
10.00	1.572	-0.142	1.800	0.705	0.000	1.095	0.095
12.00	1.565	-0.119	2.161	0.844	0.000	1.317	0.137
15.00	1.543	-0.081	2.672	1.051	0.000	1.621	0.214
20.00	1.442	-0.016	3.317	1.389	0.000	1.928	0.371
25.00	1.264	0.053	3.782	1.716	0.000	2.066	0.546
27.00	1.172	0.083	3.934	1.844	0.000	2.090	0.619
30.00	1.012	0.130	4.133	2.030	0.000	2.102	0.729
35.00	0.681	0.215	4.403	2.329	0.000	2.074	0.911
40.00	0.258	0.298	4.610	2.610	0.000	2.000	1.089

Statical angle of inclination is 0.000 degrees to starboard

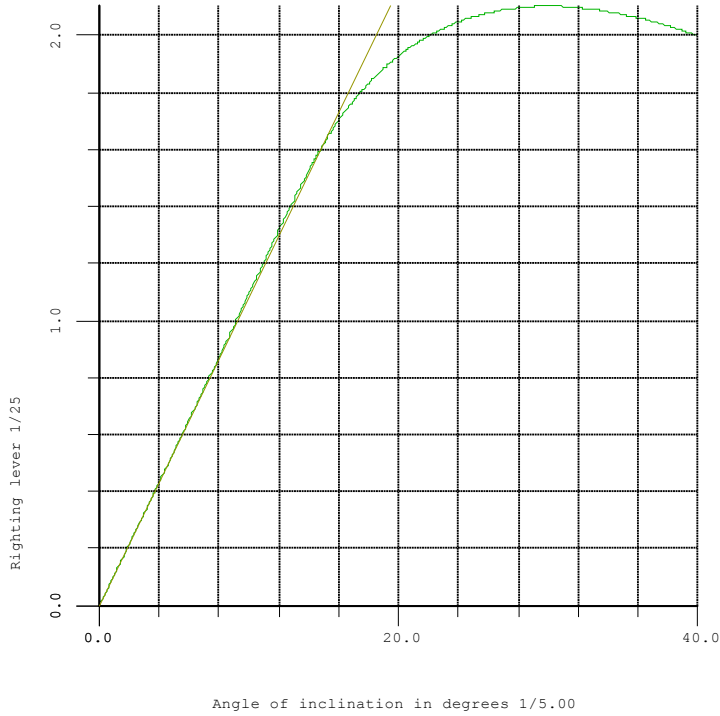
Summary

<u>Hydrostatics</u>	<u>Criterion</u>	<u>Value</u>
Draft mld.	4.500	1.585 m
Trim		-0.193 m
Statical angle of inclination		0.00 degrees SB
Flooding angle		40.00 degrees
<u>ADN intact stability tankers with tanks > 0.70 B</u>	<u>Criterion</u>	<u>Value</u>
Residual righting lever	0.100	2.102 meter
Area under the GZ curve up to 27 degrees	0.024	0.619 mrad
Minimum metacentric height G'M	0.100	6.198 meter
<u>VCG'</u>		
Actual		4.061 m
Maximum allowable		9.817 m
Loading condition complies with the stated criteria.		

TRIM AND STABILITY CALCULATION
mts "Argos GL"

27 Jan 2015 13:11:27

Condition : LSW, 98% cons. with WB1 filled



LSW, 98% consumables, fully ballasted

TRIM AND STABILITY CALCULATION

mts "Argos GL"

27 Jan 2015 13:11:56

Condition : LSW, 98% cons. fully ballasted

Description	Filling %	S.W. ton/m ³	Weight ton	VCG m	LCG m	TCG m	FSM tonm
Empty ship	-	-	1733.480	3.975	53.588	0.000	0.000
Subtotals for group : Fuel Oil Tanks							
FO aft PS	98.0	0.850	7.184	3.791	8.622	-4.713	0.652
FO aft SB	98.0	0.850	7.184	3.791	8.622	4.713	0.652
SUBTOTAL	-	-	14.368	3.791	8.622	-0.000	1.303
Subtotals for group : LNG Propulsion Tanks							
LNG propulsion tank CL	98.0	0.650	34.274	3.746	95.153	0.000	10.554
SUBTOTAL	-	-	34.274	3.746	95.153	0.000	10.554
Subtotals for group : Fresh Water Tanks							
FW aft PS	98.0	1.000	8.636	1.706	12.277	-4.282	7.211
FW aft SB	98.0	1.000	8.636	1.706	12.277	4.282	7.211
SUBTOTAL	-	-	17.272	1.706	12.277	-0.000	14.421
Subtotals for group : Miscellaneous Tanks							
DW aft PS	98.0	1.000	6.017	1.898	10.295	-4.103	6.010
DW aft SB	98.0	1.000	6.017	1.898	10.295	4.103	6.010
SUBTOTAL	-	-	12.035	1.898	10.295	0.000	12.021
Subtotals for group : Water Ballast Tanks							
Aftpeak WB	98.0	1.000	65.084	4.251	1.810	0.000	143.622
WB aft CL	98.0	1.000	32.773	1.685	6.810	0.000	30.424
WB aft PS	98.0	1.000	5.676	2.083	8.435	-3.831	5.777
WB aft SB	98.0	1.000	5.676	2.083	8.435	3.831	5.777
WB aft1 PS	98.0	1.000	22.794	1.510	15.054	-4.438	15.634
WB aft1 SB	98.0	1.000	22.794	1.510	15.054	4.438	15.634
WB 8 U-Tank	98.0	1.000	273.909	1.986	23.902	0.000	1024.719
WB 7 U-Tank	98.0	1.000	281.899	1.890	36.789	0.000	981.790
WB 6 U-Tank	98.0	1.000	255.733	1.952	48.371	0.000	926.792
WB 5 U-Tank	98.0	1.000	281.899	1.890	60.385	0.000	981.782
WB 4 U-Tank	98.0	1.000	255.336	1.950	71.958	0.000	924.704
WB 3 U-Tank	98.0	1.000	144.109	1.893	81.272	0.000	515.561
WB 2 U-Tank	98.0	1.000	120.247	2.018	87.454	0.000	464.307
WB 1 U-Tank	98.0	1.000	154.476	1.886	94.054	0.000	527.623
WB fore PS	98.0	1.000	41.356	3.299	101.698	-4.689	13.281
WB fore SB	98.0	1.000	41.356	3.299	101.698	4.689	13.281
Forepeak WB	98.0	1.000	34.670	1.894	106.568	0.000	25.660
SUBTOTAL	-	-	2039.785	2.047	56.217	-0.000	6616.367
Subtotals for group : Cargo Tanks							
Cargo 02 PS	0.0	0.850	0.000	0.750	23.610	-0.095	0.000
Cargo 02 SB	0.0	0.850	0.000	0.750	23.610	0.095	0.000
Cargo 01 PS	0.0	0.850	0.000	0.750	83.792	-0.095	0.000
Cargo 01 SB	0.0	0.850	0.000	0.750	83.792	0.095	0.000
SUBTOTAL	-	-	0.000	0.000	0.000	0.000	0.000
Subtotals for group : LNG Cargo Tanks							
LNG TANK GTT 02	0.0	0.500	0.000	1.372	42.023	0.000	0.000
LNG TANK GTT 01	0.0	0.500	0.000	1.372	65.619	0.000	0.000
SUBTOTAL	-	-	0.000	0.000	0.000	0.000	0.000

TRIM AND STABILITY CALCULATION
mts "Argos GL"

27 Jan 2015 13:11:56

Condition : LSW, 98% cons. fully ballasted

Description	Filling %	S.W. ton/m ³	Weight ton	VCG m	LCG m	TCG m	FSM tonm
Subtotals for group : Other Spaces and Compartments							
CD aft PS	0.0	1.000	0.000	0.361	11.333	-2.769	0.000
CD aft SB	0.0	1.000	0.000	0.361	11.333	2.769	0.000
CD aft1 PS	0.0	1.000	0.000	0.000	13.333	-2.764	0.000
CD aft1 SB	0.0	1.000	0.000	0.000	13.333	2.764	0.000
Void at side PS	0.0	1.000	0.000	3.800	5.294	-5.834	0.000
Void at side SB	0.0	1.000	0.000	3.800	5.294	5.834	0.000
Void at side2 PS	0.0	1.000	0.000	2.600	12.102	-5.997	0.000
Void at side2 SB	0.0	1.000	0.000	2.600	12.102	5.997	0.000
Void at side3 PS	0.0	1.000	0.000	4.950	11.536	-6.249	0.000
Void at side3 SB	0.0	1.000	0.000	4.950	11.536	6.249	0.000
POD compartment PS	0.0	1.000	0.000	1.117	6.833	-1.765	0.000
POD compartment SB	0.0	1.000	0.000	1.117	6.833	1.765	0.000
Void DB	0.0	1.000	0.000	0.000	13.794	0.026	0.000
Accommodation	0.0	1.000	0.000	2.600	13.750	0.000	0.000
Engine Room	0.0	1.000	0.000	0.600	13.236	0.143	0.000
Boxcooler aft PS	0.0	1.000	0.000	0.000	10.388	-0.522	0.000
CD aft	0.0	1.000	0.000	0.000	17.006	0.000	0.000
CD fore	0.0	1.000	0.000	-0.004	97.785	0.000	0.000
CD FO2LNG2	0.0	1.000	0.000	0.000	30.219	0.000	0.000
LNG TANK 02 W.O. GTT BLOCKS	0.0	1.000	0.000	0.950	42.018	0.000	0.000
Void above GTT	0.0	1.000	0.000	5.885	42.018	0.000	0.000
CD LNG1-2	0.0	1.000	0.000	0.000	53.816	0.000	0.000
LNG TANK 01 W.O. GTT BLOCKS	0.0	1.000	0.000	0.950	65.614	0.000	0.000
Void Above GTT	0.0	1.000	0.000	5.885	65.614	0.000	0.000
CD LNG1FO1	0.0	1.000	0.000	0.000	77.413	0.000	0.000
CD FO1-Propulsion	0.0	1.000	0.000	-0.004	90.160	0.000	0.000
Cargo hold LNG prop Tank CL	0.0	1.000	0.000	0.950	93.910	0.000	0.000
DB bowthr.rm	0.0	1.000	0.000	-0.001	101.311	0.000	0.000
Void fore PS	0.0	1.000	0.000	5.355	101.322	-5.500	0.000
Void fore SB	0.0	1.000	0.000	5.355	101.322	5.500	0.000
Bowthr.rm	0.0	1.000	0.000	0.700	101.446	0.000	0.000
Elec. Switch Room	0.0	1.000	0.000	2.855	100.360	1.465	0.000
LNG Generator Room	0.0	1.000	0.000	5.355	101.341	0.237	0.000
Forepeak	0.0	1.000	0.000	3.450	106.689	0.000	0.000
SUBTOTAL	-	-	0.000	0.000	0.000	0.000	0.000
TOTAL	-	-	3851.212	2.935	54.862	-0.000	6654.667

TRIM AND STABILITY CALCULATION
mts "Argos GL"

27 Jan 2015 13:11:56

Condition : LSW, 98% cons. fully ballasted

Hydrostatics

Volume 3822.543 m³
 LCF 53.766 m
 Mom. change trim 108.667 tonm/cm
 Ton/cm immersion 13.834 ton/cm
 Specific weight 1.000 ton/m³

Drafts and trim

Drafts above base :
 Draft mean (Lpp/2) 2.985 m
 Draft aft (App) 3.233 m
 Draft fore (Fpp) 2.736 m
 Trim -0.497 m

Transverse stability

KM transverse 6.715 m
 VCG 2.935 m
 GM solid 3.780 m
 GG' correction 1.728 m
 G'M liquid 2.052 m

VCG' 4.663 m

The stability values are calculated for the actual trim.

Statical and dynamical stability, calculated with constant LCB :

Angle(SB) degrees	Draft mld. m	Trim m	KNsinoφ m	VCG'sinoφ m	TCGcosφ m	G'Nsinoφ m	Area mrad
0.00	2.985	-0.497	0.000	0.000	-0.000	0.000	0.000
2.00	2.984	-0.496	0.234	0.163	-0.000	0.072	0.001
5.00	2.982	-0.489	0.587	0.406	-0.000	0.180	0.008
7.00	2.980	-0.481	0.823	0.568	-0.000	0.254	0.015
10.00	2.976	-0.464	1.179	0.810	-0.000	0.369	0.032
12.00	2.972	-0.449	1.418	0.969	-0.000	0.448	0.046
15.00	2.964	-0.421	1.780	1.207	-0.000	0.573	0.073
20.00	2.948	-0.363	2.396	1.595	-0.000	0.801	0.132
25.00	2.922	-0.321	3.009	1.971	-0.000	1.039	0.213
27.00	2.899	-0.314	3.237	2.117	-0.000	1.120	0.251
30.00	2.855	-0.316	3.526	2.331	-0.000	1.195	0.311
35.00	2.767	-0.309	3.884	2.674	-0.000	1.209	0.417
40.00	2.657	-0.272	4.129	2.997	-0.000	1.132	0.520

Statical angle of inclination is 0.000 degrees to starboard

Opening is submerged at [degrees]

Airvent WB 5 SB1 33.02

TRIM AND STABILITY CALCULATION
mts "Argos GL"

27 Jan 2015 13:11:56

Condition : LSW, 98% cons. fully ballasted

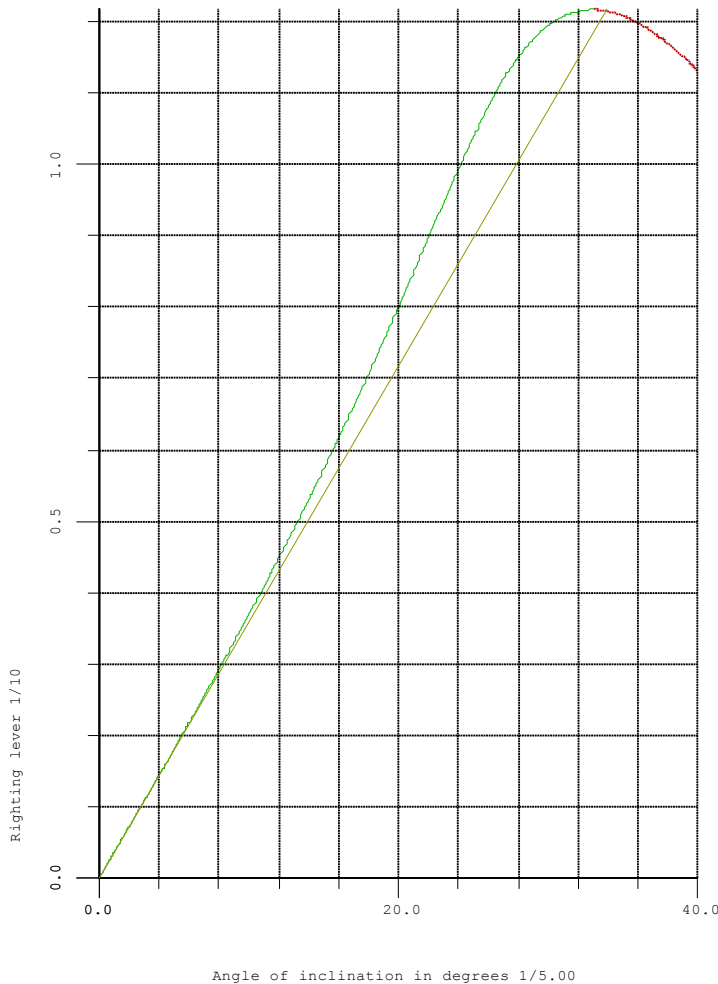
Summary

<u>Hydrostatics</u>		<u>Criterion</u>	<u>Value</u>
Draft mld.		4.500	2.985 m
Trim	-0.497 m		
Statlcal angle of inclination	0.00 degrees SB		
Flooding angle	33.02 degrees		

<u>ADN intact stability tankers with tanks > 0.70 B</u>		<u>Criterion</u>	<u>Value</u>
Residual righting lever		0.100	1.218 meter
Area under the GZ curve up to 27 degrees		0.024	0.251 mrad
Minimum metacentric height G'M		0.100	2.052 meter

<u>VCG'</u>	
Actual	4.663 m
Maximum allowable	6.614 m

Loading condition complies with the stated criteria.



LSW, 98% consumables, fully loaded FO and LNG with WB1 filled

TRIM AND STABILITY CALCULATION

mts "Argos GL"

27 Jan 2015 13:12:23

Condition : LSW, 98% cons. fully loaded FO and LNG with WB1 filled

Description	Filling %	S.W. ton/m ³	Weight ton	VCG m	LCG m	TCG m	FSM tonm
Empty ship	-	-	1733.480	3.975	53.588	0.000	0.000
Subtotals for group : Fuel Oil Tanks							
FO aft PS	98.0	0.850	7.184	3.791	8.622	-4.713	0.652
FO aft SB	98.0	0.850	7.184	3.791	8.622	4.713	0.652
SUBTOTAL	-	-	14.368	3.791	8.622	-0.000	1.303
Subtotals for group : LNG Propulsion Tanks							
LNG propulsion tank CL	98.0	0.650	34.274	3.746	95.153	0.000	10.554
SUBTOTAL	-	-	34.274	3.746	95.153	0.000	10.554
Subtotals for group : Fresh Water Tanks							
FW aft PS	98.0	1.000	8.636	1.706	12.277	-4.282	7.211
FW aft SB	98.0	1.000	8.636	1.706	12.277	4.282	7.211
SUBTOTAL	-	-	17.272	1.706	12.277	-0.000	14.421
Subtotals for group : Miscellaneous Tanks							
DW aft PS	98.0	1.000	6.017	1.898	10.295	-4.103	6.010
DW aft SB	98.0	1.000	6.017	1.898	10.295	4.103	6.010
SUBTOTAL	-	-	12.035	1.898	10.295	0.000	12.021
Subtotals for group : Water Ballast Tanks							
Aftpeak WB	0.0	1.000	0.000	1.954	2.833	0.000	0.000
WB aft CL	0.0	1.000	0.000	0.000	9.333	0.000	0.000
WB aft PS	0.0	1.000	0.000	0.838	9.333	-2.754	0.000
WB aft SB	0.0	1.000	0.000	0.838	9.333	2.754	0.000
WB aft1 PS	0.0	1.000	0.000	0.000	15.470	-3.155	0.000
WB aft1 SB	0.0	1.000	0.000	0.000	15.470	3.155	0.000
WB 8 U-Tank	0.0	1.000	0.000	0.000	24.044	0.000	0.000
WB 7 U-Tank	0.0	1.000	0.000	0.000	36.789	0.000	0.000
WB 6 U-Tank	0.0	1.000	0.000	0.000	48.142	0.000	0.000
WB 5 U-Tank	0.0	1.000	0.000	0.000	60.385	0.000	0.000
WB 4 U-Tank	0.0	1.000	0.000	0.000	71.735	0.000	0.000
WB 3 U-Tank	0.0	1.000	0.000	0.000	81.272	0.000	0.000
WB 2 U-Tank	0.0	1.000	0.000	-0.004	87.241	0.000	0.000
WB 1 U-Tank	98.0	1.000	154.476	1.886	94.054	0.000	527.623
WB fore PS	0.0	1.000	0.000	0.700	101.602	-4.249	0.000
WB fore SB	0.0	1.000	0.000	0.700	101.602	4.249	0.000
Forepeak WB	0.0	1.000	0.000	-0.010	107.244	0.000	0.000
SUBTOTAL	-	-	154.476	1.886	94.054	0.000	527.623
Subtotals for group : Cargo Tanks							
Cargo 02 PS	97.0	0.850	321.341	3.586	23.646	-2.839	163.870
Cargo 02 SB	97.0	0.850	321.341	3.586	23.646	2.839	163.870
Cargo 01 PS	97.0	0.850	311.464	3.570	83.792	-2.857	157.735
Cargo 01 SB	97.0	0.850	311.464	3.570	83.792	2.857	157.735
SUBTOTAL	-	-	1265.609	3.578	53.250	0.000	643.210
Subtotals for group : LNG Cargo Tanks							
LNG TANK GTT 02	95.0	0.500	442.703	3.310	42.023	0.000	1057.401
LNG TANK GTT 01	95.0	0.500	442.703	3.310	65.619	0.000	1057.408
SUBTOTAL	-	-	885.406	3.310	53.821	0.000	2114.809

TRIM AND STABILITY CALCULATION
mts "Argos GL"

27 Jan 2015 13:12:23

Condition : LSW, 98% cons. fully loaded FO and LNG with WB1 filled

Description	Filling %	S.W. ton/m ³	Weight ton	VCG m	LCG m	TCG m	FSM tonm
Subtotals for group : Other Spaces and Compartments							
CD aft PS	0.0	1.000	0.000	0.361	11.333	-2.769	0.000
CD aft SB	0.0	1.000	0.000	0.361	11.333	2.769	0.000
CD aft1 PS	0.0	1.000	0.000	0.000	13.333	-2.764	0.000
CD aft1 SB	0.0	1.000	0.000	0.000	13.333	2.764	0.000
Void at side PS	0.0	1.000	0.000	3.800	5.294	-5.834	0.000
Void at side SB	0.0	1.000	0.000	3.800	5.294	5.834	0.000
Void at side2 PS	0.0	1.000	0.000	2.600	12.102	-5.997	0.000
Void at side2 SB	0.0	1.000	0.000	2.600	12.102	5.997	0.000
Void at side3 PS	0.0	1.000	0.000	4.950	11.536	-6.249	0.000
Void at side3 SB	0.0	1.000	0.000	4.950	11.536	6.249	0.000
POD compartment PS	0.0	1.000	0.000	1.117	6.833	-1.765	0.000
POD compartment SB	0.0	1.000	0.000	1.117	6.833	1.765	0.000
Void DB	0.0	1.000	0.000	0.000	13.794	0.026	0.000
Accommodation	0.0	1.000	0.000	2.600	13.750	0.000	0.000
Engine Room	0.0	1.000	0.000	0.600	13.236	0.143	0.000
Boxcooler aft PS	0.0	1.000	0.000	0.000	10.388	-0.522	0.000
CD aft	0.0	1.000	0.000	0.000	17.006	0.000	0.000
CD fore	0.0	1.000	0.000	-0.004	97.785	0.000	0.000
CD FO2LNG2	0.0	1.000	0.000	0.000	30.219	0.000	0.000
LNG TANK 02 W.O. GTT BLOCKS	0.0	1.000	0.000	0.950	42.018	0.000	0.000
Void above GTT	0.0	1.000	0.000	5.885	42.018	0.000	0.000
CD LNG1-2	0.0	1.000	0.000	0.000	53.816	0.000	0.000
LNG TANK 01 W.O. GTT BLOCKS	0.0	1.000	0.000	0.950	65.614	0.000	0.000
Void Above GTT	0.0	1.000	0.000	5.885	65.614	0.000	0.000
CD LNG1FO1	0.0	1.000	0.000	0.000	77.413	0.000	0.000
CD FO1-Propulsion	0.0	1.000	0.000	-0.004	90.160	0.000	0.000
Cargo hold LNG prop Tank CL	0.0	1.000	0.000	0.950	93.910	0.000	0.000
DB bowthr.rm	0.0	1.000	0.000	-0.001	101.311	0.000	0.000
Void fore PS	0.0	1.000	0.000	5.355	101.322	-5.500	0.000
Void fore SB	0.0	1.000	0.000	5.355	101.322	5.500	0.000
Bowthr.rm	0.0	1.000	0.000	0.700	101.446	0.000	0.000
Elec. Switch Room	0.0	1.000	0.000	2.855	100.360	1.465	0.000
LNG Generator Room	0.0	1.000	0.000	5.355	101.341	0.237	0.000
Forepeak	0.0	1.000	0.000	3.450	106.689	0.000	0.000
SUBTOTAL	-	-	0.000	0.000	0.000	0.000	0.000
TOTAL	-	-	4116.919	3.614	54.942	0.000	3323.940

TRIM AND STABILITY CALCULATION
mts "Argos GL"

27 Jan 2015 13:12:23

Condition : LSW, 98% cons. fully loaded FO and LNG with WB1 filled

<u>Hydrostatics</u>		<u>Drafts and trim</u>	
Volume	4086.273 m ³	Drafts above base :	
LCF	53.646 m	Draft mean (Lpp/2)	3.177 m
Mom. change trim	110.065 tonm/cm	Draft aft (App)	3.397 m
Ton/cm immersion	13.895 ton/cm	Draft fore (Fpp)	2.957 m
Specific weight	1.000 ton/m ³	Trim	-0.440 m

<u>Transverse stability</u>			
KM transverse	6.513 m		
VCG	3.614 m		
GM solid	2.900 m		
GG' correction	0.807 m		
G'M liquid	2.092 m	VCG'	4.421 m

The stability values are calculated for the actual trim.

Statical and dynamical stability, calculated with constant LCB :

Angle(SB)	Draft mld.	Trim	KNsinφ	VCG'sinφ	TCGcosφ	G'Nsinφ	Area
degrees	m	m	m	m	m	m	mrاد
0.00	3.177	-0.440	0.000	0.000	0.000	-0.000	0.000
2.00	3.176	-0.438	0.227	0.154	0.000	0.073	0.001
5.00	3.175	-0.432	0.569	0.385	0.000	0.184	0.008
7.00	3.173	-0.424	0.798	0.539	0.000	0.259	0.016
10.00	3.169	-0.409	1.143	0.768	0.000	0.375	0.032
12.00	3.165	-0.395	1.375	0.919	0.000	0.456	0.047
15.00	3.158	-0.370	1.726	1.144	0.000	0.581	0.074
20.00	3.144	-0.325	2.319	1.512	0.000	0.807	0.134
25.00	3.124	-0.295	2.921	1.868	0.000	1.053	0.215
27.00	3.112	-0.292	3.149	2.007	0.000	1.142	0.254
30.00	3.090	-0.290	3.432	2.210	0.000	1.222	0.316
35.00	3.043	-0.268	3.786	2.536	0.000	1.251	0.425
40.00	2.980	-0.214	4.034	2.842	0.000	1.192	0.532

Statical angle of inclination is 0.000 degrees to starboard

Opening is submerged at [degrees]

Airvent WB 5 SB1 31.26

TRIM AND STABILITY CALCULATION
mts "Argos GL"

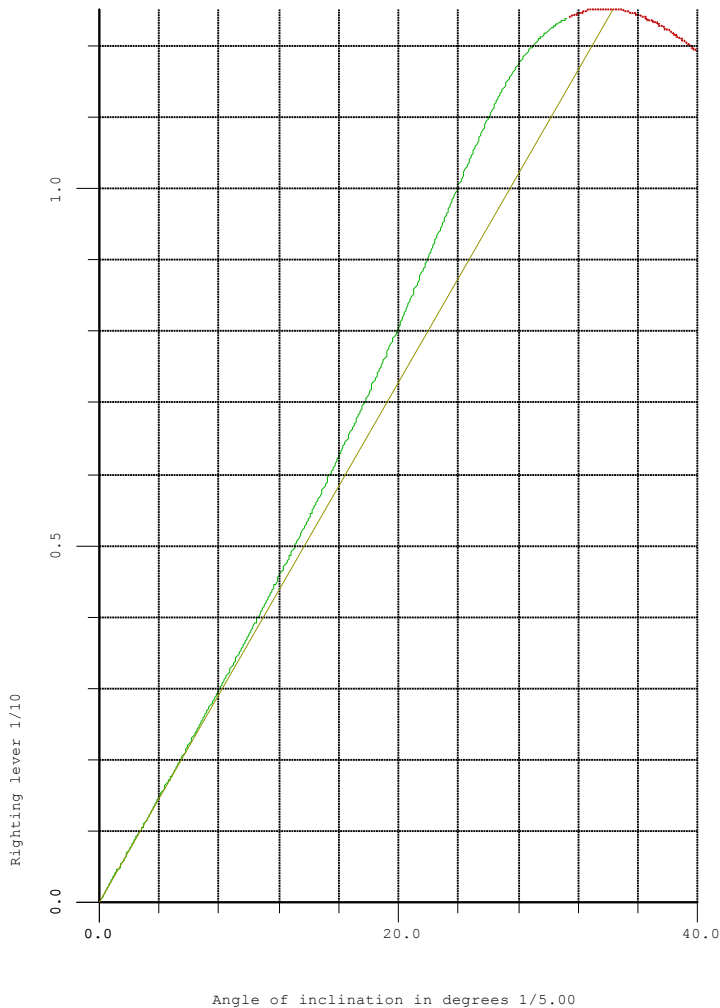
27 Jan 2015 13:12:23

Condition : LSW, 98% cons. fully loaded FO and LNG with WB1 filled

Summary

<u>Hydrostatics</u>		<u>Criterion</u>	<u>Value</u>
Draft mld.		4.500	3.177 m
Trim	-0.440 m		
Statical angle of inclination	0.00 degrees SB		
Flooding angle	31.26 degrees		
<u>ADN intact stability tankers with tanks > 0.70 B</u>		<u>Criterion</u>	<u>Value</u>
Residual righting lever		0.100	1.240 meter
Area under the GZ curve up to 27 degrees		0.024	0.254 mrad
Minimum metacentric height G'M		0.100	2.092 meter
<u>VCG'</u>			
Actual	4.421 m		
Maximum allowable	6.413 m		

Loading condition complies with the stated criteria.



LSW, 98% consumables, 97% FO, 50% LNG with WB1 filled

TRIM AND STABILITY CALCULATION

mts "Argos GL"

27 Jan 2015 13:12:35

Condition : LSW, 98% cons. 97% FO, 50% LNG with WB1 filled

Description	Filling %	S.W. ton/m ³	Weight ton	VCG m	LCG m	TCG m	FSM tonm
Empty ship	-	-	1733.480	3.975	53.588	0.000	0.000
Subtotals for group : Fuel Oil Tanks							
FO aft PS	98.0	0.850	7.184	3.791	8.622	-4.713	0.652
FO aft SB	98.0	0.850	7.184	3.791	8.622	4.713	0.652
SUBTOTAL	-	-	14.368	3.791	8.622	-0.000	1.303
Subtotals for group : LNG Propulsion Tanks							
LNG propulsion tank CL	98.0	0.650	34.274	3.746	95.153	0.000	10.554
SUBTOTAL	-	-	34.274	3.746	95.153	0.000	10.554
Subtotals for group : Fresh Water Tanks							
FW aft PS	98.0	1.000	8.636	1.706	12.277	-4.282	7.211
FW aft SB	98.0	1.000	8.636	1.706	12.277	4.282	7.211
SUBTOTAL	-	-	17.272	1.706	12.277	-0.000	14.421
Subtotals for group : Miscellaneous Tanks							
DW aft PS	98.0	1.000	6.017	1.898	10.295	-4.103	6.010
DW aft SB	98.0	1.000	6.017	1.898	10.295	4.103	6.010
SUBTOTAL	-	-	12.035	1.898	10.295	0.000	12.021
Subtotals for group : Water Ballast Tanks							
Aftpeak WB	0.0	1.000	0.000	1.954	2.833	0.000	0.000
WB aft CL	0.0	1.000	0.000	0.000	9.333	0.000	0.000
WB aft PS	0.0	1.000	0.000	0.838	9.333	-2.754	0.000
WB aft SB	0.0	1.000	0.000	0.838	9.333	2.754	0.000
WB aft1 PS	0.0	1.000	0.000	0.000	15.470	-3.155	0.000
WB aft1 SB	0.0	1.000	0.000	0.000	15.470	3.155	0.000
WB 8 U-Tank	0.0	1.000	0.000	0.000	24.044	0.000	0.000
WB 7 U-Tank	0.0	1.000	0.000	0.000	36.789	0.000	0.000
WB 6 U-Tank	0.0	1.000	0.000	0.000	48.142	0.000	0.000
WB 5 U-Tank	0.0	1.000	0.000	0.000	60.385	0.000	0.000
WB 4 U-Tank	0.0	1.000	0.000	0.000	71.735	0.000	0.000
WB 3 U-Tank	0.0	1.000	0.000	0.000	81.272	0.000	0.000
WB 2 U-Tank	0.0	1.000	0.000	-0.004	87.241	0.000	0.000
WB 1 U-Tank	98.0	1.000	154.476	1.886	94.054	0.000	527.623
WB fore PS	0.0	1.000	0.000	0.700	101.602	-4.249	0.000
WB fore SB	0.0	1.000	0.000	0.700	101.602	4.249	0.000
Forepeak WB	0.0	1.000	0.000	-0.010	107.244	0.000	0.000
SUBTOTAL	-	-	154.476	1.886	94.054	0.000	527.623
Subtotals for group : Cargo Tanks							
Cargo 02 PS	97.0	0.850	321.341	3.586	23.646	-2.839	163.870
Cargo 02 SB	97.0	0.850	321.341	3.586	23.646	2.839	163.870
Cargo 01 PS	97.0	0.850	311.464	3.570	83.792	-2.857	157.735
Cargo 01 SB	97.0	0.850	311.464	3.570	83.792	2.857	157.735
SUBTOTAL	-	-	1265.609	3.578	53.250	0.000	643.210
Subtotals for group : LNG Cargo Tanks							
LNG TANK GTT 02	50.0	0.500	233.002	2.392	42.023	0.000	1057.389
LNG TANK GTT 01	50.0	0.500	233.002	2.392	65.619	0.000	1057.394
SUBTOTAL	-	-	466.003	2.392	53.821	0.000	2114.782

TRIM AND STABILITY CALCULATION
mts "Argos GL"

27 Jan 2015 13:12:35

Condition : LSW, 98% cons. 97% FO, 50% LNG with WB1 filled

Description	Filling %	S.W. ton/m ³	Weight ton	VCG m	LCG m	TCG m	FSM tonm
Subtotals for group : Other Spaces and Compartments							
CD aft PS	0.0	1.000	0.000	0.361	11.333	-2.769	0.000
CD aft SB	0.0	1.000	0.000	0.361	11.333	2.769	0.000
CD aft1 PS	0.0	1.000	0.000	0.000	13.333	-2.764	0.000
CD aft1 SB	0.0	1.000	0.000	0.000	13.333	2.764	0.000
Void at side PS	0.0	1.000	0.000	3.800	5.294	-5.834	0.000
Void at side SB	0.0	1.000	0.000	3.800	5.294	5.834	0.000
Void at side2 PS	0.0	1.000	0.000	2.600	12.102	-5.997	0.000
Void at side2 SB	0.0	1.000	0.000	2.600	12.102	5.997	0.000
Void at side3 PS	0.0	1.000	0.000	4.950	11.536	-6.249	0.000
Void at side3 SB	0.0	1.000	0.000	4.950	11.536	6.249	0.000
POD compartment PS	0.0	1.000	0.000	1.117	6.833	-1.765	0.000
POD compartment SB	0.0	1.000	0.000	1.117	6.833	1.765	0.000
Void DB	0.0	1.000	0.000	0.000	13.794	0.026	0.000
Accommodation	0.0	1.000	0.000	2.600	13.750	0.000	0.000
Engine Room	0.0	1.000	0.000	0.600	13.236	0.143	0.000
Boxcooler aft PS	0.0	1.000	0.000	0.000	10.388	-0.522	0.000
CD aft	0.0	1.000	0.000	0.000	17.006	0.000	0.000
CD fore	0.0	1.000	0.000	-0.004	97.785	0.000	0.000
CD FO2LNG2	0.0	1.000	0.000	0.000	30.219	0.000	0.000
LNG TANK 02 W.O. GTT BLOCKS	0.0	1.000	0.000	0.950	42.018	0.000	0.000
Void above GTT	0.0	1.000	0.000	5.885	42.018	0.000	0.000
CD LNG1-2	0.0	1.000	0.000	0.000	53.816	0.000	0.000
LNG TANK 01 W.O. GTT BLOCKS	0.0	1.000	0.000	0.950	65.614	0.000	0.000
Void Above GTT	0.0	1.000	0.000	5.885	65.614	0.000	0.000
CD LNG1FO1	0.0	1.000	0.000	0.000	77.413	0.000	0.000
CD FO1-Propulsion	0.0	1.000	0.000	-0.004	90.160	0.000	0.000
Cargo hold LNG prop Tank CL	0.0	1.000	0.000	0.950	93.910	0.000	0.000
DB bowthr.rm	0.0	1.000	0.000	-0.001	101.311	0.000	0.000
Void fore PS	0.0	1.000	0.000	5.355	101.322	-5.500	0.000
Void fore SB	0.0	1.000	0.000	5.355	101.322	5.500	0.000
Bowthr.rm	0.0	1.000	0.000	0.700	101.446	0.000	0.000
Elec. Switch Room	0.0	1.000	0.000	2.855	100.360	1.465	0.000
LNG Generator Room	0.0	1.000	0.000	5.355	101.341	0.237	0.000
Forepeak	0.0	1.000	0.000	3.450	106.689	0.000	0.000
SUBTOTAL	-	-	0.000	0.000	0.000	0.000	0.000
TOTAL	-	-	3697.517	3.532	55.069	0.000	3323.914

TRIM AND STABILITY CALCULATION
mts "Argos GL"

27 Jan 2015 13:12:35

Condition : LSW, 98% cons. 97% FO, 50% LNG with WB1 filled

<u>Hydrostatics</u>		<u>Drafts and trim</u>	
Volume	3669.992 m ³	Drafts above base :	
LCF	53.896 m	Draft mean (Lpp/2)	2.874 m
Mom. change trim	107.501 tonm/cm	Draft aft (App)	3.095 m
Ton/cm immersion	13.788 ton/cm	Draft fore (Fpp)	2.653 m
Specific weight	1.000 ton/m ³	Trim	-0.442 m

<u>Transverse stability</u>			
KM transverse	6.843 m		
VCG	3.532 m		
GM solid	3.311 m		
GG' correction	0.899 m		
G'M liquid	2.412 m	VCG'	4.431 m

The stability values are calculated for the actual trim.

Statical and dynamical stability, calculated with constant LCB :

Angle(SB)	Draft mld.	Trim	KNsinφ	VCG'sinφ	TCGcosφ	G'Nsinφ	Area
degrees	m	m	m	m	m	m	mrاد
0.00	2.874	-0.442	0.000	0.000	0.000	-0.000	0.000
2.00	2.873	-0.440	0.239	0.155	0.000	0.084	0.001
5.00	2.872	-0.433	0.598	0.386	0.000	0.212	0.009
7.00	2.869	-0.425	0.839	0.540	0.000	0.298	0.018
10.00	2.865	-0.406	1.201	0.769	0.000	0.432	0.037
12.00	2.861	-0.391	1.445	0.921	0.000	0.524	0.054
15.00	2.853	-0.361	1.815	1.147	0.000	0.668	0.085
20.00	2.835	-0.295	2.444	1.516	0.000	0.928	0.155
25.00	2.803	-0.242	3.062	1.873	0.000	1.190	0.247
27.00	2.775	-0.230	3.285	2.012	0.000	1.273	0.290
30.00	2.719	-0.225	3.578	2.216	0.000	1.362	0.360
35.00	2.607	-0.211	3.937	2.542	0.000	1.395	0.481
40.00	2.470	-0.171	4.181	2.848	0.000	1.333	0.600

Statical angle of inclination is 0.000 degrees to starboard

Opening is submerged at [degrees]
Airvent WB 5 SB1 34.39

TRIM AND STABILITY CALCULATION
mts "Argos GL"

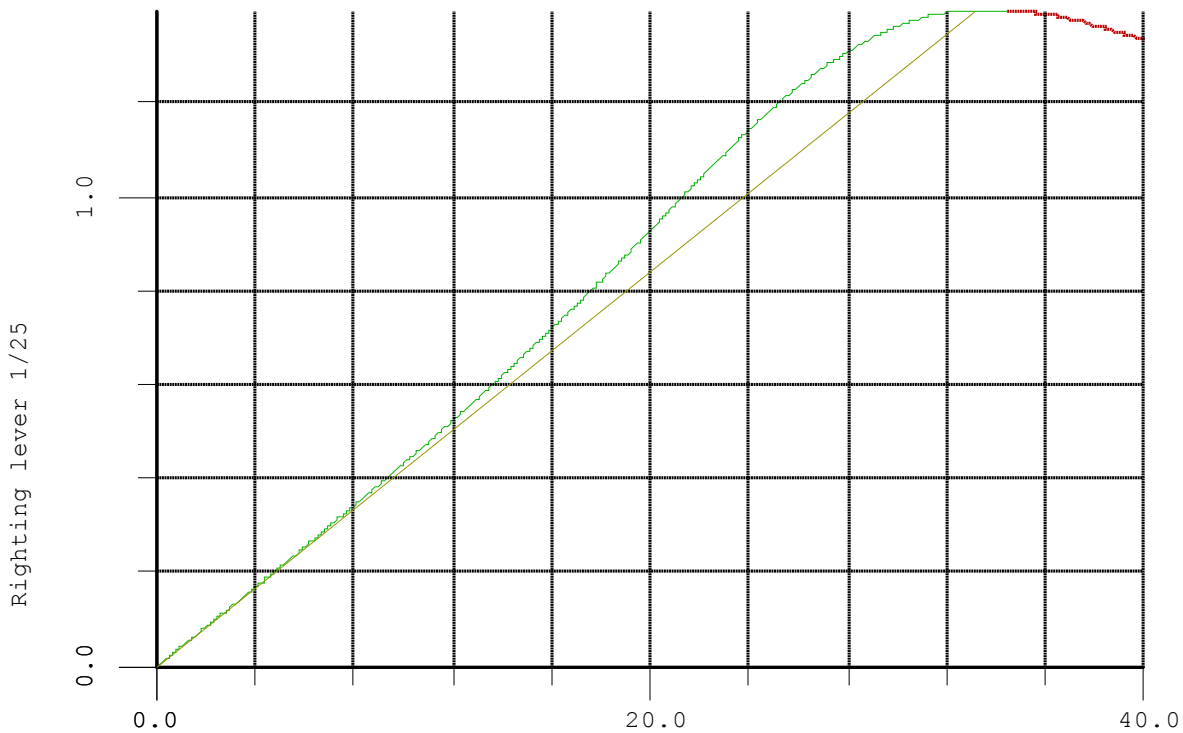
27 Jan 2015 13:12:35

Condition : LSW, 98% cons. 97% FO, 50% LNG with WB1 filled

Summary

<u>Hydrostatics</u>		<u>Criterion</u>	<u>Value</u>
Draft mld.		4.500	2.874 m
Trim	-0.442 m		
Statical angle of inclination	0.00 degrees SB		
Flooding angle	34.39 degrees		
 <u>ADN intact stability tankers with tanks > 0.70 B</u>		<u>Criterion</u>	<u>Value</u>
Residual righting lever		0.100	1.399 meter
Area under the GZ curve up to 27 degrees		0.024	0.290 mrad
Minimum metacentric height G'M		0.100	2.412 meter
 <u>VCG'</u>			
Actual	4.431 m		
Maximum allowable	6.743 m		

Loading condition complies with the stated criteria.



Angle of inclination in degrees 1/5.00

LSW, 98% consumables, 50% FO, 50% LNG with WB1 filled

TRIM AND STABILITY CALCULATION

mts "Argos GL"

27 Jan 2015 13:12:50

Condition : LSW, 98% cons. 50% FO, 50% LNG with WB1 filled

Description	Filling %	S.W. ton/m ³	Weight ton	VCG m	LCG m	TCG m	FSM tonm
Empty ship	-	-	1733.480	3.975	53.588	0.000	0.000
Subtotals for group : Fuel Oil Tanks							
FO aft PS	98.0	0.850	7.184	3.791	8.622	-4.713	0.652
FO aft SB	98.0	0.850	7.184	3.791	8.622	4.713	0.652
SUBTOTAL	-	-	14.368	3.791	8.622	-0.000	1.303
Subtotals for group : LNG Propulsion Tanks							
LNG propulsion tank CL	98.0	0.650	34.274	3.746	95.153	0.000	10.554
SUBTOTAL	-	-	34.274	3.746	95.153	0.000	10.554
Subtotals for group : Fresh Water Tanks							
FW aft PS	98.0	1.000	8.636	1.706	12.277	-4.282	7.211
FW aft SB	98.0	1.000	8.636	1.706	12.277	4.282	7.211
SUBTOTAL	-	-	17.272	1.706	12.277	-0.000	14.421
Subtotals for group : Miscellaneous Tanks							
DW aft PS	98.0	1.000	6.017	1.898	10.295	-4.103	6.010
DW aft SB	98.0	1.000	6.017	1.898	10.295	4.103	6.010
SUBTOTAL	-	-	12.035	1.898	10.295	0.000	12.021
Subtotals for group : Water Ballast Tanks							
Aftpeak WB	0.0	1.000	0.000	1.954	2.833	0.000	0.000
WB aft CL	0.0	1.000	0.000	0.000	9.333	0.000	0.000
WB aft PS	0.0	1.000	0.000	0.838	9.333	-2.754	0.000
WB aft SB	0.0	1.000	0.000	0.838	9.333	2.754	0.000
WB aft1 PS	0.0	1.000	0.000	0.000	15.470	-3.155	0.000
WB aft1 SB	0.0	1.000	0.000	0.000	15.470	3.155	0.000
WB 8 U-Tank	0.0	1.000	0.000	0.000	24.044	0.000	0.000
WB 7 U-Tank	0.0	1.000	0.000	0.000	36.789	0.000	0.000
WB 6 U-Tank	0.0	1.000	0.000	0.000	48.142	0.000	0.000
WB 5 U-Tank	0.0	1.000	0.000	0.000	60.385	0.000	0.000
WB 4 U-Tank	0.0	1.000	0.000	0.000	71.735	0.000	0.000
WB 3 U-Tank	0.0	1.000	0.000	0.000	81.272	0.000	0.000
WB 2 U-Tank	0.0	1.000	0.000	-0.004	87.241	0.000	0.000
WB 1 U-Tank	98.0	1.000	154.476	1.886	94.054	0.000	527.623
WB fore PS	0.0	1.000	0.000	0.700	101.602	-4.249	0.000
WB fore SB	0.0	1.000	0.000	0.700	101.602	4.249	0.000
Forepeak WB	0.0	1.000	0.000	-0.010	107.244	0.000	0.000
SUBTOTAL	-	-	154.476	1.886	94.054	0.000	527.623
Subtotals for group : Cargo Tanks							
Cargo 02 PS	50.0	0.850	165.640	2.273	23.680	-2.804	163.876
Cargo 02 SB	50.0	0.850	165.640	2.273	23.680	2.804	163.876
Cargo 01 PS	50.0	0.850	160.548	2.252	83.792	-2.841	157.728
Cargo 01 SB	50.0	0.850	160.548	2.252	83.792	2.841	157.728
SUBTOTAL	-	-	652.376	2.262	53.267	0.000	643.208
Subtotals for group : LNG Cargo Tanks							
LNG TANK GTT 02	50.0	0.500	233.002	2.392	42.023	0.000	1057.389
LNG TANK GTT 01	50.0	0.500	233.002	2.392	65.619	0.000	1057.394
SUBTOTAL	-	-	466.003	2.392	53.821	0.000	2114.782

TRIM AND STABILITY CALCULATION
mts "Argos GL"

27 Jan 2015 13:12:50

Condition : LSW, 98% cons. 50% FO, 50% LNG with WB1 filled

Description	Filling %	S.W. ton/m ³	Weight ton	VCG m	LCG m	TCG m	FSM tonm
Subtotals for group : Other Spaces and Compartments							
CD aft PS	0.0	1.000	0.000	0.361	11.333	-2.769	0.000
CD aft SB	0.0	1.000	0.000	0.361	11.333	2.769	0.000
CD aft1 PS	0.0	1.000	0.000	0.000	13.333	-2.764	0.000
CD aft1 SB	0.0	1.000	0.000	0.000	13.333	2.764	0.000
Void at side PS	0.0	1.000	0.000	3.800	5.294	-5.834	0.000
Void at side SB	0.0	1.000	0.000	3.800	5.294	5.834	0.000
Void at side2 PS	0.0	1.000	0.000	2.600	12.102	-5.997	0.000
Void at side2 SB	0.0	1.000	0.000	2.600	12.102	5.997	0.000
Void at side3 PS	0.0	1.000	0.000	4.950	11.536	-6.249	0.000
Void at side3 SB	0.0	1.000	0.000	4.950	11.536	6.249	0.000
POD compartment PS	0.0	1.000	0.000	1.117	6.833	-1.765	0.000
POD compartment SB	0.0	1.000	0.000	1.117	6.833	1.765	0.000
Void DB	0.0	1.000	0.000	0.000	13.794	0.026	0.000
Accommodation	0.0	1.000	0.000	2.600	13.750	0.000	0.000
Engine Room	0.0	1.000	0.000	0.600	13.236	0.143	0.000
Boxcooler aft PS	0.0	1.000	0.000	0.000	10.388	-0.522	0.000
CD aft	0.0	1.000	0.000	0.000	17.006	0.000	0.000
CD fore	0.0	1.000	0.000	-0.004	97.785	0.000	0.000
CD FO2LNG2	0.0	1.000	0.000	0.000	30.219	0.000	0.000
LNG TANK 02 W.O. GTT BLOCKS	0.0	1.000	0.000	0.950	42.018	0.000	0.000
Void above GTT	0.0	1.000	0.000	5.885	42.018	0.000	0.000
CD LNG1-2	0.0	1.000	0.000	0.000	53.816	0.000	0.000
LNG TANK 01 W.O. GTT BLOCKS	0.0	1.000	0.000	0.950	65.614	0.000	0.000
Void Above GTT	0.0	1.000	0.000	5.885	65.614	0.000	0.000
CD LNG1FO1	0.0	1.000	0.000	0.000	77.413	0.000	0.000
CD FO1-Propulsion	0.0	1.000	0.000	-0.004	90.160	0.000	0.000
Cargo hold LNG prop Tank CL	0.0	1.000	0.000	0.950	93.910	0.000	0.000
DB bowthr.rm	0.0	1.000	0.000	-0.001	101.311	0.000	0.000
Void fore PS	0.0	1.000	0.000	5.355	101.322	-5.500	0.000
Void fore SB	0.0	1.000	0.000	5.355	101.322	5.500	0.000
Bowthr.rm	0.0	1.000	0.000	0.700	101.446	0.000	0.000
Elec. Switch Room	0.0	1.000	0.000	2.855	100.360	1.465	0.000
LNG Generator Room	0.0	1.000	0.000	5.355	101.341	0.237	0.000
Forepeak	0.0	1.000	0.000	3.450	106.689	0.000	0.000
SUBTOTAL	-	-	0.000	0.000	0.000	0.000	0.000
TOTAL	-	-	3084.283	3.245	55.434	0.000	3323.913

TRIM AND STABILITY CALCULATION
mts "Argos GL"

27 Jan 2015 13:12:50

Condition : LSW, 98% cons. 50% FO, 50% LNG with WB1 filled

<u>Hydrostatics</u>		<u>Drafts and trim</u>	
Volume	3061.338 m ³	Drafts above base :	
LCF	54.497 m	Draft mean (Lpp/2)	2.426 m
Mom. change trim	102.302 tonm/cm	Draft aft (App)	2.620 m
Ton/cm immersion	13.568 ton/cm	Draft fore (Fpp)	2.232 m
Specific weight	1.000 ton/m ³	Trim	-0.387 m

<u>Transverse stability</u>			
KM transverse	7.550 m		
VCG	3.245 m		
GM solid	4.305 m		
GG' correction	1.078 m		
G'M liquid	3.227 m	VCG'	4.323 m

The stability values are calculated for the actual trim.

Statical and dynamical stability, calculated with constant LCB :

Angle(SB) degrees	Draft mld. m	Trim m	KNsinφ m	VCG'sinφ m	TCGcosφ m	G'Nsinφ m	Area mrad
0.00	2.426	-0.387	0.000	0.000	0.000	-0.000	0.000
2.00	2.425	-0.386	0.264	0.151	0.000	0.113	0.002
5.00	2.423	-0.378	0.660	0.377	0.000	0.283	0.012
7.00	2.421	-0.369	0.925	0.527	0.000	0.398	0.024
10.00	2.416	-0.348	1.325	0.751	0.000	0.575	0.050
12.00	2.411	-0.329	1.594	0.899	0.000	0.696	0.072
15.00	2.402	-0.294	2.003	1.119	0.000	0.884	0.113
20.00	2.377	-0.216	2.689	1.478	0.000	1.211	0.205
25.00	2.305	-0.136	3.290	1.827	0.000	1.463	0.322
27.00	2.257	-0.112	3.492	1.962	0.000	1.529	0.374
30.00	2.164	-0.087	3.762	2.161	0.000	1.601	0.457
35.00	1.957	-0.062	4.132	2.479	0.000	1.653	0.599
40.00	1.711	-0.029	4.377	2.778	0.000	1.599	0.742

Statical angle of inclination is 0.000 degrees to starboard

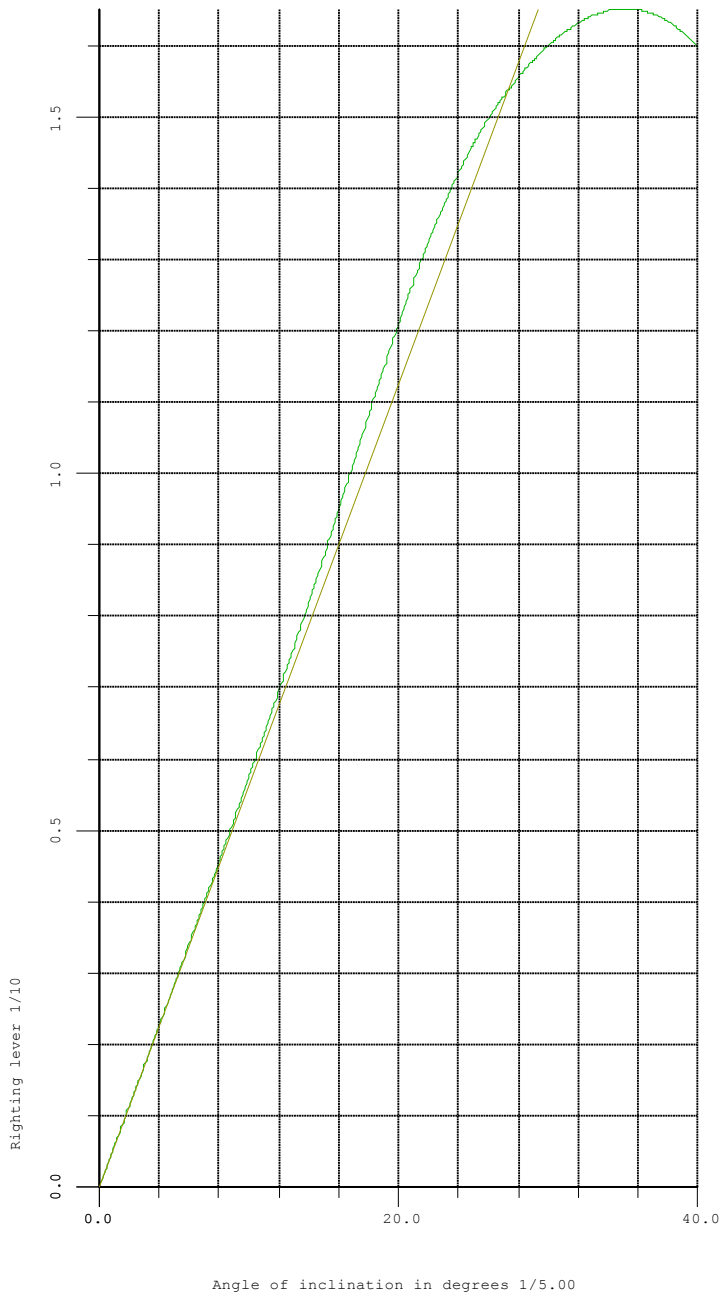
Summary

<u>Hydrostatics</u>	<u>Criterion</u>	<u>Value</u>
Draft mld.	4.500	2.426 m
Trim	-0.387 m	
Statical angle of inclination	0.00 degrees SB	
Flooding angle	40.00 degrees	
<u>ADN intact stability tankers with tanks > 0.70 B</u>	<u>Criterion</u>	<u>Value</u>
Residual righting lever	0.100	1.653 meter
Area under the GZ curve up to 27 degrees	0.024	0.374 mrad
Minimum metacentric height G'M	0.100	3.227 meter
<u>VCG'</u>		
Actual	4.323 m	
Maximum allowable	7.449 m	
<u>Loading condition complies with the stated criteria.</u>		

TRIM AND STABILITY CALCULATION
mts "Argos GL"

27 Jan 2015 13:12:50

Condition : LSW, 98% cons. 50% FO, 50% LNG with WB1 filled



LSW, 98% consumables, 10% FO, 10% LNG

TRIM AND STABILITY CALCULATION

mts "Argos GL"

27 Jan 2015 13:13:04

Condition : LSW, 98% cons. 10% FO, 10% LNG with WB1 filled

Description	Filling %	S.W. ton/m ³	Weight ton	VCG m	LCG m	TCG m	FSM tonm
Empty ship	-	-	1733.480	3.975	53.588	0.000	0.000
Subtotals for group : Fuel Oil Tanks							
FO aft PS	98.0	0.850	7.184	3.791	8.622	-4.713	0.652
FO aft SB	98.0	0.850	7.184	3.791	8.622	4.713	0.652
SUBTOTAL	-	-	14.368	3.791	8.622	-0.000	1.303
Subtotals for group : LNG Propulsion Tanks							
LNG propulsion tank CL	98.0	0.650	34.274	3.746	95.153	0.000	10.554
SUBTOTAL	-	-	34.274	3.746	95.153	0.000	10.554
Subtotals for group : Fresh Water Tanks							
FW aft PS	98.0	1.000	8.636	1.706	12.277	-4.282	7.211
FW aft SB	98.0	1.000	8.636	1.706	12.277	4.282	7.211
SUBTOTAL	-	-	17.272	1.706	12.277	-0.000	14.421
Subtotals for group : Miscellaneous Tanks							
DW aft PS	98.0	1.000	6.017	1.898	10.295	-4.103	6.010
DW aft SB	98.0	1.000	6.017	1.898	10.295	4.103	6.010
SUBTOTAL	-	-	12.035	1.898	10.295	0.000	12.021
Subtotals for group : Water Ballast Tanks							
Aftpeak WB	0.0	1.000	0.000	1.954	2.833	0.000	0.000
WB aft CL	0.0	1.000	0.000	0.000	9.333	0.000	0.000
WB aft PS	0.0	1.000	0.000	0.838	9.333	-2.754	0.000
WB aft SB	0.0	1.000	0.000	0.838	9.333	2.754	0.000
WB aft1 PS	0.0	1.000	0.000	0.000	15.470	-3.155	0.000
WB aft1 SB	0.0	1.000	0.000	0.000	15.470	3.155	0.000
WB 8 U-Tank	0.0	1.000	0.000	0.000	24.044	0.000	0.000
WB 7 U-Tank	0.0	1.000	0.000	0.000	36.789	0.000	0.000
WB 6 U-Tank	0.0	1.000	0.000	0.000	48.142	0.000	0.000
WB 5 U-Tank	0.0	1.000	0.000	0.000	60.385	0.000	0.000
WB 4 U-Tank	0.0	1.000	0.000	0.000	71.735	0.000	0.000
WB 3 U-Tank	0.0	1.000	0.000	0.000	81.272	0.000	0.000
WB 2 U-Tank	0.0	1.000	0.000	-0.004	87.241	0.000	0.000
WB 1 U-Tank	98.0	1.000	154.476	1.886	94.054	0.000	527.623
WB fore PS	0.0	1.000	0.000	0.700	101.602	-4.249	0.000
WB fore SB	0.0	1.000	0.000	0.700	101.602	4.249	0.000
Forepeak WB	0.0	1.000	0.000	-0.010	107.244	0.000	0.000
SUBTOTAL	-	-	154.476	1.886	94.054	0.000	527.623
Subtotals for group : Cargo Tanks							
Cargo 02 PS	10.0	0.850	33.128	1.135	23.785	-2.611	151.282
Cargo 02 SB	10.0	0.850	33.128	1.135	23.785	2.611	151.282
Cargo 01 PS	10.0	0.850	32.110	1.127	83.792	-2.704	157.728
Cargo 01 SB	10.0	0.850	32.110	1.127	83.792	2.704	157.728
SUBTOTAL	-	-	130.475	1.131	53.320	0.000	618.019
Subtotals for group : LNG Cargo Tanks							
LNG TANK GTT 02	10.0	0.500	46.600	1.576	42.023	0.000	1057.382
LNG TANK GTT 01	10.0	0.500	46.600	1.576	65.619	0.000	1057.382
SUBTOTAL	-	-	93.201	1.576	53.821	0.000	2114.765

TRIM AND STABILITY CALCULATION
mts "Argos GL"

27 Jan 2015 13:13:04

Condition : LSW, 98% cons. 10% FO, 10% LNG with WB1 filled

Description	Filling %	S.W. ton/m ³	Weight ton	VCG m	LCG m	TCG m	FSM tonm
Subtotals for group : Other Spaces and Compartments							
CD aft PS	0.0	1.000	0.000	0.361	11.333	-2.769	0.000
CD aft SB	0.0	1.000	0.000	0.361	11.333	2.769	0.000
CD aft1 PS	0.0	1.000	0.000	0.000	13.333	-2.764	0.000
CD aft1 SB	0.0	1.000	0.000	0.000	13.333	2.764	0.000
Void at side PS	0.0	1.000	0.000	3.800	5.294	-5.834	0.000
Void at side SB	0.0	1.000	0.000	3.800	5.294	5.834	0.000
Void at side2 PS	0.0	1.000	0.000	2.600	12.102	-5.997	0.000
Void at side2 SB	0.0	1.000	0.000	2.600	12.102	5.997	0.000
Void at side3 PS	0.0	1.000	0.000	4.950	11.536	-6.249	0.000
Void at side3 SB	0.0	1.000	0.000	4.950	11.536	6.249	0.000
POD compartment PS	0.0	1.000	0.000	1.117	6.833	-1.765	0.000
POD compartment SB	0.0	1.000	0.000	1.117	6.833	1.765	0.000
Void DB	0.0	1.000	0.000	0.000	13.794	0.026	0.000
Accommodation	0.0	1.000	0.000	2.600	13.750	0.000	0.000
Engine Room	0.0	1.000	0.000	0.600	13.236	0.143	0.000
Boxcooler aft PS	0.0	1.000	0.000	0.000	10.388	-0.522	0.000
CD aft	0.0	1.000	0.000	0.000	17.006	0.000	0.000
CD fore	0.0	1.000	0.000	-0.004	97.785	0.000	0.000
CD FO2LNG2	0.0	1.000	0.000	0.000	30.219	0.000	0.000
LNG TANK 02 W.O. GTT BLOCKS	0.0	1.000	0.000	0.950	42.018	0.000	0.000
Void above GTT	0.0	1.000	0.000	5.885	42.018	0.000	0.000
CD LNG1-2	0.0	1.000	0.000	0.000	53.816	0.000	0.000
LNG TANK 01 W.O. GTT BLOCKS	0.0	1.000	0.000	0.950	65.614	0.000	0.000
Void Above GTT	0.0	1.000	0.000	5.885	65.614	0.000	0.000
CD LNG1FO1	0.0	1.000	0.000	0.000	77.413	0.000	0.000
CD FO1-Propulsion	0.0	1.000	0.000	-0.004	90.160	0.000	0.000
Cargo hold LNG prop Tank CL	0.0	1.000	0.000	0.950	93.910	0.000	0.000
DB bowthr.rm	0.0	1.000	0.000	-0.001	101.311	0.000	0.000
Void fore PS	0.0	1.000	0.000	5.355	101.322	-5.500	0.000
Void fore SB	0.0	1.000	0.000	5.355	101.322	5.500	0.000
Bowthr.rm	0.0	1.000	0.000	0.700	101.446	0.000	0.000
Elec. Switch Room	0.0	1.000	0.000	2.855	100.360	1.465	0.000
LNG Generator Room	0.0	1.000	0.000	5.355	101.341	0.237	0.000
Forepeak	0.0	1.000	0.000	3.450	106.689	0.000	0.000
SUBTOTAL	-	-	0.000	0.000	0.000	0.000	0.000
TOTAL	-	-	2189.580	3.522	56.228	0.000	3298.706

TRIM AND STABILITY CALCULATION
mts "Argos GL"

27 Jan 2015 13:13:04

Condition : LSW, 98% cons. 10% FO, 10% LNG with WB1 filled

<u>Hydrostatics</u>		<u>Drafts and trim</u>	
Volume	2173.281 m ³	Drafts above base :	
LCF	55.620 m	Draft mean (Lpp/2)	1.756 m
Mom. change trim	93.806 tonm/cm	Draft aft (App)	1.880 m
Ton/cm immersion	13.173 ton/cm	Draft fore (Fpp)	1.633 m
Specific weight	1.000 ton/m ³	Trim	-0.247 m

<u>Transverse stability</u>			
KM transverse	9.472 m		
VCG	3.522 m		
GM solid	5.950 m		
GG' correction	1.507 m		
G'M liquid	4.443 m	VCG'	5.029 m

The stability values are calculated for the actual trim.

Statical and dynamical stability, calculated with constant LCB :

Angle(SB) degrees	Draft mld. m	Trim m	KNsinφ m	VCG'sinφ m	TCGcosφ m	G'Nsinφ m	Area mrad
0.00	1.756	-0.247	0.000	0.000	0.000	-0.000	0.000
2.00	1.756	-0.245	0.331	0.175	0.000	0.155	0.003
5.00	1.753	-0.235	0.828	0.438	0.000	0.389	0.017
7.00	1.750	-0.223	1.160	0.613	0.000	0.547	0.033
10.00	1.744	-0.198	1.662	0.873	0.000	0.789	0.068
12.00	1.738	-0.177	1.999	1.045	0.000	0.953	0.099
15.00	1.723	-0.137	2.495	1.301	0.000	1.194	0.155
20.00	1.646	-0.070	3.175	1.720	0.000	1.455	0.272
25.00	1.492	0.001	3.671	2.125	0.000	1.546	0.404
27.00	1.410	0.031	3.835	2.283	0.000	1.552	0.458
30.00	1.264	0.078	4.051	2.514	0.000	1.537	0.539
35.00	0.958	0.157	4.348	2.884	0.000	1.464	0.670
40.00	0.563	0.220	4.580	3.232	0.000	1.348	0.793

Statical angle of inclination is 0.000 degrees to starboard

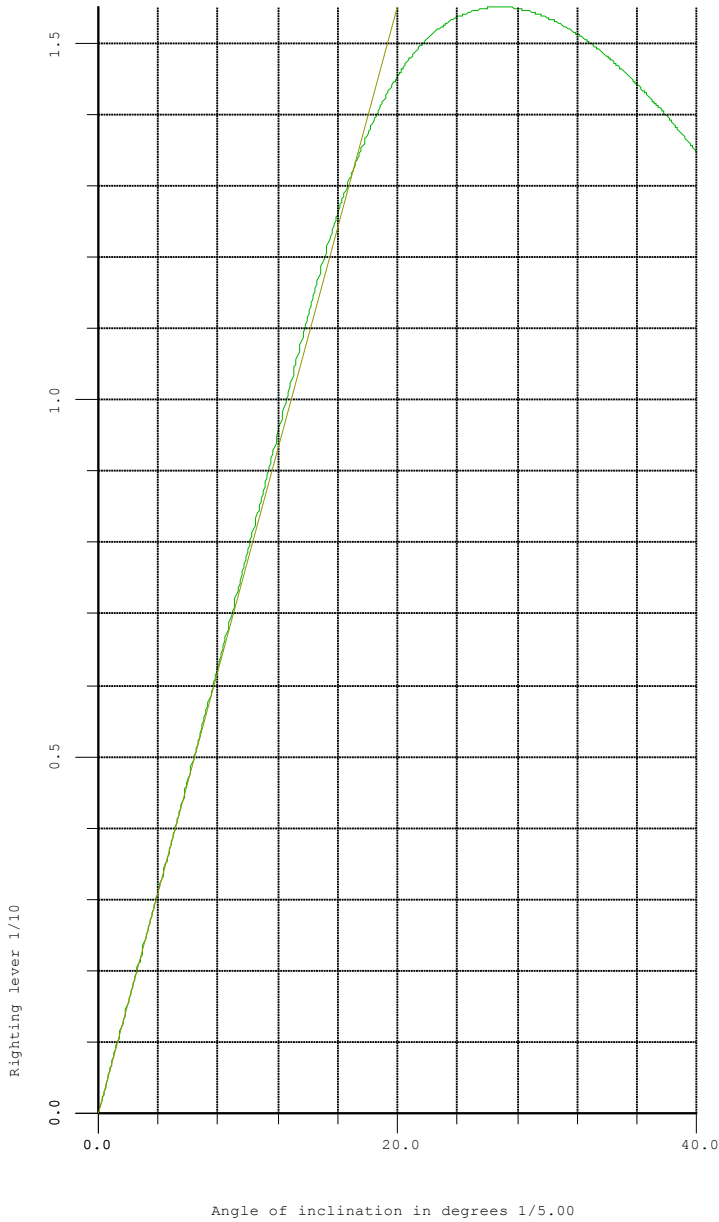
Summary

<u>Hydrostatics</u>	<u>Criterion</u>	<u>Value</u>
Draft mld.	4.500	1.756 m
Trim		-0.247 m
Statical angle of inclination		0.00 degrees SB
Flooding angle		40.00 degrees
<u>ADN intact stability tankers with tanks > 0.70 B</u>	<u>Criterion</u>	<u>Value</u>
Residual righting lever	0.100	1.552 meter
Area under the GZ curve up to 27 degrees	0.024	0.458 mrad
Minimum metacentric height G'M	0.100	4.443 meter
<u>VCG'</u>		
Actual		5.029 m
Maximum allowable		9.149 m
<u>Loading condition complies with the stated criteria.</u>		

TRIM AND STABILITY CALCULATION
mts "Argos GL"

27 Jan 2015 13:13:04

Condition : LSW, 98% cons. 10% FO, 10% LNG with WB1 filled



LSW, 98% consumables, 50% FO and 50% LNG with additional external moment

An additional moment of 337,5 tonm has been chosen because of the following assumption:

$$50[\text{ton}] \times (B/2)[\text{m}] = 50[\text{ton}] \times 6,75[\text{m}] = 337,5[\text{tonm}]$$

TRIM AND STABILITY CALCULATION

mts "Argos GL"

27 Jan 2015 14:04:15

Condition : LSW, 98% cons. 50% FO, 50% LNG with external moment

Description	Filling %	S.W. ton/m ³	Weight ton	VCG m	LCG m	TCG m	FSM tonm
Empty ship	-	-	1733.480	3.975	53.588	0.000	0.000
Subtotals for group : Fuel Oil Tanks							
FO aft PS	98.0	0.850	7.184	3.791	8.620	-4.713	0.651
FO aft SB	98.0	0.850	7.184	3.791	8.620	4.713	0.651
SUBTOTAL	-	-	14.368	3.791	8.620	0.000	1.302
Subtotals for group : LNG Propulsion Tanks							
LNG propulsion tank CL	98.0	0.650	34.274	3.746	95.152	0.000	10.561
SUBTOTAL	-	-	34.274	3.746	95.152	0.000	10.561
Subtotals for group : Fresh Water Tanks							
FW aft PS	98.0	1.000	8.636	1.706	12.276	-4.282	7.212
FW aft SB	98.0	1.000	8.636	1.706	12.276	4.282	7.212
SUBTOTAL	-	-	17.272	1.706	12.276	-0.000	14.424
Subtotals for group : Miscellaneous Tanks							
DW aft PS	98.0	1.000	6.017	1.898	10.294	-4.103	6.012
DW aft SB	98.0	1.000	6.017	1.898	10.294	4.103	6.012
SUBTOTAL	-	-	12.035	1.898	10.294	-0.000	12.023
Subtotals for group : Water Ballast Tanks							
Aftpeak WB	0.0	1.000	0.000	1.954	2.833	0.000	0.000
WB aft CL	0.0	1.000	0.000	0.000	9.333	0.000	0.000
WB aft PS	0.0	1.000	0.000	0.838	9.333	-2.754	0.000
WB aft SB	0.0	1.000	0.000	0.838	9.333	2.754	0.000
WB aft1 PS	0.0	1.000	0.000	0.000	15.470	-3.155	0.000
WB aft1 SB	0.0	1.000	0.000	0.000	15.470	3.155	0.000
WB 8 U-Tank	0.0	1.000	0.000	0.000	24.044	0.000	0.000
WB 7 U-Tank	0.0	1.000	0.000	0.000	36.789	0.000	0.000
WB 6 U-Tank	0.0	1.000	0.000	0.000	48.142	0.000	0.000
WB 5 U-Tank	0.0	1.000	0.000	0.000	60.385	0.000	0.000
WB 4 U-Tank	0.0	1.000	0.000	0.000	71.735	0.000	0.000
WB 3 U-Tank	0.0	1.000	0.000	0.000	81.272	0.000	0.000
WB 2 U-Tank	0.0	1.000	0.000	-0.004	87.241	0.000	0.000
WB 1 U-Tank	98.0	1.000	154.476	1.886	94.053	0.000	527.625
WB fore PS	0.0	1.000	0.000	0.700	101.602	-4.249	0.000
WB fore SB	0.0	1.000	0.000	0.700	101.602	4.249	0.000
Forepeak WB	0.0	1.000	0.000	-0.010	107.244	0.000	0.000
SUBTOTAL	-	-	154.476	1.886	94.053	0.000	527.625
Subtotals for group : Cargo Tanks							
Cargo 02 PS	50.0	0.850	165.640	2.273	23.664	-2.804	163.915
Cargo 02 SB	50.0	0.850	165.640	2.273	23.664	2.804	163.915
Cargo 01 PS	50.0	0.850	160.548	2.252	83.777	-2.841	157.720
Cargo 01 SB	50.0	0.850	160.548	2.252	83.777	2.841	157.720
SUBTOTAL	-	-	652.376	2.263	53.252	-0.000	643.269
Subtotals for group : LNG Cargo Tanks							
LNG TANK GTT 02	50.0	0.500	233.002	2.392	41.954	0.000	1057.374
LNG TANK GTT 01	50.0	0.500	233.002	2.392	65.550	0.000	1057.383
SUBTOTAL	-	-	466.003	2.392	53.752	0.000	2114.758

The effects of a shift in COG due to heel and trim of the tanks have been included in ALL values in this loading condition.

TRIM AND STABILITY CALCULATION
mts "Argos GL"

27 Jan 2015 14:04:15

Condition : LSW, 98% cons. 50% FO, 50% LNG with external moment

Description	Filling %	S.W. ton/m ³	Weight ton	VCG m	LCG m	TCG m	FSM tonm
Subtotals for group : Other Spaces and Compartments							
CD aft PS	0.0	1.000	0.000	0.361	11.333	-2.769	0.000
CD aft SB	0.0	1.000	0.000	0.361	11.333	2.769	0.000
CD aft1 PS	0.0	1.000	0.000	0.000	13.333	-2.764	0.000
CD aft1 SB	0.0	1.000	0.000	0.000	13.333	2.764	0.000
Void at side PS	0.0	1.000	0.000	3.800	5.294	-5.834	0.000
Void at side SB	0.0	1.000	0.000	3.800	5.294	5.834	0.000
Void at side2 PS	0.0	1.000	0.000	2.600	12.102	-5.997	0.000
Void at side2 SB	0.0	1.000	0.000	2.600	12.102	5.997	0.000
Void at side3 PS	0.0	1.000	0.000	4.950	11.536	-6.249	0.000
Void at side3 SB	0.0	1.000	0.000	4.950	11.536	6.249	0.000
POD compartment PS	0.0	1.000	0.000	1.117	6.833	-1.765	0.000
POD compartment SB	0.0	1.000	0.000	1.117	6.833	1.765	0.000
Void DB	0.0	1.000	0.000	0.000	13.794	0.026	0.000
Accommodation	0.0	1.000	0.000	2.600	13.750	0.000	0.000
Engine Room	0.0	1.000	0.000	0.600	13.236	0.143	0.000
Boxcooler aft PS	0.0	1.000	0.000	0.000	10.388	-0.522	0.000
CD aft	0.0	1.000	0.000	0.000	17.006	0.000	0.000
CD fore	0.0	1.000	0.000	-0.004	97.785	0.000	0.000
CD FO2LNG2	0.0	1.000	0.000	0.000	30.219	0.000	0.000
LNG TANK 02 W.O. GTT BLOCKS	0.0	1.000	0.000	0.950	42.018	0.000	0.000
Void above GTT	0.0	1.000	0.000	5.885	42.018	0.000	0.000
CD LNG1-2	0.0	1.000	0.000	0.000	53.816	0.000	0.000
LNG TANK 01 W.O. GTT BLOCKS	0.0	1.000	0.000	0.950	65.614	0.000	0.000
Void Above GTT	0.0	1.000	0.000	5.885	65.614	0.000	0.000
CD LNG1FO1	0.0	1.000	0.000	0.000	77.413	0.000	0.000
CD FO1-Propulsion	0.0	1.000	0.000	-0.004	90.160	0.000	0.000
Cargo hold LNG prop Tank CL	0.0	1.000	0.000	0.950	93.910	0.000	0.000
DB bowthr.rm	0.0	1.000	0.000	-0.001	101.311	0.000	0.000
Void fore PS	0.0	1.000	0.000	5.355	101.322	-5.500	0.000
Void fore SB	0.0	1.000	0.000	5.355	101.322	5.500	0.000
Bowthr.rm	0.0	1.000	0.000	0.700	101.446	0.000	0.000
Elec. Switch Room	0.0	1.000	0.000	2.855	100.360	1.465	0.000
LNG Generator Room	0.0	1.000	0.000	5.355	101.341	0.237	0.000
Forepeak	0.0	1.000	0.000	3.450	106.689	0.000	0.000
SUBTOTAL	-	-	0.000	0.000	0.000	0.000	0.000
TOTAL	-	-	3084.283	3.245	55.420	-0.000	3323.963

The effects of a shift in COG due to heel and trim of the tanks have been included in ALL values in this loading condition.

TRIM AND STABILITY CALCULATION
mts "Argos GL"

27 Jan 2015 14:04:15

Condition : LSW, 98% cons. 50% FO, 50% LNG with external moment

Hydrostatics

Volume 3061.323 m³
LCF 54.495 m
Mom. change trim 102.320 tonm/cm
Ton/cm immersion 13.568 ton/cm
Specific weight 1.000 ton/m³

Drafts and trim

Drafts above base :
Draft mean (Lpp/2) 2.426 m
Draft aft (App) 2.622 m
Draft fore (Fpp) 2.230 m
Trim -0.391 m

Transverse stability

KM transverse 7.550 m
VCG 3.245 m
GM solid 4.305 m
GG' correction 1.078 m
G'M liquid 3.227 m

VCG' 4.323 m

The stability values are calculated for the actual trim.

Statical and dynamical stability, calculated with constant LCB :

Angle(SB) degrees	Draft mld. m	Trim m	KNsinφ m	VCGsinφ m	TCGcosφ m	GNsinφ m	Area mrad
0.00	2.426	-0.391	0.000	0.000	0.109	-0.109	0.000
2.00	2.425	-0.390	0.264	0.113	0.147	0.004	0.000
5.00	2.423	-0.382	0.660	0.283	0.194	0.183	0.005
7.00	2.421	-0.372	0.925	0.396	0.225	0.304	0.013
10.00	2.416	-0.352	1.325	0.566	0.270	0.489	0.034
12.00	2.411	-0.333	1.594	0.679	0.300	0.616	0.053
15.00	2.402	-0.297	2.003	0.848	0.344	0.811	0.091
20.00	2.377	-0.218	2.689	1.130	0.415	1.144	0.176
25.00	2.305	-0.138	3.290	1.410	0.472	1.408	0.288
27.00	2.257	-0.113	3.492	1.520	0.485	1.487	0.339
30.00	2.164	-0.088	3.762	1.682	0.498	1.582	0.419
35.00	1.957	-0.063	4.132	1.946	0.508	1.678	0.562
40.00	1.711	-0.031	4.377	2.201	0.506	1.670	0.709

Statical angle of inclination is 1.939 degrees to starboard

Additional heeling moment is 337.500 tonm

Summary

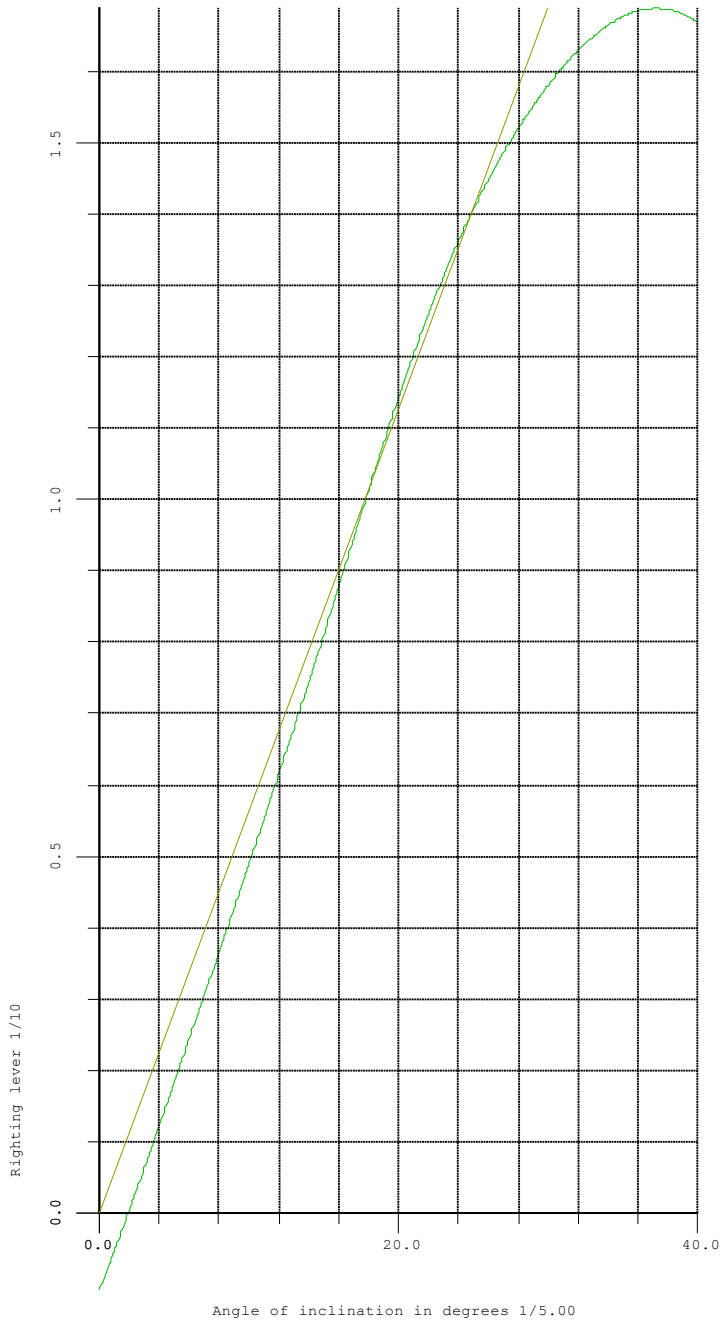
<u>Hydrostatics</u>	<u>Criterion</u>	<u>Value</u>
Draft mld.	4.500	2.426 m
Trim	-0.391 m	
Statical angle of inclination	1.94 degrees SB	
Flooding angle	40.00 degrees	
<u>ADN intact stability tankers with tanks > 0.70 B</u>	<u>Criterion</u>	<u>Value</u>
Residual righting lever	0.100	1.690 meter
Area under the GZ curve up to 27 degrees	0.024	0.339 mrad
Minimum metacentric height G'M	0.100	3.227 meter

Loading condition complies with the stated criteria.

TRIM AND STABILITY CALCULATION
mts "Argos GL"

27 Jan 2015 14:04:15

Condition : LSW, 98% cons. 50% FO, 50% LNG with external moment



Preliminary Stability information Booklet mts "Argos GL"

Date: 27 January 2015



Mr. Jean-Paul de Maat
Ministry of Infrastructure and the Environment

A. van Leeuwenhoeklaan 9
3721 MA Bilthoven
Postbus 1
3720 BA Bilthoven
www.rivm.nl
KvK Utrecht 30276683
T 030 274 91 11
F 030 274 29 71
info@rivm.nl

memo

Interaction between LNG spills on water or gas oil

Date

April 2015

Dealt with by

ir. S. Mahesh
Centre for Environmental
Safety and Security

soedesh.mahesh@rivm.nl

I. Introduction

The bunker ship Argos-GL is currently being designed. Argos-GL will transport liquefied natural gas (LNG) and gas oil for bunkering seagoing vessels and inland waterway vessels in the harbour of Rotterdam. The LNG on board will be stored in membrane tanks. For the use of membrane tanks for the carriage of LNG a derogation from the ADN Committee is necessary.

The ADN Committee discussed the request for this derogation during its meeting in August 2014 and decided to ask a technical expert group to further examine this issue. The expert group discussed this matter last November during its meeting which was attended by delegates from Germany, Netherlands, Lloyds Register, Argos and Gaz Transport & Technigaz SA (GTT).

The report of this meeting was discussed during the meeting of the ADN Committee in January.

Germany had questions about what actually happens when after a collision there is a crack in the wall(s) of the tank and LNG release in or on the water. Also the consequences of contact between LNG and regular gas oil was discussed.

The Ministry of Infrastructure and the Environment requested the Dutch National Institute for Public Health and the Environment (RIVM) for an expert judgment on these two topics.

II. Assessment of LNG spills over water

LNG cargo tank breaches

In this section is discussed the variables that influence an LNG cargo tank breach and the LNG spill dispersion after a breach. The potential hazard consequences after ignition are not discussed here, because these are described in the literature.

The variables that influence an LNG cargo tank breach include:

- Type and location of the breach and the energy involved;
- The vessel's geometry, its construction and materials, hold spaces, distance between hulls, tonnage, and event mitigation systems;
- LNG cargo tank construction and size; and
- The fluid mechanics and thermodynamic characteristics of LNG.

If the membrane tank is punctured, LNG driven only by weight of the fluid itself and will traverse the ship's below decks spaces plus the ballast space between the two hulls, which are empty when a full cargo is on board. The speed at which an LNG spill will progress will depend on the size and location of the breach in the LNG cargo tank. The pressure in the membrane tank is slightly above the atmospheric pressure, so the outflow will be lower than a regular pressure tank and the LNG will not be forced out as in a regular pressure tank.

For LNG cargo tank designs, a realistic estimate of tanker losses (i.e., the fraction of the spill that reaches the water) must be reduced to account for LNG diverted to the ballast space or vacant hold areas. Spill damage to the ship from contact with the cryogenic LNG and/or from fire damage to the ship or its other LNG cargo tanks are consequences. Based on the analyses, the potential for damage to the ship cannot be ruled out, especially for large spills. However, it was concluded for Argos GL that releases from no more than one tank would be involved in a spill at any one time. This release is not expected to increase significantly the overall hazard ranges, but would increase the expected duration of the consequences.

LNG spill dispersion after a breach

Following a tank breach or other spill event, depending on the size and location, LNG can be expected to spill onto or into the vessel itself, escape through a breach onto the water surface, or both. LNG dispersion can occur through either volatilization of the LNG into the air and transport as a vapor cloud or transport as a liquid on the surface of the water.

Several variables must be addressed in developing an assessment of an LNG spill, its general dispersion and the potential hazards. Assumptions made in addressing or analyzing these variables can have a significant impact on estimates of the potential hazards associated with an LNG spill.

Potential consequences from an LNG spill over water

The consequences of an LNG spill include a wide range of potential events. Here we discuss the analyses that should be considered to assess the consequences and hazards of an LNG spill for a specific site.

- ***Rapid Phase Transitions (RPT)***

Rapid Phase Transitions occur when the temperature difference between a hot liquid and a cold liquid is sufficient to drive the cold liquid rapidly to its superheat limit, resulting in near spontaneous boiling of the cold liquid. When a cryogenic liquid such as LNG is suddenly heated by contacting a warm liquid such as water or gas oil, rapid boiling of the LNG can occur, resulting in localized overpressure releases. The impacts of this phenomenon will be localized near the spill source and should not cause extensive structural damage.

Rapid Phase Transitions are more likely to occur in LNG mixtures containing very high fractions of ethane and propane. LNG composition is a critical parameter.

Spill rate, spill duration, and the spill surface conditions influence the rapid

phase transition process. Higher spill rates and longer spill durations are more likely to produce Rapid Phase Transitions. Critical temperature difference leading to nucleate/pool boiling heat transfer is more likely to be reached if more cold liquid is spilled or if cold liquid is spilled over a long duration. Only a small fraction of the spilled LNG was observed to undergo Rapid Phase Transitions. The hazard potential of Rapid Phase Transitions can be severe, but as mentioned earlier is highly localized within the spill area.

Date
26 April 2015

- ***Brittle fracture and cryogenic burns***

Potential degradation of the structural integrity of an LNG ship could occur, because LNG can have a very damaging impact on the integrity of many steels and common ship structural connections, such as welds. Both the ship itself and other LNG cargo tanks could be damaged from a large spill.

The very low temperature of LNG suggests that a breach of an LNG cargo tank that could cause the loss of a large volume of liquid LNG might have negative impacts on people and property near the spill, including crew members or emergency personnel. If LNG liquid contacts the skin, it can cause cryogenic burns.

III. Assessment of LNG spills over gas oil

If LNG comes in contact with gas oil it will respond mainly in the same manner as when it comes in contact with water. Therefore gas oil is not separately considered in this analysis. The recommendations for LNG apply to both gas oil and water.

IV. General considerations

In this part of the report the RIVM gives some general considerations what could happen when LNG is released in or on the water or when it comes in contact with gas oil.

- If LNG is suddenly released in greater amounts to water, there will be a very fast evaporation of LNG. LNG shall withdraw the heat of evaporation from the (excess) water or the gas oil.
- The rapid formation of methane gas also means a rapid increase in volume and Rapid Phase Transition.
- The interaction between LNG spills on gas oil will lead to similar effects as the interaction between LNG and on water.

References

- Guidance on Risk Analysis and Safety Implications of Large Liquefied Natural Gas (LNG) Spill Over Water. Mike Hightower, et. al. Sandia Report SAND2004-6258. December 2004.
- LNG Properties and Hazard. Understanding LNG Rapid Phase Transitions (RPT). G.A. Melhem, et. al. ioMosaic Corporation. 2006.

reference ADN Approval Procedure Argos GL
revision E10152-40-AP

Page 1/27
Date 15-09-2014

Type G-tanker Argos GL

**Determination of Energy absorption capacity for inland waterway tank vessel “Argos GL” with tanks larger than 380 m³ and a reference ship for approval procedure enlarged cargo tanks
ADN**

reference ADN Approval Procedure Argos GL
revision E10152-40-AP

Page 2/27
Date 15-09-2014

Contents

<i>Summary</i>	3
<i>Conclusion</i>	3
<i>Introduction</i>	5
<i>Step 1: Drawings</i>	6
<i>Step 2: Identification of collision locations</i>	7
Longitudinal striking locations	7
Vertical striking positions	7
<i>Step 3: Weighting factor by location</i>	10
Horizontal weighting factors	10
Vertical weighting factors	15
<i>Step 4: Determination of energy absorption capacity</i>	15
Striking angles	16
Bow types	18
Crash calculations	18
Striking cases with no failure	18
Results Crash calculations	19
Y-type structure	19
Reference structure	19
<i>Step 5: Probability calculation</i>	20
<i>Step 6: Calculate weighted failure probabilities</i>	25
<i>Step 7: Adding weighted probabilities</i>	25
<i>Step 8: Multiply probabilities by location weighting factor</i>	25
<i>Step 9: Adding weighted probabilities for each scenario</i>	25
<i>Step 10+11: Calculate weighted averages</i>	26
<i>Step 12: Consequence increase</i>	26
<i>Step 13: Compare tank failure ratio with effect ratio</i>	26
<i>Conclusion</i>	27
<i>References</i>	27

reference ADN Approval Procedure Argos GL
 E10152-40-AP
revision

Page 3/27
Date 15-09-2014

Summary

In this report it is shown that an increase in tank volume from 380 m³ to 935 m³ is possible for the inland waterway tanker 'Argos GL' according to the ADN 2013, Part 9, Section 9.3.4, 'Alternative Constructions' for acceptance of cargo tanks larger than 380 m³. The report is written according to the 13 basic steps described in the approval procedure.

In the document a description is given of both the reference structure and the alternative structure and the striking bow shapes. Decisive horizontal and vertical collision cases have been identified for both striking bow shapes and struck ship designs. This has resulted in 18 collision scenarios that are modelled and calculated for the reference ship and 18 scenarios for the alternative structure. These locations have been defined in accordance with Lloyd's Register. As the structural design for this type G tanker resembles the design of a type C tanker with structurally integrated tanks, the procedure for determining striking locations and weighing factors as described for a Type C tanker in AND (2013) has been followed.

The modelling of the striking and struck ships in the explicit finite element code LS-DYNA is described. The critical failure strain used for the calculations is a critical thickness reduction dependent on both plate thickness and element size. Regarding this failure criterion the authors are convinced that the energy absorption capacity of the alternative structure is higher than currently assessed because of the used critical values. The followed approach is considered to be conservative for the alternative construction.

For each scenario the energy absorption capacity has been determined at the point of failure of both inner and outer hull or just before an inner hull or deck displacement in y- respectively z-direction of 0.30 [m] is reached. It is assumed that the GTT containment system for the LNG cargo fails at a displacement larger than 0.30 [m]. Plots are made of both local thickness reduction, displacements and global stress and strain distributions. A short description of the failure mode is given for each case. For each case the force-indentation and contact energy indentation curves are presented in the report "FE Crash calculations Argos GL".

The calculated location weighting factor and energy absorption capacity for each case has been filled in the approval procedure. This results in a probability reduction factor of 2.73 for the alternative crashworthy ship with increased cargo tanks from 380 m³ to 935 m³. As laid down in the approval procedure the effect increase of a tank size increase from 380 m³ to 935 m³ is a factor 2.46.

The effect increase of a size increase of cargo tanks from 380 m³ to 935 m³, can be compensated by building a crashworthy side structure which protects the cargo tanks, thus reducing the probability of failure. For the alternative ship the risk is a factor 0.90 times the risk associated with the reference ship.

Conclusion

The calculated location weighting factor and energy absorption capacity for each case have been entered in the approval procedure. This results in a probability reduction factor of 2.73 for the alternative crashworthy ship with increased cargo tanks from 380 m³ to 760 m³. As laid down in the approval procedure the effect increase of a tank size increase from 380 m³ to 935 m³ is a factor 2.46.

reference ADN Approval Procedure Argos GL
 E10152-40-AP
revision

Page 4/27
Date 15-09-2014

The effect increase of an increase of cargo tanks from 380 m³ to 760 m³, is adequately compensated by the alternative crashworthy side structure which protects the cargo tanks, thus reducing the probability of failure. For the alternative ship the risk is a factor 0.74 times the risk associated with the reference ship.

reference ADN Approval Procedure Argos GL
E10152-40-AP
revision

Page 5/27
Date 15-09-2014

Introduction

Inland waterway tankers, with tanks larger than the maximum allowable size according to ADN 2013, Part 9, Section 9.3.4, “Alternative Constructions”, may be acceptable from a safety point of view, when the tanks are sufficiently protected against collisions through a crashworthy side structure. This can be shown by comparing the risk associated with a conventional design (reference design) featuring tanks complying with the ADN (2013) regulations, to the risk of a crashworthy design (alternative design) fitted with enlarged cargo tanks. In the described risk concept the probability of tank rupture is related to the energy absorption capacity of the ship structure in a collision scenario up to failure of the inner and outer hull, deck plating in way of tank or a displacement in y- or z-direction of the tank boundary larger than 0,30 [m].

In this document the approval procedure is reported to determine the energy absorption capacity of both reference and alternative design.

reference ADN Approval Procedure Argos GL
 revision E10152-40-AP

Page 7/27
 Date 15-09-2014

Step 2: Identification of collision locations

In consultation with the classification authority Lloyd’s Register the following collision locations have been identified.

Longitudinal striking locations

For both striking bow shapes and structure types three striking locations in longitudinal direction have been identified:

- Direct striking on a transverse bulkhead
- Direct striking on a web frame
- Striking between two web frames

Vertical striking positions

The vertical striking position is exclusively dependent on the draught differences between striking and struck vessels restricted in the range of maximum and minimum draught of both vessels. Therefore first the maximum and minimum drafts of both striking and struck vessels together with the dimensions that determine the different vertical collision locations have to be described. These are given in table 1.

Striking vessel Europe II type push barge	T _{1min}	0.60 [m]
	T _{1max}	4.00 [m]
	Height of upper edge vertical part in way of corner	5.20 [m]
	Height of lower edge vertical part in way of corner	4.20 [m]
Striking vessel V-shape bow	T _{1min}	1.50 [m]
	T _{1max}	5.00 [m]
	Height of upper edge vertical part	6.70 [m]
	Height of lower edge vertical part	6.39 [m]
Struck vessel Conventional	T _{2min}	1.54 [m]
	T _{2max}	3.38 [m]
	Side depth	5.89 [m]
	Breadth of sheerstrake	0.52 [m]
Struck vessel Alternative structure	T _{2min}	1.54 [m]
	T _{2max}	3.38 [m]
	Side depth	6.53 [m]
	Breadth of sheerstrake	0.78 [m]

Table 1 Typical dimensions for vertical striking locations

reference ADN Approval Procedure Argos GL
E10152-40-AP
revision

Page 8/27
Date 15-09-2014

Graphically this can be illustrated by a rectangular area to be framed with values of maximum and minimum draughts of both striking and struck vessels. Each point in this area is a possible collision situation. An equal probability distribution is assumed over all the situations possible. The points on each inclined line, that has an angle of 45 degrees to the horizontal and vertical axes, have the same draught difference and therefore this line represents one vertical collision location. For each scenario representative vertical collision locations can be defined. This is graphically represented in figures 1 and 2.

P2 For both structures the point P2 is the point where the lower edge of the vertical part of EuropeII / V-bow touches the deck level of the struck ship.

P3 Is the point where the upper vertical part of EuropeII / V-bow touches the lower part of the sheerstrake.

In order to clarify the positions of P2 and P3 in relation to the structural arrangement, they are schematically given in Figure 1

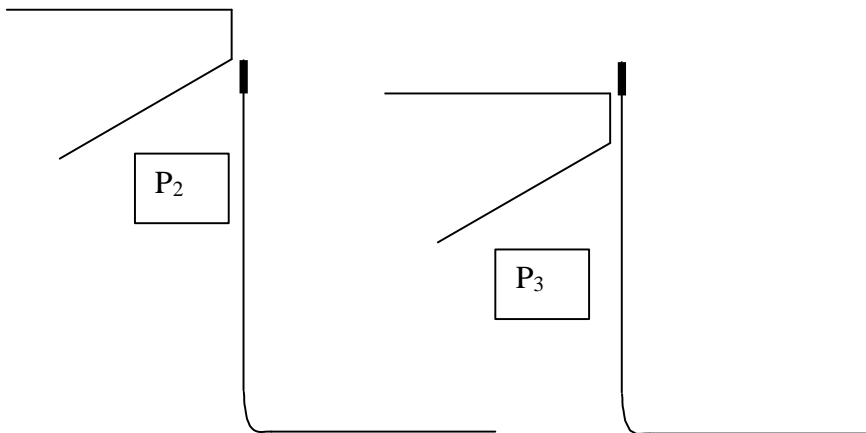


Figure 1 Distinctive vertical locations reference structure

reference E10152-40-AP
 revision

Page 9/27
 Date 15-09-2014

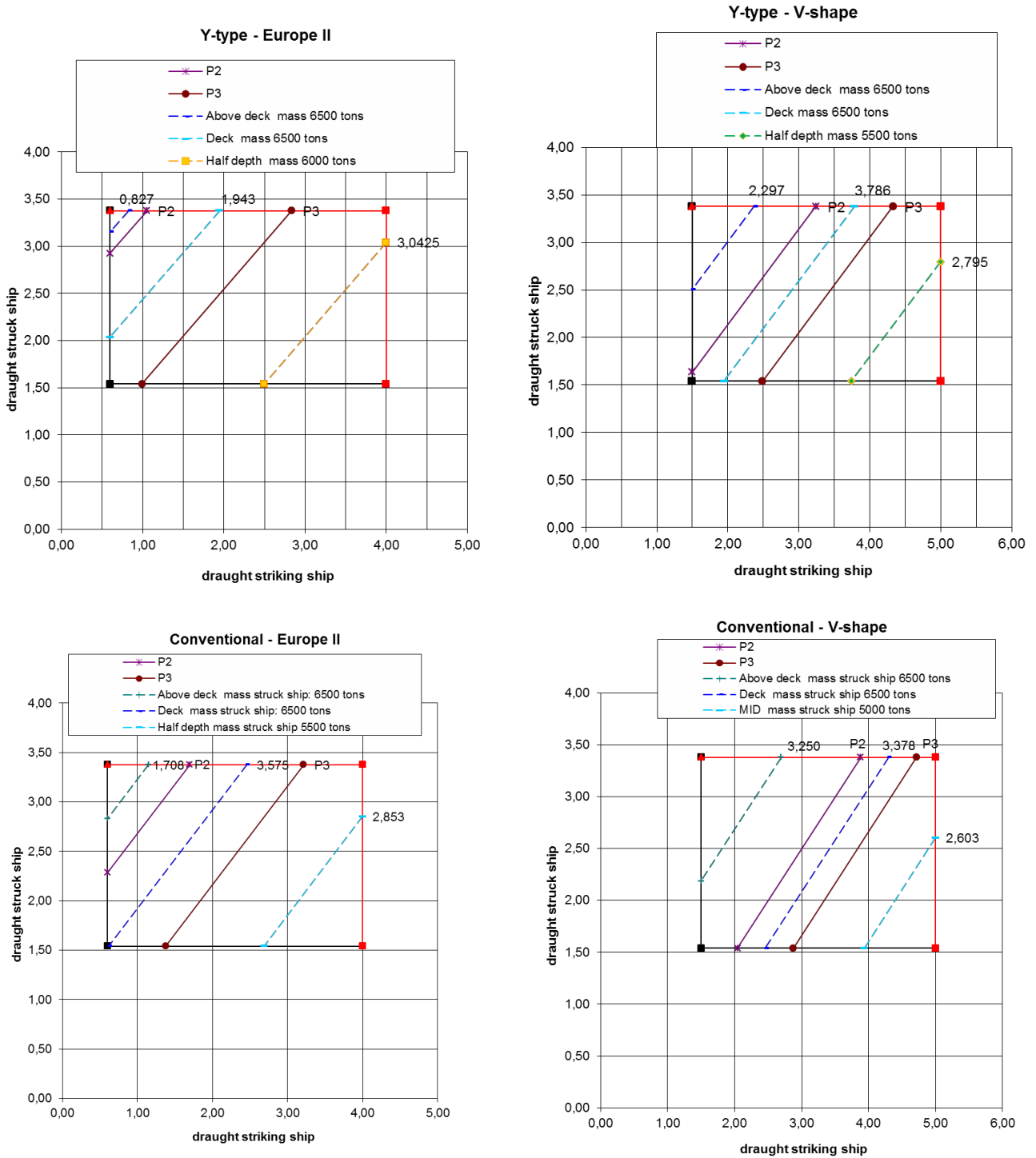


Figure 2 Vertical striking locations

reference ADN Approval Procedure Argos GL
 E10152-40-AP
revision

Page 10/27
Date 15-09-2014

Step 3: Weighting factor by location

The weighting factors corresponding to the collision locations have also been determined in consultation with Lloyd's Register.

Horizontal weighting factors

The horizontal weighting factors have been related to the number of frame spacings in the cargo hold. 20 percent of the webframe spacing is assigned to a distinct horizontal striking location. In table 2a till 2d the calculation of the horizontal weighting factors are given for the conventional and the alternative structural layout.

reference ADN Approval Procedure Argos GL
 revision E10152-40-AP

Page 12/27
 Date 15-09-2014

Table 2b Weighting factors alternative Structure

Collision	At Bulkhead		nr frame	nr. BHD's	spacing	total			
	web	frame spacing fore	3	2	560				
			1		378	4116			
	web	frame spacing fore	3	1	560				
			1		460	2140			
	web	frame spacing fore	2	4	500	4000			
	web	frame spacing fore	3	2	560	3360			
	web	frame spacing aft	3	2	560	3360			
	web	frame spacing aft	2	4	500	4000			
	web	frame spacing aft	3	2	560				
			1		378	4116			
	web	frame spacing aft	3	1	556	1668			
						26760		check:	
					20%	5352		297,33	< 450
	Weighfactor		0,06700						
	At Web								
			nr frame	nr. Webs	spacing	total			
	web	frame spacing fore	3	36	560	60480			
	web	frame spacing fore	3	2	560				
			1		378	4116			
	web	frame spacing fore	3	1	556	1668			
	web	frame spacing aft	3	1	560				
			1		460	2140			
	web	frame spacing fore	3	2	560				
			1		378	4116			
	web	frame spacing aft	3	36	560	60480		check:	
						133000		341	< 450
					20%	26600			
	Weighfactor		0,33300						
	Between Webs								
			nr frame	nr. Webs	spacing	total			
			3	1	560				
			1		460	2140			
			3	38	560	63840			
			1	4	378				
			3		560	8232			
			3	1	556	1668			
			2	4	500	4000			
						79880			
	Weighfactor		0,60000				60%		47928

reference ADN Approval Procedure Argos GL
 E10152-40-AP
 revision

Page 13/27
 Date 15-09-2014

Table 2c Conventional structural layout

Fuel oil cargo tank 2						
	frame spacing	1	460			
	frame spacing	3	560			
number of	webframes with	4 frame spacings		1	total spacing	2140
	frame spacing		560			
number of	webframes with	3 frame spacings		6	total spacing	10080
Cofferdam						
	frame spacing		540			
number of	webframes with	3 frame spacings		2	total spacing	3240
LNG cargo tank 2						
	frame spacing		560			
number of	webframes with	3 frame spacings		4	total spacing	6720
number of	webframes with	2 frame spacings		1	total spacing	1120
	frame spacing	1	560			
	frame spacing	2	429			
number of	webframes with	3 frame spacings		1	total spacing	1418
					sum LNG tank	9258
number of LNG tanks	4				total spacing	37032
Cofferdam						
	frame spacing		473,3333			
1 cofferdam with	3 frame spacings				total spacing	1420
number of 1 [m] cofferdams	3				total spacing	4260
Cofferdam						
	frame spacing	1	420			
	frame spacing	3	540			
number of	webframes with	4 frame spacings		1	total spacing	2040
	frame spacing		540			
number of	webframes with	3 frame spacings		1	total spacing	1620
Fuel Oil Cargo tank 1						
	frame spacing		560			
number of	webframes with	3 frame spacings		7	total spacing	11760
Cofferdam						
	frame spacing		500			
1 cofferdam with	2 frame spacings				total spacing	1000
LNG Propulsion tank						
	frame spacing		560			
number of	webframes with	3 frame spacings		3	total spacing	5040
	frame spacing		556			
number of	webframes with	3 frame spacings		1	total spacing	1668
						79880

reference ADN Approval Procedure Argos GL
 revision E10152-40-AP

Page 14/27
 Date 15-09-2014

Table 2d Weighting factors conventional Structure

Collision	At Bulkhead								
			nr frame	nr. BHD's	spacing	total			
	web frame spacing fore		3	6	560	10080			
	web frame spacing fore		3	1	540	1620			
	web frame spacing fore		3	1	560				
			1		460	2140			
	web frame spacing fore		3	3	473,3333	4260			
	web frame spacing fore		3	1	540				
			1		420	2040			
	web frame spacing fore		2	1	500	1000			
	web frame spacing aft		3	2	560	3360			
	web frame spacing aft		3	2	540	3240			
	web frame spacing aft		2	4	429				
			1		560	5672			
	web frame spacing aft		3	3	473,3333	4260	check:		
	web frame spacing aft		2	1	500	1000		310,31	< 450
	web frame spacing aft		3	1	556	1668			
						40340			
					20%	8068			
	Weighfactor	0,10100							
	At Web								
			nr frame	nr. Webs	spacing	total			
	web frame spacing fore		3	26	560	43680			
	web frame spacing fore		3	2	540	3240			
	web frame spacing fore		2	4	560	4480			
	web frame spacing fore		2	4	429				
			1		560	5672			
	web frame spacing fore		3	1	556	1668	check:		
	web frame spacing aft		3	1	560			323	< 450
			1		460	2140			
	web frame spacing aft		3	30	560	50400			
	web frame spacing aft		3	1	540	1620			
	web frame spacing aft		2	4	560	4480			
	web frame spacing aft		3	1	540				
			1		420	2040			
						119420			
					20%	23884			
	Weighfactor	0,29900							
	Between Webs								
			nr frame	nr. Webs	spacing	total			
			3	1	560				
			1		460	2140			
			3	32	560	53760			
			3	3	540	4860			
			2	4	560	4480			
			2	4	429				
			1		560	5672			
			3	1	540				
			1		420	2040			
			3	3	473,3333	4260			
			3	1	556	1668			
			2	1	500	1000			
						79880			
	Weighfactor	0,60000			60%	47928			

reference ADN Approval Procedure Argos GL
 E10152-40-AP
 revision

Page 15/27
 Date 15-09-2014

Vertical weighting factors

Figure 2 is used for the determination of the weighting factors corresponding to the different vertical locations. The weighting factor of the different representative vertical collision locations is determined as the ratio between the area corresponding with the representative case and the total rectangular area. For both structures the point P2 is the point where the lower edge of the vertical part of EuropeII / V-bow touches the deck level of the struck ship. The triangular area bounded by P2 corresponds to the representative vertical collision location: *striking above deck*.

The point P3 is the point where the upper vertical part of EuropeII / V-bow touches the lower part of the sheerstrake. The area bounded by P2 and P3 is corresponds to the representative vertical collision location: *striking on deck*.

For the conventional structure the triangular lower right corner of the rectangle corresponds to the representative vertical collision scenario: *striking at half depth*

The positions of P2 and P3 are schematically given in figure 1.

In table 3 the combined horizontal and vertical weighting factors are given for each location.

Push barge					V-shape				
New design					New design				
		at bkhd	at web	btwn webs			at bkhd	at web	btwn webs
		0,07	0,33	0,60			0,07	0,33	0,60
location 1, above deck	0,02	0,001	0,005	0,010	location 1, above deck	0,24	0,016	0,079	0,142
location 2, at deck	0,37	0,025	0,123	0,222	location 2, at deck	0,31	0,021	0,103	0,185
location 3, Mid	0,61	0,041	0,204	0,368	location 3, Mid	0,46	0,030	0,152	0,273
Reference design					Reference design				
		at bkhd	at web	btwn webs			at bkhd	at web	btwn webs
		0,10	0,30	0,60			0,10	0,30	0,60
location 1, above deck	0,10	0,010	0,029	0,058	location 1, above deck	0,44	0,045	0,132	0,265
location 2, at deck	0,40	0,041	0,120	0,242	location 2, at deck	0,21	0,022	0,064	0,128
location 3, mid	0,50	0,051	0,150	0,301	location 3, mid	0,35	0,035	0,103	0,207

Table 2 Combined weighting factors for each striking location

Step 4: Determination of energy absorption capacity

The calculations have to be carried out for two collision scenarios. Collision scenario I must be analyzed assuming a Europe II type push barge bow of which the scantlings are shown in Figure 4. Collision scenario II must be analyzed assuming a V-Shape bow of which the scantlings are shown in Figure 5. For a better description of the contact definitions in the Finite element calculations the sharp edges on deck level of both striking bow shapes have been rounded with a radius of 40[mm].

reference ADN Approval Procedure Argos GL
revision E10152-40-AP

Page 16/27
Date 15-09-2014

Striking angles

- The V-shape bow will strike at an angle of 90 degrees with respect to the longitudinal axis of the struck vessel
- The Europe II push barge bow will strike at an angle of 55 degrees with respect to the longitudinal axis of the struck ship (Figure 3).

These striking angles are prescribed in the approval guideline.

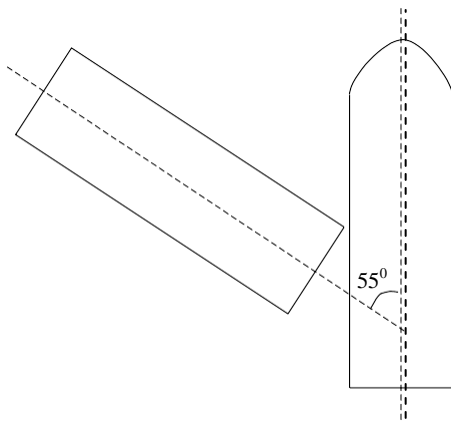


Figure 3 Striking angle for push barge bow

reference ADN Approval Procedure Argos GL
revision E10152-40-AP

Page 17/27
Date 15-09-2014

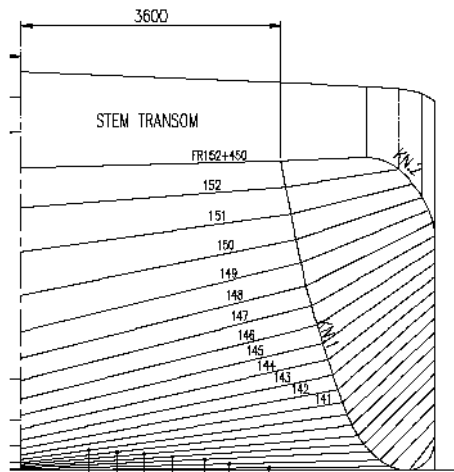
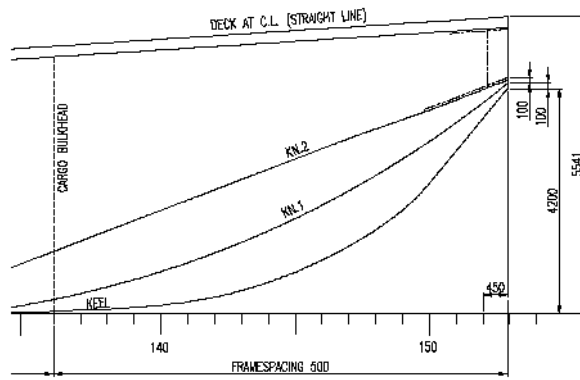


Figure 4 Scantlings Europe II type push barge bow

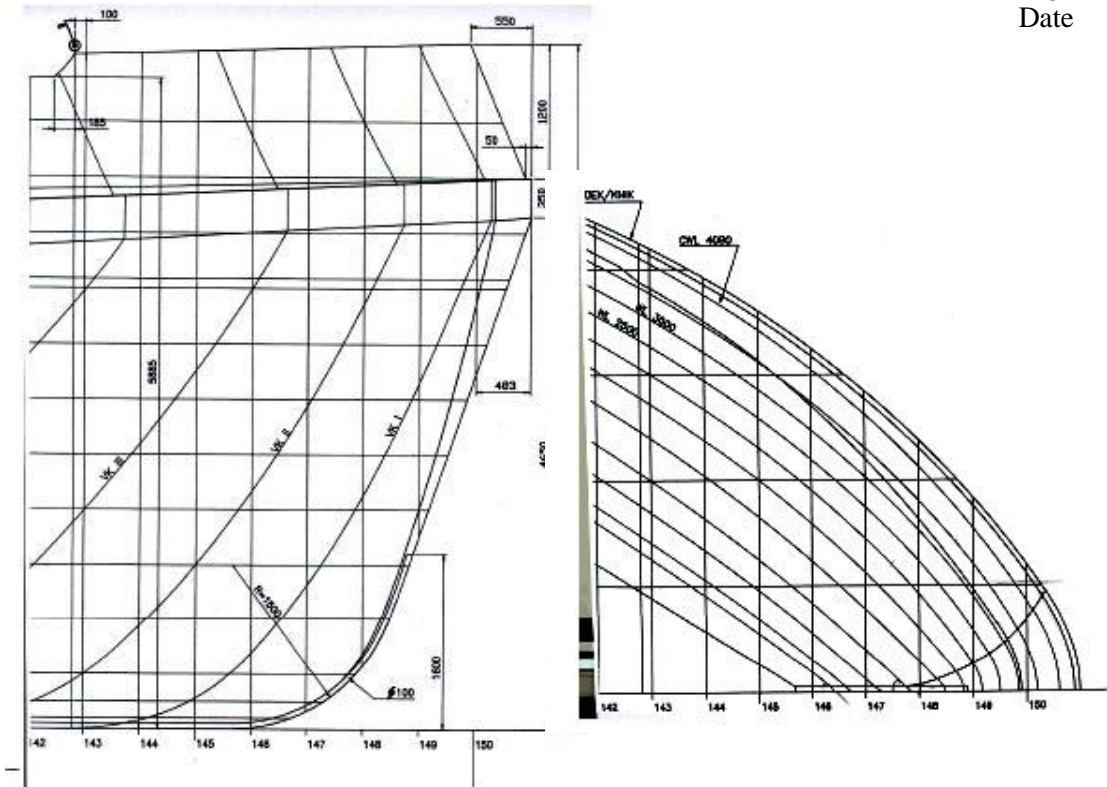


Figure 5 Scantlings V-bow

Crash calculations

All the 36 identified collision scenarios have been calculated and the energy absorption capacity for each case has been determined and is entered into the probability matrices defining the overall probability comparison of penetration upon collision. This results in the probability reduction factor given hereunder. The results of the calculations are plotted in Table 3 and Table 4.

Striking cases with no failure

In one of the collision scenarios no failure of both inner and outer hull or deck plating occurs and the maximum deformation of 0.3 [m] from the tank boundary is also not reached. This is the scenario for striking with the Europe II type bow on the alternative structure at bulkhead above deck. The energy absorption capacity for this scenario has risen till 28.40 [MJ] at 2.53 [m] of indentation. This amount of energy exceeds the maximum striking energy available on the river Rhine which is 28.30 [MJ] assuming an inelastic collision for this scenario.

In this way the probability of cargo outflow has been reduced to zero for those cases. This means that these cases are not taken into account in the probability reduction calculation.

Results Crash calculations

For all calculations the energy values are read just before the first element removal of the inner or outer hull. The numbers in red indicate that no failure occurs.

Y- type structure

New						
Bow type	Collision location		Energy [MJ]	Penetration [m]		0.3 [m] displacement tank boundary
				Outer hull	inner hull	
Europe II	Above deck	bulkhead	28.40	2.53	2.530	
		at web	26.80	1.9	NOT	2.530
		between webs	27.30	NO	NOT	2.530
	On deck	bulkhead	21.40	0.3	NOT	1.620
		at web	15.80	0.5	NOT	1.430
		between webs	16.80	0.4	NOT	1.490
	On half depth	bulkhead	15.60	0.37	1.620	
		at web	11.50	0.4	NOT	1.490
		between webs	11.60	0.4	NOT	1.460
V-Shape	Above deck	bulkhead	11.90	NO	NOT	1.210
		at web	11.40	NO	1.080	1.280
		between webs	12.30	0.8	NOT	1.320
	On deck	bulkhead	13.50	NO	NOT	1.210
		at web	12.90	NO	1.080	1.260
		between webs	9.48	1.08	1.080	
	On half depth	bulkhead	11.30	0.29	1.200	
		at web	10.10	0.3	NOT	1.230
		between webs	8.12	0.1	NOT	1.080

Table 3 Summary results Y-type structure

Reference structure

Reference						
Bow	Collision Location		Energy [MJ]	Penetration [m]		0.3 [m] displacement
				Outer hull	inner hull	
Europe II	Above deck	at bulkhead	10.46	3,100	3,100	
		at web	12.44	3,300	3,000	
		between webs	10.98	3,000	3,000	
	On deck	at bulkhead	5.71	0.430	NOT	0.770
		at web	4.61	0.450	NOT	0.690
		between webs	4.59	0.450	NOT	0.720
	Mid	at bulkhead	5.38	0.150	1,000	
		at web	4.36	0.330	1,050	
		between webs	6.54	0.440	NOT	1,260
V-shape	Above deck	at bulkhead	4.27	NO	NOT	0.820
		at web	3.96	NO	NOT	0.800
		between webs	3.98	NO	NOT	0.800
	On deck	at bulkhead	4.18	NO	NOT	0.690
		at web	1.66	NO	NOT	0.400
		between webs	4.31	0.740	0.74	0.74
	Mid	at bulkhead	4.35	0.150	0.820	
		at web	3.98	0.300	0.925	
		between webs	5.81	0.160	1,120	1,120

Table 4 Summary results reference structure

reference revision
ADN Approval Procedure Argos GL
E10152-40-AP

Page 20/27
Date 15-09-2014

Step 5: Probability calculation

The probability of tank failure is calculated according to the ADN guideline [1]. The CPDF-curves are related to the mass of the struck ship and the velocity of the striking ship. The CPDF curves are prescribed by the following formula of which the appropriate coefficients have to be determined.

$$P_{x\%} = C_1 E_{loc(i)}^3 + C_2 E_{loc(i)}^2 + C_3 E_{loc(i)} + C_4$$

with: $P_{x\%}$ probability of tank failure,
 C_{1-4} coefficients as listed in table 2 of the ADN guideline,
 $E_{loc(i)}$ Energy absorbing capacity.

For the calculations reported the coefficients for the CPDF-curves are listed in table 6. The alternative structure and the reference structure have the same distinctive vertical striking locations with matching depth and mass for the struck ship. This means that for both the alternative and the reference structure use has been made of the same CPDF curves.

Bow Type	Collision location	CPDF corresponding to Mass struck ship	Speed	C1	C2	C3	C4
Push barge	Above deck	6.500 tonnes	1*Vmax	7,503E-05	-4,225E-03	2,571E-02	9,616E-01
			2/3*Vmax	8,405E-04	-2,099E-02	5,468E-02	9,657E-01
			0.5*Vmax	4,789E-03	-6,728E-02	1,010E-01	9,635E-01
	On deck	6.500 tonnes	1*Vmax	7,503E-05	-4,225E-03	2,571E-02	9,616E-01
			2/3*Vmax	8,405E-04	-2,099E-02	5,468E-02	9,657E-01
			0.5*Vmax	4,789E-03	-6,728E-02	1,010E-01	9,635E-01
	Half depth	6.000 tonnes	1*Vmax	7,902E-05	-4,431E-03	2,719E-02	9,590E-01
			2/3*Vmax	9,115E-04	-2,269E-02	6,285E-02	9,573E-01
			0.5*Vmax	5,349E-03	-7,407E-02	1,186E-01	9,517E-01
Bow Type	Collision location	CPDF corresponding to Mass struck ship	Speed	C1	C2	C3	C4
V-Shape	Above deck	6.500 tonnes	1*Vmax	7,503E-05	-4,225E-03	2,571E-02	9,616E-01
			0.3*Vmax	1,088E-01	-5,403E-01	3,017E-01	9,610E-01
	On deck	6.500 tonnes	1*Vmax	7,503E-05	-4,225E-03	2,571E-02	9,616E-01
			0.3*Vmax	1,088E-01	-5,403E-01	3,017E-01	9,610E-01
	Half depth	5.500 tonnes	1*Vmax	8,334E-05	-4,684E-03	2,935E-02	9,542E-01
			0.3*Vmax	1,328E-01	-6,365E-01	3,669E-01	9,471E-01

Table 5 Coefficients for CPDF formula for both Alternative Structure and reference structure

In figures 7 to 10 the calculated probabilities are named $P_{100\%}$, $P_{66\%}$, $P_{50\%}$ and $P_{100\%}$, $P_{30\%}$ with reference to the percentage of the maximum striking velocity. They are plotted in the yellow marked cells

scen.I	Eloc1	CPDF50%	P50%	0,00	w f 50%	0,2	Pw 50%	0,00								
		28,4	CPDF66%	P66%	0,00	w f 66%	0,5	Pw 66%	0,00							
			CPDF100%	P100%	0,00	w f 100%	0,3	Pw 100%	0,00	+		w flocshe	et			
								sum	0,00	Ploc1	0,00	w f loc1	0,001	Pw	9E-07	
scen.I	Eloc2	CPDF50%	P50%	0,00	w f 50%	0,2	Pw50%	0,00								
		26,8	CPDF66%	P66%	0,00	w f 66%	0,5	Pw66%	0,00							
			CPDF100%	P100%	0,06	w f 100%	0,3	Pw100%	0,02	+						
								sum	0,02	Ploc1	0,02	w f loc1	0,005	Pwlo	1E-04	
scen.I	Eloc3	CPDF50%	P50%	0,00	w f 50%	0,2	Pw50%	0,00								
		27,3	CPDF66%	P66%	0,00	w f 66%	0,5	Pw66%	0,00							
			CPDF100%	P100%	0,04	w f 100%	0,3	Pw100%	0,01	+						
								sum	0,01	Ploc1	0,01	w f loc1	0,010	Pwlo	1E-04	
scen.I	Eloc4	CPDF50%	P50%	0,00	w f 50%	0,2	Pw 50%	0,00								
		21,4	CPDF66%	P66%	0,00	w f 66%	0,5	Pw 66%	0,00							
			CPDF100%	P100%	0,31	w f 100%	0,3	Pw 100%	0,09	+						
								sum	0,09	Ploc1	0,09	w f loc1	0,025	Pw	0,0023	
scen.I	Eloc5	CPDF50%	P50%	0,00	w f 50%	0,2	Pw50%	0,00								
		15,8	CPDF66%	P66%	0,00	w f 66%	0,5	Pw66%	0,00							
			CPDF100%	P100%	0,61	w f 100%	0,3	Pw100%	0,18	+						
								sum	0,18	Ploc1	0,18	w f loc1	0,123	Pwlo	0,023	
scen.I	Eloc6	CPDF50%	P50%	0,00	w f 50%	0,2	Pw50%	0,00								
		16,8	CPDF66%	P66%	0,00	w f 66%	0,5	Pw66%	0,00							
			CPDF100%	P100%	0,56	w f 100%	0,3	Pw100%	0,17	+						
								sum	0,17	Ploc1	0,17	w f loc1	0,222	Pwlo	0,037	
scen.I	Eloc7	CPDF50%	P50%	0,00	w f 50%	0,2	Pw50%	0,00								
		15,6	CPDF66%	P66%	0,00	w f 66%	0,5	Pw66%	0,00							
			CPDF100%	P100%	0,60	w f 100%	0,3	Pw100%	0,18	+						
								sum	0,18	Ploc1	0,18	w f loc1	0,041	Pwlo	0,007	
scen.I	Eloc8	CPDF50%	P50%	0,00	w f 50%	0,2	Pw50%	0,00								
		11,5	CPDF66%	P66%	0,07	w f 66%	0,5	Pw66%	0,03							
			CPDF100%	P100%	0,81	w f 100%	0,3	Pw100%	0,24	+						
								sum	0,27	Ploc1	0,27	w f loc1	0,204	Pwlo	0,056	
scen.I	Eloc9	CPDF50%	P50%	0,00	w f 50%	0,2	Pw50%	0,00								
		11,6	CPDF66%	P66%	0,06	w f 66%	0,5	Pw66%	0,03							
			CPDF100%	P100%	0,80	w f 100%	0,3	Pw100%	0,24	+						
								sum	0,27	Ploc1	0,27	w f loc1	0,368	Pwlo	0,099	

Figure 6 Probability calculation, Alternative design, scenario I, collision with push barge

reference ADN Approval Procedure Argos GL
 revision E10152-40-AP

Page 22/27
 Date 15-09-2014

scen.II	Eloc1	CPDF30%	P30%	0,00	wf 50%	0,2	Pw 50%	0,00						
	11,9	CPDF100%	P100%	0,80	wf 100%	0,3	Pw 100%	0,24	+		w flocsheet			
							sum	0,24	Ploc1	0,24	wf loc1	0,016	Pw loc1	0,0038
scen.II	Eloc2	CPDF30%	P30%	0,00	wf 50%	0,2	Pw50%	0,00						
	11,4	CPDF100%	P100%	0,82	wf 100%	0,3	Pw100%	0,25	+					
							sum	0,25	Ploc1	0,25	wfloc1	0,079	Pwloc1	0,019
scen.II	Eloc3	CPDF30%	P30%	0,00	wf 50%	0,2	Pw50%	0,00						
	12,3	CPDF100%	P100%	0,78	wf 100%	0,3	Pw100%	0,23	+					
							sum	0,23	Ploc1	0,23	wfloc1	0,142	Pwloc1	0,033
scen.II	Eloc4	CPDF30%	P30%	0,00	wf 50%	0,2	Pw 50%	0,00						
	16,2	CPDF100%	P100%	0,59	wf 100%	0,3	Pw 100%	0,18	+					
							sum	0,18	Ploc1	0,18	wf loc1	0,021	Pw loc1	0,0037
scen.II	Eloc5	CPDF30%	P30%	0,00	wf 50%	0,2	Pw50%	0,00						
	15,48	CPDF100%	P100%	0,63	wf 100%	0,3	Pw100%	0,19	+					
							sum	0,19	Ploc1	0,19	wfloc1	0,103	Pwloc1	0,019
scen.II	Eloc6	CPDF30%	P30%	0,00	wf 50%	0,2	Pw50%	0,00						
	11,38	CPDF100%	P100%	0,82	wf 100%	0,3	Pw100%	0,25	+					
							sum	0,25	Ploc1	0,25	wfloc1	0,185	Pwloc1	0,045
scen.II	Eloc7	CPDF30%	P30%	0,00	wf 50%	0,2	Pw50%	0,00						
	11,3	CPDF100%	P100%	0,81	wf 100%	0,3	Pw100%	0,24	+					
							sum	0,24	Ploc1	0,24	wfloc1	0,030	Pwloc1	0,007
scen.II	Eloc8	CPDF30%	P30%	0,00	wf 50%	0,2	Pw50%	0,00						
	10,1	CPDF100%	P100%	0,86	wf 100%	0,3	Pw100%	0,26	+					
							sum	0,26	Ploc1	0,26	wfloc1	0,152	Pwloc1	0,039
scen.II	Eloc9	CPDF30%	P30%	0,00	wf 50%	0,2	Pw50%	0,00						
	8,12	CPDF100%	P100%	0,93	wf 100%	0,3	Pw100%	0,28	+					
							sum	0,28	Ploc1	0,28	wfloc1	0,273	Pwloc1	0,076

Figure 7 Probability calculation, Alternative design, scenario II, collision with V-shape bow

reference ADN Approval Procedure Argos GL
 revision E10152-40-AP

Page 23/27
 Date 15-09-2014

scen.I	Eloc1	CPDF50	P50%	0,00	wf 50%	0,2	Pw50%	0,00										
	10,46	CPDF66	P66%	0,20	wf 66%	0,5	Pw66%	0,10										
		CPDF10	P100%	0,85	wf 100%	0,3	Pw100%	0,26	+									
							sum	0,36	Ploc1	0,36	wf loc1	0,010	Pwloc1	0,0035				
scen.I	Eloc2	CPDF5	P50%	0,00	wf 50%	0,2	Pw50%	0,00										
	12,44	CPDF6	P66%	0,02	wf 66%	0,5	Pw66%	0,01										
		CPDF1	P100%	0,77	wf 100%	0,3	Pw100%	0,23	+									
							sum	0,24	Ploc1	0,24	wf loc1	0,029	Pwloc1	0,007				
scen.I	Eloc3	CPDF5	P50%	0,00	wf 50%	0,2	Pw50%	0,00										
	10,98	CPDF6	P66%	0,15	wf 66%	0,5	Pw66%	0,07										
		CPDF1	P100%	0,83	wf 100%	0,3	Pw100%	0,25	+									
							sum	0,32	Ploc1	0,32	wf loc1	0,058	Pwloc1	0,019				
scen.I	Eloc4	CPDF50	P50%	0,24	wf 50%	0,2	Pw50%	0,05										
	5,71	CPDF66	P66%	0,75	wf 66%	0,5	Pw66%	0,38										
		CPDF10	P100%	0,98	wf 100%	0,3	Pw100%	0,30	+									
							sum	0,72	Ploc1	0,72	wf loc1	0,041	Pwloc1	0,0292				
scen.I	Eloc5	CPDF5	P50%	0,47	wf 50%	0,2	Pw50%	0,09										
	4,61	CPDF6	P66%	0,85	wf 66%	0,5	Pw66%	0,43										
		CPDF1	P100%	1,00	wf 100%	0,3	Pw100%	0,30	+									
							sum	0,82	Ploc1	0,82	wf loc1	0,120	Pwloc1	0,099				
scen.I	Eloc6	CPDF5	P50%	0,47	wf 50%	0,2	Pw50%	0,09										
	4,59	CPDF6	P66%	0,86	wf 66%	0,5	Pw66%	0,43										
		CPDF1	P100%	1,00	wf 100%	0,3	Pw100%	0,30	+									
							sum	0,82	Ploc1	0,82	wf loc1	0,242	Pwloc1	0,199				
scen.I	Eloc7	CPDF50	P50%	0,24	wf 50%	0,2	Pw50%	0,05										
	5,38	CPDF66	P66%	0,77	wf 66%	0,5	Pw66%	0,39										
		CPDF10	P100%	0,99	wf 100%	0,3	Pw100%	0,30	+									
							sum	0,73	Ploc1	0,73	wf loc1	0,051	Pwloc1	0,037				
scen.I	Eloc8	CPDF5	P50%	0,47	wf 50%	0,2	Pw50%	0,09										
	4,36	CPDF6	P66%	0,87	wf 66%	0,5	Pw66%	0,44										
		CPDF1	P100%	1,00	wf 100%	0,3	Pw100%	0,30	+									
							sum	0,83	Ploc1	0,83	wf loc1	0,150	Pwloc1	0,125				
scen.I	Eloc9	CPDF5	P50%	0,01	wf 50%	0,2	Pw50%	0,00										
	6,54	CPDF6	P66%	0,64	wf 66%	0,5	Pw66%	0,32										
		CPDF1	P100%	0,97	wf 100%	0,3	Pw100%	0,29	+									
							sum	0,61	Ploc1	0,61	wf loc1	0,301	Pwloc1	0,184				

Figure 8 Probability calculation, Reference design, Scenario I, collision with push barge

reference ADN Approval Procedure Argos GL
 E10152-40-AP
 revision

Page 24/27
 Date 15-09-2014

scen.II	Eloc1	CPDF30%	P30%	0,00	wf 30%	0,7	Pw 50%	0,00											
	4,27	CPDF100%	P100%	1,00	wf 100%	0,3	Pw 100%	0,30	+				wflocshe et						
							sum	0,30		Ploc1	0,30	wfloc1	0,045	Pwloc1	0,0134				
scen.II	Eloc2	CPDF30%	P30%	0,00	wf 30%	0,7	Pw50%	0,00											
	3,96	CPDF100%	P100%	1,00	wf 100%	0,3	Pw100%	0,30	+										
							sum	0,30		Ploc1	0,30	wfloc1	0,132	Pwloc1	0,04				
scen.II	Eloc3	CPDF30%	P30%	0,00	wf 30%	0,7	Pw50%	0,00											
	3,98	CPDF100%	P100%	1,00	wf 100%	0,3	Pw100%	0,30	+										
							sum	0,30		Ploc1	0,30	wfloc1	0,265	Pwloc1	0,08				
scen.II	Eloc4	CPDF30%	P30%	0,00	wf 30%	0,7	Pw 50%	0,00											
	4,18	CPDF100%	P100%	1,00	wf 100%	0,3	Pw 100%	0,30	+										
							sum	0,30		Ploc1	0,30	wfloc1	0,022	Pwloc1	0,0065				
scen.II	Eloc5	CPDF30%	P30%	0,47	wf 30%	0,7	Pw50%	0,33											
	1,66	CPDF100%	P100%	0,99	wf 100%	0,3	Pw100%	0,30	+										
							sum	0,63		Ploc1	0,63	wfloc1	0,064	Pwloc1	0,04				
scen.II	Eloc6	CPDF30%	P30%	0,00	wf 30%	0,7	Pw50%	0,00											
	4,31	CPDF100%	P100%	1,00	wf 100%	0,3	Pw100%	0,30	+										
							sum	0,30		Ploc1	0,30	wfloc1	0,128	Pwloc1	0,039				
scen.II	Eloc7	CPDF30%	P30%	0,00	wf 30%	0,7	Pw 50%	0,00											
	4,35	CPDF100%	P100%	1,00	wf 100%	0,3	Pw 100%	0,30	+										
							sum	0,30		Ploc1	0,30	wfloc1	0,035	Pwloc1	0,0105				
scen.II	Eloc8	CPDF30%	P30%	0,00	wf 30%	0,7	Pw50%	0,00											
	3,98	CPDF100%	P100%	1,00	wf 100%	0,3	Pw100%	0,30	+										
							sum	0,30		Ploc1	0,30	wfloc1	0,103	Pwloc1	0,031				
scen.II	Eloc9	CPDF30%	P30%	0,00	wf 30%	0,7	Pw50%	0,00											
	5,81	CPDF100%	P100%	0,98	wf 100%	0,3	Pw100%	0,29	+										
							sum	0,29		Ploc1	0,29	wfloc1	0,207	Pwloc1	0,061				

Figure 9 Probability calculation, Reference design, Scenario II, collision with V-shape bow

reference revision
ADN Approval Procedure Argos GL
E10152-40-AP

Page 25/27
Date 15-09-2014

Step 6: Calculate weighted failure probabilities

The weighted failure probabilities are calculated by multiplying each failure probability $P_{(##)\%}$ with the weighting factor as shown below.

			weighting factor
Scenario I	CPDF 50%	wf50%	0.2
	CPDF 66%	wf66%	0.5
	CPDF 100%	wf100%	0.3
Scenario II	CPDF 30%	wf30%	0.7
	CPDF 100%	wf100%	0.3

Table 6 Weighting factors for collision speeds

In Figure 6 to Figure 9, these weighted failure probabilities are named $P_{W50\%}$, $P_{W66\%}$, $P_{W100\%}$ and $P_{W30\%}$, $P_{W100\%}$ respectively.

Step 7: Adding weighted probabilities

By adding the weighted failure probabilities, the probabilities for each location are obtained. In Figure 6 to Figure 9, the probabilities for each location are named P_{loc1} to P_{loc9} for both scenarios for the Alternative design and P_{loc1} to P_{loc9} for both scenarios for the Reference design.

Step 8: Multiply probabilities by location weighting factor

Multiplying these probabilities with the weighting factors $w_{loc(i)}$ from table3, gives the weighted probabilities $P_{wloc(i)}$. In Figure 6 to Figure 9, the weighted probabilities for each location are named P_{wloc1} to P_{wloc9} for both scenarios for the Alternative design and the Reference design.

Step 9: Adding weighted probabilities for each scenario

Adding the weighted probabilities gives the weighted failure probabilities $P_{wloc(i)}$ for collision scenario I and II.

Alternative design:

- the weighted failure probability for scenario I = 0.225
- the weighted failure probability for scenario II = 0.247

reference ADN Approval Procedure Argos GL
revision E10152-40-AP

Page 26/27
Date 15-09-2014

Reference design:

- the weighted failure probability for scenario I = 0.702
- the weighted failure probability for scenario II = 0.320

Step 10+11: Calculate weighted averages

The weighted averages of both scenarios for both designs are:

$$\text{Probability Reference design} = P_r = 0.8 * 0.702 + 0.2 * 0.320 = 0.625$$

$$\text{Probability Alternative design} = P_n = 0.8 * 0.225 + 0.2 * 0.247 = 0.229$$

Step 12: Consequence increase

The tank size for the alternative design is 935 m³ compared to 380m³ for the reference design. In case of tank failure, the consequence will increase with a factor 935/380 = 2.46.

Step 13: Compare tank failure ratio with effect ratio

The consequence for the alternative design increases with a factor 2. The probability decreases with a factor

$$\frac{P_r}{P_n} = \frac{0.625}{0.229} = 2.73.$$

Hence the risk for sailing with the 760 m³ tank will decrease with a factor $\frac{2.46}{2.72} = 0.90$.

The following equations are true:

$$\frac{C_n}{C_r} \leq \frac{1}{P_n/P_r}$$
$$\frac{935}{380} = 2.46 < \frac{1}{0.229/0.626}$$

reference ADN Approval Procedure Argos GL
E10152-40-AP
revision

Page 27/27
Date 15-09-2014

Conclusion

The effect increase of an increase of cargo tanks from 380 m³ to 935 m³ for the type G tanker “Argos GL” is adequately compensated by the application of the alternative crashworthy side structure which protects the cargo tanks as presented in this document. This is demonstrated according to [1] “ADN 2013 Part 9 section 9.3.4. Alternative Constructions”.

References

1. ADN 2013 Part 9, Rules for Construction, part 9.3.4 Alternative constructions.



Technical Division

**GTT REPORT TO ADN - MEMBRANE CONTAINMENT
SYSTEM FOR LNG**

Report




DT-RPT-001158

Revision : 01

20/02/2015

Page : 1 / 16

Technical Division
**GTT REPORT TO ADN - MEMBRANE CONTAINMENT
SYSTEM FOR LNG**
Report

01	First issue	20/02/2015	 MAL	 ENMR	 ARB
REVISION	DESCRIPTION	DATE DD/MM/YYYY	BY	CHECKED	APPROVED

document_simple-rev09



Technical Division

**GTT REPORT TO ADN - MEMBRANE CONTAINMENT
SYSTEM FOR LNG**

Report

DT-RPT-001158

Revision : 01

20/02/2015

Page : 2 / 16

CONTENTS

1. ABBREVIATIONS	5
2. INTRODUCTION	5
3. MEMBRANE DESIGN	6
3.1. INTEGRATED TANKS.....	6
3.2. ATMOSPHERIC TANKS	7
3.3. INSULATION MATERIALS.....	7
3.4. STRUCTURAL VALIDATION	8
3.4.1. FATIGUE.....	8
3.4.2. STRENGTH ASSESSMENT	8
3.4.3. SLOSHING.....	8
3.4.4. CONCLUSION TO STRUCTURAL VALIDATION	12
4. ARGOS GL GENERAL ARRANGEMENT AND SPECIFICITIES	12
4.1. LNG PROPULSION.....	12
4.2. SHIP COMPARTEMENTS	13
4.3. STABILITY	13
4.4. PROTECTION TO SIDE COLLISION RISK.....	13
4.5. LNG PUMPS.....	15
4.6. RELIQUEFACTION	15
APPENDIX 1. GENERAL ARRANGEMENT	16



	Technical Division	DT-RPT-001158 Revision : 01 20/02/2015 Page : 3 / 16
	GTT REPORT TO ADN - MEMBRANE CONTAINMENT SYSTEM FOR LNG	
	Report	

TABLE OF ILLUSTRATIONS

Figure 1: IMO classification of LNG Containment System.....	6
Figure 2: Tank volume optimisation according to LNG containment system.....	7
Figure 3: 3D view of two LNG tanks at small scale.....	9
Figure 4: Picture of the 6 degree of freedom test rig	10
Figure 5: Experimental and numerical assessment of the CS.....	10
Figure 6: Probability of failure definition	11
Figure 7: ARGOS GL General Arrangement	13
Figure 8: DAMEN "Schelde-huid" structure, intact and deformed	14
Figure 9: Corrugated stainless steel primary membrane	14

REFERENCE DOCUMENTS

- [1] SIGTTO - Gas concentrations in the insulation spaces of membrane LNG carriers date March 2007
- [2] ISOPE - Reliability-based Methodology for Sloshing Assessment of Membrane LNG Vessels, E. Gervaise and al. ISOPE 2009
- [3] DAMEN - Royal Schelde Shipyard - Construction aspects for the Schelde Y-shape crashworthy hull structure, Bob van de Graaf
- [4] TU Delft - Ship collision, Joep Broekhuijzen , Flushing, Feb. 2003
- [5] ARGOS .b.v. - Gasoil/LNG bunker ship project - update
- [6] United Nations Economic and Social Council, Working Party on the Transport of Dangerous Goods - Joint Meeting of the RID Committee of Experts and the Working Party on the Transport of Dangerous Goods; Bern 17-21 March 2014 / Tanks.
ref.: ECE/TRANS/WP.15/AC.1/2014/24
- [7] Economic Commission for Europe , Inland Transport Committee, Working Party on the Transport of Dangerous Goods - Joint Meeting of Experts on the Regulation annexed to the European Agreement concerning the International Carriage of Dangerous Goods by Inland Waterways (ADN); Geneva, 26-30 January 2015 /
Report of the meeting of the informal Expert Group "Bunker vessel Argos-GL
ref.: INF 27 -

	Technical Division	DT-RPT-001158 Revision : 01 20/02/2015 Page : 4 / 16
	GTT REPORT TO ADN - MEMBRANE CONTAINMENT SYSTEM FOR LNG	
	Report	


EXECUTIVE SUMMARY

At present, LNG fuel transportation with inland vessels has only been allowed in pressurized, cylindrical tanks. The GTT membrane tank system offers several advantages but does not comply with some of the requirements of the ADN rules.

The membrane technology is the most used LNG cargo containment system for seagoing vessels, integrated into the ship structure. It is operated in near atmospheric conditions with advantages in case of a hypothetical failure and it features a proven, redundant tightness and insulation system.

Its robustness has been thoroughly tested with detailed investigations including very extensive model testing of the sloshing phenomenon, allowing to determine precisely the loads applied on the insulation in all conditions. However, the relevance of sloshing for inland vessels is substantially lower than for seagoing vessels.

The ARGOS GL bunker vessel is the very first application of the membrane system to inland vessels, adequately integrated in the vessel design, structure and systems in order to provide a safe and efficient storage solution, approved by the Classification Society.

	Technical Division	DT-RPT-001158 Revision : 01 20/02/2015 Page : 5 / 16
	GTT REPORT TO ADN - MEMBRANE CONTAINMENT SYSTEM FOR LNG	
	Report	

1. ABBREVIATIONS

ADN: European Agreement concerning the International Carriage of Dangerous Goods by Inland Waterways
BLEVE: Boiling Liquid Expanding Vapour Explosion
BOG: Boil-Off Gas
CFD: Computerized Fluid Dynamics
CS: Containment System
EPF: Exceedance Probability Function
FEM: Finite Element Model
GTT: Gaztransport & Technigaz
IGC Code: International Code for the Construction and Equipment of Ships Carrying Liquefied Gases in Bulk
IMO: International Maritime Organisation
ISOPE: The International Society of Offshore and Polar Engineers
LNG: Liquefied Natural Gas
LR: Lloyd's Register of Shipping
NG: Natural Gas (at vapour stage)
PDF: Probability Density Function
PUF: PolyUrethane Foam
PS: Portside
R-PUF: Reinforced PolyUrethane Foam
RVIR: Rhine Vessels Inspection Regulations
SB: Starboard
SIGGTO: Society of International Gas Tanker and Terminal Operators Ltd

2. INTRODUCTION

With the implementation of new pollution regulation and the probable long term increase of fuel cost, the gas propulsion becomes a competitive alternative to the standard HFO fuelled Ship. The following years will see the development of LNG fuelled Ship designs. These Ships will need to bunker. Shipping and LNG distribution industries are currently developing LNG bunker Ships.

In this context, ARGOS as main bunker fuel operator wants to develop its activities in LNG bunkering. Thus, the ARGOS GL project is currently under development. This ship is designed for bunkering both seagoing vessels and inland waterway vessels, but can also be used for delivering LNG to bunkering stations.

The vessel is designed as an inland waterway Type G tanker, according to ADN 2015, to the Rhine Vessels Inspection Regulations (RVIR) and to the Lloyd's Register Rules and Regulations for Inland Waterway Ships. The working area of this ship is mainly Amsterdam, Rotterdam and Antwerp ports. This ship will be able to bunker as well Gasoil (four tanks of 380 m³ each) and LNG (two tanks of 935 m³ each). It will be the first combined LNG / Gasoil bunker vessel. This LNG bunker ship is not a standalone item, but an opportunity for the total chain.

This development is included in LNG Masterplan for Rhine-Main-Danube and will be co-financed by the European Union. This project is under development since beginning of 2013. The main next target dates are the followings:

- March 2015: signing contracts, beginning of hull construction in Romania
- October 2015: arriving of hull in the Netherlands for outfitting
- February 2016: tests and power up LNG gas generator systems
- March 2016: LNG cargo system tests finalisation
- April 2016: LR approvals and ship delivery

The technology chosen for LNG containment system is Mark III Flex membrane system developed by GTT.

GTT is a world leader in the LNGC market, thanks to its membrane containment system. The company is continuously adapting its technologies to meet new challenges. GTT's membrane technology is recognised by all industry players thanks to its compactness, reduced construction time, cost effectiveness, etc. These advantages, together with the large network of Shipyards proposing GTT systems have allowed GTT's market share to continuously increase.

This document aims at giving technical justification of the safety of the membrane system for inland waterway navigation.

3. MEMBRANE DESIGN

IMO classification of LNG containment system considers separately independent tanks from integrated tanks as explained in the following figure:

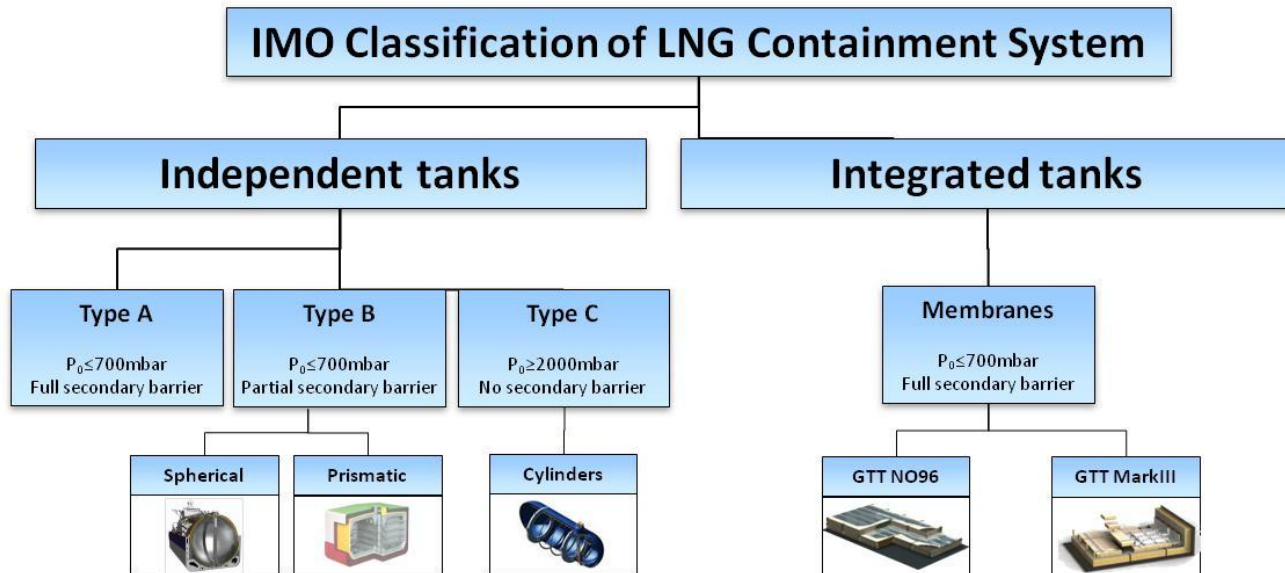


Figure 1: IMO classification of LNG Containment System

Membrane systems have two main characteristics:

- Integrated system: the tank is integrated into the ship structure;
- "Atmospheric" system: the pressure is maintained under 700 mbarg.

All GTT LNG containment systems are fully validated by the major Classification Societies including Lloyds Register which is in charge of the classification of ARGOS GL ship.

3.1. INTEGRATED TANKS

The tank is integrated to the ship: the insulation is supported by the adjacent hull structure. The functions of thermal insulation and tightness are realised by two separated components. For Mark III GTT containment system, the components are the following:

- Insulation is achieved by: R-PUF: Polyurethane Foam (PUF) reinforced (R) by glass fibre;
- Tightness is ensured by two barriers: Triplex – composite: two glass clothes and aluminium foil in between (so-called secondary barrier) - and Stainless steel 304L thickness 1.2mm (so-called primary barrier).

This separation of function allows optimizing the weight of the solution. GTT membrane systems are light (around 70 kg/m²). Thus, for the same cargo capacity, the ship lightweight is reduced with membrane system.

This LNG containment system does not create any particular points or stress concentrations on the ship structure because it is integrated: the loads are transferred in a uniform way to the hull structure. No thermal loads are transferred to the ship structure.

Because the system is integrated, no loss of space is induced by inspection room between hull structure and insulation. For ARGOS GL project, LNG cargo capacity is increased by 55,8% with membrane containment system compared to type C system as illustrated in the following figures:

Conceptual design: Type C LNG cargo tanks

$$4 \times 300 \text{ m}^3 = 1\,200 \text{ m}^3$$

Final design: Membrane LNG cargo tanks

$$2 \times 935 \text{ m}^3 = 1\,870 \text{ m}^3$$

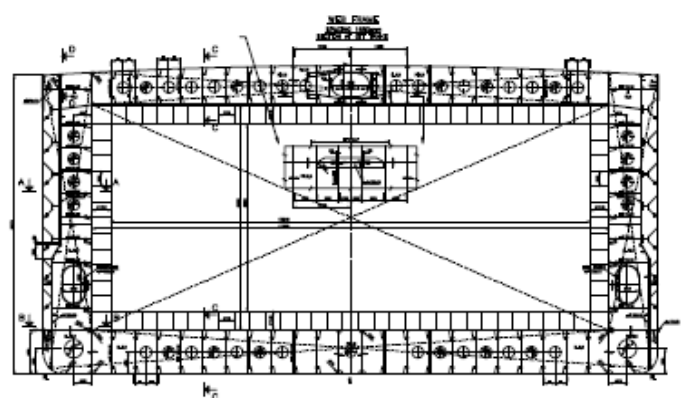
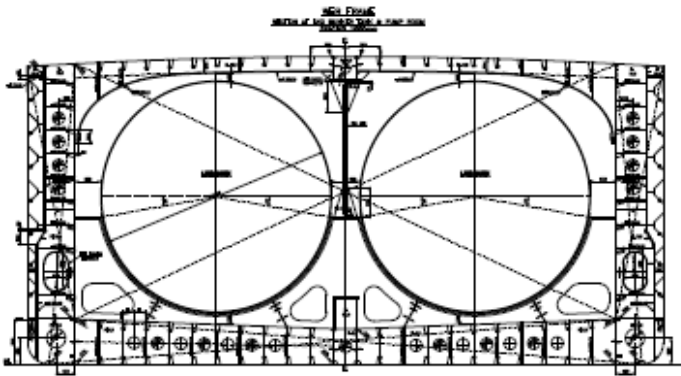


Figure 2: Tank volume optimisation according to LNG containment system

In addition type C tank cannot be filled up to the same level than the membrane tanks because of the higher pressure setting of their safety valves.

3.2. ATMOSPHERIC TANKS

According to IMO classification, membrane tanks are atmospheric tanks. The pressure is controlled under 700 mbarg.

From a safety point of view, as opposed to pressurized tank, this means:

- No risk of BLEVE (Boiling Liquid Expanding Vapour Explosion);
- No jet fire;
- Limited amount of spill and reduced dispersion range in case of an hypothetic catastrophic containment failure, as the leaking flowrate would be purely generated by gravity instead of pressure.

Pressure is permanently monitored inside the tank and controlled between 50 and 150 mbarg in order to keep LNG as cold as possible.

3.3. INSULATION MATERIALS


Mark III (and Mark III Flex) containment system is made of plywood, mastic, reinforced polyurethane foam, triplex and stainless steel. The selection of material is done according to classification society and GTT cooperation.

Testing methods are defined, after in-house GTT laboratory tests.

For each material used, a dedicated material specification is issued including explanation on performance characteristics. Suppliers are approved by GTT and classification society.

The main requirements are the following:

- To withstand LNG temperature (-163°C) and warming up temperature (up to 60°C);
- To be chemically compatible with LNG, water, sea water and nitrogen;

	Technical Division	DT-RPT-001158 Revision : 01 20/02/2015 Page : 8 / 16
	GTT REPORT TO ADN - MEMBRANE CONTAINMENT SYSTEM FOR LNG	
	Report	

- To withstand dynamic pressure loads due to LNG motions inside the tank;
- To withstand pressure variations from - 800 mbarg to 3 barg.

All the insulation materials including R-PUF are enclosed between hull structure and primary barrier made of 1,2 mm thick Stainless steel sheet. This primary barrier is in direct contact with LNG. The fire risk within these spaces is null since there is no ignition source and no oxygen in the insulation spaces and inside the tank itself. So this situation is totally different from externally insulated tank of road trucks which may be exposed to ignition source in the presence of ambient air / oxygen - see ref. [6]

In case of fire, the heat ingress will increase and the BOG flow as well. The pressure safety valves are designed according to this fire case. In case of fire, the integrity of the tank is ensured.

Moreover, the insulation spaces are permanently inerted by nitrogen. The pressure is permanently controlled ensuring that no air ingress is possible. The insulation spaces are continuously monitored for detection of hydrocarbon traces.

For more explanations and risk assessment about the nitrogen system and insulation spaces of GTT membrane system, please refer to the document from SIGGTO *Gas concentrations in the insulation spaces of membrane LNG carriers* dated March 2007 - ref. [1]

3.4. STRUCTURAL VALIDATION

3.4.1. FATIGUE

The membrane system itself plus load standing associated elements are designed and validated for fatigue:

- in extreme conditions: 40 years of operation worldwide including in North Atlantic Winter Conditions
- in addition, consideration of 2,000 full thermal cycles (from ambient to -163°C temperature).

This fatigue calculations are done considering a combination of the following loads:

- Hull bending moment
- Cargo pressure
- Thermal gradient.

3.4.2. STRENGTH ASSESSMENT

The membrane strength assessment combines the loads due to:

- internal cargo pressure;
- external ballast pressure;
- thermal loads;
- ship global and local deflection;
- dynamic loads due to ship motions;
- sloshing loads.

3.4.3. SLOSHING

3.4.3.1. Preamble

This section deals with the sloshing phenomenon in relation with the membrane system, because:

- this issue has been raised repeatedly during previous ADN discussions about the membrane;
- in the past, it has caused some concern in the LNG maritime industry, as opposed to pressurized tank.

However, sloshing does not occur on inland waterway vessels as discussed in section 3.4.3.6 below. Tanks are too small and ship motions are reduced. This load case is not to be considered for ARGOS GL project.

3.4.3.2. Nature of sloshing and GTT experience

Sloshing is the result of global cargo motions within a partially filled tank resulting from ship motions. When ship motions become significant, waves are generated inside the tank and lead to liquid impacts when they hit the tank walls. This local and dynamic phenomenon has no impact on the general stability of the ship but only with ship structure and containment system. Anyhow, the stability of any ship - inland or seagoing - is ensured by the compliance of the compulsory Stability Booklet with IMO and ADN regulations as well as Classification Societies rules for ships carrying a liquid cargo, including the free surface effect.

Sloshing is a resonance phenomenon, it means that the frequency of the impacts and their magnitude will tend to increase when the liquid natural periods coincides with the natural period of the excitation source (the ship motions in relation with the sea state and heading).

Sloshing is by nature a non-deterministic phenomenon. While the global ship motions are predictable, the magnitude, the location and the instant of a sloshing impact are rather unpredictable. Sloshing is hence studied through statistical approaches based on the description of the statistical pressure distributions and the frequency of the impacts.

GTT has developed a unique expertise in:

- assessing the impact of sloshing on the membrane system and its components;
- determining the areas of the tank where membrane reinforcement is required;
- designing suitably reinforced membrane components.

The methodology used for validation can be divided into three parts:

- 1) The sloshing load evaluation;
- 2) The Containment System strength evaluation;
- 3) The final strength assessment which compares both the loads and the containment strength.

The resistance of insulation material in cryogenic conditions (vs. ambient temperature) is tested separately in depth by GTT:

- in its own material laboratory, equipped with state-of-the art equipment, with a long experience considered as a worldwide reference;
- through measurements on board seagoing vessels in operation.

3.4.3.3. Loads evaluation

The sloshing loads are derived from laboratory tests at small scale (1/40).

The tests consist in shaking with pre-determined motions a model tank filled with water and a specific gas mixture at ambient conditions in order to measure representative pressures of the real scale, at various locations of the model tank and for a set of conditions (filling level, heading, sea state).

Tank motion excitations at small scale are derived from the motions at full scale calculated through numerical simulations by means of the Froude similitude.

The model tanks made of PMMA (Plexiglas) represent the tanks shape at model scale:

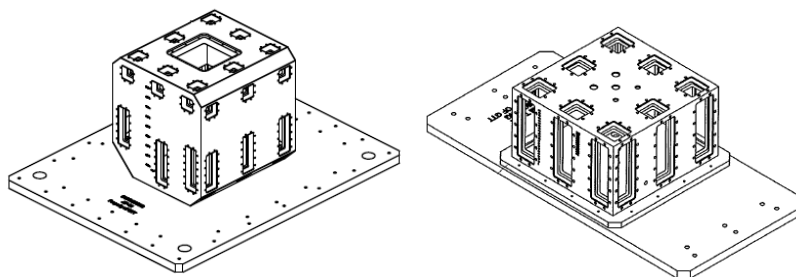



Figure 3: 3D view of two LNG tanks at small scale

	Technical Division	DT-RPT-001158 Revision : 01 20/02/2015 Page : 10 / 16
	GTT REPORT TO ADN - MEMBRANE CONTAINMENT SYSTEM FOR LNG	
	Report	

Six (6) degrees of freedom motion generator called HEXAPOD is being used as a routine for the model tests (see Figure 4). It is based on the "Stewart Platform" principle, with six mechanical jacks and their associated electric-driven motors.



Figure 4: Picture of the 6 degree of freedom test rig

A long-term approach is considered for the sloshing study to determine the maximum expected sloshing loads on the containment system. This approach integrates the sloshing response of all the sea states the vessel will potentially face during her life. It is applied by determining short-term probability density functions (PDF) obtained at the critical filling level for a large set of sea states and headings. These PDFs are then combined, taking occurrence frequency of each sea state and heading into account, to generate the long-term exceedance probability function (EPF).

3.4.3.4. Containment System strength evaluation

The Containment System (CS) is submitted to both thermal (cryogenic conditions) and mechanical (dynamic loads) effects. The modeling of these effects in order to apprehend them from an experimental approach is very challenging.

In-service CS strengths are consequently determined through two complementary approaches:

- Experimental: GTT's finite elements models are calibrated with several kinds of experimental results, like static compression of the CS at ambient temperature or subsystems experiments under dynamic and temperature conditions;
- Numerical: The numerical models which have been validated during the previous step are used to determine the in-service capacities of the CS.

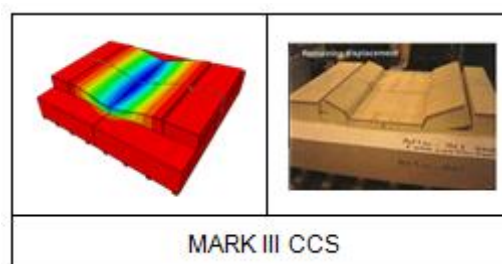


Figure 5: Experimental and numerical assessment of the CS

3.4.3.5. Reliability approach

A reliability method is proposed. Probabilities of failure are calculated for each failure mode of the CS and compared with GTT design acceptance criteria. GTT design acceptance criteria have been determined taking into account the type of CS and the consequences of a failure of one (or several) of its components.

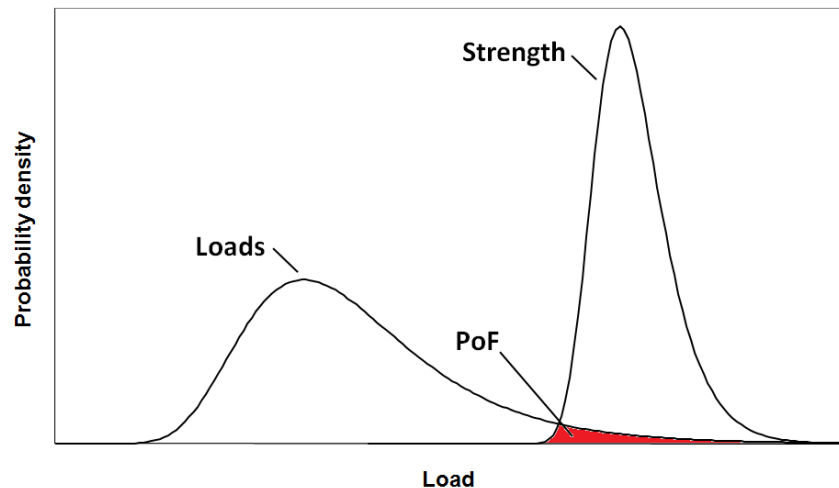


Figure 6: Probability of failure definition

The limit conditions considered for Mark III is the permanent crushing of the foam.

It can be noticed that the sloshing load evaluation is only based on model tests. Indeed, even if CFD simulations can give a good idea of the global liquid flow, today's computers and today's CFD programs are not powerful enough to model all the phenomena occurring during an impact and predict the sloshing pressure accurately enough.

From a liquid motion point-of-view, the overall design can be optimized by:

- modifying the tank shape;
- improving containment strength;
- shifting from one-row of tanks to two-row tanks design.

GTT has developed technical solutions to be able to adapt the containment system to the loads it copes with, even in very severe conditions.

For more details on this subject please refer to: *Reliability-based Methodology for Sloshing Assessment of Membrane LNG Vessels*, - ref. [2]


3.4.3.6. Inland waterway specificities

Seagoing vessels are concerned by sloshing loads because of the tank size allowing wave formation and sea states with large waves creating important ship motions.

Inland waterway vessels are not concerned by sloshing: tank sizes are relatively small (limited mass of liquid moving) and ship structure is anyway not designed to sustain wave patterns generating important ship motion.

Possible LNG accelerations and impacts on board inland vessels are of another nature and amplitude:

- in case of collision with another vessel or a fixed obstruction in the river (e.g. a bridge column), the liquid acceleration will not generate any fatigue stress due to repeated loads. According to GTT calculations, the risk of damaging the containment system by on shock is negligible (multiplied by 10^{-6}) compared to the risk of sloshing in North Atlantic condition navigation. In case of collision, the tank might be probably damaged by the impact itself and not by the wave caused by this impact. This point is specifically addressed by naval architect when calculating the scantling of ship structure according to applicable class rules (about the tank structure reinforcement, please refer to section 4.4);

	Technical Division	DT-RPT-001158 Revision : 01 20/02/2015 Page : 12 / 16
	GTT REPORT TO ADN - MEMBRANE CONTAINMENT SYSTEM FOR LNG	
	Report	

- the liquid accelerations inside the tanks due to the turning of the vessel e.g. in a Rhine turn are much lower than the accelerations to be considered according to the maritime Classification Rules; typically 0.7g transverse - 0.4g vertical.

3.4.4. CONCLUSION TO STRUCTURAL VALIDATION

All the causes of the following loads on membrane have to be taken into account for the design of the ship whatever the LNG containment system chosen. It has to be done according to class rules and ADN regulation.

- Local and global deformations of the tank structure and internal and external pressure impact the scantling of the ship.
- Thermal loads imply a specific choice of steel grade for the tank structure.
- Free surface has an impact on the calculation of ship stability.

It is worth mentioning that after 50 years of operations not a single failure of the primary membrane has occurred, even after a few significant accidents and frequent rough sea conditions.

4. ARGOS GL GENERAL ARRANGEMENT AND SPECIFICITIES

As explained in introduction, this ship will be able to load Gasoil (four tanks of 380 m³ each) as well as LNG (two tanks of 935 m³ each).

4.1. LNG PROPULSION

Three LNG-electric generators are installed for the ship's propulsion and power generation. In a separate engine room in the aft ship a diesel generator is installed for emergency power. For LNG propulsion a separate LNG fuel tank of 40 m³ (volume 100%) is installed. Type C LNG containment system was chosen here.

LNG propulsion system and LNG cargo system are totally independent by design according to ADN §7.2.4.9. This implies that tank monitoring system, safety equipments, pressure management, piping for LNG fuel and LNG cargo parts are totally independent.

4.2. SHIP COMPARTMENTS

The ship is divided into the following compartments:

Forepeak – generator room – cofferdam – LNG fuel storage tank room – cofferdam – Diesel cargo tank 1 (PS and SB) – cofferdam – LNG cargo tank 1 – cofferdam – LNG cargo tank 2 – cofferdam – Diesel cargo tank 2 (PS and SB) – cofferdam – tanks – aft engine room and PS and BS thrusters rooms – aft peak.

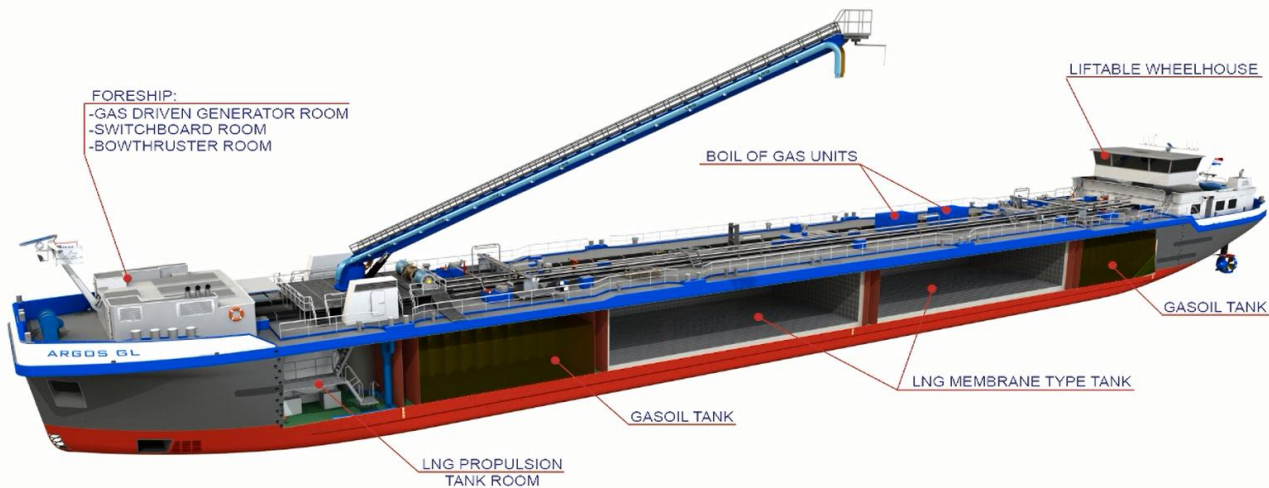


Figure 7: ARGOS GL General Arrangement

The General Arrangement of the vessel is shown in APPENDIX 1.

With the use of so many cofferdams, not only the cargo zone is separated from the fore and aft ship but also the LNG cargo tanks are separated from the gasoil tanks. All cofferdams can be flooded with water. Thus in case of an improbable leakage of a LNG cargo tank or of a Diesel tank, surrounding cofferdams would be flooded in order to avoid any ignition possibility.

Interaction of LNG and Diesel can therefore be considered as not possible.

Moreover, NG is extracted from the same underground oil well as the crude oil from which Diesel is extracted as well. Consequently NG and Diesel are chemically compatible without any risk. Cold NG or LNG in contact with Diesel would just have the physical effect of freezing Diesel.

4.3. STABILITY

The ship fully complies with the stability requirements of the ADN (refer §9.1.0.93 to 9.1.0.95).

The LNG will be carried in tanks with a large breadth, but the free surface moment is included in the ship's stability calculations and this does not lead to a large reduction in stability due to the light density of the LNG (around 0.45 t/m³). The gasoil tanks are divided into a PS and SB tank with a bulkhead in between, so their contribution to the free surface moment is limited but has, of course, been taken into account.

4.4. PROTECTION TO SIDE COLLISION RISK

The ship will be built with a double bottom, a double hull and a double deck. Inside this double hull, the membrane tanks will be placed. As the tanks are integrated inside the double hull of the vessel the risk of being damaged by a collision is limited.

1) However, due to the size of the tanks, the whole vessel needs to comply with the requirements of ADN §9.3.4. Thus, the vessel is equipped with a DAMEN patented 'Schelde-huid'. This Y-shaped crashworthy hull structure allows to sustain high impact loads by increasing the energy absorbing capability of the side shell.

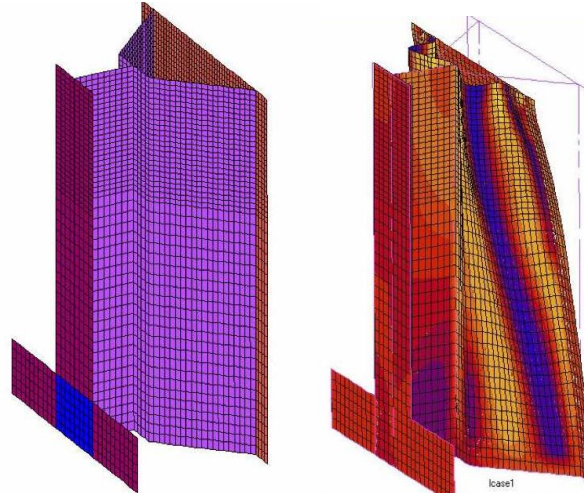


Figure 8: DAMEN "Schelde-huid" structure, intact and deformed

For more details on this crashworthiness structure, please refer to *Construction aspects for the Schelde Y-shape crashworthy hull structure*, ref. [3] and *Ship collision*, ref. [4].

2) The double hull width is 1,065 mm, which is more than required by legislation.

3) Lastly, the GTT membrane containment systems have a great flexibility to withstand the large deformations of the tank structure. For Mark III system, the primary barrier is folded corrugated stainless steel, 1.2mm thick.

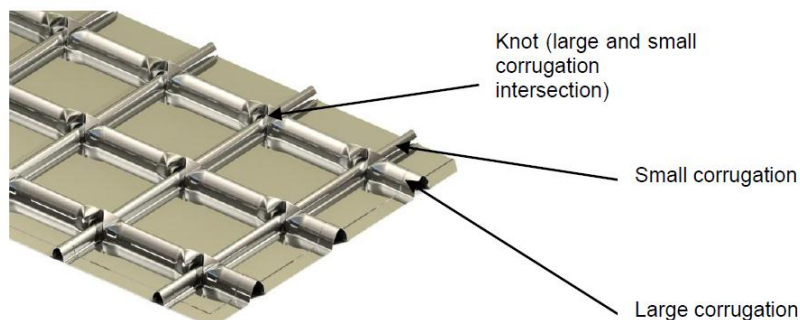



Figure 9: Corrugated stainless steel primary membrane

Tests have been performed at ambient temperature and cryogenic temperature: it is possible to totally unfold primary membrane without any crack apparition. Tightness of primary membrane is ensured under important deformation: the maximum transverse out of plane of tank structure is 150 mm/m

The calculations according to the requirements of ADN §9.3.4 have been made and have showed that the damage of the inner hull of the vessel will be limited, so that the transverse deformation is less that the above limit, and no leakage will occur. The membrane tanks have sufficient flexibility to withstand the deformation of the inner hull of the vessel due to the calculated collisions

	Technical Division	DT-RPT-001158 Revision : 01 20/02/2015 Page : 15 / 16
	GTT REPORT TO ADN - MEMBRANE CONTAINMENT SYSTEM FOR LNG	
	Report	

4.5. LNG PUMPS

Submerged pumps (with electrical motor inside LNG tank) are commonly used in any LNG installation onshore or offshore. Pressure inside tank is above atmospheric pressure ensuring that no oxygen is inside tank. There are no risks of explosion or fire.

ARGOS GL project will use deep well pumps which motor is installed on deck according to ADN requirement §9.3.1.52.1. No electric wire will be inside LNG tank.

4.6. RELIQUEFACTION

Membrane tanks pressure limitation to 0.7 barg requires the installation of a BOG treatment system to be started after a certain time of standstill without gas consumption.

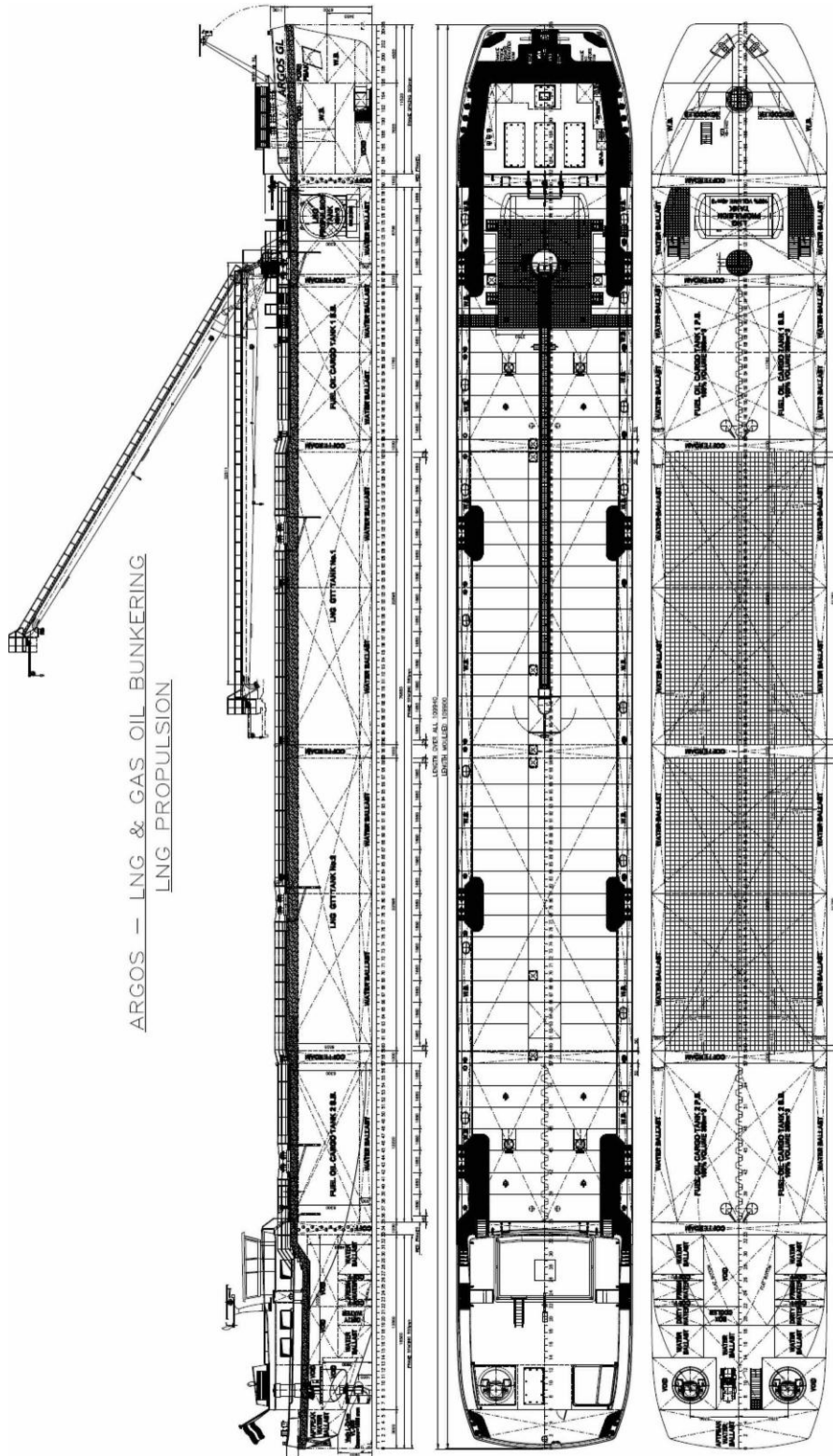
In case of ARGOS GL, BOG is treated by a reliquefaction plant as follows:

- 4 units are fitted, operating in parallel;
- each unit is capable of treating 50% of the design BOG, so a total of 2 x 100% of design BOG;
- therefore, the performance of the system will be sufficient even after a double equipment failure; it should be noted that usually a single failure-proof system is considered as sufficient for safety;
- the ship is equipped with an emergency diesel generator independent from LNG fuel part of the installation ensuring energy for reliquefaction plant;
- the system has been approved by LR for this project.

By design, even in case of failure, the risk to completely lose the reliquefaction function is so low that it can be considered as not possible.



APPENDIX 1. GENERAL ARRANGEMENT



A Mark III panel subjected to a flip-through wave impact: results from the *Sloshel* project

L. Brosset⁽¹⁾, W. Lafeber⁽²⁾, H. Bogaert⁽²⁾, M. Marhem⁽¹⁾, P. Carden⁽³⁾, J. Maguire⁽³⁾

¹GTT (Gaztransport & Technigaz), Saint-Rémy-lès-Chevreuse, France

²MARIN, Hydro Structural Services, Wageningen, The Netherlands

³Lloyd's Register EMEA, London, United Kingdom

ABSTRACT

Within the *Sloshel* Joint Industrial Project, a new full scale wave impact test campaign has been carried out in April 2010. Unidirectional focused waves were generated in a flume in order to impact a rigid wall in which an instrumented Mark III LNG containment system panel had been embedded. The wall was entirely covered with the Mark III corrugated membrane in the same way as on board a LNG carrier.

During one of the last tests of the campaign a flip-through type of impact was generated and very high local pressures were measured. The horizontal small corrugations of the membrane were significantly deformed but no permanent deformation of the foam was observed by initial visual inspection. After removing the Mark III panel and cutting it into small blocks, no discernible cracking, no discernible permanent deformation and no discernible change of the initial properties were observed.

This paper describes the main lessons obtained from this flip-through impact, through measurements related to the hydrodynamic loads, and through the structural response of the different components of the Mark III panel.

KEY WORDS: Sloshing, LNG carrier, Mark III, Corrugation, Containment System, Flip-Through, impact pressure, *Sloshel*

INTRODUCTION

The aim of the *Sloshel* full scale Mark III tests was to study some key issues related to sloshing impacts in tanks of Mark III LNG vessels through impact tests of breaking waves in a flume. Although obviously not identical to the real conditions, the conditions induced by impacts of breaking waves in a flume with water and air on a real Mark III containment system are considered to be relevant for studying fluid-structure interactions, scaling effects by comparison with a previous test campaign at scale 1:6 and wave-corrugation interactions. These tests also enabled the building of a reference data base for validation of numerical simulations.

As the loads generated by the water are almost twice as large as those generated by LNG for similar waves due to the ratio of densities, caution was taken in order to not damage the membrane or the containment system before having stored enough data. The wooden-wedge-reinforced version of the membrane was used and only large air-pocket type or slosh type of impacts (inducing large but not extreme loads) were generated at first. These types of impacts, described in Brosset et al (2009), are believed to be the most representative of

sloshing impacts for low and partial fill levels in tanks of LNG carriers.

After 139 tests with such waves, without any discernible deformation of the corrugations, it was decided to generate intentionally a flip-through type of impact, less likely to occur onboard a ship but potentially capable to deform the corrugations and to damage the foam or the plywood plates of the Mark III panel.

During test 140 a real flip-through impact was created, inducing a maximum measured pressure of 56 bar, the highest ever measured during the different campaigns of the *Sloshel* project. The horizontal corrugations of the membrane were significantly deformed with a maximum deflection of 5 mm. No permanent deformation of the foam was observed by initial visual inspection. After two subsequent tests generating moderate impacts, it was decided to end the campaign in order to allow a careful check of the Mark III panel, including search for cracks after cutting the panel into small blocks and material tests. No residual deformation of the foam and no discernible change of the initial mechanical properties were observed.

This paper describes in detail test 140, through the numerous measurements (pressures, strains, forces) and high speed videos recorded, related to both the loads and the response of the containment system including the corrugations. Reasons are proposed to explain why the foam was not crushed after the panel withstood a maximum pressure of 30 bar while its notional capacity is only 14 bar at ambient temperature in static conditions.

TEST SET-UP

The full scale Mark III tests were carried out in the outdoor Delta flume operated by Deltares in The Netherlands. The flume is 240 m long, 7 m high and 5 m wide. At one end it features a piston-type second order wave making system. Details of the set-up are given by Kaminski and Bogaert (2010). For the sake of simplicity, only the elements that are relevant to the present paper are described in the section below.

General set-up

A transverse concrete test wall was placed 145 m from the wave maker. A horizontal steel test panel was embedded into the test wall, enabling the mounting of two instrumented blocks at a height in between 5.0 m and 6.0 m above the bottom of the flume as indicated in **Figure 1**. The two blocks were 1.2 m wide and 1.0 m high. The first one, on the left in **Figure 1**, was a thick block of aluminium. The second one, on the right in **Figure 1**, was a Mark III panel cut in order to fit within the opening (1.2 m wide instead of 3 m originally). The panel was assembled from

components delivered by a Mark III certified manufacturer. The two blocks were bonded at their back sides to metallic plates (force plates) lying on load cells. The Mark III panel was glued on the force plate using horizontal mastic ropes running over its whole width and spaced every 100 mm.

The test wall was completely covered by the Mark III corrugated membrane in the same way as on board a LNG carrier, as shown in **Figure 1**. The large corrugations were set vertically. This choice was motivated by the fact that, when deformed corrugations have been observed on board LNG carriers in the lower part of the tanks, they were most of the time located on the longitudinal bulkheads. As the tests were performed with water, thus with a density more than twice the density of LNG, the reinforced version of the Mark III membrane was used. In this version, installed recently on board some Mark III ships, the large corrugations have ribs and all corrugations are strengthened by wooden wedges.

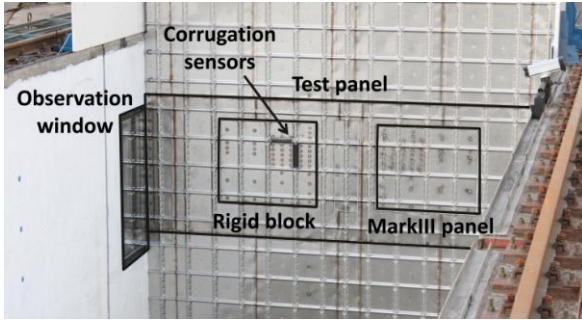


Figure 1 - Test set-up of full scale Mark III tests. Test panel, rigid block, Mark III panel, corrugation sensors and observation window.

Instrumentation

Each block was instrumented with 52 pressure sensors placed flush on its surface running through and welded to the membrane. The configurations of sensors on both blocks were symmetrical to the middle vertical line of the wall. The sensors can be distinguished on **Figure 1**. These configurations with the numbering of the sensors are detailed in **Figure 2**. The letters ‘R’, ‘M’ and ‘P’ stand respectively for ‘Rigid block’, ‘Mark III block’ and ‘Pressure sensor’.

Two especially-designed *corrugations sensors* were developed by MARIN. Such sensors have the shape of real corrugations and were set-up on the wall instead of the original corrugations. Each sensor measured two forces exerted by the flow on each side of the corrugation, perpendicular to the corrugation in the wall plane. The forces are positive when oriented towards the centre of the corrugation. A vertical and a horizontal corrugation sensor were set up on the rigid block. They can be readily distinguished on **Figure 1**.

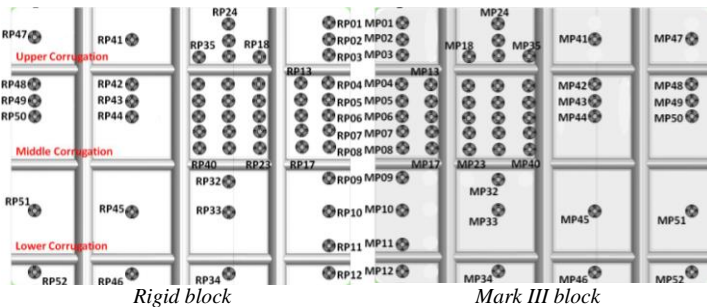


Figure 2 - Configuration of pressure sensors on Rigid block and Mark III panel.

The Mark III panel was also instrumented with strain gauges and accelerometers on (1) the inside of the plywood cover plate, (2) the triplex membrane and (3) both sides of the bottom plywood plate. **Figure 3** shows the sensor configurations for both plywood plates. The letters ‘S’ and ‘A’ stand respectively for ‘Strain gauge’ and for ‘Accelerometer’.

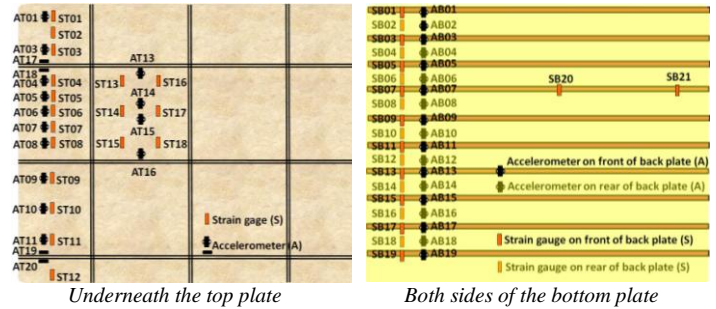


Figure 3 – Configuration of accelerometers (black) and strain gauges (orange) for the top and the bottom plates of Mark III block. Top views.

Transient foam displacements were captured by an optical system based on two high speed cameras observing a section of the foam coated by a speckle raster. The two cameras were fixed as rigidly as possible at the left upper side of the Mark III panel inside the wall. The speckle pattern and the two high speed cameras observing the pattern are shown in **Figure 4**. The area observed by the cameras spans the whole thickness of the foam on a total height of 250 mm in between $h_1=5.650$ m and $h_2=5.900$ m. This area is centred on the upper corrugation of the Mark III block. It is the area targeted to be impacted by the crests of the waves and to withstand the highest pressures. This area is also covered by the largest density of pressure sensors and strain gauges.

An observation window was fitted in the longitudinal flume wall, adjacent to the impacted wall, at the same height as the test panel. The window was 1.5 m high and 1 m wide and can be seen on the white painted flume wall in **Figure 1**. Behind the thick glass of the observation window three high speed video cameras were installed. For each impact, the first camera (HSC1) recorded the full view, the second camera (HSC2) focused on the area in between the middle and the upper corrugations and the third camera (HSC3) zoomed closer around the upper corrugation.

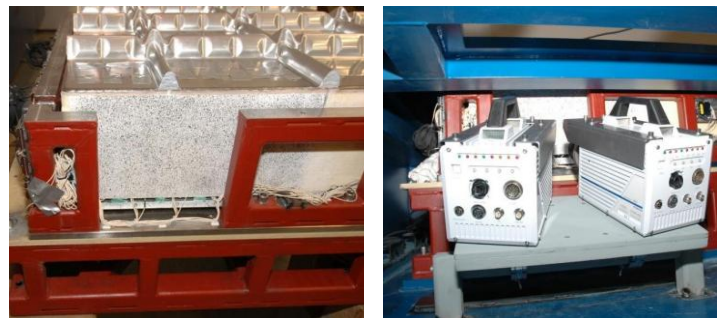


Figure 4 - Speckle pattern at the left side of the Mark III panel (left), and high speed cameras observing the speckle pattern (right).

The data acquisition system for the pressure sensors, strain gauges, accelerometers and load cells sampled at 50 kHz. The cameras observing the displacements of the foam section recorded at 15 kHz. The three cameras inside the observation window were recording respectively at 5 kHz, 5 kHz and 1.2 kHz. All the cameras were synchronized with the data acquisition system.

The maximum measured pressure (55.6 bar) was obtained on sensor RP36 of the rigid block. The instant for which the maximum is reached is taken as the origin of time throughout this paper.

HYDRO-DYNAMICS AND LOADS

All impacting waves during this campaign were generated by a focusing technique (see Hofland et al., 2010 and Kimmoun et al., 2010). Wave packets were generated by the paddle in order to meet at a theoretical focal point. The main parameter enabling the adjustment of the shape of the wave just before the impact was the location of the focal point with regards to the wall. Test 140 was a Flip-Through type of impact, which is considered as a limit case in between the air-pocket type and the slosh type of impact (see Kaminski et al., 2011, Bogaert et al., 2010, Brosset et al., 2009). It is difficult to realize such a flip-through impact in laboratory conditions. Here, the waves have been designed very carefully with an accurate tuning of the parameters at first in a small flume in order to master better the repeatability of the global flow (shape of the wave just in front of the wall) and to obtain as high a pressure as possible. It is considered that this kind of wave is very unlikely to happen in real (in-service) conditions. Nevertheless it is interesting because it brings insight about fluid-structure interaction in highly dynamic conditions.

The Flip-Through impact

Figure 5 shows three pictures recorded by the high speed camera HSC1 inside the observation window at three instants just before the impact. There is a time step of 30 ms between the pictures.

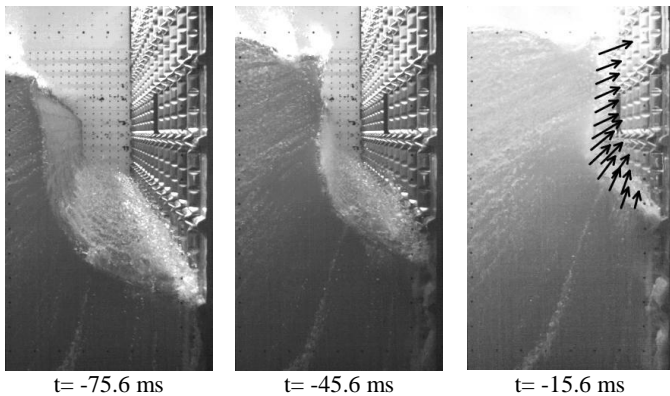


Figure 5 – Wave shape for test 140 just before the impact (Camera HSC1). The black arrows represent the velocities of the bubbles inside the water near the free surface. $V_{max}=8$ m/s.

The first observation that can be made from these pictures is that, as intended, the flow is globally 2D, if the boundary effects on the two longitudinal walls are disregarded. Actually, a close look at the pictures shows that the liquid section close to the observation window is slightly delayed, by a few centimetres compared to the section on the opposite wall. This is confirmed by the analysis of the pressure signals on the horizontal lines of sensors. The signal pattern is globally reproduced from the right to the left but with an almost constant delay of 2.3 ms from pressure sensor column of sensor MP47 (right part of the Mark III block) to column of sensor RP47 (left part of the rigid block). Another consequence is that what is seen from the observation window happens around 2 ms after it has happened on the Mark III block and 1 ms after it has happened on the rigid block.

There are two main global processes that are progressing together: the run-up of the wave trough and the forward moving of an almost vertical wave front.

The run-up process of the wave trough is a general process that would also appear for Air-pocket-type or Slosh-type of impacts. This process mitigates the impact whatever the type because it converts smoothly a part of the horizontal momentum of the wave to a vertical momentum. For a Flip-Through impact the speed of the run-up is higher than for the two other types. Here the maximum vertical velocity of the trough is 4.7 m/s. If the wall were smooth (without corrugations), this run-up process would not induce any significant load on the wall until the wave front is close enough. These conditions have been called *restricted wave trough* in Bogaert et al. (2010). In these conditions, an upward vertical jet would start building from the trough and a pressure pulse would arise from the root of the jet at the wave trough intersection with the wall and travel with the wave trough along the wall. Until these restricted trough conditions are met, the free surface of the trough intersects the wall perpendicularly.

The moving forward of the wave front is also a general process for all types of waves. It can lead to an overturning crest for an Air-Pocket type of impact which would hit directly the wall. The maximum horizontal speed of the front was 8 m/s for test 140. As both the wave front is moving forward and the trough is running up, the space filled by the air in between the front, the trough and the wall is decreasing quickly. This induces an upward vertical air flow. This flow shears the free surface, drawing drops of water out of the bulk of liquid and creating strong irregularities on the free surface and a spray around it. This instability of the free surface is known as the Kelvin-Helmholtz instability (see Drazin, 2004) and is believed to be the main cause of the non-repeatable impact pressure measurements on the wall when repeating accurately the impact conditions. The speed of the extracted drops can be evaluated from high speed camera records and gives an estimation of the air flow vertical velocity. Here the maximum vertical speed of air is evaluated at 50 m/s. Another influence of the air flow is to shape the free surface. For test 140 there is no clear crest. The action of the air jet helps preventing the overturning of the crest.

The loading processes

The trough run-up and the forward move of the wave front are global processes. At each time the trough passes by a corrugation, the same local phenomena happen:

1. immersion of the corrugation (water entry of the corrugation in a reference system linked to the corrugation) and separation of the flow;
2. reattachment of the flow to the wall;
3. entrapment of a small air pocket in between the corrugation and the reattachment point, and compression of this air pocket.

These local phenomena are quite smooth as long as the trough is unrestricted, and do not generate significant loading of the wall or the corrugations. When the wave front is very close, these phenomena become stronger and generate new local phenomena that interact also with the corrugations. These phenomena are detailed in this subsection through the video recordings, the pressure measurements and the force measurements on the horizontal corrugation sensor. For the sake of simplicity, only pressure signals of sensors RP1 to RP8 of the rigid block (see **Figure 2**) are given in this section to illustrate the different phenomena. These sensors, located on the first right column of the rigid block, give the longest

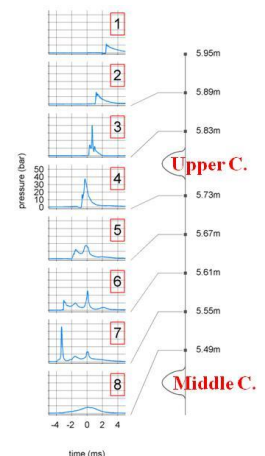


Figure 6 – Pressure signals at RP1 to RP8.

series of working sensors in a column.

As there is a good 2D behavior of the wave, with good duplication of the signal patterns horizontally (at least on the rigid block), this column of sensors is representative of the loading processes on the whole rigid block. The eight pressure signals and the locations of the related sensors are given in **Figure 6**.

- **Direct impact due to the reattachment of the trough**

When the trough is restricted by the close presence of the wave front, the reattachment of the flow, after separation imposed by the run-up along the corrugation, may be very violent. This is the case during test 140 for the reattachment following the separation from the middle horizontal corrugation of the blocks, as illustrated by **Figure 7** by a succession of pictures taken by camera HSC2 at very short time intervals.

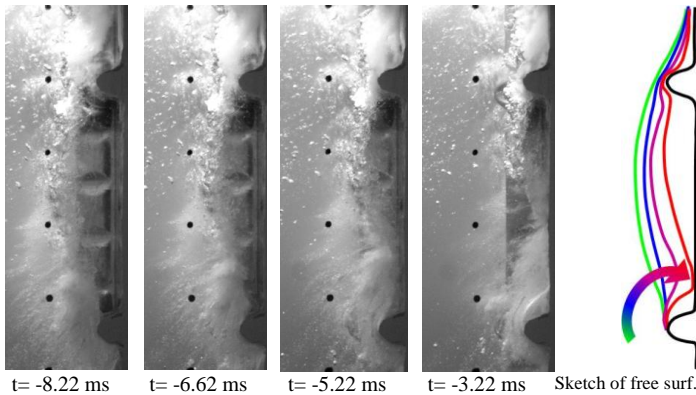


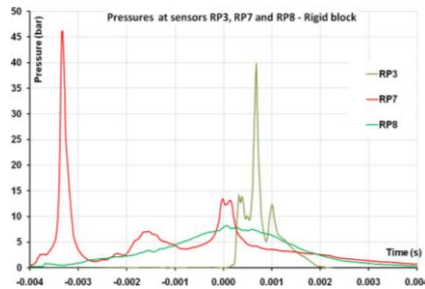
Figure 7 – Separation and reattachment of the flow after the run-up along the middle corrugation (HSC2).

This reattachment leads to a local impact close to sensor row of RP7 with a horizontal velocity evaluated from the videos at 16 m/s. The maximum impact pressure recorded for this local impact is 46.1 bar at RP7. This kind of hydrodynamic impact is very localized: the sensors RP6 and RP8, only 60 mm away from RP7, felt the consequences of the hydrodynamic impact (described later) but not directly the pressure peak. It is also very short: around 0.5 ms at RP7.

The reattachment of the flow leads to the entrapment and the compression of a small air pocket in between the middle corrugation and the impact point. Sensor RP8 is located inside this small air pocket. The boundary of the pocket is clearly visible on the picture at instant $t = -3.22$ ms of **Figure 7**. As a consequence the white cloud around the pocket must be considered as aerated water.

There is also such a reattachment a few milliseconds later after the separation due to the run-up along the upper horizontal corrugation of the blocks. The reattachment is not obvious from the videos but is logically expected and can be deduced from the pattern of the pressure signals at sensor RP3. **Figure 8** shows the pressure signals at RP8, RP7 and RP3.

Figure 8 – Pressure signals at RP3, RP7 and RP8. Impact pressures due to the reattachments after separation at middle (RP7) and upper (RP3) corrugation. Pressure in the entrapped gas pocket (RP8).



The reattachment of the flow to the wall is a direct impact that

generates locally a pressure wave into the liquid and a strain wave into the impacted structure. The pressure wave into the liquid after the first reattachment is clearly visible on the high speed videos. As the water is aerated, the color of the water becomes darker when the front of the wave is passing by, because the bubbles are compressed. This reason has been clearly demonstrated by a close observation of large bubbles crossed by the pressure wave. The speed of the pressure wave has been evaluated around 250 m/s from the videos. This value corresponds to a speed of sound in water with 1% of aeration. With such a speed of sound of the aerated water and the impact velocity of 16 m/s already given, the acoustic pressure on a rigid wall would be 40 bar. The maximum impact pressure of 46.1 bar obtained on the rigid block is in line with this scenario.

The direct impacts due to the reattachment of a restricted wave trough after separation from a horizontal corrugation are very much like wave crest impacts. They lead to non-traveling pressure pulses of large amplitude and short duration, much localized (radius of less than 60 mm here). Such events are thus difficult to capture and might be missed by the network of pressure sensors although actually present.

- **Vertical jet building from the reattaching trough**

After each impact due to a reattachment, a vertical upward liquid jet is building from the impact point. The development of this jet after the first reattachment around pressure sensor RP7 is described in **Figure 9** by a succession of pictures taken by HSC2 at very short time intervals.

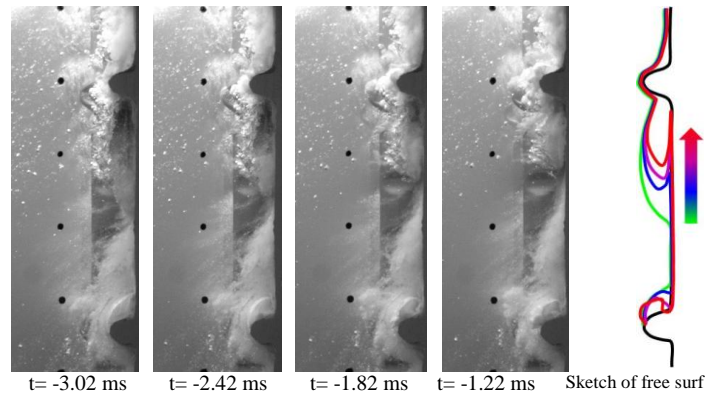


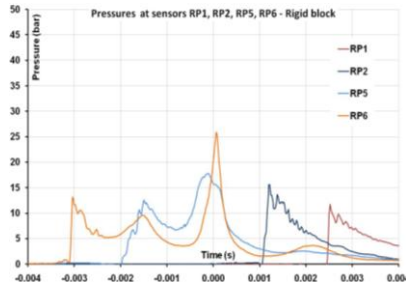
Figure 9 – Building upward vertical jet from the reattaching trough (HSC2).

The root of the jet is located at a point on the wall which is moving upwards because the wave front is still feeding the impact area. This area is thus becoming larger. Close to this point, the velocities in the fluid have to take a very sharp turn, which leads to a pressure pulse on the wall traveling upwards with the point. This traveling pulse is very much like the traveling pressure pulse induced by a drop of a wedge into water initially at rest, a good approximation of which is given by the so-called Wagner solution (see Wagner, 1932).

Such a traveling pulse is captured by pressure sensors RP6 and RP5 due to the liquid jet building from the first reattachment above the middle corrugation and afterwards by pressure sensors RP2 and RP1 due to the liquid jet building from the second reattachment above the upper corrugation.

Figure 10 shows the pressure signals at RP6, RP5, RP2 and RP1. Only the first rise and decrease of the pressure signals at RP6 and RP5 is explained by the traveling pulse due to the building jet. From these signals, a vertical velocity of the root of the jet can be estimated, which is around 60 m/s for the first event and around 43 m/s for the second event.

Figure 10 – Pressure signals at RP6, RP5, RP2 and RP1. Traveling pulses at the root of vertical jets following the reattachment above the middle corrugation (RP6 and RP5) and above the upper corrugation (RP2 and RP1).



• **Direct impact of the jet on the upper corrugation**

The upward jet induced by the reattachment will hit the upper corrugation. At the same time the gas below the corrugation is still escaping, turning around the corrugation. These processes are described in **Figure 11** by a succession of pictures taken by camera HSC2 at very short time intervals.

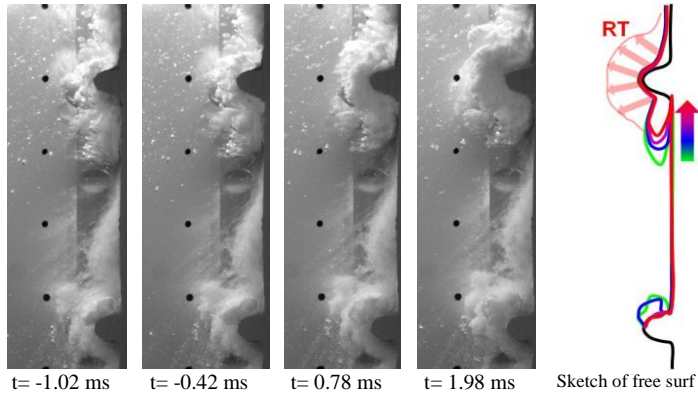
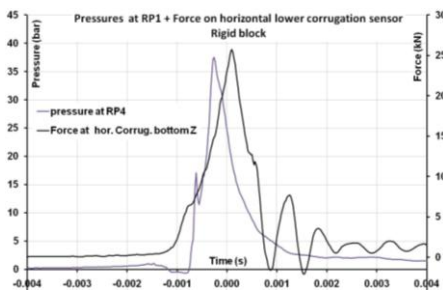


Figure 11 – Impact of the jet on the upper corrugation. Compression of the escaping gas below the corrugation until a sudden Rayleigh-Taylor (RT) gas/liquid mixing process (HSC2).

The volume of air in between the upper corrugation, the trough and the front is decreasing quickly. However the gas is not entrapped and can escape along the corrugation. The white cloud that is seen in the first three pictures of **Figure 11** is due to the Kelvin-Helmholtz instability of the free surface induced by the air jet tangential to the free surface.

Two sensors can help to understand in more in depth what happens locally - they are the bottom part of the horizontal corrugation sensor and the pressure sensor RP4 just under the upper corrugation. Their signals are shown on **Figure 12**.

Figure 12 – Pressure signals at RP4 and force signal at the bottom part of the horizontal corrugation sensor.



It can be seen that there are two parts in the pressure signal at RP4. The first slope is due to the traveling pressure pulse at the root of the jet. So after passing along sensors RP6 and RP5 (see **Figure 10**), the trough is reaching sensor RP4. There is no increase of the pressure before this sharp raise which confirms that the sensor was not within an entrapped air pocket and the air was still able to escape along the corrugation.

The force on the corrugation sensor starts rising before the root of the jet reaches sensor RP4 although there is no gas pocket compression.

Hence, this first rise is due to the impact of the jet on the root of the corrugation. The jet is very thin and cannot alone be responsible for the following rise of the force. A possible scenario is that the thin layer of gas flowing below the corrugation starts to be highly compressed because the gas cannot escape quickly enough. This scenario would explain that very suddenly during the rise of the force on the corrugation, a new cloud of bubbles appears as can be seen on the fourth picture of **Figure 11** (t=1.98 ms). It looks as though the layer of gas explodes, penetrating the free surface by means of bubbles and preventing reaching an even higher pressure. This intrusion of the gas through a liquid free surface is known as the Rayleigh-Taylor process (see Drazin, 2004). It appears as a mitigating process that should be studied carefully in the context of sloshing.

• **Other phenomena**

If one wishes to understand any details of the pressure signals on the rigid block, one needs to be aware that, at any point of the liquid, there is not only the influence of local events but also an influence of remote events. This influence decreases rapidly with the distance ($\sim 1/r^2$). When the liquid is considered as incompressible the information is supposed to be transmitted instantaneously. In the reality, it is traveling continuously through the liquid at the speed of sound by means of pressure waves from one pressure source to any remote point.

Four main elementary loading processes have been described above: the direct impact while the surrounding gas can escape freely, the traveling pulse at the root of a jet, the compression/expansion of an entrapped gas pocket, and the quick compression of a thin jet of escaping gas. Most of the time, only the last three processes are directly measured by pressure sensors. The direct impact process is much localized and it is unlikely to have a sensor just at the right point. What is measured when the phenomenon is captured by a sensor is the remote influence transmitted from the source by a pressure wave. This is likely to be the case for pressure peaks measured at RP3 and RP7 shown on **Figure 8**. This also implies that the maximum pressure measured is not necessarily the maximum pressure actually reached in the vicinity.

The second bump of the pressure signal at RP5 and the third bumps of pressure signals at RP6 and RP7 can also be considered as the remote influence of the final impact on the corrugation. This can be seen more clearly on **Figure 13** gathering all pressure time traces of sensors RP1 to RP8.

The analysis of the remote influence of a loading process is made complex by the fact that these loading processes are very local and some particular events may have occurred that were not captured by the high speed camera recordings. Moreover the level of aeration in the vicinity of the wall can quickly vary in space and in time (presence of bubble clouds for instance), which induces strong variations of the speed of sound.

• **Summary**

All pressure signals of sensors RP1 to RP8 are gathered on **Figure 13**.

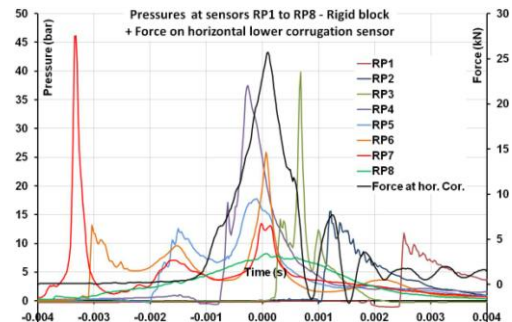


Figure 13 – Pressure signals at sensors RP1 to RP8 and force signal at the bottom part of the horizontal corrugation sensor.

The different parts of the pressure signals recorded during test 140 have been induced by only four different types of elementary local loading processes plus remote influences propagated by pressure waves. These local phenomena are similar as those already seen during drop-tests of wedges into water initially at rest in case of the surface of the dropping wedge includes transverse corrugations or raised edges. For more details about these local loading processes, refer to Lafeber et al., 2011.

HYDRO-STRUCTURAL INTERACTION

The Mark III block was instrumented with many sensors. In this section, we will focus on the top left part of the block, from the middle corrugation to the top and from its left section to the first vertical corrugation (see **Figure 1**, **Figure 2** and **Figure 3**). As the top part was the targeted impact area for all tests, supposed to withstand the highest loads, the left section of this top part was watched by the optical system (two high speed cameras inside the wall) and the top left area was instrumented with the highest density of sensors.

Figure 14 shows the locations of these different sensors and their numbering, including Pressure sensors (MP), Strain gauges (ST) and Accelerometers (AT) behind the Top plate, Strain gauges (SB) and Accelerometers (AB) on both sides of the Bottom plate. The section of the foam as seen by the optical system (in grey) corresponds to a state at rest. The triplex membrane is represented by a vertical line - it could not be detected from the pictures of the optical system. The top and back plates have also been added. The top plate is out of shot but the back plate is in shot of the two high speed cameras.

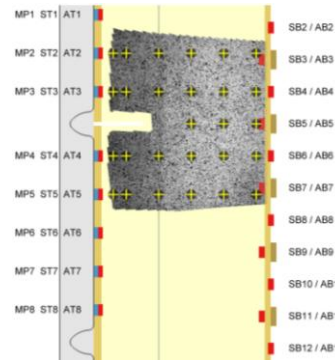


Figure 14 – Instrumentation of the top left part of the Mark III block. Pressure sensors in blue. Strain gauges and accelerometers, both in red.

The pictures from the optical system presented in this paper have been corrected from optical distortions and rigid body motion. After post-processing, the displacements and thus the strains can be derived from the pictures at every point. A grid of reference points has been added on **Figure 14**. The time traces of the normal strains presented later have been post-processed at these locations.

Maximum deflections in the Mark III panel

The maximum transient displacement of the foam normal to its thickness is 2.6 mm and is obtained just under the slit at $t=-0.29$ ms, almost when the maximum pressure is reached on the Mark III block. The maximum normal strain is 1.5%. At the same time the foam is sheared due to the upward vertical force exerted by the flow on the corrugation and transmitted to the top plate. The maximum vertical displacement is 1.4 mm. These values are relatively low compared to the threshold for permanent deflection of the foam as it will be described in the next section dedicated to Strength.

Figure 15 shows the deformed foam and back plate at this instant with a magnification factor of ten. The foam is colored according to the level of normal strains, as post-processed from the pictures recorded by the optical system.

The relaxation slit in the primary foam underneath the upper corrugation avoids the generation of high shear stresses in the top plate. As a consequence there is a higher concentration of normal stresses in

the primary barrier just below the upper corrugation. The presence of the very stiff mastic ropes induces also a concentration of normal stresses in their vicinity. The bottom plate behaves as a beam stiffened by the foam and supported by several almost rigid mastic ropes. The different displacements in the normal direction (x) between the two sides of the slit behind the upper corrugation induce necessarily a slight rotation downwards of the corrugation and of the inner wooden wedge.



Figure 15 – Deformed foam with coloration according to normal strains (left). Deformed back plywood plate (red line on the right) - Instant $t=-0.29$ ms. Both obtained from post-processing of two high speed cameras inside the wall (optical system).

Comparison of the loads on the two blocks

The different local loading processes on the rigid block have been described in detail in the previous section. **Figure 13** summarizes all pressure signals recorded by the pressure sensors RP1 to RP8 on the same column of sensors of the rigid block (see **Figure 2** for the exact locations). The mirror column of pressure sensors on the Mark III block also had 8 sensors MP1 to MP8. Their locations are shown in **Figure 2** and **Figure 14**. Unfortunately four of them were out of order during test 140. Sensors MP1, MP4, MP5 and MP8 were working satisfactorily. Their time traces are shown in **Figure 16**.

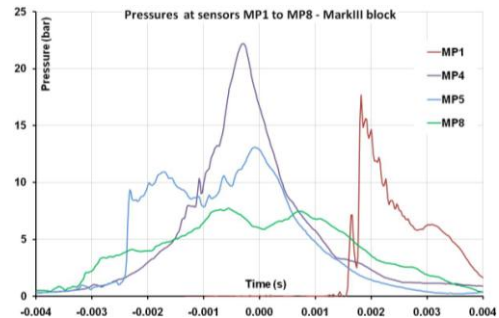


Figure 16 – Pressure signals at MP1, MP4, MP5, MP8 on the Mark III block.

The same main events happened in front of the Mark III block as in front of the Rigid block although a few millisecond earlier, as already mentioned. The reattachment of the flow to the wall, after separation from the middle corrugation, induced the entrapment of an air pocket in between the middle corrugation and the reattachment point. MP8 was inside the pocket or close to its boundary. Signals at MP8 and RP8 are therefore very similar. There was no working sensor available at the reattachment location (around MP7) and thus the much localized pressure pulse due to the impact was not captured. But from the impact point arose an upward vertical jet. The quick rise of the MP5 pressure signal at -2.5 ms is due to the root of the jet passing by the sensor. The same kind of traveling pulse at the root of a vertical jet was also seen on pressure sensors RP6, RP5 and RP4 of the rigid block.

The main difference between the two blocks is that the reattachment on Mark III side also entrapped a gas pocket below the upper corrugation. Both MP4 and MP5 were inside the gas pocket at the reattachment time, which explains that they recorded the same pressures until MP5

went out of the pocket around -2.5 ms. It can be checked on **Figure 13** that the sharp rise of pressure due to the traveling pulse on signals RP6, RP5 and RP4 started from a null pressure, which proves that the air around could escape quickly enough and thus that there was no gas pocket below the upper corrugation of the rigid block.

The presence of a gas pocket underneath the upper corrugation of the Mark III block also explains the significantly smoother pressure peak at MP4 compared to RP4 even though the maximum pressure obtained is not only due to the compression of air.

This local difference of the loading processes could be explained by 3D effects, as only a tiny difference on the incident flows would be needed to make it. In that case, the reduction of maximum pressure on Mark III block with regards to the rigid block would be pure chance. Nevertheless, one can also consider that the entrapment of the gas pocket underneath the upper corrugation has been favored by the receding of the primary foam and the rotation downwards of the corrugation. This could thus have been considered as a result of the fluid-structure interaction on the Mark III panel. The hydro-elasticity would not only be a simple mass/spring issue but could also cause the switch between different local loading processes.

Time traces of strains in the Mark III panel

There are five different parts in the Mark III structure that should be scrutinized separately: the plywood top plate, the foam (primary and secondary), the plywood back plate, the triplex sheet and the mastic ropes. Due to the concision requested for a conference paper, only the first three parts, considered as the weak structural points, are presented. For the triplex sheet, it is apparent that its influence is moderate as there is no discontinuity of the normal strains in the foam in its vicinity (see **Figure 15**). Only a selection of signals among many others is presented here in order to give a sense of what is considered to have really mattered during the impact.

• Top plate

Figure 17 presents the strain time traces as measured by the strain gauges underneath the plywood top plate (ST1 to ST8, see **Figure 14**). These are longitudinal strains, the direction of the gauges being vertical. Positive strains mean tension of the lower fibers.

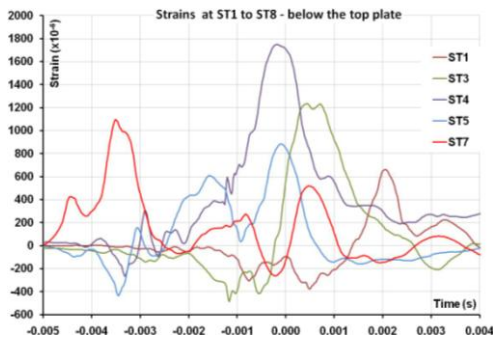


Figure 17 – Strain (microstrain) time traces measured by gauges ST1 to ST8 under the top plate of the Mark III block.

The signal ST2, ST6 and ST8 have been voluntarily excluded of **Figure 17** for the sake of readability and because they did not bring much insight. Reference is made to **Figure 16** for comparison with the pressure signals on sensors MP1, MP4, MP5 and MP8 on top of the plate. Colors are the same for signals from strain gauges and pressure sensors at the same height.

The strains in **Figure 17** are most of the time positive (tension of the fibers) because the main events (reattachment near MP7 and strong compression of the gas pocket under the corrugation) lead to a local

bending of the top plate which has to be counterbalanced further by an opposite bending inducing a global dynamic behavior of the plate. This is particularly clear when looking at ST7 strain around -0.7 ms: while the load is increasing quickly just below the slit, the shape of the plate is forced to accommodate at ST7, far from the event.

The response at ST4 follows closely the load at MP4. This gauge gives the maximum strain which is still low ($1.8 \cdot 10^{-3}$). It is reached only with a small delay (0.2 ms) after the maximum at MP4.

Due to the relaxation slit behind the corrugations, the top plate is split in independent parts vertically. Strains at ST1 to ST3 above the upper slit and at ST4 to ST8 below the upper slit should be largely decoupled as they are located on two separate parts of the plate. Actually, the drop of the strain on gauge ST3 while the pressure rises at MP4 (and thus the strain rises at ST4) indicates that the corrugation and its inner wooden wedge transmit a part of the load to the upper part of the plate which tends to bend its edge towards the interior of the panel.

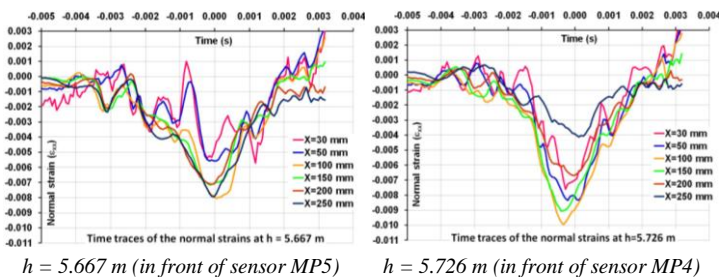
These signals bring indirect information about loading processes that could not be recorded directly because of broken pressure sensors (MP2, MP3, MP6, MP7): (1) the reattachment after the flow separation from the middle corrugation that was captured on the rigid block by sensor RP7 (see **Figure 8**) occurred also on the Mark III panel. The first two peaks of ST7 are the response of this impact; (2) the reattachment after the flow separation from the upper corrugation that was captured by sensor RP3 (see **Figure 8**) occurred also on the Mark III panel around broken sensor MP3. The large peak around $t=0.5$ ms is the consequence of this impact. The peak of ST1 around $t=2$ ms is due to the passage of the root of the vertical jet (maximum just a little delayed compared to maximum of MP1) following the reattachment.

The accelerometers AT1 to AT8 located under the top plate show an intense dynamic activity from the impact due to the reattachment with a saturation of the sensors at around 400 g. Fast Fourier Transforms of both strains and accelerations do not show clear modes.

The maximum level of strain recorded in the whole top plate is 0.002 (0.2%).

• Foam

The post-processing of the images recorded at 15 kHz by the two high speed cameras inside the wall provides relevant information on the structural behavior of the Mark III panel like, for instance, the displacement, the strains in the main directions ϵ_{xx} (normal to the wall) and ϵ_{zz} (vertical), the shear strain ϵ_{xz} or ϵ_{zx} , and the acceleration at any point in the image. **Figure 18** shows the time traces of the normal strains at the six points through the thickness of the foam on the same horizontal line as sensor MP4 and on the same line as sensor MP5 (see **Figure 14** for the exact location of the points). Starting from the top of the top plate, the first point on a horizontal line is 30 mm away. The next points are located every 50 mm.



$h = 5.667$ m (in front of sensor MP5) $h = 5.726$ m (in front of sensor MP4)

Figure 18 – Time traces of the normal strains ϵ_{xx} as post-processed by the optical system at six points at the same height as MP5 (left), at six points at the same height as MP4 (right).

Negative values of the normal strain mean that the foam is in

compression.

A simple verification of these values consists in comparing the mean value over a horizontal line (say, the line starting from MP4) at a time this value is at a maximum (mean(ϵ_{xx}) = -0.0074) with the difference of maximum displacements at the two ends of the line divided by the thickness of the panel ((0.5-2.5)/270=-0.0074).

The normal strain field at $t=-0.29$ ms, corresponding to the maximum pressure (recorded at MP4) and approximately to the maximal strain, is given in **Figure 15**. The coloration helps to understand the distribution of the strains in the foam and therefore the distribution along the two horizontal lines from MP5 and MP4. For instance, it can be noticed from **Figure 18** (left) that the maximum strains on the line starting from MP5 is reached after the maximum on the line at MP4, although the maximum load at MP5 is reached much before the maximum load at MP4. This is clearly due to a 2D behavior within the foam imposed mainly by the global dynamic behavior of the top plate leading to a spreading of the strain field from the load source. This influence of the top plate explains also a more dynamic behavior of the points in the vicinity of the top plate.

The maximum strain in the foam obtained from the optical system is around 1.5% just under the slit. We will come back on this point in the next section and compare it with the strength.

• **Back plate**

Figure 19 presents the strain time traces as measured by the strain gauges SB3 to SB7 alternatively on both sides of the plywood back plate in view of the optical system (see **Figure 3** and **Figure 14** for exact locations). These are longitudinal strains, the direction of the gauges being vertical. Positive strains mean tension of the fibers.

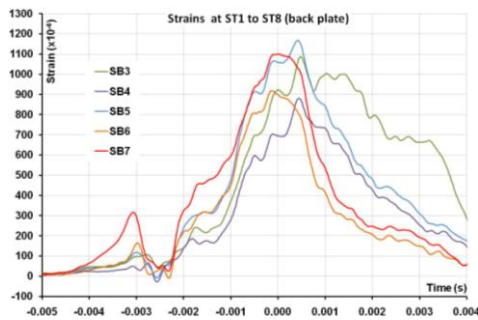


Figure 19 – Strain (microstrain) time traces measured by gauges SB3 to SB7, over and underneath the back plate of the Mark III block.

All strains are positive, which corresponds to the bending behavior of a beam stiffened by the foam supported by the rigid mastic ropes. Maximum strain in the whole back plate is around 0.002 (0.2%).

STRENGTH ANALYSIS

Before test 140, two tests had already induced large pressures though smaller than during test 140. A visual inspection had been conducted after these two tests and no deformation of the corrugations had been observed. Therefore, it is considered very unlikely that any deformation of the corrugations was present before test 140. After test 140 clear deformations of the small horizontal corrugations, but no deformations of the large vertical corrugations, were observed visually. A thorough inspection of the corrugations was carried out with precise measurements of the indentations. During this inspection no visible permanent depression of the membrane in front of the Mark III block was noticed. It was then decided to reproduce twice a moderate wave impact that had already been tested in order to compare the new strain measurements with the previous ones and detect a potential damage of the panel. As no clear modification was observed in the response of the

containment system, it was decided to stop the test campaign and check carefully the foam and the plywood plates of the Mark III test panel.

This section describes the state of the Mark III test panel after test 140 through the results of the different investigations. Strength curves from static tests at ambient are provided for the different components of Mark III and a short analysis is done for a comparison between the Sloschel measurements and what would have been expected from these curves.

Small reinforced Corrugations

As already mentioned, the reinforced version of the membrane was used during the Sloschel Mark III test campaign. **Figure 20** (left) shows the distribution of the wooden wedges inside the small (horizontal) and large (vertical) corrugations. It can be seen that there is a gap of 80 mm in the central part of the small corrugations in between the two long wooden wedges.

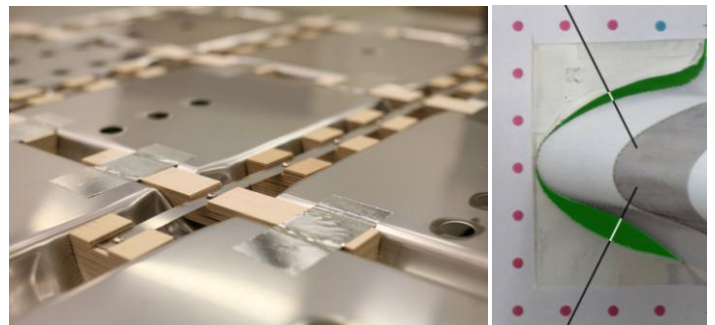
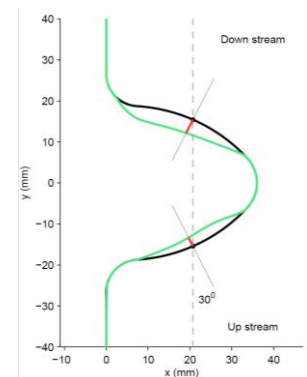
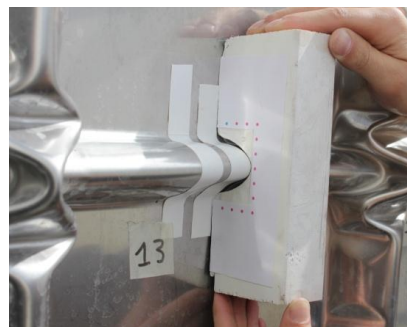


Figure 20 – Reinforcement of the primary membrane by wooden wedges (left) – Most deformed corrugation during test 140: comparison with a template (right).

Only three rows of horizontal corrugations, around the top part of the test blocks, presented visible deformations. All the deformations were in the form of dents on both sides of the corrugations but more pronounced on the lower side. The dents were visible only in the central part of the corrugation, where there was no support of the wooden wedges. No upward or downward global bending was noticed.

The measurements of the indentations for each corrugation of the three rows were performed with the help of a template made directly with a spare part of the primary membrane (overlap membrane part). The template was put over the deformed corrugations as shown in **Figure 21** (left).



Small corrugation template

Definition of the indentations

Figure 21 – Measurement of the indentation of horizontal corrugations.

Photos of the gap between the template and the deformed corrugation were made and post-processed in order to derive two values of deflections according to GTT’s recommendations as shown in **Figure 21** (right). The uncertainty on the final result was estimated to

be plus or minus 0.5 mm.

The maximum indentation measured was 5 mm on the lower side of an upper corrugation of the rigid block, just above pressure sensor RP48. This sensor recorded a maximum pressure of 51.7 bar. The upper side of the corrugation was also the most deformed with an indentation of 2 mm. The picture obtained during the inspection for this corrugation is presented in **Figure 20** (right) after geometrical correction by reference to the locations of the pink dots.

The permanent deformations on both sides of all the horizontal corrugations together with the maximum pressure measured by the sensors are presented in **Figure 22**.

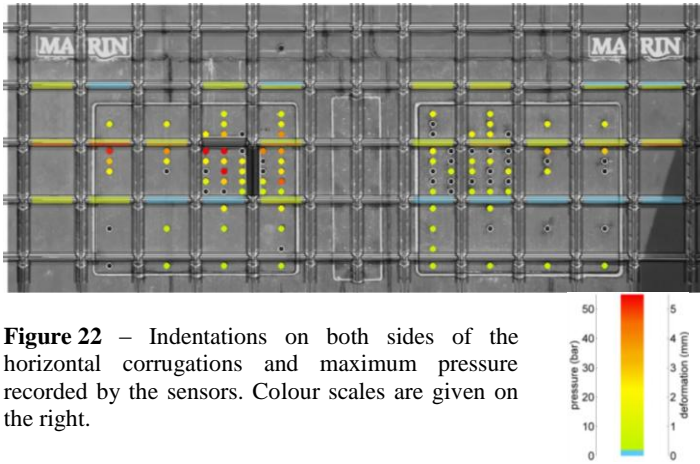


Figure 22 – Indentations on both sides of the horizontal corrugations and maximum pressure recorded by the sensors. Colour scales are given on the right.

When the corrugation is coloured in blue, it means that no visible deformation was observed. A quick look at **Figure 22** allows one to notice that both the pressures and the permanent deflections on the corrugations are lower on the Mark III block than on the rigid. It is difficult to determine conclusively whether this is due to a fluid-structure interaction influence or simply to 3D effects. Nevertheless, it is interesting to notice that the maximum deflections on the lower side of the upper corrugations of the Mark III block range from 1.5 to 2.8 mm whereas the corresponding deflection is 3.8 mm on the next corrugation on the right of the wall lying directly on the concrete. One could argue that it is due to boundary effects along the wall but this increase of deflection does not exist on the other side of the wall.

Bogaert et al. (2010), describing a similar SlosheI test campaign but at a scale of 1:6, mentioned that there is a correlation between the upstream pressure close to a horizontal corrugation and the vertical force measured on this corrugation even though the distance to the corrugation has obviously a large influence on the pressure result. It is therefore interesting to compare the permanent deformation measured on the down side of a horizontal corrugation to the maximum upstream pressure measured by the closest sensor when available. **Figure 23** shows the results for the seven deformed corrugations having an upstream pressure sensor in their vicinity (distance of 50 mm between the sensor and the centre of the corrugation).

All the deformations and corresponding pressures on the Mark III panel are lower than those on the rigid block for the upper line of corrugations (RP09 is located below the middle corrugation).

The curve in red on **Figure 23** is a strength curve of the small reinforced corrugation obtained from static tests at ambient temperature. The pressure was uniform around the corrugation during the tests and the deformations were symmetrical.

There is a good linear correlation between the deflection and the maximum upstream pressure. Although the minimum visible permanent deformation (around 2 mm) was obtained for an upstream pressure very close to the static pressure for the same deflection, the trends given by

the two curves diverge progressively when the pressure increases: to obtain a given deformation, a much lower static pressure is needed than the maximum dynamic pressure measured upstream of the corrugation during test 140.

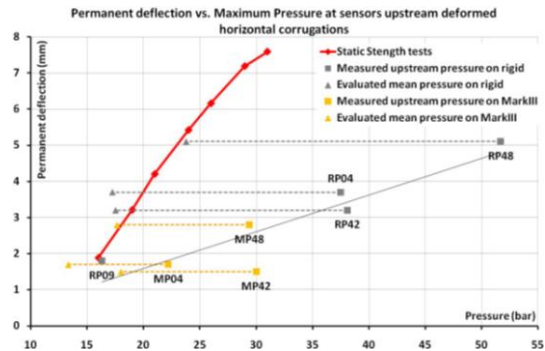


Figure 23 – Permanent deflection of horizontal corrugation vs. Maximum measured upstream pressure (square dots) and maximum evaluated mean pressure (triangles). Labels of the pressure sensors are given. Yellow dots for Mark III, grey dots for Rigid. Static strength curve in red.

Two different reasons could be proposed: (1) the spatial distribution of the load on the corrugation; (2) an increase of the strength due to the load rate.

For the first reason, one has indeed to consider that the pressure measured at the root of the corrugation is very high but in a strong region of the corrugation. The local pressure could be much lower in the central part of the lower corrugation side, which is structurally more sensitive. The corrugation sensor just above sensor RP27 can give some insight about this point. The maximum pressure at RP27 is 55.5 bar. The maximum vertical upward force measured by the corrugation sensor is 25.6 kN (see **Figure 12**). As the length of the corrugation is about 270 mm and its height is 37.2 mm, the surface on which the mean pressure is to be calculated is 0.01 m². It means that the value of the force in kN is precisely the value of the mean pressure in bar. Therefore, the maximum mean pressure on the corrugation sensor is 46% of the maximum upstream pressure. This ratio should be relevant for all upper corrugations on the rigid block as they withstood the same kind of loading process. Assuming this ratio for defining a relevant pressure associated to the permanent deformations of the upper corrugations of the rigid blocks leads to a move of the grey square-shaped dots of **Figure 23** until the grey triangles. These new locations match reasonably well with the static strength curve at ambient. For such a comparable match for the corrugations on Mark III a ratio around 60% is to be assumed. The orange square dots are thus replaced by the orange triangles.

Such ratios fit rather well with the local loading processes proposed for the two blocks. Indeed the compression of an entrapped gas pocket underneath the corrugation (Mark III block) would lead to an almost uniform pressure underneath the corrugation on a large part of it. Having a smaller ratio for the compression of an escaping air jet is expected as the pressure at the free end of the jet is the atmospheric pressure.

Therefore the distribution of the loads below the upper corrugations is enough to explain the difference between the static strength curve and the strength curve from test 140 built simply from the maximum upstream pressure. No special increase of strength due to a load rate influence is required. The static strength curve of the reinforced horizontal corrugations at ambient temperature is therefore relevant for highly dynamic impacts: for a given deflection during an impact, the related pressure from the curve gives a valuable estimation of the maximum average pressure really withstood by the corrugation.

Mark III panel (foam + plywood plates)

The Mark III block used for the Sloshe campaign was a reinforced version: the spaces between adjacent mastic ropes was 100 mm instead of 140 mm for the standard version.

- **State of the Containment system (plywood and foam)**

After the test campaign, the Mark III panel was dismantled and sawn into 16 blocks, through the slits of the primary foam behind the corrugations. Every side of the blocks was carefully inspected visually, by several Sloshe partners, especially in the vicinity of the slit where plastic deformation were expected. No crack or residual deformation was detected either in the plywood plates or in the foam.

Some small samples of foam were cut in the areas where plastic deformation had been expected and static compression tests were performed for comparison with static tests carried out before the campaign. The results in term of Young modulus and offset yield stress (0.2%) were not significantly changed and all in the usual range of characteristics. The conclusion was that the Mark III panel was essentially intact after all Sloshe tests and therefore after test 140.

- **Comparison of measured Strains and Strength from static tests at ambient temperature: Strain rate influence**

Table 1 summarizes the maximum absolute transient values for the relevant strains as measured (1) below the top plate, (2) on the section of the foam in view of the optical system and (3) on both sides of the back plate, together with the different material characteristics (offset (0.2%) yield strain (ϵ_0) and Young modulus (E)) obtained from static tests at ambient. For the plates, the strains are the longitudinal ϵ_{zz} strains measured by all gauges available (see **Figure 3**). For the foam, the strains are the normal ϵ_{xx} strains as deduced from the optical system on all points in view of the cameras.

Table 1 - Maximum strains in the Mark III panel and characteristics of materials from static tests at ambient

	Max(ϵ_{zz})	Max(ϵ_{xx})	ϵ_0	% ϵ_0	σ_0 (Bar)	E (Bar)
Top plate	0.002	-	0.007	29%	700	100000
Foam	-	0.015	0.02	75%	14	780
Back plate	0.002	-	0.007	29%	700	100000

ϵ_0 , σ_0 : offset yield strain and stress (0.2%)

The utilization factor of the static strength at ambient, defined as the ratio of the maximum strain to the maximum corresponding offset yield strain, is around 30% for both plywood plates and 75% for the foam. It must be kept in mind that for the foam we have only information on a boundary section where the maximum load recorded was only 2/3 of the maximum recorded on the Mark III panel. If we considered the most highly loaded section and applied a magnification factor of 3/2 on the corresponding strains, the utilization factor would be 113%. Therefore, in the vertical boundary section observed by the two high speed cameras of the optical system, the static strength was sufficient to withstand the load without any plastic deformation. But in more inner sections, small areas in the foam below the upper slit should have experienced plastic deformations if only the static strength was available. This means that the strength was higher than the static strength at least in the most loaded areas.

Now, the maximum strain rate in the foam derived from the optical system data was around 10 /s. The highest values were obtained just under the upper slit. At the level of pressure sensor MP4, namely 50 mm underneath the slit, the strains shown in **Figure 18** (right) have a highest rate of 7 /s. For a strain rate around 10/s, the Young modulus is quite similar (slightly increased) compared to quasi-static conditions,

whereas the offset yield stress is highly increased. Therefore, in the local areas concerned by such a strain rate (just behind the top plate), the higher strength of the foam due to the strain rate influence prevented any plastic deformation into the foam.

However this strain rate influence does not explain the low level of strains measured.

- **Influence of the dynamic behavior of the top plate on the load distribution**

Figure 24 shows the normal stresses σ_{xx} into the foam at six points on a horizontal line starting from pressure sensor MP4, five centimeters below the slit behind the upper corrugation. The reference points are shown on **Figure 14**. The strains have been presented at the same points on **Figure 18**. The stresses have been deduced from the strains using the Young modulus in **Table 1**, obtained from static tests at ambient. This is relevant because the Young modulus does not change much for strain rates lower than 10 /s. The pressure at MP4 has been added on **Figure 24** as it is also the normal stress on the skin of the top plate at MP4.

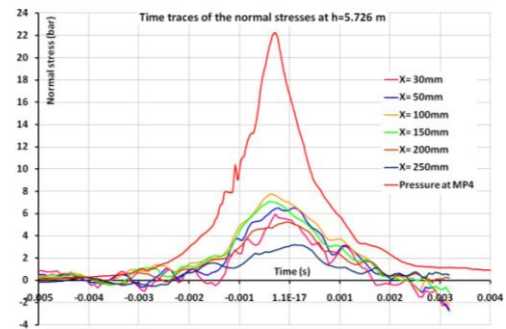


Figure 24 - Time traces of the pressure at MP4 and of the normal stresses σ_{xx} at six points at the same height as MP4.

There is a strong attenuation of the normal stress from the skin of the top plate ($x = 0$) to the first point in the foam in view of the optical system ($x = 30$ mm). The reduction factor is 3.6 when the pressure is at its maximum at MP4. It can also be noticed that the oscillations of the strains are stronger close to the plate than further into the foam but these oscillations are not clearly correlated with those at the strain gauge ST4 under the top plate on the same horizontal line.

What would have been expected from a more traditional analysis with only the records from the pressure sensors? A first well known reason for a reduction of stress into the foam is the distribution of the load by the cover plate. A current approach (see LR Sloshing Assessment Guidelines, 2009 or Gervaise, 2009) proposes to compare the mean maximum pressure calculated on different loaded areas (loading curve) to a static strength curve evaluated by static tests with patch loads. The pressure may be corrected by a Dynamic Amplification Factor evaluated by Finite Element dynamic analysis for different rise times of the load. Such a static strength curve takes benefit of the load distribution by the cover plate.

Let us first construct a loading curve: the minimum loaded area considered is $0.06 \text{ m} \times 0.06 \text{ m} = 0.0036 \text{ m}^2$, which corresponds to the area of influence of a single pressure sensor (60 mm between sensors). The maximum pressure to be considered for this smallest area is 30 bar obtained on sensor MP42. In contrast, when considering the entirety of the Mark III panel, an associated peak pressure may be calculated as peak transient force, namely 726 kN as measured by the load cells behind the panel, divided by associated area, namely 1.2 m^2 , which gives 6 bar. The intermediate areas have been chosen considering a row of sensors (area: $0.08 \text{ m} \times 1.2 \text{ m} = 0.096 \text{ m}^2$; mean pressure from MP4, MP42 and MP48=20 bar) and a more complete collection of sensors (0.33 m^2 , 11 bar).

For choosing a strength curve a special attention must be paid to the criterion. Criteria adopted on board ships can be related to two limit states: (1) failure of the back plywood in between two mastic ropes by shear or bending fracture. The criterion for the strength is a maximum residual deflection of 0.5 mm of the back plywood; (2) fatigue of a membrane knot by rotation when not well supported due to foam crushing – the criterion for which is 10 mm crushing. GTT has built several experimental strength curves by static tests of the standard and reinforced version of Mark III with patch loads at ambient or in service conditions. At ambient and for a standard version of Mark III, the criterion on the back plywood is more severe and thus the tests are conducted with several displacement sensors located behind the back plywood. The foam is checked at the end of the tests. Such a strength curve would provide significantly higher values than the loading curve for test 140 but would not help understanding. For the reinforced version the foam crushes before the failure of the back plywood occurs but there is no experimental strength curve available at ambient temperature. Therefore, for the purposes of this paper we propose a strength curve based on numerical simulations for the reinforced version at ambient temperature. The criterion chosen is the occurrence of a first plastic deformation into the foam.

The loading curve for test 140 and numerical strength curve at ambient temperature are presented on **Figure 25**. A numerical strength curve based on the same criterion of no plastic deformation into the foam but with a thermal gradient from -162°C on the membrane to 20°C at the mastic ropes level has also been added.

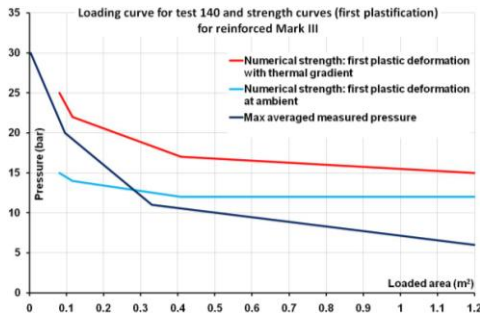


Figure 25 – Loading curve from test 140 (dark blue) - Numerical static strength (first plastic deformation) for reinforced Mark III panel at ambient (light blue) and with a thermal gradient in the Mark III panel (red).

This approach appears to be conservative as for the small loaded areas large zones of plastic deformation into the foam would have been expected from the strength curve at ambient temperature, which was not the case in reality. With an in-service thermal gradient of temperature through the thickness of the foam, the strength would increase significantly when considering smaller and smaller patch loads - this is not the case at ambient temperature. It suggests that the distribution of the load for small patches is efficient at cold temperature but not at ambient, due to a stiffening of the foam at low temperature which limits the local bending of the top plate. Therefore, the distribution of the load by the top plate seems not to be the right explanation for the low level of strains during test 140, at least when the spatial distribution of the loads is made by averaged patch loads.

A 2D Finite Element (FE) model of a vertical section of the Mark III panel was built in order to perform static and dynamic calculations and compare both behaviors. The linear material properties of the plywood and the foam described in **Table 1** were adopted. The plywood plates and the foam were discretized with 10x10 mm² elements. Static and dynamic calculations were performed with a load uniformly distributed on a patch area of 80 mm just under the upper slit. For the dynamic calculation, the load was given directly by the pressure recorded at

sensor MP4. For the static calculation, a load of 22 bar, corresponding to the maximum pressure at sensor MP4, was applied.

Figure 25 shows the results in terms of normal stresses for both calculations. The black area corresponds to higher stresses than the offset yield stress for static tests at ambient (14 bar).

For both calculations, there is a large area under the slit for which the offset yield stress is exceeded. No reduction of stress behind the top plate is noticed. Moreover, there is a significant amplification of the strains into the foam when considering the dynamic load and therefore the *black area* is even larger. The maximum displacements under the slit are respectively 5 mm for the static calculation and 5.9 mm for the dynamic calculation, to be compared to the 2.6 mm obtained in reality. Whatever the size of the loaded area, the patch load approach would always lead to a dynamic amplification (even small) of the strains. Only for very small rise times (lower than 0.2 ms) a dynamic attenuation might occur. This is not the case here as the rise time of pressure sensor MP4 is larger than 1 ms. Therefore, the dynamic behavior of the plywood plates and the foam does not seem to be the right explanation for the attenuation of the strains behind the top plate, at least when the spatial distribution of the loads is made by averaged patch loads.

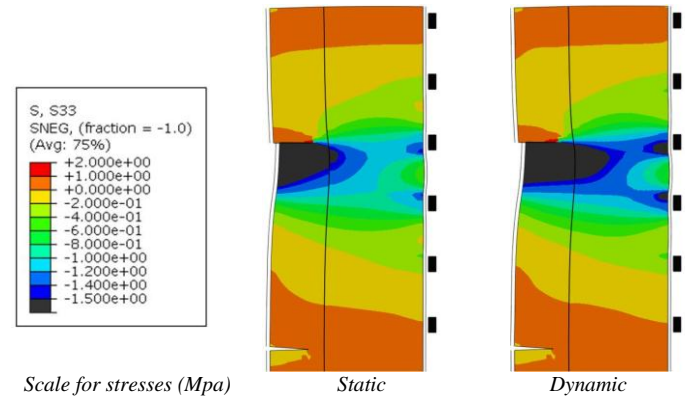


Figure 25 – normal stresses in the foam calculated by static and dynamic FEA on a 2D model of Mark III reinforced panel with a patch load on an area of 80 mm under the upper slit. Dynamic load = pressure recorded at MP4. Static load= 22 bar = max at MP4.

Whichever the way a static load would be interpolated from the sensor signals MP4, MP5 and MP8 when pressure at MP4 is at maximum, the resultant strains would be significantly higher, but for a larger loaded area, thus for a smaller strength, as it has been verified with several calculations. So, a better spatial distribution of the loads does not appear to explain the attenuation of the strains into the foam at least for static loads.

All the above results combine two main parameters: (1) the spatial distribution of the loads (patch load/real distribution); (2) the dynamic behavior (static/dynamic). The results of test 140 indicate that there is an attenuation of the strains into the foam when the load is correctly distributed in space and time. Other results obtained by calculations for simplified spatial or time distributions are summarized in **Table 2** by an amplification factor of the maximum deflection *with regards to the measured one*. These factors are given here just as an indication of a general trend related to possible simplifications of load modeling.

Table 2 – amplification factors on the maximum displacement from FE calculations for different simplifications of the load modeling for test 140.

	Static load	Real time distribution
Patch load	1.8	2.1
Real space distribution	3.0	1

The simplifications of the spatial and time distributions of the loads that are commonly used lead to an overestimation of the strains into the foam and of the maximum displacement for the conditions of test 140. Therefore only a realistic dynamic loading with explicit FE calculations on the whole loaded area should be able to explain the real results.

This is not as simple as it could be first thought because the knowledge on the load through the pressure sensors is incomplete. For instance, among the eight sensors (MP1 to MP8) on the same column, that are of interest for the behavior of the foam in view of the optical system, only 4 sensors were working correctly and a major event such as the reattachment of the flow on the wall after its separation from the middle corrugation was not captured. Even with a complete column of close working sensors, as shown in Figure 6 for the rigid block, the continuity between the signals is not obvious and a relevant interpolation is not straightforward. Nevertheless work is in progress on this matter.

It is believed that when considering a realistic time-space distribution for such globally upwards traveling loads obtained with breaking waves, the dynamic bending behavior of the top plate stiffened by the foam is different than with patch loads and leads to a much better distribution of the loads into the foam. It appears as though the high frequency content of the pressure peaks were filtered by the global dynamic behavior of the top plate.

CONCLUSIONS

During a Sloshel wave impact campaign in a flume involving a fully instrumented reinforced Mark III panel, a Flip-Through impact inducing high pressures was generated (referred to as test 140). Such a Flip-Through impact is considered to be very unlikely on board a LNG carrier but the highly dynamic loading conditions it generates bring insight about fluid-structure interaction in extreme conditions.

During a Flip-Through, the moving forward of the wave front and the run-up of the wave trough progress simultaneously until the front and the trough meet in a very restricted area (*restricted trough* conditions).

The combined analysis of the pressure signals and the videos from high speed cameras watching closely the impact through an observation window enabled the decomposition of the loading mechanisms.

The elementary loading processes (ELP) appear to be very general as far as wave impacts on a structure are concerned. They are: (1) the actual impact (discontinuity of velocity), very localized and inducing acoustic pressure with the local velocity of sound of the aerated water; (2) the building of a jet along the wall from the impact area. The sharp turn of the velocities induces a traveling pressure pulse at the root of the jet; (3) the compression of entrapped gas pockets or escaping gas jets.

All these processes generate loads directly in their vicinity. They have also a more remote influence transmitted by pressure waves through the fluids.

In the particular case of test 140, the situations in which the ELPs developed are related to the nature of the impact (Flip-Through) and to the interactions with the corrugated membrane are: (a) violent reattachment of the flow after separation from a corrugation during the trough run-up (ELP1); (b) building jet from the reattachment point (ELP2); (c) compression of the gas pockets entrapped above the corrugation during the reattachment or entrapped in between the reattachment point, the wave front and the upper corrugation (ELP3); (d) impact of the jet on the root of the upper corrugation (ELP1); (e) compression of a jet of escaping gas below a corrugation (ELP3).

The development of different kinds of free surface instabilities appears to be also a general process associated to wave impacts - these are: (1) Kelvin-Helmoltz (KH) instabilities due to the tangential jet of

escaping gas; (2) Rayleigh-Taylor (RT) instabilities when entrapped gas tends to penetrate the free surface.

During test 140, KH developed during the forward move of the wave front and also below the corrugations. It is believed the KH instability is the main cause of the non repeatability of wave impact pressure measurements even on a flat wall. RT developed underneath the upper corrugation during the final compression of the escaping air jet or the entrapped air pocket. RT might be a mitigating process preventing higher compression. RT creates locally clouds of fine bubbles which eventually increase the aeration of the water. Both phenomena should be studied further in the context of sloshing as they seem to have a large influence on the impact pressures.

The maximum pressure recorded on the rigid block was 56 bar whereas it was 30 bar on the Mark III panel. In both cases the maximum pressure occurred under the upper corrugation. Although the flow was predominantly 2D, the loading processes involved were different on the rigid block and the Mark III panel. On the rigid block, the gas was escaping until the last moment whereas it was entrapped much earlier on the Mark III panel. This difference was considered to be the main reason for the discrepancy on the maximum pressures. It could be simply attributed to small 3D variations of the flow. Nevertheless, the entrapment of gas was favored by the receding of the foam just below the upper corrugation and the related rotation of the corrugation. Therefore, the gap between the maximum pressures could also be attributed to fluid-structure interactions. In such a case, hydro-elasticity appears as more complex than a mass/spring system interacting with a given wave loading process, and could be the cause of a switch from one loading process to another.

Three rows of horizontal reinforced corrugations were deformed during test 140. The vertical corrugations were not deformed. Indentations on both sides of the horizontal corrugations occurred in their central part where there was no support from the wooden wedges. The deflections were significantly more pronounced on the lower side. No global bending of the corrugations was observed. Maximum measured deflection was 5 mm.

This type and level of permanent deflection of the membrane corrugations is not considered as damage since fatigue tests conducted by GTT have shown that deformed corrugations still behave in the same way as non deformed corrugations and their lifetime is not shortened.

The level of deflection is clearly correlated to the maximum upstream pressure (50 mm below the center of the corrugation, thus very close to the foot of the corrugation). Consequently, the deflections are lower on the Mark III panel than on the rigid block. As on both sides of the Mark III panel the deflections on the rigidly supported corrugations are larger than on the Mark III supported corrugations, hydro-structure interaction appears to be a better explanation than random 3D effects.

The maximum mean pressure on the lower side of a corrugation is lower than the corresponding maximum upstream pressure. The ratio deduced from comparison between the force measurement by the horizontal corrugation sensor and the upstream pressure measurement (sensor RP27) is 46%. This ratio should be relevant for all upper corrugations of the rigid block as the loading process remains the same. When applying this ratio to the measured upstream pressures for defining a relevant pressure corresponding to a deflection of any horizontal upper corrugations of the rigid block and to be compared with the strength curve obtained by GTT with static tests at ambient, the points match rather well with the curve. For a comparable match with the corrugations on Mark III a ratio of 60% is suggested. These ratios fit quite well with the two loading processes proposed for the rigid block and Mark III panel, namely the compression of respectively a jet of escaping air or an entrapped gas pocket. Therefore, considering

a static strength curve for the corrugations appears to be relevant: no special reinforcement due to a load rate influence appears to be needed to be taken into account.

Although having experienced local pressures of up to 30 bar, exceeding by far the offset yield stress in quasi-static conditions at ambient temperature, the foam of the Mark III panel did not exhibit any discernible cracking or discernible plastic deformation area after the test, according to visual inspection after cutting the panel in 12 blocks and according to material tests on small samples.

From the post-processing of the optical system measurement, the strains exceeded the quasi-static offset yield strain inside the foam, at least locally under the relaxation slit behind the upper corrugation. As the strain rate in this area was around 10 /s and as the strength (offset yield strain) of the foam is much larger for this range of strain rate, the dynamics of the material played a clear positive role to prevent any plastic deformation.

Moreover, the maximum transient displacement deduced from the optical system measurements was only 2.6 mm. A significant attenuation of the stress level just behind the top plate was observed which could not simply be explained by just the dynamics of the material, as the Young modulus was only moderately increased for the considered range of strain rates. It appears that the pressure signal was filtered by the top plate stiffened by the foam.

According to the current approach, consisting of comparing maximum averaged pressures on different loaded areas (loading curve) to strengths obtained under corresponding quasi-static patch loads (strength curve), the most relevant loading areas for test 140 are the small areas for which the load exceeds the strength. For such areas chosen just under the upper slit, the distribution of the load by the cover plate turns out not to be efficient at ambient temperature. Finite element calculations with the maximum averaged pressure on this area would lead to a large overestimation of the maximum displacement. Introducing the dynamics of the load would amplify the maximum displacement. Introducing the spatial distribution of the loads for quasi-static conditions would lead to an even worse theoretical result.

It seems that only a realistic distribution of the load in space and in time can lead to the actual structural response. This can unfortunately not be easily tested by FE calculations because the density of working pressure sensors is too scarce for a relevant interpolation of the load in space and time domains. Fully coupled fluid-structure interaction analysis (FSI) is seen as a way forward. Nevertheless some efforts are being made to reconstruct the actual interpolated load by an iterative process taking benefit of the knowledge gained from the loading process analysis.

Finally it is interesting to note that the Mark III structural behavior seems to adjust favorably to the worse in service conditions, by:

- large increase of the elastic domain for strain rates around 10 /s;
- strain attenuation for a realistic space and time distribution of the load, at least in case of highly dynamic loading conditions;
- better load distribution by the top plate under cryogenic temperatures;
- large increase of the Young modulus and of the offset yield stress of the foam under cryogenic temperatures.

ACKNOWLEDGEMENTS

The views expressed in the paper are those of the authors and do not necessarily represent the unanimous views of all the SlosheL consortium members.

The authors would like to acknowledge the support provided by the SlosheL consortium members that have made the SlosheL project

possible: American Bureau of Shipping, Bureau Veritas, Ecole Centrale Marseille, Chevron, ClassNK, Det Norske Veritas, GDF SUEZ, GTT, Lloyd's Register EMEA, MARIN, Total and Shell.

REFERENCES

- Bogaert, H., Brosset, L., Kaminski, M.L., (2010) "*Interactions between wave impacts and corrugations of Mark III Containment System for LNG carriers: findings from the SlosheL project*", 20th (2010) Int. Offshore and Polar Eng. Conf., Beijing, China, ISOPE.
- Brosset, L., Mravak, Z., Kaminski, M., Collins, S., Finnigan, T., (2009) "*Overview of SlosheL project*", 19th (2009) Int. Offshore and Polar Eng. Conf., Osaka, Japan, ISOPE.
- Carden, E.R., Maguire, J.R., Durley-Boot, N.J., (2011) "*Modal testing and model reconciliation of the SlosheL Mk III test panel*", 21st (2011) Int. Offshore and Polar Eng. Conf., Maui, (HI), USA, ISOPE.
- Drazin, P.G., Reid, W.H., "*Hydrodynamic Stability*", Cambridge University Press, 2004
- Gervaise, E., de Sèze, P.E., Maillard, S., (2009) "*Reliability-based methodology for sloshing assessment of membrane LNG vessels*", 19th (2009) Int. Offshore and Polar Eng. Conf., Osaka, Japan, ISOPE.
- Hofland, B., Kaminski, M.L., Wolters, G., (2010) "*Large Scale Wave Impacts on a Vertical Wall*", 32nd Int. Conf. on Coastal Engineering, ICCE 2010, Shanghai, China, June 30 – July 5, 2010.
- Kaminski, M.L., Bogaert, H., (2010). "*Full-Scale Sloshing Impact Tests Part II*", 20th (2010) Int. Offshore and Polar Eng. Conf., Beijing, China, ISOPE.
- Kaminski, M.L., Bogaert, H., Brosset, L., (2011). "*Full and large scale wave impact tests for a better understanding of sloshing – Results of the SlosheL project*", 30th (2011) Int. Conf. on Ocean, Offshore and Arctic Eng. OMAE 2011-49992, Rotterdam, the Netherlands
- Kimmoun, O., Ratouis, A., Brosset, L., (2010) "*Sloshing and scaling: experimental study in a wave canal at two different scales*", 20th (2010) Int. Offshore and Polar Eng. Conf., Beijing, China, ISOPE.
- Lafeber, W., Brosset, L., Bogaert, H., (2011) "*Loads on Mark III corrugated primary membrane: findings from the SlosheL project*", 21st (2011) Int. Offshore and Polar Eng. Conf., Maui, (HI), USA, ISOPE.
- Lloyds Register, (2009) "*Sloshing Assessment Guidelines (SAG), Version 2*", May 2009
- Wagner, H., (1932) "*Über Stoss- und Gleitvorgänge an der Oberfläche von Flüssigkeiten*", Z. Angew. Math. Mech. 12, pp 193-215 (English transl: "*Phenomena associated with impacts and sliding on liquid surfaces*", NACA Translation 1366.)
- Copyright ©2010 The International Society of Offshore and Polar Engineers (ISOPE). All rights reserved.